Development of an improved two-stage seeding process for a nanocomposite vascular graft using human peripheral-blood derived endothelial cells.

Geoffrey Punshon

Royal Free and University College Medical School

PhD thesis submitted to University College London

Declaration of originality

I, Geoffrey Punshon, confirm that the work presented in this thesis is my own. Where information has been derived from other sources I confirm that this has been indicated in the thesis.

This thesis is dedicated to my wife Alison

Without her love and support it would never have been completed.

Acknowledgements

Firstly, I would like to acknowledge the fantastic support and help I received from my supervisors, Professor Alex Seifalian and Professor George Hamilton and my deepest thanks go to both of them. They gave me the confidence to publish my work initially and then to carry on and study for a PhD. Alex especially was always there for me when I had a problem or was not sure how to proceed even though he had so many claims on his time.

Dina Vara and I collaborated on many projects some of which are included as part of this thesis, especially the cell adhesion under flow work, both while she was a student and after she was awarded her PhD. Dina was always a pleasure to work with.

Arnold Darbyshire prepared the entire polymer for my work and kindly taught me how to do the preparation myself as well as how to extrude the graft samples. Arnold's advice and enthusiasm was invaluable to my work and was most appreciated.

I'd also like to thank Karen Cheetham for her enthusiastic support of my carrying out the PhD and my colleagues Kevin Sales, Barry Fuller, Max Ahmed, Alok Tiwari, Achala de Mel, Sandip Sarkar and Jerry Kirk for all their help, support and advice over the years.

Innes Clatworthy processed all the Scanning Electron Microscope samples. He was always available for advice on the interpretation of the scans and contributed to many of our publications as well as this thesis.

Michael Olbrich from the Vienna group collaborated with me on the surface modification work and carried out both the preparation and analysis of the modified polymer which I used to do the cell work. It was an interesting experience to work with another group so closely.

Abstract

Background:

Currently available prosthetic small calibre vascular grafts have poor medium and long term outcomes due to the development of neo-intimal hyperplasia caused by their non-compliant properties and lack of an endothelial cell lining.

Here a nanocomposite based on polyhedral oligomeric silsesquioxane (POSS) attached by direct reaction onto a urethane segment was employed as a potential vascular graft material. It has been demonstrated to have similar viscoelastic properties to a native artery and be resistant to degradation.

Initially Human Umbilical Vein Endothelial Cells (HUVEC) were employed as the cell source of choice after which investigations were carried out into the suitability of human peripheral blood derived circulating endothelial cells (CEC) and endothelial progenitor cells (EPC) for graft seeding.

Aim:

The aim of this study was to develop a system with the potential to deliver an EPC/CEC-seeded bypass graft in a realistic time-frame.

Methods:

The cytocompatibility of the nanocomposite was initially investigated using HUVEC as a cell source. Surface modification of the nanocomposite to improve cell adhesion and proliferation was then attempted using UV exposure. Seeded nanocomposite grafts were then exposed to flow and the effect of preconditioning investigated. Following this the use of human peripheral blood derived EPC and CEC as a potential cell seeding source was investigated. Studies were also carried out into the sterilization of the nanocomposite.

Results:

The nanocomposite was able to support the attachment and growth of both HUVEC and EPC/CEC. Nanocomposite grafts were successfully seeded and exposed to flow with cells being retained on the graft surface following exposure to flow.

Conclusions:

The results obtained suggest that the nanocomposite graft and the use of EPC/CEC derived from human peripheral blood process has potential both for a realistic and achievable two-stage seeding process for vascular bypass grafts.

Contents

List of Figures and Tables

Figures

14

Fig 2.2e. Toluidine Blue staining of HUVEC exposed to 24 hours nanocomposite-treated CCM$_{100}$ (Magnification X20).

Fig 2.2f. Toluidine Blue staining of HUVEC exposed to 24 hours nanocomposite-treated CCM$_{ST}$(Magnification X20).

Fig.2.3a. LDH assay test on HUVEC seeded directly onto nanocomposite for 24 hours. Absorbance was measured in arbitrary units at 450nm wavelength. Data are mean ± SD(n=6).

Fig. 2.3b. Alamar blue^{TM} viability assay test on HUVEC seeded directly onto nanocomposite for 24 hours. Absorbance was measured in arbitrary units at 570nm wavelength and background at 630nm subtracted. Data are mean ± SD(n=6).

Fig. 2.3c. Alamar blue^{TM} viability assay test on HUVEC seeded directly onto nanocomposite for 96 hours. Absorbance was measured in arbitrary units at 570nm wavelength and background at 630nm subtracted. Data are mean ± SD(n=6).

Fig. 2.4a: Unseeded nanocomposite 24 hours(Magnification x640).

Fig. 2.4b: Unseeded nanocomposite 96 hours(Magnification x 160)

Fig. 2.4c: HUVEC seeded nanocomposite 24 hours(Magnification x 160).

Fig 2.4d: HUVEC seeded nanocomposite 96 hours(Magnification x160)

Fig.2. 5. Alamar blue^{TM} viability assay test on HUVEC seeded directly onto nanocomposite for 16 days. Absorbance was measured in arbitrary units at 570nm wavelength and background at 630nm subtracted. Data are mean ± SD(n=6).

Figure 3.1 Structure of nanocomposite

Figure 3.2 SEM image of nanocomposite: nanocomposite exposed to 172 nm UV-light in 5 mbar NH$_3$ for 30 minutes. For recording of the SEM image, a thin Au layer was deposited onto the surface by sputter deposition.

Figure 3.3 AFM image of nanocomposite: nanocomposite exposed to 172 nm UV-light in 5 mbar NH$_3$ for i) 0 minutes (untreated), ii) 5 minutes, iii) 10 minutes, iv) 15 minutes and v) 30 minutes. The image shows an area of 4 x 4 µm, while the colour-scale encodes the height

information. Due to an image processing artefact, the largest features are accompanied by slightly deeper stripes in horizontal and vertical direction.

Figure 3.4 CA of UV-irradiated nanocomposite: advancing water contact angle at nanocomposite versus irradiation time (exposure to 172 nm UV-light in 5 mbar NH_3).

Figure 3.5 XPS spectra of nanocomposite: (a) nanocomposite untreated, (b) nanocomposite exposed to 172 nm UV-light in 5 mbar NH_3 for 30 seconds, (c) nanocomposite exposed for 5 minutes and (d) nanocomposite exposed for 30 minutes.

Figure 3.6 ATR-FTIR spectra of nanocomposite: nanocomposite untreated and nanocomposite exposed to 172 nm UV-light in 5 mbar NH_3 for 30 seconds, 5 minutes and 30 minutes, respectively. For sake of clarity, an off-set is added to the spectra of irradiated samples.

Figure 3.7 Peak assignment in ATR-FTIR spectra: peak assignment in spectrum of (a) untreated nanocomposite and (b) nanocomposite exposed to 172 nm UV-light in 5 mbar NH_3 for 30 minutes. Ph is the abbreviation of phenol-ring.

Figure 3.8a Pico green assay for total DNA amount from cells seeded on unmodified nanocomposite graft after two hour seeding with 0.5, 1, 2 and 4 x 10^5 HUVEC/ml (n=4). [+] indicates p<0.001 vs. previous column.

Figure 3.8b Percentage of cells seeded on nanocomposite after two hour seeding with 0.5, 1, 2 and 4 x 10^5 HUVEC/ml (n=4).

Figure 3.8c LDH activity for unmodified (0), 5, 10, 15 and 30 minutes irradiated at 5mbar NH_3 atmosphere modified Prep 11 graft after 2 hours seeding (n=4). Cell seeding density 1 x 10^5 cells/well.

Figure 3.9: AB assay for unmodified (0), 5, 10, 15 and 30 minutes irradiated at 5mbar NH_3 atmosphere modified nanocomposite a) after initial seeding, b) 24 hours; c) 48 hours and d)

72 hours after initial 1 hour and 2 hour seeding (n=4). Cell seeding density 1 x 10^5 cells/well. * indicates $p<0.05$ vs. 2 hour unmodified.

Figure 4.1: Cell isolations by density centrifugation from 20ml human blood. Cells counted by haemocytometer and number adjusted for volume of blood taken. Alphanumeric on the X axis refer to extract codes.

Figure 4.2: FACS analysis of initial cell isolations. Number of CD133+ and CD133+/VEGFR2+ (EPC) cells shown per ml of cell isolation.

Figure 4.3: Cell metabolism determined by an Alamar blue^{TM} assay up to 35 days (n=5).

Figure 4.4a) 2% agarose gel of RT-PCR for three initial cell isolations (A, B and C) with CD14, CD34, CD133 and VEGFR2

Figure 4.4b) 2% agarose gel of RT-PCR for three confluent cell isolations A, B and C with CD14, CD34, CD133 and VEGFR2

Figure 4.4c) 2% agarose gel of RT-PCR for an initial cell isolation A and two Day 35 nanocomposite confluent seeded samples B and C with CD14, CD34, CD133 and VEGFR2

Figure 4.4d) 2% agarose gel of RT-PCR for two HUVEC cell isolations A, B, two initial cell isolations C, D and two Day 35 nanocomposite confluent seeded samples E, F for PECAM-1 and vWF

Figure 4.5a): Cells seeded on nanocomposite and stained with Giemsa at Day 5 (x10 magnification)

Figure 4.5b): Cells seeded on nanocomposite and stained with Giemsa at Day 14 (x10 magnification)

Figure 4.5c): Cells seeded on nanocomposite and stained with Giemsa at Day 21 (x10 magnification)

Figure 4.5d): Cells seeded on nanocomposite and stained with Giemsa at Day 35 (x10 magnification).

Figure 4.6: Cells were observed in a confluent layer on the nanocomposite at day 35 demonstrated with SEM.

Figure 4.7. Initial cell isolation stained for CD34 and CD133. a) unstained, b) CD34 stained, c) CD133 stained and d) dual stained. All views are of the same cell population (magnification X100).

Figure 4.8: Staining of Hill Colonies: three views each stained for i) no fluorescence ii) CD34 (FITC(green)) and iii) CD133 (Allophycocyanin(red)).

Figure 4.9: Confluent cell culture stained for CD34 and CD133: a) unstained, b) CD34 stained, c) CD133 stained and d) dual stained. All views are of the same cell population (magnification X100).

Figure 4.10: Initial cell isolation and confluent cells stained for vWF: a) initial isolation unstained b) confluent cells unstained, c) initial isolation stained for vWF and d) confluent cells stained for vWF (magnification X100).

Figure 4.11: Initial cell isolations and confluent cells stained for PECAM-1: a) initial isolation unstained b) confluent cells unstained, c) initial isolation stained for PECAM-1 and d) confluent cells stained for PECAM-1 (magnification X100).

Figure 5.1: The flow circuit comprising a variable-speed electromagnetic centrifugal pump, flexible plastic tubing, fluid reservoir and circulating solution oxygenated through a Maxima hollow fibre oxygenator with 95% air and 5% CO_2. Automatic pH, pO_2 and pCO_2 controller.

Figure 5.2: Vessel distension detected with ultrasound wall tracking system and pressure with Millar Mikro-tip catheter transducer from circuit in Figure 4.1.

Figure 5.3: A typical time dependent velocity (a) and shear rate distribution (b) acquired by the duplex ultrasound coupled with on-line vessel wall tracking system.

Figure 5.4: A schematic representation of the experimental procedure illustrating a summary of the treatment carried out to each set of conduits. Group A conduits were exposed to either

1 or 4 hours static (S_1 or S_4) or preconditioning (P_1 or P_4) prior to exposure to 4 hours physiological flow while Group B conduits were exposed to either 1 or 4 hours static (SR_1 or SR_4) or preconditioning (PR_1 or PR_4) followed by a 24 hour static recovery period prior to exposure to 4 hours physiological flow.

Figure 5.5: Alamar blue^{TM} cell viability assay post HUVEC seeded on TCP and nanocomposite conduits at cell seeding densities of 0.5 x 10^6 cells/cm^2, 1 x 10^6 cell/cm^2 and 2 x 10^6 cells/ cm^2 after A) 4 hours, B) 8 hours, C) 12 hours and D) 24 hours of seeding time.

Figure 5.6: LDH assay test measuring cell toxicity on HUVEC seeded on TCP and nanomposite conduits at 0.5 x 10^6, 1 x 10^6 and 2 x 10^6 for A) 4 hours, B) 8 hours, C) 12 hours and D) 24 hours of seeding time. *P < 0.05, **P < 0.01and ***P < 0.001 using one-way ANOVA with Tukeys

Figure 5.7: Cell seeding efficiency and viability post 1 and 4 hour static and flow exposed on A) glass and B) PCSBU conduits. No significant differences were seen between PSCBU groups (one-way ANOVA).

Figure 5.8: Typical SEM of a PCSBU conduit: A) unseeded, B) seeded with 1 x 10^6 HUVEC overnight

Figure 5.9: Assessment of cell viability by an Alamar blue^{TM} metabolic assay: Figure 3A shows Pre-flow, S_1, S_4, P_1 and P_4 groups. Figure 3B shows Pre-flow, SR_1, SR_4, PR_1 and PR_4 groups. Statistical analysis was carried out by one-way ANOVA (n = 4) with ** P < 0.01 and *** P < 0.001

Figure 5.10: Typical SEM of nanocomposite conduits: A (unseeded conduit), B (Pre-flow conduit), C (S_1 conduit), D (S_4 conduit), E (P_1 conduit), F (P_4 conduit), G (SR_1 conduit), 4.8 H (SR_4 conduit), I (PR_1 conduit) and J (PR_4 conduit).

Figure 5.11: Typical 2% agarose gels of PCR products with a 100 bp marker. Each sample was analysed for GAPDH, TGF-β1, VEGFR-1, PECAM-1 and VEGFR-2 expression: Figure 4A shows S_1, S_4, P_1 and P_4 samples. Figure 4B shows SR_1, SR_4, PR_1 and PR_4 samples.

Figure 5.12: Intensity analysis of PCR products to determine gene expression levels following normalisation for GAPDH: Figure 5A shows S_1, S_4, P_1 and P_4 samples for TGF-β1, VEGFR-1, PECAM-1 and VEGFR-2. Figure 5B shows SR_1, SR_4, PR_1 and PR_4 samples for TGF-β1, VEGFR-1, PECAM-1 and VEGFR-2. Statistical analysis was carried out by one-way ANOVA (n = 4) with * P<0.05, ** P < 0.01 and *** P < 0.001

Figure 6.1: Typical Hill Colonies isolated using Histopaque 1077 (left) and Lymphoprep (right).

Figure 6.2: Effect of Isolation Technique. Cells isolated by: Histopaque 1077 (H) or Lymphoprep (L). Cell Group: Initially adherent at Day 2 (IA), Adherent at D7 (A) or Non-adherent at D7 (NA). Time point: Day 7 (D7) or Day 14 (D14). * p<0.001 L A D14 vs. L A D7; $^{\&}$ p<0.001 H A D14 vs. L A D7; $^{\#}$ p>0.05 H A D7 vs. L A D7 and $^{+}$ p>0.05 H A D7 vs. H A D14.

Figure 6.3a): RNA analysis for CD14, CD34 and CD133 on cell extracts isolated by either Histopaque (H) or Lymphoprep (L) techniques from initial (I) or Day 14 (D14) samples. N = Negative Control.

Figure 6.3b): RNA analysis for vWF, VEGFR-2 and PECAM-1 on cell extracts isolated by either Histopaque (H) or Lymphoprep (L) techniques from initial (I) or Day 14 (D14) samples. N = Negative Control.

Figure 6.4: Effect of Gelatin or Fibronectin Coating on Cell Metabolism. Coating type: Uncoated (UC); Gelatin Coated (GC) or Fibronectin Coated (FC). Cell Group: Initially adherent at Day 2 (IA), Adherent at D7 (A) or Non-adherent at D7 (NA). Time point: Day 7

(D7) or Day 14 (D14). [+] $p > 0.05$ FC A D7 vs. UC A D7; [$] $p < 0.001$ GC A D7 vs. UC A D7 or FC A D7; [*] $p < 0.001$ UC A D7 vs. UC A D14 and [&] $p > 0.05$ FC A D7 vs. FC A D14.

Figure 6.5: The Effect of FBS concentration on cell metabolism. Percentage Fetal Bovine Serum (FBS) 5%, 10% or 20%. Cell Group: Initially adherent at Day 2 (IA), Adherent at D7 (A) or Non-adherent at D7 (NA). Time point: Day 7 (D7) or Day 14 (D14). [*] $p < 0.05$ 20% FBS A D7 vs. 20% FBS A D14.

Figure 6.6: The effect of various media on cell metabolism. Media types: RPMI1640; M199; DMEM; IMDM and EGM-2. Cell Group: Initially adherent at Day 2 (IA), Adherent at D7 (A) or Non-adherent at D7 (NA). Time point: Day 7 (D7) or Day 14 (D14). [*] $p < 0.001$ IMDM A D7 vs. M199 A D7; [&] $p < 0.001$ M199 A D7 vs. RPMI A D7; [+] $p < 0.001$ RPMI A D7 vs. DMEM A D7 or EGM-2 A D7; [#] $p > 0.05$ IMDM A D14 vs. M199 A D14 and [$] $p < 0.001$ M199 A D14 or IMDM A D14 vs. RMPI 1640 A D14.

Figure 7.1: ATR-FTIR analysis of (A) cast POSS-PCU, (B) porous POSS-PCU, (C) cast POSS-PCL, and (D) porous POSS-PCL nanocomposites after sterilization with EtOH (10 min and 24 h), autoclave, and gamma irradiation. A summary of the changes in key peak intensities are inset (n ¼ 6, $p < 0.05$).

Figure 7.2: ATR-FTIR analysis of POSS-PCU nanocomposites following sterilisation with EtOH (10 mins and 24 hrs), Autoclave and gamma irradiation. With each spectra is a summary of any changes in key peak intensities (n=6, $p < 0.05$).

Figure 7.3: The percentage change (compared with unsterilized control) in number average (M_n, top) and weight average (M_w, bottom) molecular weight of POSS-PCU and POSS-PCL, both cast and porous samples after sterilization via a 10-min incubation in EtOH, 24 h incubation in EtOH, autoclaving, and gamma irradiation (mean ± SD, n=3). The molecular weights of the unsterilized controls were as follows: POSS-PCU (M_w = 108 500, M_n = 42,600), POSS-PCL (62 800, M_n = 31,200).

Figure 7.4: Cell viability after 7-day incubation, as determined by Alamar blue[TM] assay. Results (mean ± SD) are presented as a percentage of the control cells grown on tissue culture plastic (n=4, * = p<0.001). Gamma irradiation appeared to reduce the number of viable cells by approximately 50% on POSS-PCU whereas no significant differences were observed in cell growth on casted POSS-PCL samples. No cell growth was seen on the coagulated samples of POSS-PCL.

Tables

Table 3.1: Detailed evaluation of XPS spectra. Key: UN; Untreated Nanocomposite, IN; Irradiated Nanocomposite (30 minutes exposure to 172nm UV-light in 5 mbar NH_3)

Table 4.1: Primer sequences for CD14, CD34, CD133, VEGFR2, CD31 and vWF gene expression analysis.

Table 5.1: Flow circuit haemodynamic data including peak and mean shear stresses

Table 5.2: GAPDH, TGFβ-1, PECAM-1, VEGFR-1and VEGFR-2 Primer Sequences.

Table 5.3: RNA yield was measured at absorbance of 260nm and 280nm and quantity determined as ng/μl. Group A shows S_1, S_4, P_1 and P_4 samples. Group B shows SR_1, SR_4, PR_1 and PR_4 samples.

Table 6.1: Primer sequences for CD14, CD34, CD133, VEGFR2, PECAM-1 and vWF gene expression analysis.

Table 7.1: Mechanical properties (Young's Modulus, ultimate tensile strength and elongation at break) of POSS-PCU and POSS-PCL samples after sterilization by a variety of techniques (n=6).

Table 7.2: Bacterial Growth Observed on Each Sample After Incubation in Tryptone Soya Broth (TSB) and Fluid Thioglycollate Medium (THY) for Cultivation of Microorganisms.

1

1 Introduction

Cardiovascular disease has become an increasing health issue with a significant economic impact (Mozaffarian *et al.*, 2016). The World Health Organisation estimates that in 2012 17.5 million people died from cardiovascular disease worldwide. In the USA for example 38% of all deaths recorded were due to cardiovascular disease (World Health Organisation, 2016). It is believed that over 800,000 coronary artery bypass procedures are carried out annually (Cleveland Clinic 2011) and the overall demand for vascular grafts is growing substantially with an estimated annual growth of 8.4% in the USA for example (Freedonia Group 2011).

For the past five decades, there has been considerable interest in the development and use of synthetic vascular grafts as an integral part of vascular surgery. Initial work in the 1950's focused on the use of autologous vein segments for small (less than 4mm) to medium (less than 7mm) vessel peripheral vascular bypass in distal limbs. While the use of autologous

grafts has been successful (Klinkert *et al.*, 2004; Klinkert *et al.*, 2003; Chamiot-Clerc *et al.*, 1998) it is limited by the fact that in approximately one third of patients a suitable autologous vein is not available either because the existing veins are in poor condition or suitable ones have been used in previous procedures (Veith *et al.*, 1979; Kerdjoudj *et al.*, 2007; Twine and McLain, 2010).

There are a number of features and challenges which must be taken into consideration when designing the ideal vascular conduit such as minimizing patient waiting time for a suitable conduit, ensuring that the conduit has adequate mechanical properties (suture retention strength, burst pressure, resistance to degradation and compliance similar to native vessels), low permeability at arterial pressures to limit transmural bleeding and seroma formation, minimal thrombogenicity and consistency between production runs all of which must be addressed.

One possibility is to use natural biological scaffolds as a basis for a vascular conduit. These can be either autologous or derived from human or animal donors. There are two major advantages to these natural scaffolds compared to synthetic models, firstly that they can be infiltrated more easily by host cells than synthetic materials such as polytetrafluoroethylene (PTFE) giving the potential to be repopulated with autologous cells from the host and secondly that the scaffold itself is composed of proteins and other components of the extracellular matrix necessary to support cell adhesion and growth unlike synthetic scaffolds (Nemeno-Guanzon *et al.*, 2012). The difficulty with these biological scaffolds is the issue of immune-mediated rejection which is difficult to overcome (Schuurman *et al.*, 2003; Seetharam *et al.*, 2010). In order to try to reduce the effect of this decellularization of allo- or xeno-grafts is usually performed to remove the antigenic cellular components while leaving the extra-cellular matrix structure intact (Mathapati *et al.*, 2011). Such decellularized scaffolds have shown promise as implantable biomaterials or as the basis for tissue-

engineered constructs (L'Heureux *et al.*, 2007; Fiore *et al.*, 2011). However, while decellularizing the scaffold reduces the risk of immune-mediated rejection the methods used to accomplish this such as the use of organic solvents, detergents or ionic solutions (Dahl *et al.*, 2003; Mangold *et al.*, 2015) and the mechanical techniques such as agitation, sonication or freeze-thawing (Wilshaw *et al.*, 2012; Azhim *et al.*, 2011; Pellegata *et al.*, 2012) may have a detrimental effect on scaffold integrity following implantation (Moroni and Mirabella, 2014). Investigations into these effects are complicated by the fact that there is no generally agreed method for achieving decellularization in part due to the varied composition of the extracellular matrix in different tissues.

As a result, it has been necessary to employ synthetic vascular graft replacements for those patients who cannot provide a suitable autologous vein (Veith *et al.*, 1979; Desai *et al.*, 2011). To date the outcome of using the various synthetic vascular grafts employed clinically has been poor with low long-term patency rates resulting in high re-intervention rates, increased morbidity and low quality of life when compared to grafts employing an autologous vein (Baiguera and Ribatti, 2013). The reasons for this decrease in patency are varied with issues such as the thrombogenicity and mechanical characteristics of the material surface (Sarkar *et al.*, 2007a), lack of a suitable endothelial cell (EC) layer (Kannan *et al.*, 2005a) and increased rates of infection (Chiesa *et al.*, 2002) which can be life-threatening (Harish and Allon, 2011) all being implicated.

Considering that according to a recent report by Hirsch *et al* cardiovascular diseases still account for more than 20% of global mortality and are the primary cause of death worldwide this is an issue which still needs to be addressed (Hirsch *et al.*, 2012).

One of the first studies to look at a successful suitable synthetic replacement for an autologous vein was that of Voorhees' and Blakemore published in 1954 which used tubes

constructed from Vinyon "N" cloth initially in thirty canine subjects followed by a clinical trial in eighteen human subjects (Blakemore and Voorhees, 1954). Ten of the human subjects survived the trial with a maximum follow up of ten months. All the survivors were symptom free and had functional prosthesis.

These early studies encouraged further investigation into other textiles including Nylon and Orlon. The major difficulty encountered with these textiles was that over time they lost tensile strength and failed. The next major breakthrough was the introduction of Dacron in 1957 by DeBakey (Debakey *et al.*, 1957). Dacron consists of polyester fibres bundled into multi-filament yarns and has been either woven or knitted into a fabric material. Woven Dacron tends to result in narrow spaces for tissue in-growth while knitted Dacron is looser and favours tissue in-growth. However knitted Dacron is prone to low bursting strength and a tendency to deform when placed under stress. Dacron was demonstrated to have much improved post-implantation mechanical properties and rapidly became the material of choice for synthetic aortic aneurysm repair which has not been bettered since. Some improvements have been made to the initial Dacron prosthesis including adding a velour coating to the inner and outer surface to encourage cell attachment and growth as well as making the prosthesis easier to pre-clot. A further addition was external support to the prosthesis to prevent prosthesis kinking when crossing joints.

Unfortunately, when employed in low flow small diameter vessel replacement the positive outcomes seen in large calibre high flow vessels were not observed. The major reason for this failure was twofold, firstly the low flow experienced in the smaller vessels and the inherent thrombogenicity of the Dacron lead to thrombotic occlusion and secondly neointimal hypoplasia was a significant problem at the anastomotic sites. These issues resulted in a poor long-term patency for small diameter Dacron prosthesis and resulted in other materials being investigated for this application.

The next breakthrough in peripheral artery bypass came in 1959 with the introduction of PTFE by Edwards (Edwards, 1959). PTFE is a durable inert fluorocarbon polymer which can be extruded to increase the number of micropores as extended PTFE Polytetrafluoroethylene (ePTFE). PTFE has high flexibility, demonstrates good resistance to biodegradation and has an anti-thrombogenic electronegative luminal surface. It has been used as an haemodialysis vascular access conduit (Baker *et al.*, 1976) and synthetic membranes. It has also been used in cosmetic and reconstructive surgery (Liu *et al.*, 2016). In 1973 PTFE was successfully used for small calibre artery replacement (Matsumoto *et al.*, 1973). Studies such as those by Raithel (Raithel and Groitl, 1980) and Veith (Veith *et al.*, 1979) came to the conclusion that PTFE was as effective as autologous vein when employed for infrainguinal bypass. However medium to long term usage of PTFE grafts suffered from the development of neointimal hypoplasia resulting in graft occlusion (Echave *et al.*, 1979) which may result either from changes in matrix and cytokine constituents (Sarkar *et al.*, 2006) and from the relative stiffness of the material compared to native vessels. These issues are exacerbated in small diameter conduits (Kannan *et al.*, 2005a). PTFE also does not support cell seeding very well with extensive cell loss when exposed to physiological flow (Carr *et al.*, 1996; Rosenman *et al.*, 1985).

Another material with low compliance which has been considered for use in small diameter vascular prosthesis is polypropylene, a thermoplastic polymer made from the monomer propylene. Polypropylene has a crystalline structure which gives it strength and is relatively resistant to chemical degradation. It also has a low thrombogenicity and inflammatory reaction rarely being rejected by the body. These properties lead to studies using polypropylene as a small calibre vascular prosthesis. Initial results based on medium term implantations suggested that polypropylene was superior to PTFE (Greisler *et al.*, 1992) but further long term studies demonstrated that the long term biostability of polypropylene in

vivo was less successful with surface cracking, erosion and serious wall weaknesses developing in grafts implanted for a number of years (Mary *et al.*, 1998) resulting in polypropylene falling out of favour as a potential prosthesis base.

Various reasons have been suggested for the development of neointimal hyperplasia in small calibre PTFE and Dacron grafts. A study by Kidson and Abbott made a direct association between the lack of compliance of PTFE and Dacron and neoinitimal hyperplasia particularly in small diamer (<6mm) grafts (Kidson and Abbott, 1978). The mechanism of intimal hyperplasia was investigated in depth by Sottiurai in 1999 who demonstrated that intimal hyperplasia consisted principally of multiple layers of extracellular matrix (ECM) and cells. Adjacent to the lumen the cells were mesenchymal type cells, deeper in the lumen myofibroblasts were more prominent (Sottiurai, 1999). Earlier studies by the same group had already demonstrated that physical stresses on smooth muscle cells (SMC) result in the synthesis of ECM (Sottiurai *et al.*, 1983). More recent studies have shown that the geometry of the anastomosis affects the occurrence of initmal hyperplasia (Kannan *et al.*, 2005a) as does the lack of compliance demonstrated by PTFE, Dacron and polypropylene (Sarkar *et al.*, 2006).

As a result, there has been considerable interest in the possibility of utilizing materials with a compliance more similar to natural veins to reduce the likelihood of neointimal hyperplasia developing in long term implanted small diameter vascular prosthesis. To date two major groups of material have been investigated, silicones and polyurethanes.

Silicone has several advantages as a potential graft material. It is very elastic resulting in potentially good compliance, a property it retains even after implantation and tissue incorporation (White *et al.*, 1987). It is also largely inert (Habal, 1984). Silicone has a long history of use for medical devices as diverse as breast implants and feeding tubes with long

term implantation (Moss *et al.*, 1990) {153} and biostability (Christenson *et al.*, 2005). While silicone has low leucocyte and complement activation (Kottke-Marchant *et al.*, 1987) one major disadvantage is that the hydrophobicity of pure polysiloxane results in a high affinity for fibrinogen resulting in unacceptable levels of thrombogenicity. In an attempt to overcome this either the use of hydrophilic copolymer coploymerisation (Julio *et al.*, 1994) or the attachment of organic groups (Whalen *et al.*, 1992) has been investigated.

The use of silicone in breast implants has, however, lead to a reconsideration of the long term stability of silicone in the body due to reports of silicone breast implants rupturing and migrating (Puckett *et al.*, 2004) due to the degradation of silicone in vivo following the breakdown of silicone bonds by oxidation and hydrolysis as reported by Garrido et al (Garrido *et al.*, 1993). As a result of these issues the use of silicone for long-term implants has become problematical.

Another potential material to address the need for conduits which has been explored are the polyurethanes. Polyurethanes are more compliant than Dacron and PTFE resulting in a reduction in compliance mismatch between the conduit and the native vasculature (Sarkar *et al.*, 2006). Polyurethane conduits can be produced via two methods, either fibrillar in which fibres of polyurethane are woven, knitted, spun electrostatically or wound into a conduit or foam which can be produced by phase inversion, foam flotation and dip coating. Initial studies reported issues with high rates of aneurysm and thrombogenicity compared to Dacron or ePTFE (Brothers *et al.*, 1990) but these issues have been addressed using modified forms of polyurethane which demonstrate biostability (Salacinski *et al.*, 2002b), improved thrombogenicity (Kannan *et al.*, 2006) and the potential for successful cell seeding (Punshon *et al.*, 2005; Vara *et al.*, 2008).

It was recognised very early on that apart from the deficiencies of the various materials explored as potential vascular conduits one of the other major issues was the lack of an EC layer on the conduit either at implantation or through spontaneous in-growth post-implantation. The lack of an endothelial layer which can interact with circulating blood to provide an anti-thrombogenic surface preventing the initiation and development of the process of intimal hyperplasia is a major factor in graft failure.

Many studies have demonstrated that spontaneous formation of an endothelial layer along the full length of the vessel does not occur in humans either by in-growth through the vessel wall or in-growth from the adjacent vessel. There is some limited in-growth in a narrow zone limited to the immediate anastomotic area in humans (Pennel *et al.*, 2013; Berger *et al.*, 1972). Even after numerous studies the maximum transanastomotic growth in grafts implanted for a number of years has been found to be no more than 1 to 2 cm (Pennel *et al.*, 2013) which, given that the usual graft length is 50 to 60 cm. is inadequate. Several animal models have been utilized to study EC seeding but these are somewhat compromised by the fact that many animal species demonstrate rapid and extensive transanastomotic endothelialisation and is further complicated by the fact that relatively young animals are used in studies compared to the human patient population requiring intervention (Zilla *et al.*, 2007).

Other than relying on the spontaneous in-growth of an endothelial layer from the anastomotic region there are two main strategies for creating an endothelial layer on vascular prosthesis. The first method investigated was to seed the conduit with EC's prior to implantation. There have been two approaches with this method, 'single-stage' seeding in which cells are extracted and immediately seeded on the conduit without expansion in culture and 'two-stage' seeding where cells are harvested from a suitable source followed by culture and expansion in the laboratory prior to conduit seeding and implantation. These two

approaches have their own advantages and disadvantages when potentially used in a clinical situation.

'Single-stage' seeding requires the patient to undergo a single operation during which cells are extracted and the conduit seeded and implanted which seemed an ideal way to produce a seeded conduit.

Early studies by Herring in 1978 (Herring *et al.*, 1978) looked at single-stage seeding in a canine model replacing the infrarenal aorta with a Dacron conduit which was seeded immediately pre-implantation with endothelium scraped from the saphenous vein and resulted in the successful development of an endothelial layer after six weeks' implantation. Graham in 1980, again in a canine model, reported on a series of twenty-eight subjects which underwent thoracoabdominal bypass using a 6mm Dacron conduit (Graham *et al.*, 1980b; Graham *et al.*, 1980a). The cell source in this study was autologous external jugular vein extracted by enzymatic digestion using trypsin and collagenase. Extracted cells were similarly seeded immediately pre-implantation of the conduit and the implanted conduits examined between one and twenty-eight days' post-implantation. Again, the seeded conduits demonstrated an endothelial coverage (greater than 80% by day twenty-eight) and showed an increase in clot-free surfaces compared to unseeded conduits. Building upon his earlier canine work Herring in 1984 reported on a trial in human subjects which looked at single-stage seeding (Herring *et al.*, 1984). 186 operations were carried out on 161 patients over the course of the four-year study and again Dacron was the conduit of choice. In eleven patients' axillary-femoral and axilliary femoral-femoral bypasses were carried out (six seeded and five unseeded) with 28 patients undergoing femoral-femoral bypasses (thirteen seeded and fifteen unseeded). Femoral-popliteal conduits were implanted in 147 limbs (112 vein, 18 seeded and 17 unseeded). Unfortunately, the results of this trial were not encouraging. For femoral-femoral and femoral-popliteal bypasses there was no significant difference in patency

between seeded and unseeded conduits. There was an increase in patency in axillary-popliteal seeded conduits compared to unseeded conduits. Vein grafts were significantly better than both seeded and unseeded Dacron grafts (p = 0.016). Interestingly this study also reported on the effect of smoking on the patency of conduits and suggested that patients who smoked had worse outcomes than those that did not.

A later study reported in 1989 by Fasol *et al* looked at the effect of single-stage seeding using PTFE conduits and compared unseeded conduits, seeded with autologous EC conduits or reversed saphenous vein conduits with a one-year follow-up period (Fasol *et al.*, 1989). Assessment was by scanning electron microscopy (SEM) of circulating platelets to determine active platelet levels. It was demonstrated that there was a significant increase in activated platelets in PTFE conduits regardless of seeding when compared to patients with reversed vein implantation suggesting that the cell seeding had failed to develop a functional EC layer on the conduits.

Studies such as the ones above lead to a consideration of the difficulties inherent in the single-stage seeding process. It is very difficult to extract sufficient cells to provide a realistic seeding density (Tiwari *et al.*, 2003a; Ivarsson *et al.*, 1998) compounded by the fact that as the cells have a very limited time to attach to the conduit there are substantial losses when the conduit is implanted and exposed to physiological blood flow post-implantation (Salacinski *et al.*, 2000). As mentioned previously the issue of self-endothelialisation which was not so apparent at the time also affected the value of the animal studies on which this work was based.

As a result, interest moved on to two-stage seeding which by comparison allows the production of substantial numbers of cells over a number of week's culture which can be seeded on the conduit prior to implantation.

One of the earliest clinical studies into two-stage seeding was reported in 1992 by Magometschnigg   who carried out a prospective non-randomised clinical trial on 26 human subjects all of whom had chronic end stage peripheral vascular disease and required repeat reconstruction. EC were extracted between 4 and 7 weeks prior to implantation, expanded in culture, and seeded onto PTFE conduits for 13 patients. The other 13 patients were given unseeded PTFE conduits. Initial patency after 30 days was 92% for the seeded group compared to 53% for the unseeded group. After an 18 month follow-up the amputation rate was 15% for the endothelialised conduit group whereas for the control group the amputation rate was 31%. This study therefore suggested that EC seeding in a two-stage process was a potential method to improve clinical outcomes in human patients (Magometschnigg *et al.*, 1992).

In 1994 Zilla *et al* reported a study carried out on 49 human subjects who did not have suitable saphenous vein's available for harvest (Zilla *et al.*, 1994). EC were harvested from the external jugular vein and cultured to provide an adequate cell number to endothelialise PTFE conduits coated with fibronectin glue. 33 patients were provided with an endothelialised conduit and 16 with an unseeded conduit. The efficiency of seeding was measured using angiography, platelet labelling studies, assessment of the ankle-brachial index and duplex sonography for up to 32 months' post-implantation. To obtain the 16 million EC required to produce a confluent layer on a 70-cm length 6 mm conduit took an average of 25 days' post-harvest with a 27% failure rate where the harvested cells failed to grow. The results for the successfully seeded conduits were impressive with an 84% patency at 32 months compared to only 55% for the unseeded conduits demonstrating a significant difference ($p < 0.041$) while there was also a significant lowering of the ankle-brachial index at 24 months ($p < 0.0023$) and a significant reduction in platelet uptake at all time points measured.

A similar study in humans by Leseche *et al (Leseche et al., 1997)* using EC harvested from autologous vein followed by cell culture to increase cell numbers prior to PTFE conduit seeding at high density comprised 32 patients. In 11 patients (34%) insufficient cells were obtained to seed the conduit due to failed isolation or culture (nine patients), preoperative infarction (one patient) or contamination of the isolated cells (one patient). In the remaining 21 patients it took an average of 23.5 days to achieve sufficient EC for seeding from an average vein segment 10.5 cm long. All the patients underwent above-knee femoro-popliteal bypass with a 7mm PFTE conduit. Immediately post-operation there were no complications reported. Two patients died of non-related causes after 2 and 36 months respectively. One patient required the conduit to be removed after 75 days due to the development of an abscess in the femoral triangle and three patients suffered bypass failure (at 3, 10 and 53 months). The cumulative patency rates for the implanted conduits were 95% at 3 months, 89% at 48 months and 67% at 76 months. While no direct comparison was made with unseeded conduits these rates demonstrated that such seeding was viable and may result in improved patency.

The long-term outcome of such two-stage seeding techniques has also been examined by Deutsch *et al* who reported on a fifteen-year study partly based on their previous work mentioned earlier (Zilla *et al.*, 1994) and two later investigations in 1997 (Meinhart *et al.*, 1997) and 1999 (Deutsch *et al.*, 1999). This involved 318 non-acute patients 310 of whom received a total of 381 endothelialised PTFE grafts (308 femoropopliteal and 33 femorodistal). The source of the EC was short segments of subcutaneous veins (80% cephalic, 11% basilica, 2% external jugular and 7% saphenous) with an average culture time of 19 days. The expanded cells were then seeded onto fibronectin coated PTFE conduits (6mm diameter 64%, 7mm diameter 36%). In only 2.5% of cases growth failure prevented successful seeding which was a considerable improvement on the approximately 30% failure

rate in the studies mentioned earlier. Reported outcomes of primary patency were 69% for the femoropopliteal conduits at 5 years with a 61% patency at 10 years, for the femorodistal conduits was 52% after 5 years and 3% at 10 years. This study demonstrated that two-stage endothelialisation for vascular conduits was a viable routine procedure with significant benefits for the patients involved and patency rates resembling those of vein grafts assuming that they could wait for the EC to be extracted and grown up.

Such seeded conduits can further be subjected to regimes such as pre-conditioning (in which seeded conduits are exposed to a gradually increasing flow in an *in vitro* flow circuit which has been demonstrated to improve cell retention on conduits when exposed to physiological flow) to improve cell adhesion when the conduit is implanted in the patient (Vara *et al.*, 2008).

Despite the apparent success of the two-stage seeding method it has failed to be adopted clinically generally and remains limited to very few groups. The process exposes the patient to the necessity for two procedures (one to extract the cells and a second to implant the conduit) with the associated risk to the patient of the procedures themselves. There is also the possibility that the cell extraction and expansion may fail resulting in the patient undergoing an additional operation and not having a suitable seeded conduit for implantation anyway. Such a process also has significant cost implications both from the expense of carrying out two procedures per patient rather than one for an un-seeded conduit or a 'single-stage' process and the additional cell culture facilities and staff required to expand and seed the conduits which may be the main reason behind the failure of this process to be adopted more widely despite it's apparent advantages. Finally the fact that it can take several weeks to expand the cells means that this approach is not suitable if the patient cannot wait for a seeded conduit to be produced.

Given the problems encountered with the various synthetic conduit materials another approach which has gained considerable interest over the last twenty-five years is that of a tissue engineered vascular graft. As a concept, such tissue engineered vascular conduits would have mechanical properties which mimicked those of native vessels with a diameter matched to that of the site of the anastomosis and have a viable endothelium present on the inner surface. This would be achieved without the use of either synthetic materials (such as PTFE or Dacron) or foreign materials (such as allo- or xeno-grafts} to provide an initial scaffold thus ideally avoiding the issues with chronic inflammatory responses.

One of the first proponents of the tissue-engineered approach was the group of Bell who reported a living blood vessel developed *in vitro* developed using a cell-seeded collagen gel tube system in 1986 (Weinberg and Bell, 1986). The resulting conduit demonstrated a multilayered structure resembling that of an artery with SMC in the vessel wall and EC's lining the lumen. That the endothelial layer was functional was demonstrated by the production of von Willebrand factor and prostacyclin. Unfortunately, however, the resulting conduit was not mechanically strong enough to withstand implantation at physiological pressures and flow rates resulting in the necessity to incorporate a Dacron sleeve to strengthen the conduit and re-introducing the problems associated with synthetic materials.

Following this pioneering works other groups have looked at using collagen or fibrin (Bu *et al.*, 2010; Sgarioto *et al.*, 2012; Assmann *et al.*, 2013; Filova *et al.*, 2014) based or coated conduits but the issues with achieving a conduit with a clinically acceptable burst pressure have remained. The issues with the burst pressure of such conduits are multiplied when such conduits are implanted as they are also susceptible to attack and degradation by the immune system weakening them further.

Given these challenges with either using permanent synthetic materials or tissue-engineered conduits without synthetic materials a variation on the process has been increasingly investigated in which the synthetic material used in the conduit is composed of resorbable polymers. The concept behind this system is that the polymer gives the conduit the initial strength to allow implantation under physiological flow conditions to occur while over time the resorbable nature of the polymer results in the polymer gradually degrading in a controlled manner to be replaced by native tissue which maintains structure (Weber *et al.*, 2011). In animal models this method has proved successful but it has proved less so in humans where there are complications resulting from the reproducibility and safety of the manufacturing process which must be taken into account unlike in animal models.

In conclusion, there is still a considerable challenge to be addressed in developing a widespread clinically acceptable process for overcoming the lack of a suitable autologous vessel for use as a vascular conduit. The amount and variety of research carried out to date suggests that no single approach will be successful and that in order to develop a clinically viable system numerous obstacles must still be overcome.

Financially the costs related to the use of cells in a proposed conduit must be addressed and the long-term potential cost savings of improved outcomes investigated. Any such system will require commercialization both to fund research into the field and to overcome the high production costs involved. However, the fact that there is a large potential market and that the treatment is potentially life-saving or limb saving suggest that financing a potentially successful process may be viable.

Clinically the long lead time associated with many of the approaches taken to date for systems involving cell seeding which can require weeks or even months of preparation to produce a viable conduit also need to be considered. To some extent these can be reduced by

appropriate patient management but this has to date been one of the major reasons why such methods are not routinely employed clinically. There have been some investigations into this of invasive versus medical therapy in elderly patients suffering from chronic symptomatic coronary-artery disease with some studies showing no difference in either myocardial infarction or mortality between patients receiving either optimum medical treatment or surgical intervention while the benefits of improved patency may also outweigh the increased risk associated with a longer waiting time to produce an improved conduit (Simoons and Windecker, 2010). By contrast systems which focus on improving the materials from which conduits are made and not involving cellularization avoid the problems associated with long waiting times and reliability and reproducibility of cellularization systems but generally have worse outcomes.

Finally, there are a number of regulatory and ethical issues which must be considered both for cell-based conduits and synthetic materials. The model of regulation used in organ transplantation may be the most appropriate basis for such regulation which is still in a development phase in tissue engineering where much of the regulatory practice is based on the mass production of pharmaceuticals which does not tailor well with the relatively small scale nature of tissue engineered vascular conduits.

The work presented in this thesis was carried out over a number of years during which there were exciting developments in the field of vascular tissue engineering.

Initially the concept was to look at the potential of a novel material, POSS-PCU, to support EC seeding and improve blood compatibility. In order to demonstrate this initially the cytotoxicity of POSS-PCU was investigated thoroughly using HUVEC following which investigations were performed into optimising seeding of a POSS-PCU conduit and exposing the seeded conduit to simulated physiological flow to investigate the effect of pre-

conditioning on cell retention. Additional studies included looking at surface modification of the POSS-PCU to improve cell adhesion and growth and investigating the blood compatibility of the unseeded POSS-PCU.

During the course of this work it became apparent that there was the potential to investigate new sources of EC's for use in vascular tissue engineering. Traditional studies had used primary cell sources such as autologous vein or various types of fat (omentum and subcutaneous) which were difficult to obtain and failed to result in adequate cell numbers for successful conduit seeding without extensive cell culture prior to implantation. As a result, many studies looked at HUVEC which, while easier to obtain and expand, were not suitable for use in a clinical situation.

The potential of stem cells extracted from bone marrow, embryonic tissue or umbilical cord blood lead to considerable interest in the use of stem-cell derived EC's for vascular tissue engineering. However, these sources of cells have some drawbacks either from ethical considerations (for embryonic tissue), difficulty in obtaining samples for research (bone marrow) and lack of clinical relevance (cord blood with its immune compatibility issues) were all potential drawbacks. As a result, other potential sources of EPC have been considered such as lipoaspirates. Marchal *et al* reported extracting and culturing multi-potent endothelial-like cells from 15 patients using liposuction-derived subcutaneous adipose tissue (Marchal *et al.*, 2012).

Asahara's paper in 1997 demonstrating that EPC could be extracted from human peripheral blood was interesting in that it postulated a source of cells which would be readily available for research (taking blood samples being considerably less invasive than collecting bone marrow samples), free from any ethical considerations other than informed consent and clinically relevant in that patients could have a conduit seeded with autologous cells collected

from their own peripheral blood (Asahara *et al.*, 1997). Peripheral blood derived EPC have subsequently been used in a number of areas such as vascular stents (Banerjee *et al.*, 2012), human pulmonary valves (Cebotari *et al.*, 2006) and prosthesis (Liu *et al.*, 2014; Goh *et al.*, 2014).

It thus became apparent that it might be possible to combine the clinically proven success of the 'two-stage' seeding system reported by Deutch and Zilla with this new cell source to produce a seeded graft which would overcome some of the disadvantages of the 'two-stage system'. Peripheral blood could be extracted from the patient without the need for an operation, EPC and circulating EC's extracted and either the conduit seeded immediately and implanted or the cells expanded and differentiated then seeded on the conduit. Such a system would remove the need for the patient to undergo two operations with the associated risks and expense, not require expansion and culture of the extracted cells if sufficient cells could be extracted from blood without culture and still provide all the benefits of an EC seeded conduit with no tissue compatibility issues as well. There are still some drawbacks with using peripheral blood as a source of cells such as the low numbers of EPC which can be isolated from peripheral blood which may be exacerbated in elderly patients or those with high morbidity associated with vascular disease (Stauffer *et al.*, 2008; Singh *et al.*, 2012) and the lack of a generally accepted method of isolation and characterisation (Igreja *et al.*, 2007; Punshon *et al.*, 2011) but it is possible that these can be overcome by further research in the field.

1.2 Aim of the Thesis

Current techniques for vascular grafting have many limitations but there has been some progress using EC seeding. The aim of this thesis is to explore possible solutions to this clinical challenge. A variety of approaches to this problem, using culture and seeding of peripheral blood derived EPC and circulating EC's was investigated to further the development of two-stage seeding process for vascular conduits.

1.3 Ethical Approval and Informed Consent

All of the work carried out in this study had ethical approval from the UCL Research Ethics Committee. When the studies in this thesis were carried out informed consent was not required for the collection of human umbilical cords used as a cell source in Chapters 2, 3 and 5. Under current legislation for research access to human cells and tissues as developed under the Human Tissue Authority (HTA), informed consent from the mother is required for all donations of human umbilical cord tissue and should be obtained prior to donation. This also dictates development of appropriate traceability, storage, audit and disposal policies. In the case of the use of human blood used for the extraction of peripheral blood derived stem cells in Chapters 4, 6 and 7, informed consent was obtained from the volunteer donors under the procedures relevant at the time. Nowadays, such procedures equally must form part of any HTA-related research access in the institutes undertaking the research. Full details on HTA policies and procedures can be seen at https://www.hta.gov.uk/.

2

2 Endothelial Cell Cytocompatibility of the Nanocomposite

2.1 Introduction

The biomaterials available for clinical applications such as stents or bypass grafts are largely made from two different polymers, poly(ethylene terephthalate) (PET or Dacron) and polytetrafluoroethylene (PTFE) (Seifalian *et al.*, 2002; Kannan *et al.*, 2005a). Dacron is very reactive towards both surrounding tissue and blood when used for cardiovascular applications , and this results in neo-intimal proliferation and inflammation when used for both grafts (Zenni *et al.*, 1994; Greisler *et al.*, 1996a) and stents (Peng *et al.*, 1996; Murphy *et al.*, 1992). PTFE is the other commonly employed polymer in applications such as cardiovascular grafts and stents as it displays a relatively high bio-stability and is tolerated reasonably well by the

human body. However, in a similar manner to Dacron there is a high adherence of platelets and blood proteins to the surface of the graft or stent (Kannan *et al.*, 2005d).

As a result, a number of alternatives to polymers have been investigated in an attempt to overcome these difficulties. One such alternative is Polyurethanes which have been investigated for applications in cardiovascular biomedical devices and have advantages in both their durability and their ability to extrude flexibly. In an artificial bypass graft their properties can simulate the viscoelastic properties found in native arterial wall, which can be a significant factor in improving the patency of cardiovascular devices (Salacinski *et al.*, 2001). In comparison to Dacron and PTFE, Polyurethanes demonstrate a lower level of surface thrombogenicity. This reduction in thrombogenicity can be enhanced by the fact that the surface of polyurethanes can be modified with smart bio-molecules such as Arginine-Glycine-Aspartate (RGD) or heparin (Kidane *et al.*, 2004).

An bypass graft based on poly(carbonate-urea)urethane (PCU) was developed in the Division of Surgery at UCL where it underwent testing and assessment. This material is currently marketed as an access graft (Salacinski *et al.*, 2002a; Salacinski *et al.*, 2002b) in kidney patients who require an access graft for a short period while they are waiting for a suitable kidney donor. This material has some issues with thrombogenicity, but to a lesser extent than other polyurethanes due to its soft segment being based on carbonate linkages rather than ester or ether as in the majority of conventional polyurethanes. It was felt that there remained a need for a material which did not require surface modification that employed a carbonate amorphous segment in order to reduce the issues associated with surface thrombogenicity. Ideally such a polymer should be able to demonstrate both anti-platelet and protein inhibitory qualities together with the ability to allow cells to grow on its surface due to showing good   cytocompatibility. In an attempt to achieve these requirements a polymer based on polyurethane and bridged monomers of silsesquioxane (pendant nano-

bridge); poly(carbonate-silsesquioxane-bridge-urea)urethane (PCBSU) nanocomposite was developed. By the incorporation of these bridged monomers into polyurethanes anti-thromogenic qualities may occur in the resultant polymer. Due to their inorganic nature silsesquioxanes do not have the issues and complexities which occur when drugs and biomaterials such as heparin are incorporated into the material. The silesquioxane being bridged and pendant on the polymer surface allows the anti-platelet and anti-coagulant function to occur and may reduce the cytotoxic effects often associated with materials containing silicon. This should allow EC's to grow on the material surface as ideally required in tissue engineered cardiovascular medical devices.

Previous studies into the cytocompatibility of similar materials have investigated the effect on cells of either contract directly with the material or via indirect contact using cell culture medium exposed to samples of the material for a period prior to exposure to cells. Techniques used to evaluate cytocompatibility include examining cell morphology by light microscopy and SEM, [3-(4,5-dimethylthiazol-2-yl)-2,5-diphenyltetrazolium bromide] (MTT) metabolic activity assays, Neutral Red viability staining and cell counting by using Tryphan Blue (Ramires *et al.*, 2000; Belanger *et al.*, 2000; Marois *et al.*, 1996; Armitage *et al.*, 2003).

In this Chapter the direct and indirect outcome of exposing HUVEC to nanocomposite is investigated to determine if it may provide a suitable material for cell seeding. This was ascertained by looking at the total amount of DNA present in the cells using a Pico Green assay system, examining cell metabolism using an Alamar blue™ (AB) metabolic assay and looking at cell damage by measuring Lactate Dehydrogenase (LDH) release. Cell

morphology was studied by staining with Toluidine blue in the case of indirect contact and carrying out SEM studies in the case of direct contact.

2.2. Materials and Methods

2.2.1. Polymer production

The synthesis of poly(carbonate-bridged silsesquioxane-urea)urethane nanocomposite was carried out as follows. The inorganic urethane is made from 4,4'-methylenebis(phenyl isocyanate) (MDI), poly(hexamethylene carbonate)diol, and silsesquioxane dissolved in tetrahydrofuran here bis[3-(trimethoxysilyl)propyl]amine and chain extended with DMAC.

Nanocomposite graft material was cast by pouring 3ml of polymer (diluted 1:1 in DMAC) solution into a 10cm diameter glass dish and leaving for 18 hours in a circulating air oven at 55-65°C. Following casting graft material was thoroughly washed with phosphate buffered saline (PBS) prior to use.

2.2.2. Endothelial cell culture

HUVEC were isolated from human umbilical cord vein following a previously described method (Seifalian *et al.*, 2001). Cell numbers were amplified by tissue culture in Cell Culture Medium (CCM) which was prepared as follows: 157 ml M199 medium, 4.5 ml Sodium Bicarbonate (7.5%), 1.5 ml Penicillin/Streptomycin (10,000 U/ml and 10 mg/ml respectively), 40 ml Fetal Bovine Serum and 3.6 ml 200 mM L-Glutamine (Invitrogen Ltd, Paisley, U.K.). At confluence cells were removed using 0.25% Trypsin-EDTA (Sigma-

Aldrich Company Ltd, Poole, U.K.) and split in a 1:2 ratio. Confluent cultures at passage three were used in all experiments.

2.2.3 Assessment of Cytocompatibility

2.2.3.1 Indirect effect of nanocomposite on HUVEC

A sample of the nanocomposite was powdered using a Mikro Dismembartor U (B. Braun Biotech International, Melsungen, Germany). Following powdering nanocomposite samples were sterilised by autoclaving. Powdered nanocomposite was then added at concentrations of 1, 10 and 100mg/ml to CCM and shaken for seven days at 37°C on a shaker. Following exposure to powdered nanocomposite the treated CCM samples were centrifuged to remove the powdered nanocomposite.

24-well plates were seeded with 1ml HUVEC at a concentration of 2×10^5 cells/ml for 24 hours. Cells were then exposed to the following treatments: Untreated CCM (CCM_0), 1mg/ml treated CCM (CCM_1), 10mg/ml treated CCM (CCM_{10}), 100mg/ml treated CCM (CCM_{100}) and, in order to show the efficiency of the assays used, 1µM Staurosporine (CCM_{ST}) which is a potent inhibitor of phospholipids/calcium-dependant protein kinase and causes cell death. LDH, AB and Pico Green assays were carried out 24 and 96 hours post-exposure.

2.2.3.2 Direct effect of nanocomposite on HUVEC

Sections of nanocomposite material were cut into 16mm diameter discs and autoclaved to sterilise them. The discs were then placed into a 24-well plate (Helena Biosciences, Sunderland, U.K). Twelve nanocomposite discs were seeded with 1ml HUVEC at a

concentration of $2x10^5$ cells/ml for 24 hours (nanocomposite-seeded). Twelve wells containing discs of nanocomposite were left unseeded with only CCM in them as a control (nanocomposite-unseeded). LDH, AB and Pico Green assays were carried out 24 and 96 hours post-seeding and samples of nanocomposite sent for SEM studies.

2.2.3.3 Assessment of cell proliferation on nanocomposite

Thin films of nanocomposite were cast in 60mm x 120mm glass Petri dishes and sterilized by autoclaving. 2×10^5 HUVEC were then seeded in six dishes with a further six being left unseeded as a control. As a comparison, uncoated dishes were seeded with the same number of cells. At 1, 3, 6, 10, 13 and 16 days post-seeding a 4-hour AB assay was carried out on all samples.

2.2.4. Lactate dehydrogenase assay to assess cell damage on nanocomposite

LDH was measured using a CytoTox 96® Non-Radioactive Cytotoxicty assay kit (Promega, Southampton, U.K.). LDH is a stable cytosolic enzyme released upon cell lysis into the CCM. The amount of LDH released is measured using a 30-minute coupled enzymatic assay based on the conversion of a tetrazolium salt INT (2-p-iodophenyl-3-p-nitrophenyl-5-phenyl tetrazolium chloride) into a red formazin product, with the amount of colour formed being proportional to the number of lysed cells.

50µl CCM from each sample was transferred to a 96-well plate (Helena Biosciences, Sunderland, U.K). 50µl Substrate Mix (1 vial substrate plus 12mls assay buffer) was added to each well and the plate covered in foil to prevent light access. Samples were then incubated at room temperature for 30 minutes after which the reaction was stopped by the addition of 50µl

stop solution (1M acetic acid). Absorbance was then read at 450nm using a Multiscan MS UV visible spectrophotometer (Labsystems, Ashford, U.K.).

2.2.5. Alamar blue^{TM} assay to assess cell viability and metabolism on nanocomposite

AB (Serotec, Kidlington, U.K.) is a commercially available assay which aims to measure quantitatively cell proliferation, cytotoxicity and viability. This is achieved by incorporating resazurin and resarfurin as colourimetric oxidation reduction indicators. These indicators respond to chemical reduction resulting from cell metabolism by changing colour. This colour change may be measured by monitoring absorbance at 570 and 630 nm. The advantages of this assay are that it is soluble in media, stable in solution, minimally toxic to cells and produces changes that are easily monitored (Seifalian *et al.*, 2001).

AB was added to CCM at a concentration of 10% (v/v). At each AB assay timepoint grafts/wells were washed with 1 ml PBS and 1 ml of the AB/CCM mixture added to each graft/well. 1 ml AB/CCM mixture was placed into each of 6 empty wells as a negative control. After 4 hours' a 100μl sample of the AB/CCM mixture was removed and the absorbance at 570 nm and 630 nm measured in a 96-well plate (Helena Biosciences, Sunderland, U.K.) using a Multiscan MS UV visible spectrophotometer (Labsystems, Ashford, U.K.). The absorbance at 630 nm (background) was subtracted from that at 570 nm.

2.2.6 Pico green assay to assess cell quantity on nanocomposite

The Pico green assay (Molecular Probes Europe BV, Leiden, The Netherlands) quantifies double stranded DNA in solution using an ultrasensitive fluorescent nucleic acid stain. Stock

standard DNA solution (100µg/ml) was diluted in tris-EDTA (TE) assay buffer to provide a standard curve of 0 to 1000ng/ml DNA. Cell samples were trypsinised as above and the cell disrupted by being passed through a small-bore needle three times. 100µl of standard/sample was added to a 96-well plate and 100µl of diluted Pico Green (Pico Green Dimethylsulfoxide stock solution diluted x200 in TE assay buffer) was added to each standard/sample well. Plates were then incubated for 5 minutes in the dark. Standards/samples were then excited at 480nm and the flouresence emission intensity measured at 520nm using a Fluroskan Ascent FL spectrofluorometer (Thermo Life Sciences, Basingstoke, U.K.).

2.2.7 Assessment of cell morphology on nanocomposite

2.2.7.1 Toluidine blue staining

Cells were washed with PBS and then fixed in formaldehyde for 10 minutes at room temperature. 500µl of an 0.1% solution of Toluidine blue in distilled H_2O (Sigma Chemical Company, Poole, Dorset, U.K.) was then added to each well and incubated for 30 minutes at room temperature. Cells were then destained in water and photographed.

2.2.7.2 Scanning Electron Microscopy

Sections of unseeded nanocomposite and nanocomposite seeded with HUVEC were washed 3 times with PBS and prepared for SEM. The specimens were then attached to aluminium stubs and an SC500 (EM Scope) sputter coater used to coat them with gold. The stubs were then examined and photographed using a Phillips 501 SEM.

2.2.8. Data analysis and statistical methods

Data are presented in mean±SD. Comparison between groups was made by One Way ANOVA (Kruskal-Wallis) test with post comparison using Bonferroni's Multiple Comparison test. *indicates $P < 0.05$ and *** that $P < 0.001$.

2.3. Results

2.3.1. Indirect effect of nanocomposite on HUVEC

2.3.1.1. Lactate dehydrogenase assay

After 24 hours' indirect exposure there was no significant difference ($P > 0.05$) between the CCM_0 group and any of the nanocomposite treated CCM groups. Cells treated with CCM_{ST} had a significantly higher level of LDH activity compared to the CCM_0 group ($p < 0.001$) (Fig. 2.1a).
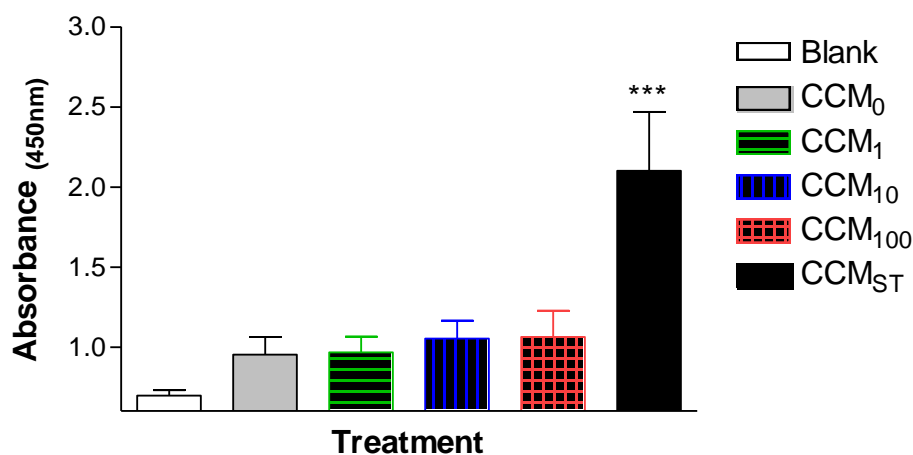
Fig. 2.1a. LDH assay test on HUVEC exposed to nanocomposite-treated CCM for 24 hours. Absorbance was measured in arbitrary units at 450nm wavelength. Data are mean ± SD(n=6).

2.3.1.2. Alamar blue^{TM} assay

Indirect exposure to nanocomposite for 24 hours showed no significant difference between the CCM_0 group and the three nanocomposite-treated CCM groups. The cells treated with CCM_{ST} showed significantly less AB activity than the CCM_0 group (p<0.001) (Fig. 2.1b). In the case of the indirectly exposed 96 hour cells there was no significant difference in AB activity between the CCM_0 cells and the CCM_1 or CCM_{10} groups, however there was a significant reduction in AB activity in the case of the CCM_{100} sample (p<0.05). After 96 hours exposure to CCM_{ST} no viable cells were present (Fig. 2.1c).
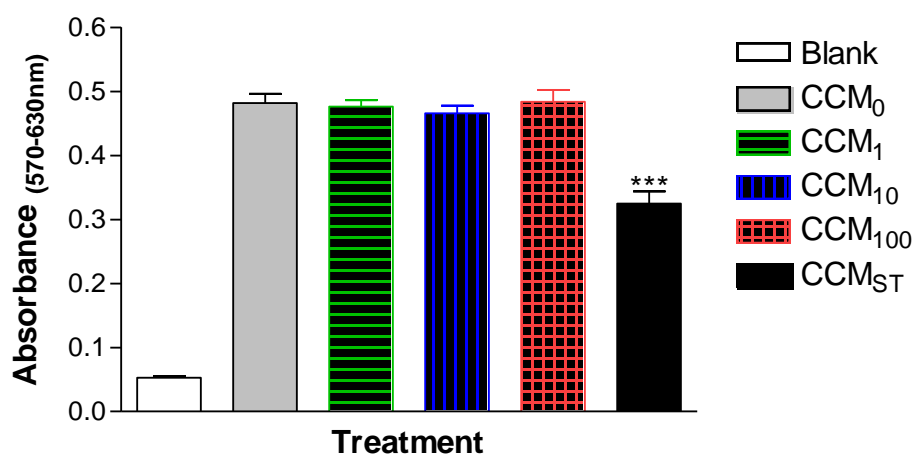
Fig. 2.1b. Alamar blue^{TM} viability assay test on HUVEC exposed to nanocomposite-treated CCM for 24hours. Absorbance was measured in arbitrary units at 570nm wavelength and background at 630nm subtracted. Data are mean ± SD(n=6).
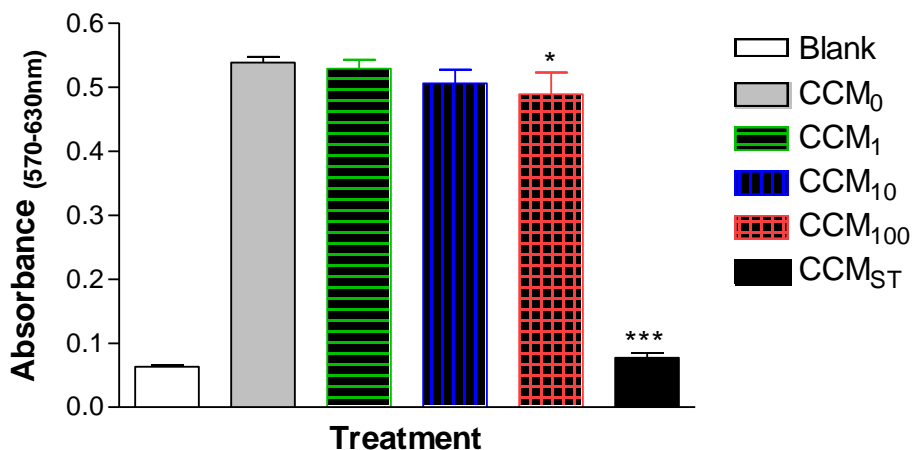
Fig. 2.1c. Alamar blue^{TM} viability assay test on HUVEC exposed to nanocomposite-treated CCM for 96 hours. Absorbance was measured in arbitrary units at 570nm wavelength and background at 630nm subtracted. Data are mean $\pm$ SD(n=6).

2.3.1.3. Pico Green assay

After 24 hours' indirect exposure to nanocomposite treated CCM between 780.1$\pm$55.3 and 916.9$\pm$38.0 µg/ml DNA was extracted, with no significant difference being observed between the CCM_0 cells and any of the test groups (Fig. 2.1d). In the case of the 96hr indirect exposure experiment again there was no significant difference between the CCM_0 cells and the three different concentrations of nanocomposite-treated medium exposed cells. However, there was significantly less DNA in the staurosporine exposed group (Fig. 2.1e).
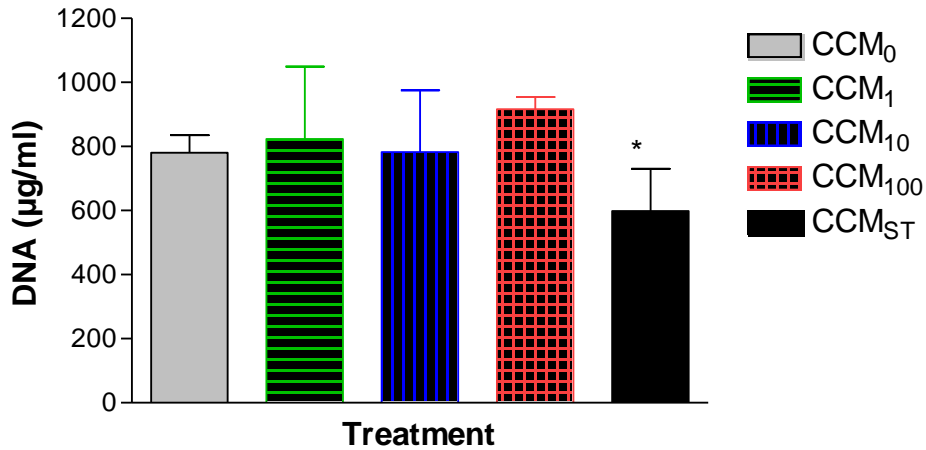
Fig. 2.1d. Pico Green assay test on HUVEC exposed to nanocomposite-treated CCM for 24 hours. Data is presented as DNA amount in µg/ml. Data are mean ± SD(n=5).
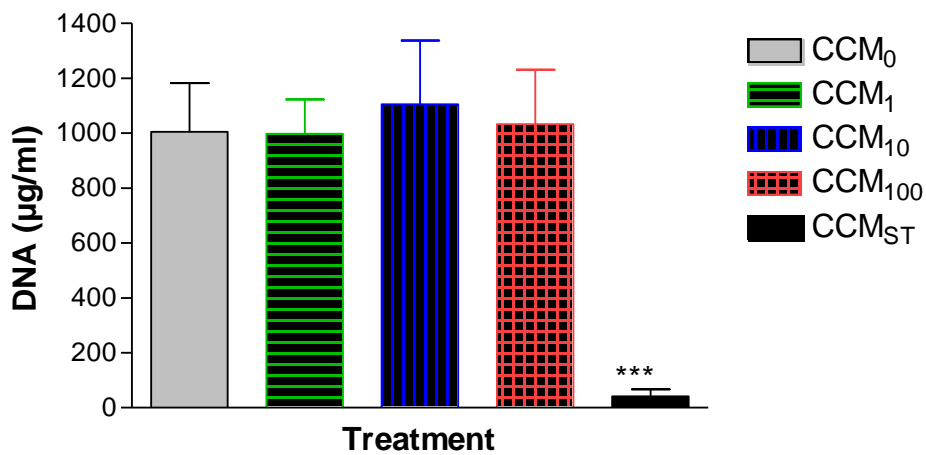
Fig. 2.1e. Pico Green assay test on HUVEC exposed to nanocomposite-treated CCM for 96 hours. Data is presented as DNA amount in µg/ml. Data are mean ± SD(n=5).

2.3.1.4. Toluidine Blue staining

The results from the Toluidine Blue staining can be seen in Fig. 2.2. It can be seen that at both 24 and 96 hours post exposure to CCM_{100} cell appearance and numbers are comparable

to cells exposed to untreated CCM (Fig. 2.2a, 2.2b, 2.2d and 2.2e). However, exposure to CCM$_{ST}$ clearly results in cell damage at both time points (Fig. 2.2c and 2.2f).
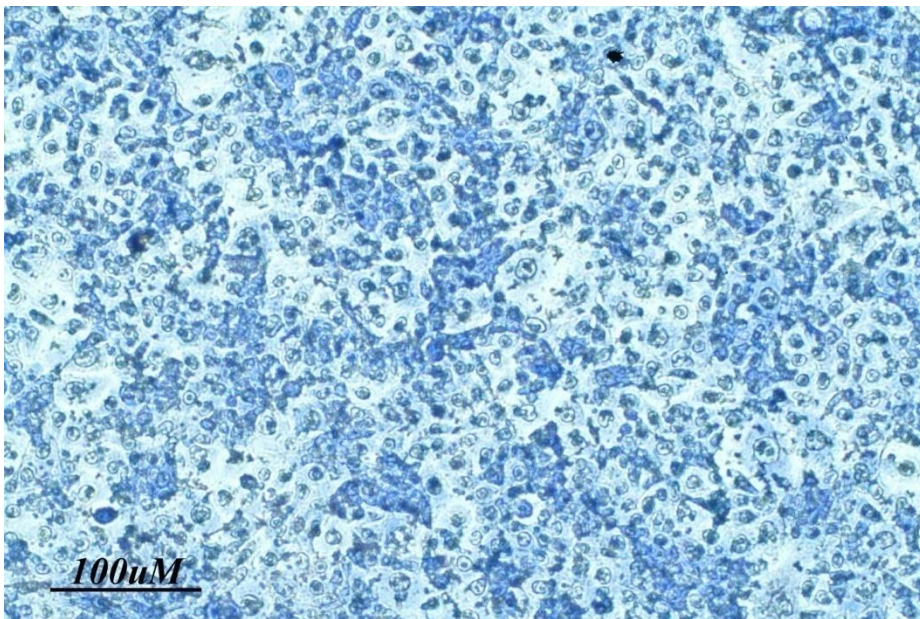
Fig 2.2a. Toluidine Blue staining of HUVEC exposed to 24 hours nanocomposite-treated CCM$_0$ (Magnification X20).
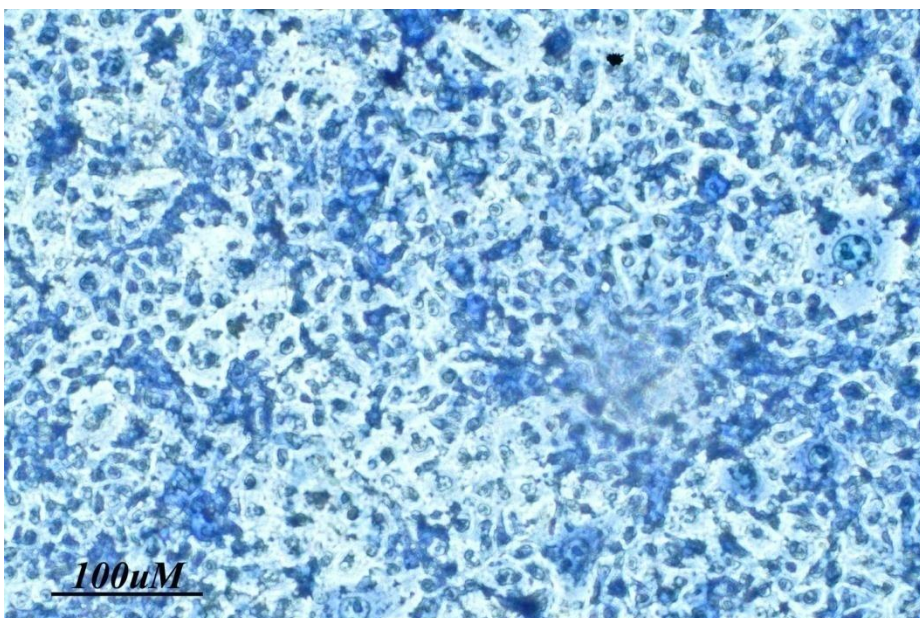
Fig 2.2b. Toluidine Blue staining of HUVEC exposed to 24 hours nanocomposite-treated CCM$_{100}$ (Magnification X20).
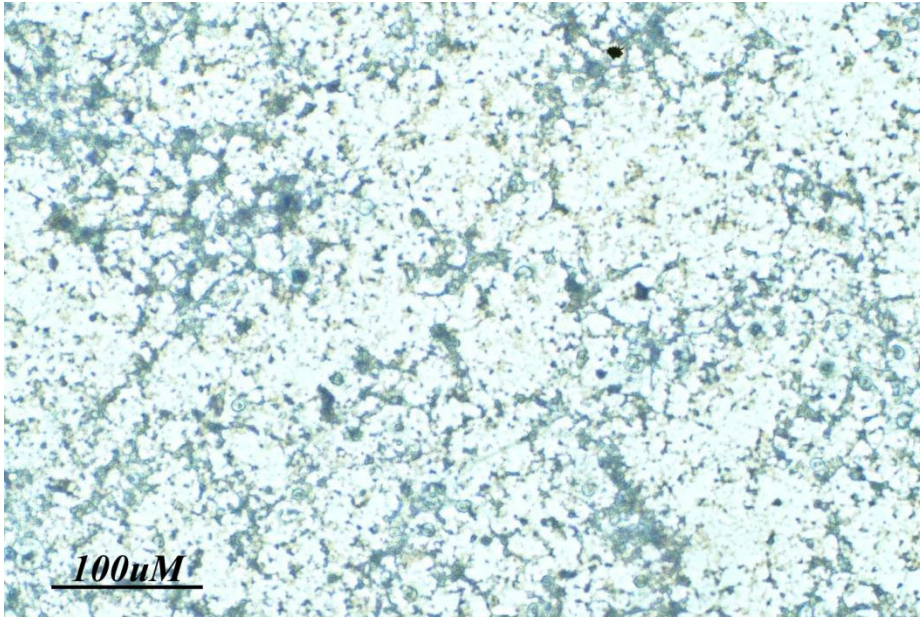
Fig 2.2c Toluidine Blue staining of HUVEC exposed to 24 hours nanocomposite-treated

CCM_{ST} (Magnification X20).
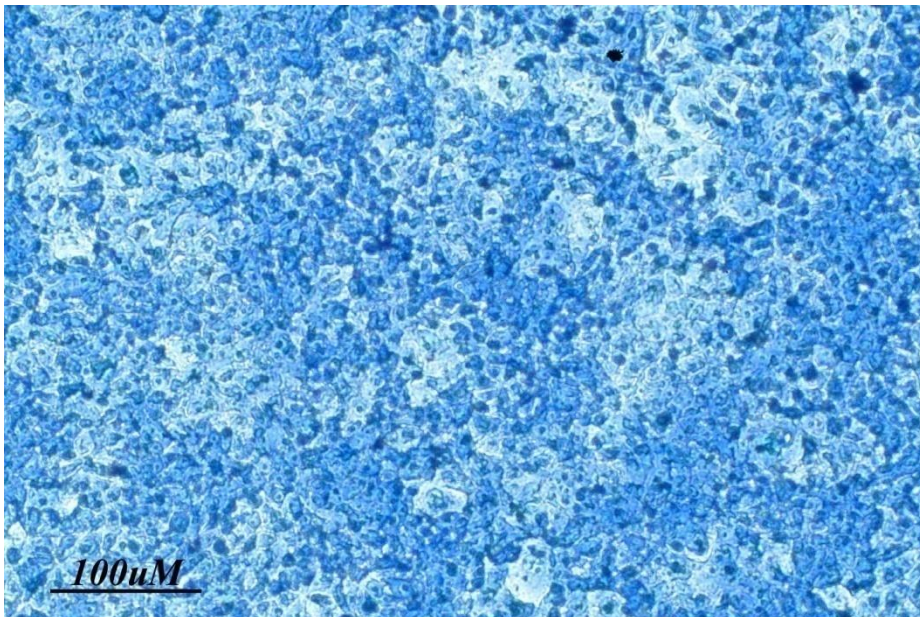
Fig 2.2d. Toluidine Blue staining of HUVEC exposed to 96 hours nanocomposite-treated
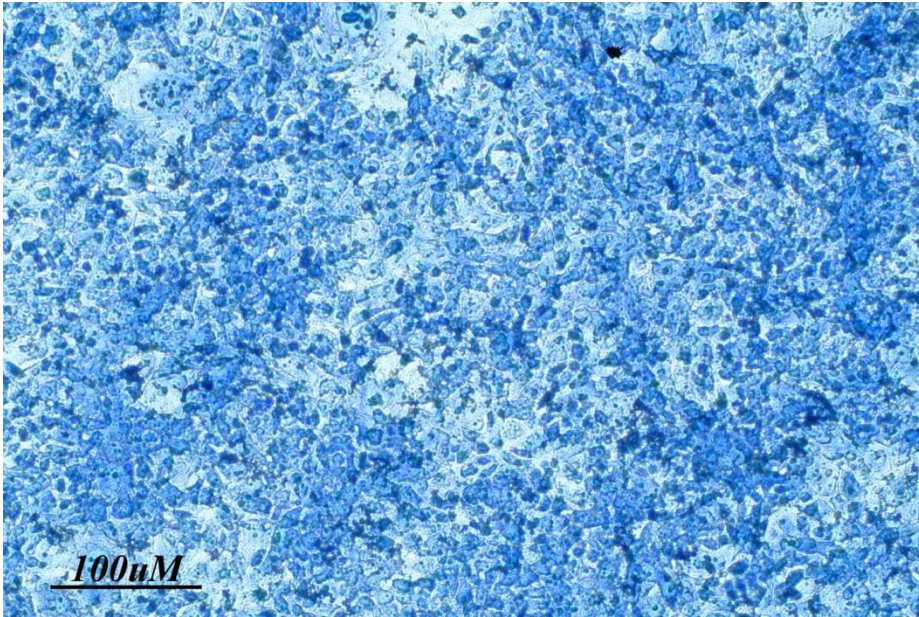
CCM_0 (Magnification X20).

Fig 2.2e. Toluidine Blue staining of HUVEC exposed to 24 hours nanocomposite-treated CCM$_{100}$ (Magnification X20).
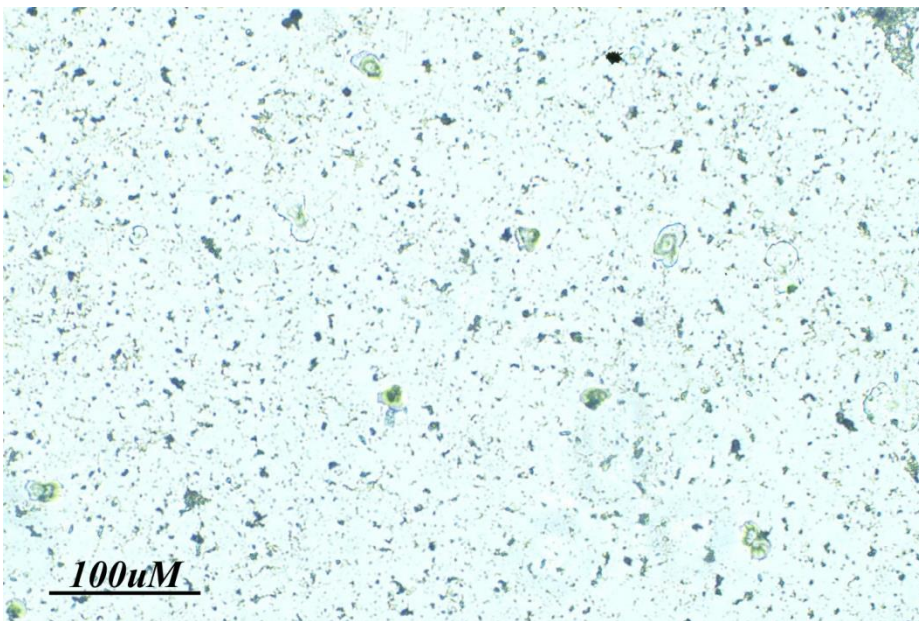
Fig 2.2f. Toluidine Blue staining of HUVEC exposed to 24 hours nanocomposite-treated CCM$_{ST}$(Magnification X20).

2.3.2. Direct effect of nanocomposite on HUVEC

2.3.2.1. Lactate dehydrogenase assay

After 24 hours direct exposure a significantly higher level (p<0.001) of LDH activity was found from the nanocomposite-seeded group compared to the CCM_0 group (Fig. 2.3a).
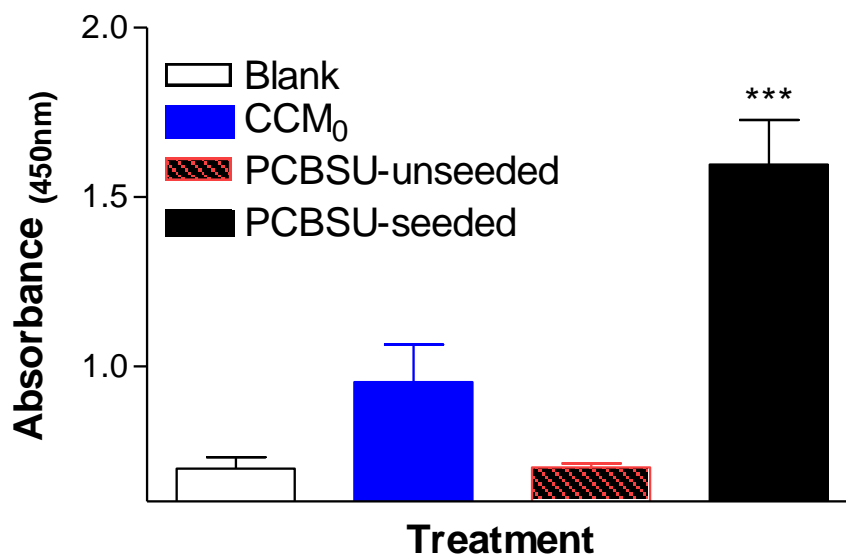
Fig.2.3a. LDH assay test on HUVEC seeded directly onto nanocomposite for 24 hours. Absorbance was measured in arbitrary units at 450nm wavelength. Data are mean ± SD(n=6).

2.3.2.2. Alamar blue^TM assay

Direct exposure to nanocomposite for 24 hours showed viable cells present, though at a lower level of AB activity compared to the CCM_0 group (p<0.001) (Fig. 2.3b). After 96 hours direct exposure viable cells were still present on the PCBSU-seeded, again at a lower level compared to the CCM_0 cells (p<0.001) (Fig. 2.3c).
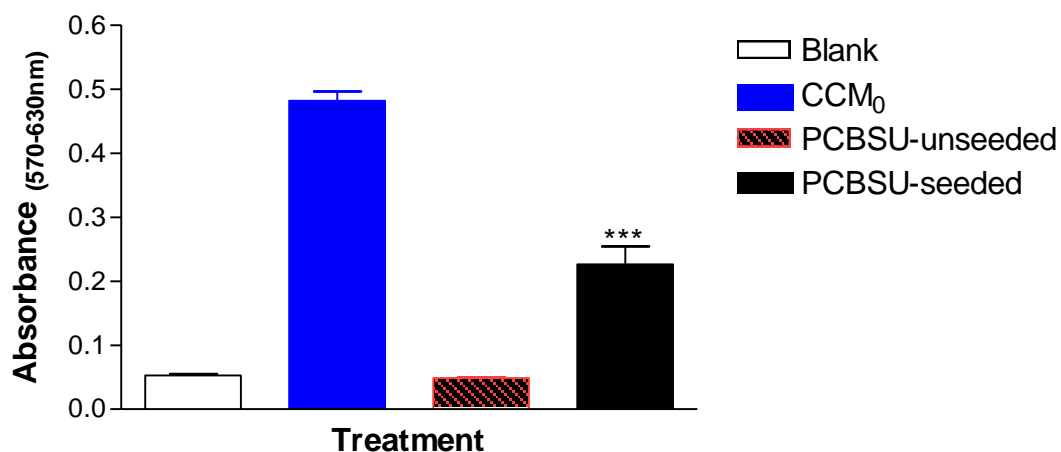
Fig. 2.3b. Alamar blue^{TM} viability assay test on HUVEC seeded directly onto nanocomposite for 24 hours. Absorbance was measured in arbitrary units at 570nm wavelength and background at 630nm subtracted. Data are mean $\pm$ SD(n=6).
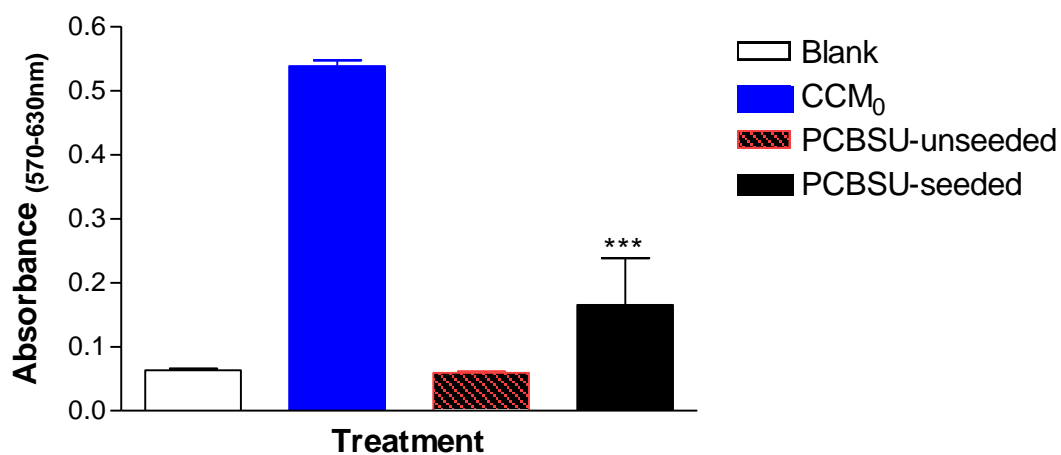
Fig. 2.3c. Alamar blue^{TM} viability assay test on HUVEC seeded directly onto nanocomposite for 96 hours. Absorbance was measured in arbitrary units at 570nm wavelength and background at 630nm subtracted. Data are mean $\pm$ SD(n=6).

2.3.2.3. Pico green assay

24 hours direct exposure to nanocomposite resulted in the presence of 417.3±50.4 µg/ml DNA. After 96 hours direct exposure 323.6±232.9 µg/ml of DNA was extracted from the graft samples.

2.3.2.4. SEM studies

SEM studies showed that the surface of the nanocomposite graft material was uniform and demonstrated that EC were present on the graft material at both 24 and 96 hours post-seeding (Fig. 2.4).
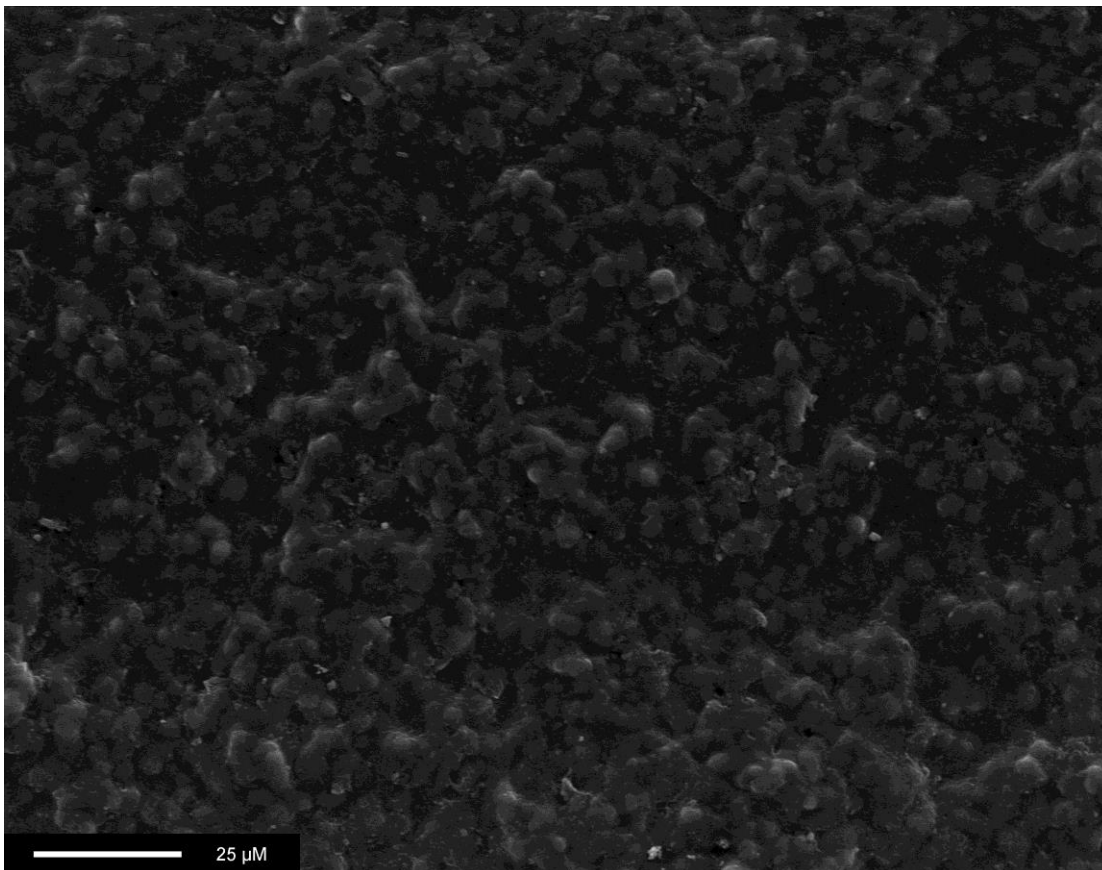
Fig. 2.4a: Unseeded nanocomposite 24 hours(Magnification x640).
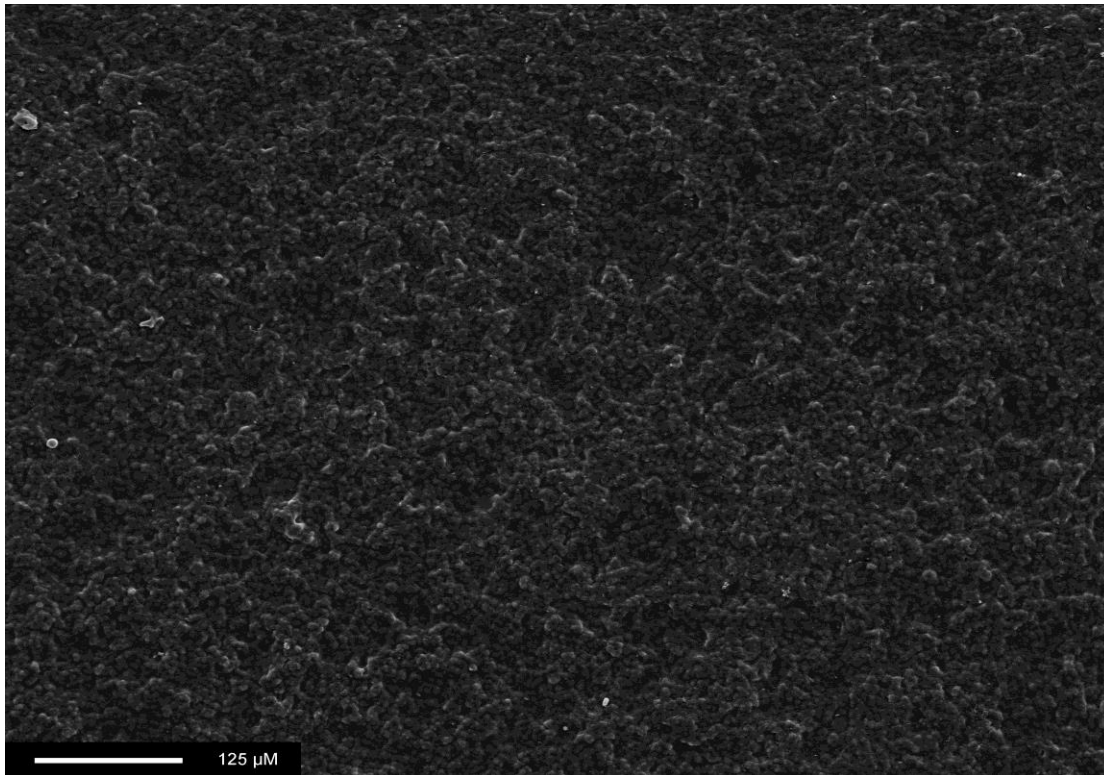
Fig. 2.4b: Unseeded nanocomposite 96 hours(Magnification x 160)
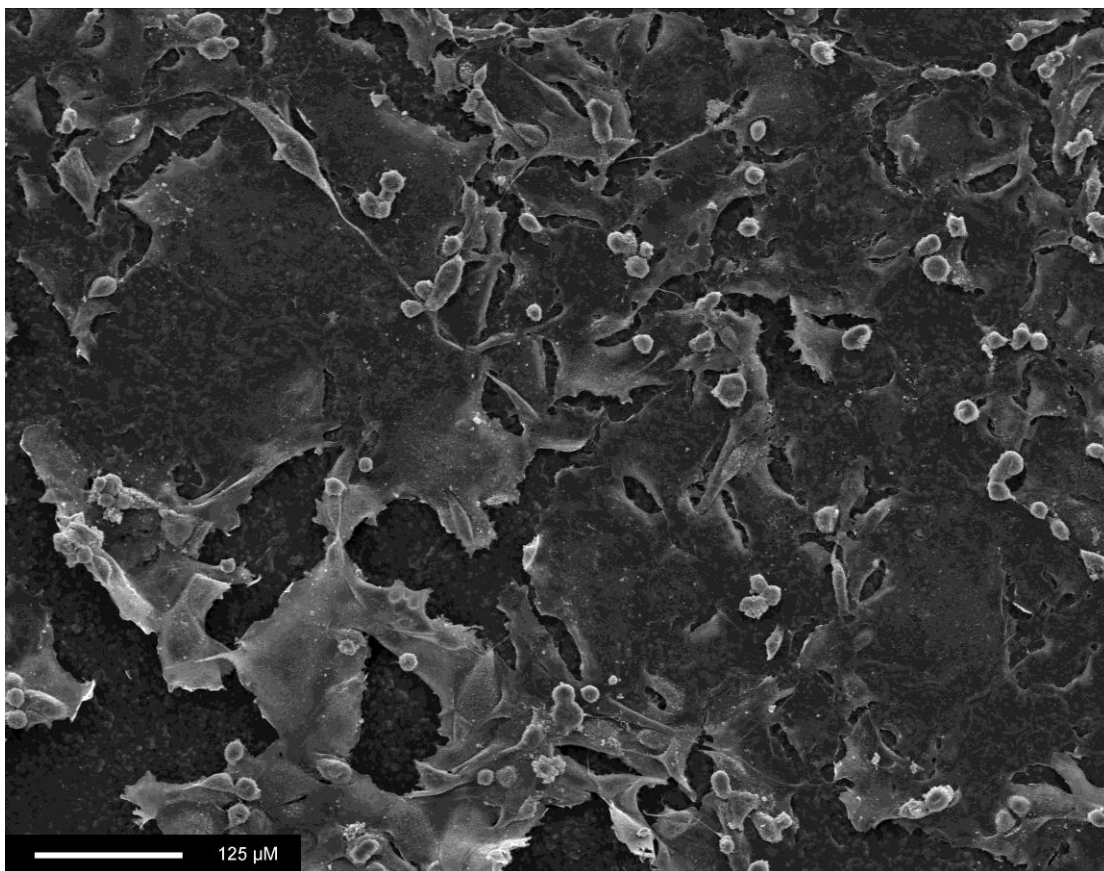
Fig. 2.4c: HUVEC seeded nanocomposite 24 hours(Magnification x 160).
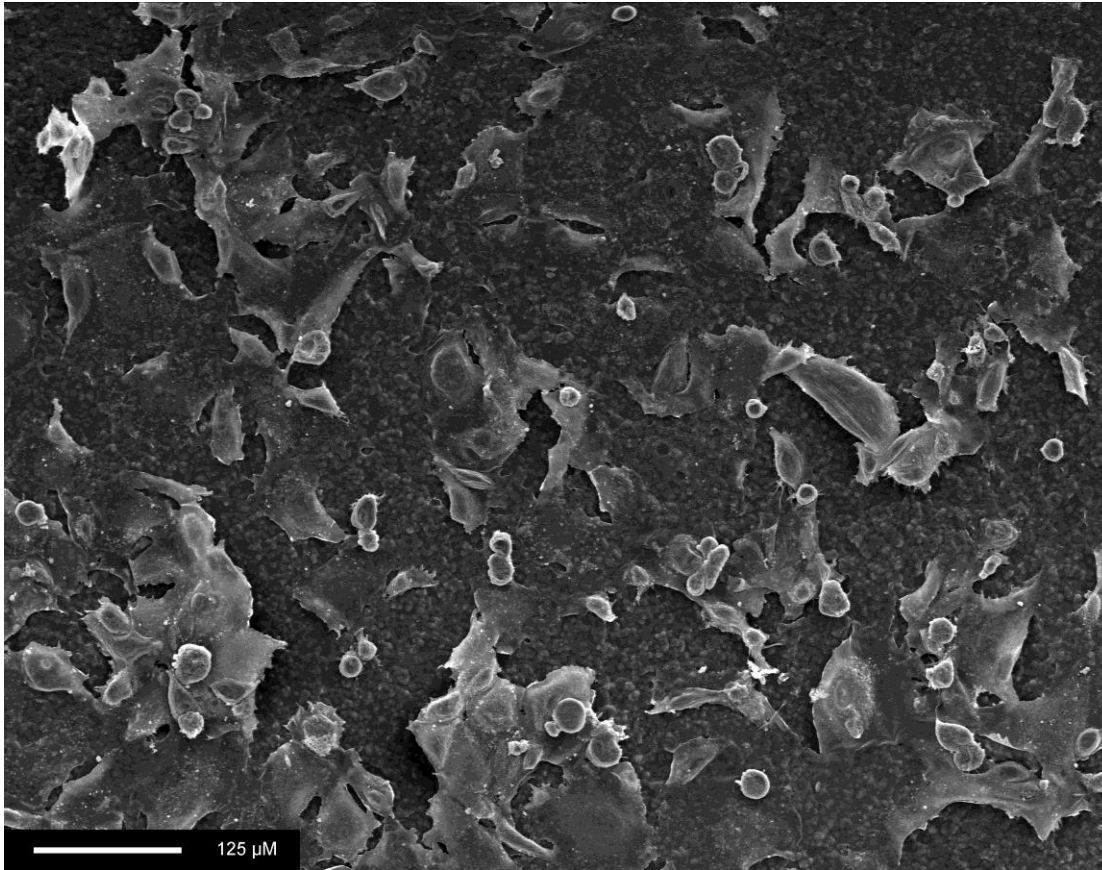
Fig 2.4d: HUVEC seeded nanocomposite 96 hours(Magnification x160)

2.3.3. Assessment of cell proliferation on nanocomposite

Fig. 2.5 shows the results from the proliferation study. It can be seen that the HUVEC exhibit a typical growth curve on both nanocomposite and glass, with confluence being reached at day 10. Again, the AB results are lower for the cells seeded on nanocomposite compared to those seeded on glass.
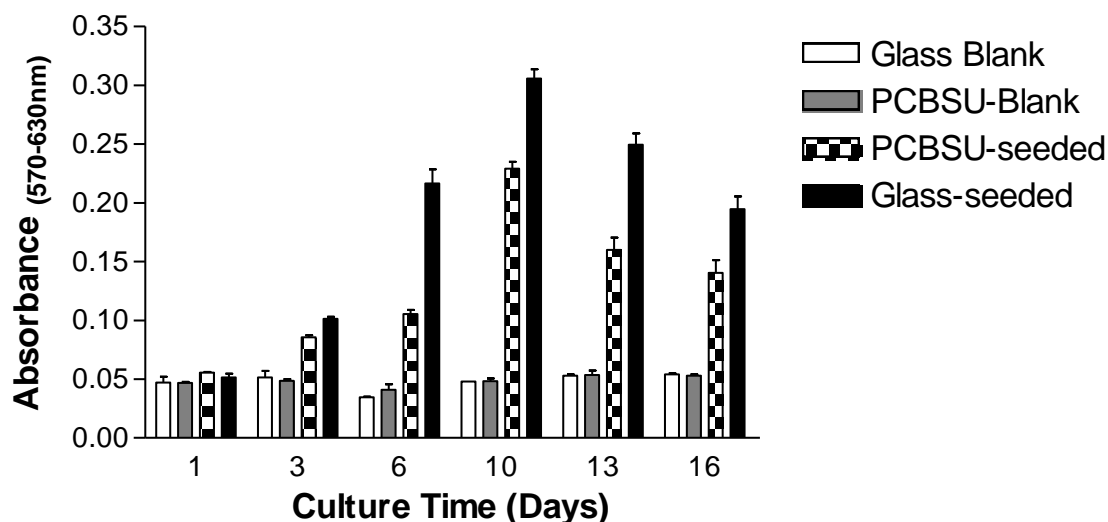
Fig.2. 5. Alamar blue^{TM} viability assay test on HUVEC seeded directly onto nanocomposite for 16 days. Absorbance was measured in arbitrary units at 570nm wavelength and background at 630nm subtracted. Data are mean ± SD(n=6).

2.4. Discussion

A greater understanding of the importance and need to improve the surface thrombogenicity of biomaterials has become a vital field of research. Studies in tissue engineering have demonstrated that silicon and its analogues (for example oxides) can have the effect of reducing both protein adsorption and platelet adhesion (Zhang *et al.*, 2001). It has been suggested that this reduction is related to the surface charge on the material (Nylander *et al.*, 2001; Amaral *et al.*, 2002) which can result in structural changes to blood proteins (Xu *et al.*, 2003; Buijs *et al.*, 2003) with fibrinogen (Lasseter *et al.*, 2004) being one example. One property of silicon is that it is very un-reactive and as a result research has been focused on moieties such as siloxane, in particular poly(dimethysiloxane) (PDMS) either by itself or in conjunction with either rubbers or polyurethanes (Chen *et al.*, 2002; Prokopowicz *et al.*, 2003; Cunningham *et al.*, 2002). However, PDMS by itself or combined with rubbers

is mechanically very weak and as a result is generally unsuitable for use in biomedical devices. Therefore, a number of different methodologies have been investigated with the aim of combining it with a polyurethane. The outcomes *in vivo* have not been good as a result of the dramatic losses in bio-stability caused by the non-reaction of PDMS with either the soft or hard segments of the polyurethane resulting in a tendency to form two separate polymers (Martin *et al.*, 2000; Park *et al.*, 1999). Silicon and siloxane based materials have also been demonstrated to have poor growth characteristics when seeded with human cells such as EC's (Peters *et al.*, 2004) resulting in an inability to seed a prospective biomedical device based on these materials.

There is still therefore a requirement for a polyurethane containing silicon which would be mechanically strong, able to demonstrate bio-stability and also possesses the advantageous properties of reduced protein and platelet adsorption. This material should also permit the seeding and growth of cells such as EC without deleterious cytotoxic effects.

The material used in this investigation, a polyurethane containing silsesquioxane, was developed for its potential to become an inorganic-polymer which would possess all the required properties described above (Duchateau *et al.*, 2004).

In the clinical scenario, the choice of a material to be used for cardiovascular prostheses must incorporate cytocompatibility to EC in two areas; indirect and direct contact of EC with the material. In this study in the case of indirect contact an initial exposure for 24 hours to CCM treated with powdered nanocomposite produced no significant effect on either cell metabolism or cell numbers compared to the CCM_0 as shown by the results of the AB and PG assays. The use of Staurosporine as a positive control proves the principle that these assays are capable of demonstrating cell damage and further suggests that the toxicity of the

nanocomposite is low. A longer 96-hour exposure again produced no significant change in cell numbers though metabolism was reduced significantly in the case of the CCM_{100} group. In contrast by 96 hours' post-exposure the CCM_{ST} group showed no cell metabolism and extremely low cell numbers. This indicated that toxicity by nanocomposite on EC was not apparent other than mildly at CCM_{100}.

24 hours post-seeding of EC onto nanocomposite showed the presence of viable EC from the Pico Green DNA analysis results and SEM analysis and that the cells were metabolising. Whilst both the cell numbers and metabolism were significantly less than for the CCM_0 cell group this may be due to improved seeding and attachment on TCP (which is optimal for cell attachment and growth) compared to nanocomposite and is similar to the results obtained in previous studies on ePTFE and compliant polyurethane (CPU) (Seifalian *et al.*, 2001). There was a significantly increased level of LDH activity compared to the CCM_0 cells suggesting that seeding efficiency on nanocomposite was lower than on TCP or glass or that initial cell damage had occurred. Extended 96-hour direct exposure showed similar results to the 24-hour period and again demonstrated the presence of viable cells on the material. The cell proliferation study showed that HUVEC can be maintained on nanocomposite for an extended period (16 days) and that the growth pattern is similar to that for HUVEC grown on a glass surface.

2.5. Conclusion

In conclusion, it can be said that the results presented in this chapter demonstrate that indirect exposure to nanocomposite does not result in serious damage to EC at concentrations likely to be encountered in a clinical situation. Furthermore, the nanocomposite can be

successfully seeded with EC and, once seeded, the EC remain viable and proliferate for a period of days. This combined with its other advantages suggests that the nanocomposite is suitable for further development in cardiovascular devices.

3

3 Ultra violet Surface Modification of Nanocomposite

3.1 Introduction

In clinical usage at present the vast majority of medical devices such as bypass grafts and stents are manufactured from two polymers, either polytetrafluroethylene (PTFE) or poly(ethylene terephthalate) (PET or Dacron) (Seifalian *et al.*, 2002). Dacron has a long history of clinical employment, being first used as a vascular graft in 1957 (Hess, 1985) but is highly reactive both to blood and the surrounding tissues producing inflammation and neo-intimal proliferation in both grafts (Zenni *et al.*, 1994; Greisler *et al.*, 1996b) and stents (Peng *et al.*, 1996; Murphy *et al.*, 1992). PTFE was first introduced in the 1960's for use as artificial heart valves and, due to its properties such as biostability and tolerance in the body, has been extensively used since then and indeed is still the most popular choice for bypass grafts today. However, the long-term patency of PTFE, especially in small diameter grafts, is poor

and there is a high adherence of platelets and blood proteins to the surface (Kannan *et al.*, 2005a).

A variety of different types of polymer have been studied as alternatives to PTFE and Dacron in an attempt to develop an improved device (Xue and Greisler, 2003). Our group initially developed a poly(carbonate-urea)urethane in collaboration with an industrial partner which was demonstrated to be cytocompatible (Salacinski *et al.*, 2000; Tiwari *et al.*, 2002) and resistant to degredation (Salacinski *et al.*, 2002b; Salacinski *et al.*, 2002a; Seifalian *et al.*, 2003). In order to further improve the anti-thrombogenicity of the material a number of nanocomposites based upon polyurethane and incorporating silsesquioxane (Kannan *et al.*, 2005b) were then developed. One uses bridged monomers of silsesquioxane (pendant nano-bridge); poly(carbonate-silsesquioxane-bridge-urea)urethane (PCBSU) nanocomposite. The cytocompatibility of the nanocomposite has been demonstrated in a previous study which showed that EC are not significantly damaged by indirect exposure to nanocomposite at concentrations likely to be encountered in a clinical situation (1 to 100μg/ml) and that cast nanocomposite films can be successfully seeded with EC which remain viable and proliferate for a period of days (Punshon *et al.*, 2005). Another is poly(carbonate-urea)urethane with silsequioxane nano-cages namely herein a mixture of two polyhedral oligomeric silsequioxanes. This nanocomposite has been demonstrated to be resistant to degradation.

The other major area of investigation in this field is the potential modification of the surface of the polymer to improve the biocompatibility of the material. One approach to this is to coat or incorporate a variety of moeties such as heparin or Arginine-Glycine-Aspartate (RGD) onto or into the polymer (Kidane *et al.*, 2003; Kidane *et al.*, 2004). A variety of chemical modfication techniques have also been investigated which have been believed to have potential in this area such as exposure of materials to plasmas (Tseng and Edelman,

1998), ion beams (Lee *et al.*, 2004), electrons (Lappan *et al.*, 1999), synchrotron and γ radiation (Sato *et al.*, 2003) or UV light (Heitz *et al.*, 2003). In general these methods rely upon creating new chemical groups on the polymer surface favouring cell adhesion. Previous studies have demonstrated that the biocompatibility of PTFE could be markedly improved by exposure of the polymer to UV-light at a wavelength of $\lambda < 200$ nm in a reactive NH_3 atmosphere (Heitz *et al.*, 2003; Heitz *et al.*, 2004; Mikulikova *et al.*, 2005).

This chapter examines the possibility of applying a UV-light based surface modification technique previously shown to be successful to the nanocomposite with the aim of demonstrating successful surface modification and improving cell attachment and proliferation on the nanocomposite surface.

3.2 Materials and methods

3.2.1 Nanocomposite synthesis and graft preparation

Polycarbonate polyol and trans-cyclohexanediolisobutyl-silsesquioxane (Figure 2.1) were placed in a reaction flask equipped with stirrer and nitrogen. The mixture was heated to dissolve the nanocage. To this, methylene di-isocyanate (MDI) was added and then reacted at 70 ºC for 90 minutes to form a pre-polymer. Then DMAC was added. Chain extension of the pre-polymer was carried out by the addition of ethylenediamine and diethylamine in DMAC. 1-butanol in DMAC was added to the mixture to form a 2% polyhedral oligomeric silsesqioxane-poly (carbonate-urea) urethane solution. All chemicals and reagents were purchased from Aldrich Limited, Gillingham, UK.

3.2.2 Nanocomposite Preparation

Nanocomposite foils with a thickness of approximately 10 µm were cast from a DMAC solution. 1.5 g of the nanocomposite was dissolved in 12 g of DMAC. 10.25 g of this solution was poured into a metal mould (10 x 10 x 0.5 cm) and the nanocomposite solidified in a polymer drying oven at 51°C for 30 hours. In all subsequent discussions, the polymer will be addressed as nanocomposite to avoid confusion once it is diluted for casting.
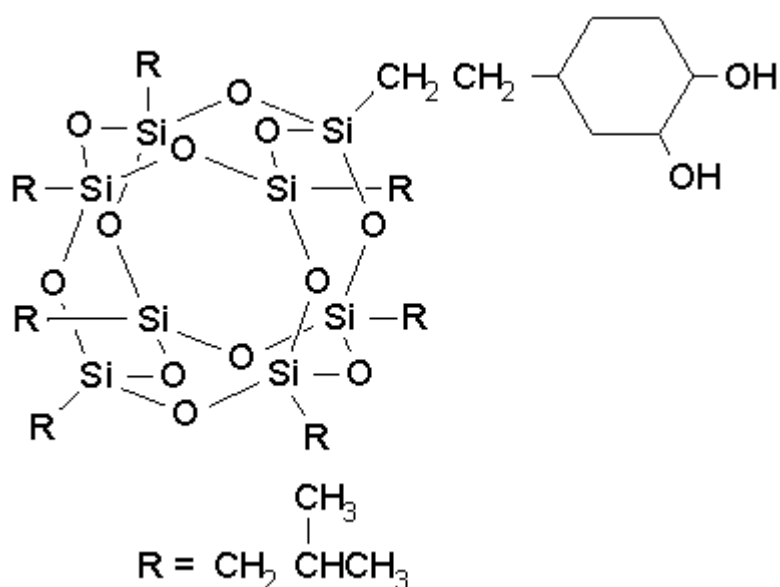
Figure 3.1 Structure of nanocomposite

3.2.3 UV-modification of the nanocomposite

The foils were irradiated by means of a Xe_2^*-excimer lamp (Heraeus-Noblelight, Hanau, Germany) for times of between 30 seconds and 30 minutes. The lamp was emitting quasi-continuously with a centre wavelength of 172 nm, a spectral bandwidth of approximately 16 nm and an intensity of approximately 17 mW/cm^2. The samples were flushed with a moderate flow of NH_3 at a total pressure of 5 mbar. The NH_3 gas employed during irradiation had a purity of 99.995%. (Linde, Höllriegelskreuth, Germany). The

distance between the sample surface and the chamber window was 5 mm. The time intervals between surface modification and the biological experiments were between 1 and 9 weeks. Between modification and biological experiments, the samples were stored covered by aluminium foils under atmospheric conditions without special provisions. Investigations involved untreated and 30 second, 5 minute, 10 minute, 15 minute and 30 minutes' surface modified nanocomposite foils. Prior to cell seeding nanocomposite films were cut into discs to fit 24-well plates and sterilized by autoclaving.

3.2.4 Nanocomposite characterisation methods

The sample morphology was investigated by contact mode atomic force microscopy (AFM) in air (Resolver, Quesant Instrument, Agoura Hills, CA) and by SEM (JSM-6400 Scanning Microscope, Joel, Tokyo, Japan). Measurements of advancing water contact angle were performed according to a standard procedure (Adamson and Gast, 1997). In brief, a small drop of de-ionised water (volume about 10 µl) was put onto the flat sample surfaces using a syringe in such a way that the drop volume at the surface expands. The resulting advancing contact angle was evaluated by optical methods using a digital camera. The measurements were performed in an air-conditioned laboratory at 22° C. For each sample the measurement was repeated 12 times. The chemical composition of the surface of nanocomposite samples was investigated by means of X-ray induced photo-electron spectroscopy (XPS) employing the monochromatic Al K□ line (Axis 165, Kratos Analytical, Manchester, UK). The typical analysed depth was about 7 nm and the analysed area 0.3 x 0.7 mm. Attenuated total reflection – fourier transformed infrared spectroscopy (ATR-FTIR) was employed to analyse infrared active bonds in the surface of the samples. In this case an FTIR spectrometer (Equinox, Bruker, Karlsruhe, Germany) with a single reflection attenuated total

reflectance (ATR) diamond system (Golden Gate, Specac, Orpington, UK) was employed. The analytical depth of this methodology depends on the refractive index of the material under investigation and the position in the spectrum. For a typical nanocomposite we estimated a penetration depth of 0.2 µm at 7500 cm^{-1} and 4.6 µm at 370 cm^{-1}, respectively. A spectra library (Mentor Pro, Biorad, Hercules, CA) together with an heuristic approach was used to identify the peaks and the corresponding bond vibrations.

3.2.5 Cell Seeding of nanocomposite foils

Experiments for evaluation of cell adhesion and proliferation were performed using HUVEC at passage 3. HUVEC were isolated from human umbilical cord vein following a previously described method (Jaffe *et al.*, 1973). Cell numbers were amplified by tissue culture in Cell Culture Medium (CCM) which was prepared as follows: 157 ml M199 medium, 4.5 ml Sodium Bicarbonate (7.5%), 1.5 ml Penicillin/Streptomycin (10,000 U/ml and 10 mg/ml respectively), 40 ml Fetal Bovine Serum and 3.6 ml 200 mM L-Glutamine (Invitrogen Ltd, Paisley, U.K.). At confluence cells were removed using 0.25% Trypsin-EDTA (Sigma-Aldrich Company Ltd, Poole, U.K.) and split in a 1:2 ratio.

3.2.6 Determination of optimal seeding density

In order to determine the optimum seeding density for HUVEC unmodified nanocomposite foils (n=4) were placed in standard polystyrene 24-well tissue culture plates (Helena Biosciences, Sunderland, U.K.) and seeded with cells at a density of 0.5, 1.0, 2.0 and 4.0 x 10^5 cells/well in 0.5 ml culture medium for two hours. Following the two-hour seeding period seeding the cell culture medium was removed and frozen at -20°C for total DNA

analysis to assess the number of cells which did not attach and the seeded cells were extracted for total DNA analysis.

LDH was measured using a CytoTox 96® Non-Radioactive Cytotoxicty assay kit (Promega, Southampton, U.K.). LDH is a stable cytosolic enzyme released upon cell lysis into the cell culture medium. The amount of LDH released is measured using a 30-minute coupled enzymatic assay based on the conversion of a tetrazolium salt INT (2-p-iodophenyl-3-p-nitrophenyl-5-phenyl tetrazoliumchloride) into a red formazin product, with the amount of colour formed being proportional to the number of lysed cells.

50µl cell culture medium from each sample was transferred to a 96 well plate (Helena Biosciences, Sunderland, U.K). 50µl Substrate Mix was added to each well and the plate covered in foil to prevent light access. Samples were then incubated at room temperature for 30 minutes after which the reaction was stopped by the addition of 50µl stop solution (1M acetic acid). Absorbance was then read at 450nm using a Multiscan MS UV visible spectrophotometer (Labsystems, Ashford, U.K.).

The Pico green assay (Molecular Probes Europe BV, Leiden, The Netherlands) quantifies double stranded DNA in solution using an ultrasensitive fluorescent nucleic acid stain. Stock standard DNA solution (100µg/ml) was diluted in tris-EDTA (TE) assay buffer to provide a standard curve of 0 to 1000ng/ml DNA. Cell samples were trypsinised as above and the cell disrupted by being passed through a small-bore needle three times. 100µl of standard/sample was added to a 96 well plate and 100µl of diluted Pico Green (Pico Green Dimethylsulfoxide stock solution diluted x200 in TE assay buffer) was added to each standard/sample well. Plates were incubated for 5 minutes in the dark. Standards/samples were then excited at

480nm and the flouresence emission intensity measured at 520nm using a Fluroskan Ascent FL spectrofluorometer (Thermo Life Sciences, Basingstoke, U.K.).

3.2.7 Nanocomposite seeding to determine the effect of UV modification of nanocomposite

Untreated polymer foils and foils of 5 minute, 10 minute, 15 minute and 30 minutes irradiation times were placed in a 24-well untreated tissue culture plates (n=4). Foils were seeded with HUVEC at a concentration of 1×10^5 cells/well in 0.5ml cell culture medium for either 1 or 2 hours. Following seeding the medium was removed and used for LDH analysis. The initially seeded cells were initially examined by Alamar blue[TM] assay and again after 24, 48 and 72 hour's culture.

3.2.8 Assessment of cell viability and metabolism on UV modified nanocomposite

AB (Serotec, Kidlington, U.K.) is a commercially available assay which aims to measure quantitatively cell proliferation, cytotoxicity and viability. This is achieved by incorporating resazurin and resarfurin as colourimetric oxidation reduction indicators. These indicators respond to chemical reduction resulting from cell metabolism by changing colour. This colour change may be measured by monitoring absorbance at 450 nm. AB was added to cell culture medium (CCM) at a concentration of 10% (v/v). At each AB assay timepoint grafts/wells were washed with 1 ml PBS and 1 ml of the AB/CCM mixture added to each graft/well. 1 ml AB/CCM mixture was placed into each of 6 empty wells as a negative control. After 4 hours' a 100μl sample of the AB/CCM mixture was removed and the

absorbance at 450 nm measured in a 96-well plate (Helena Biosciences, Sunderland, U.K.) using a Multiscan MS UV visible spectrophotometer (Labsystems, Ashford, U.K.).

3.2.9 Statistical Evaluation

Data are presented in mean±SD. Comparison between groups was made by One Way ANOVA (Kruskal-Wallis) test with post comparison using Bonferroni's Multiple Comparison test. *indicates $P< 0.05$ and *** that $P< 0.001$.

3.3 Results

3.3.1 Atomic Force Microscopy/Scanning Electron Microscopy of nanocomposite

Figure 3.2 shows an SEM micrograph of the top side of a nanocomposite sample cast from DMAC solution. The surface appearance consists of a bulky round rough structure with a periodicity of about 5 µm and ribbon-like finer layered structure which is not distributed homogeneously over the whole sample area. Also visible are fine inclusions. The surface morphology accessible by the SEM investigation is independent of the UV-irradiation. The sample in Figure 2 has been irradiated for 30 minutes by the UV-lamp in 5 mbar NH_3 (the longest irradiation time used in this study), but shows the same features as an untreated surface demonstrating that the process of irradiation does not affect the surface. The fine inclusions were investigated in more detail by AFM measurements. Figure 3.3 shows the micrograph of nanocomposite samples UV-irradiated for 0 to 30 minutes in NH_3. The pronounced cage-like features are the mixture of silsequioxane nano-cages. Again, the features were similar for untreated and irradiated samples.
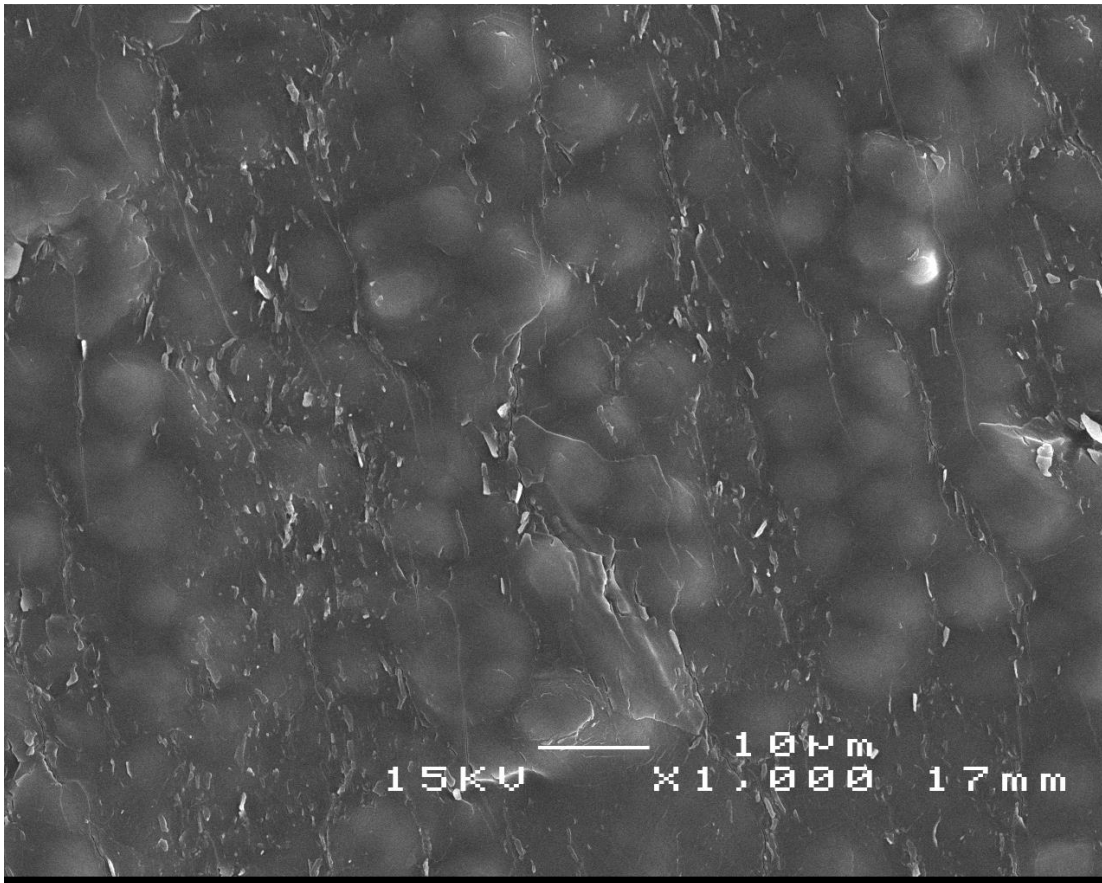
Figure 3.2 SEM image of nanocomposite: nanocomposite exposed to 172 nm UV-light in 5 mbar NH_3 for 30 minutes. For recording of the SEM image, a thin Au layer was deposited onto the surface by sputter deposition.

3.3.2 Chemical and Surface Analysis

Atomic Force Microscopy (AFM). Scans were performed with an 'Quesant Instruments Corp' AFM Serial Number: 752010 and the results are shown in Figure 3.3 which are set out in the series below.
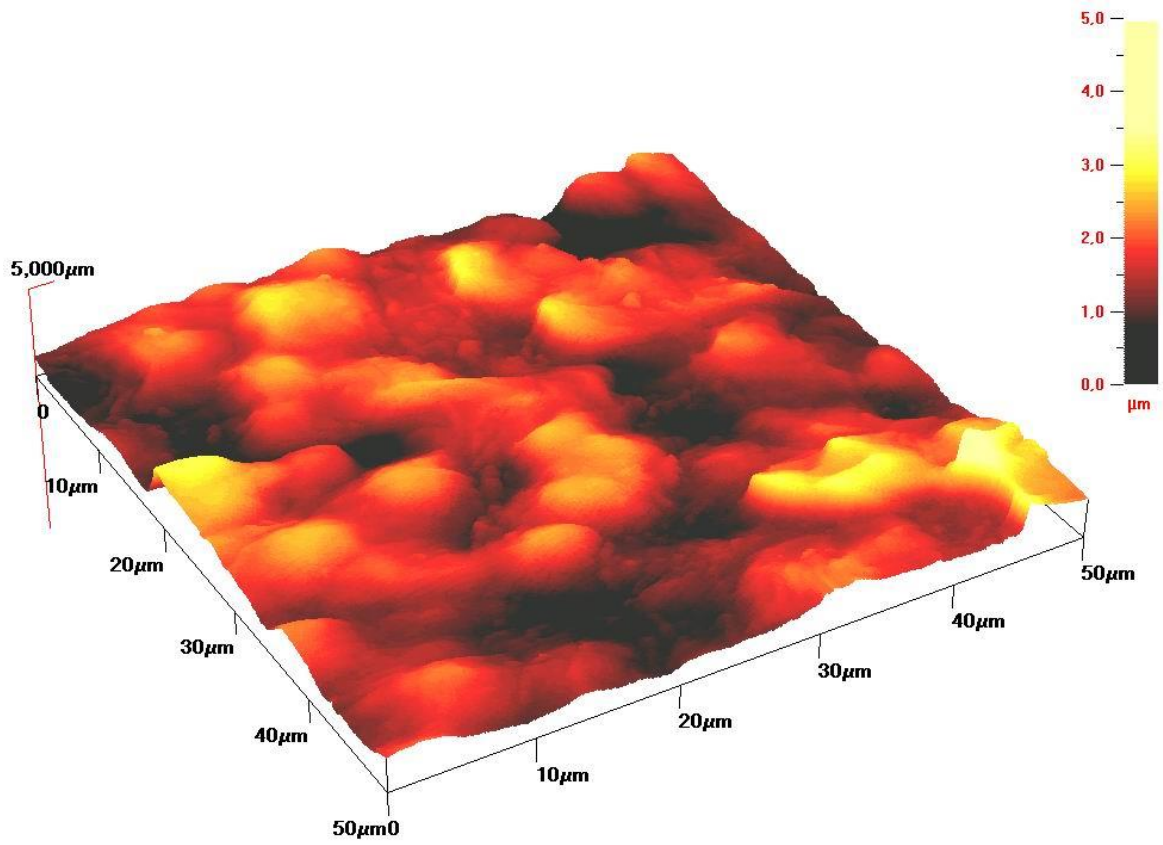
i) O minutes irradiation
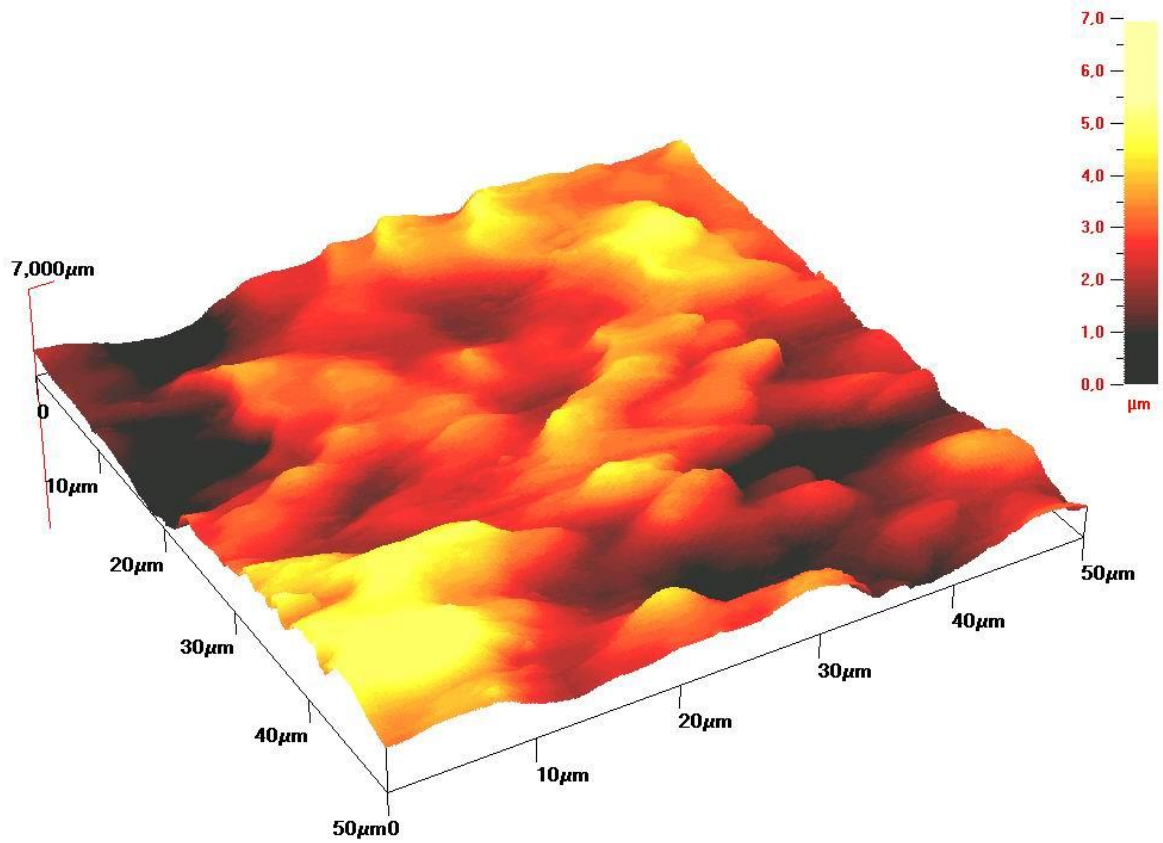
ii) 5 minutes
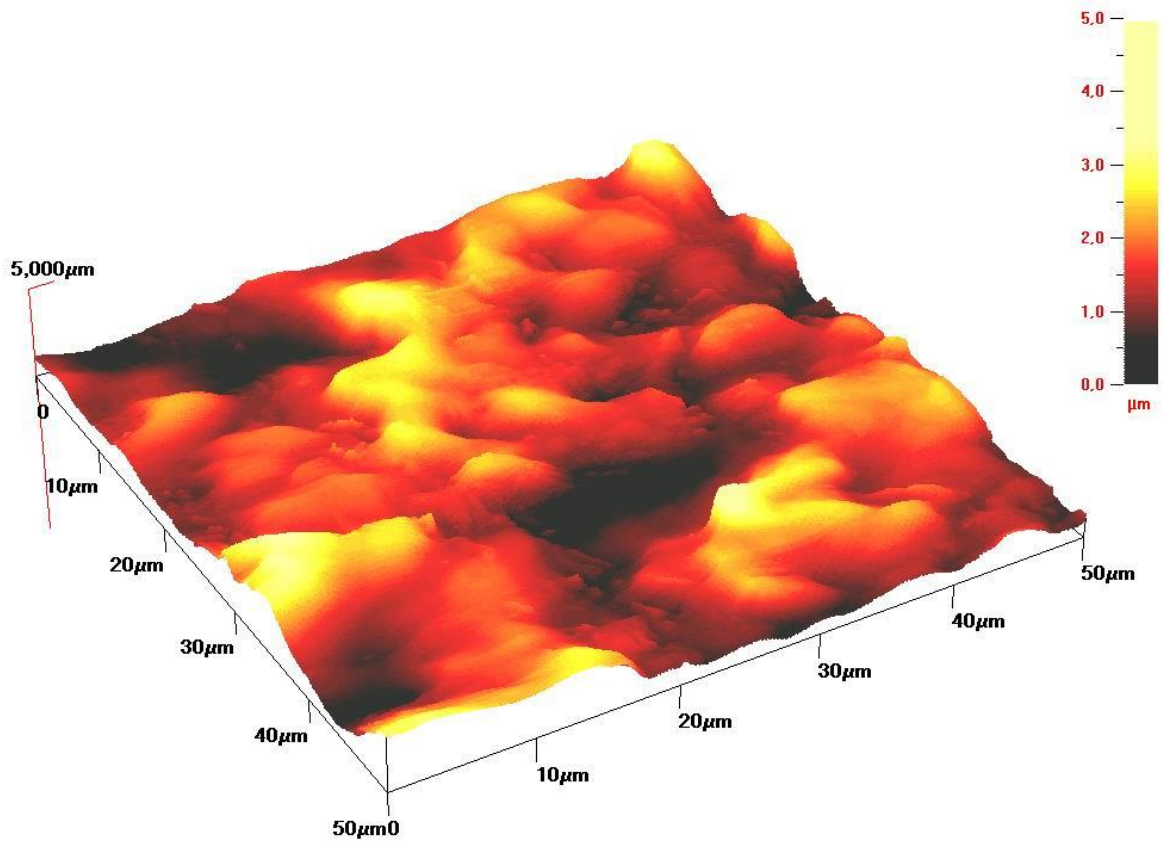
iii) 10 minutes
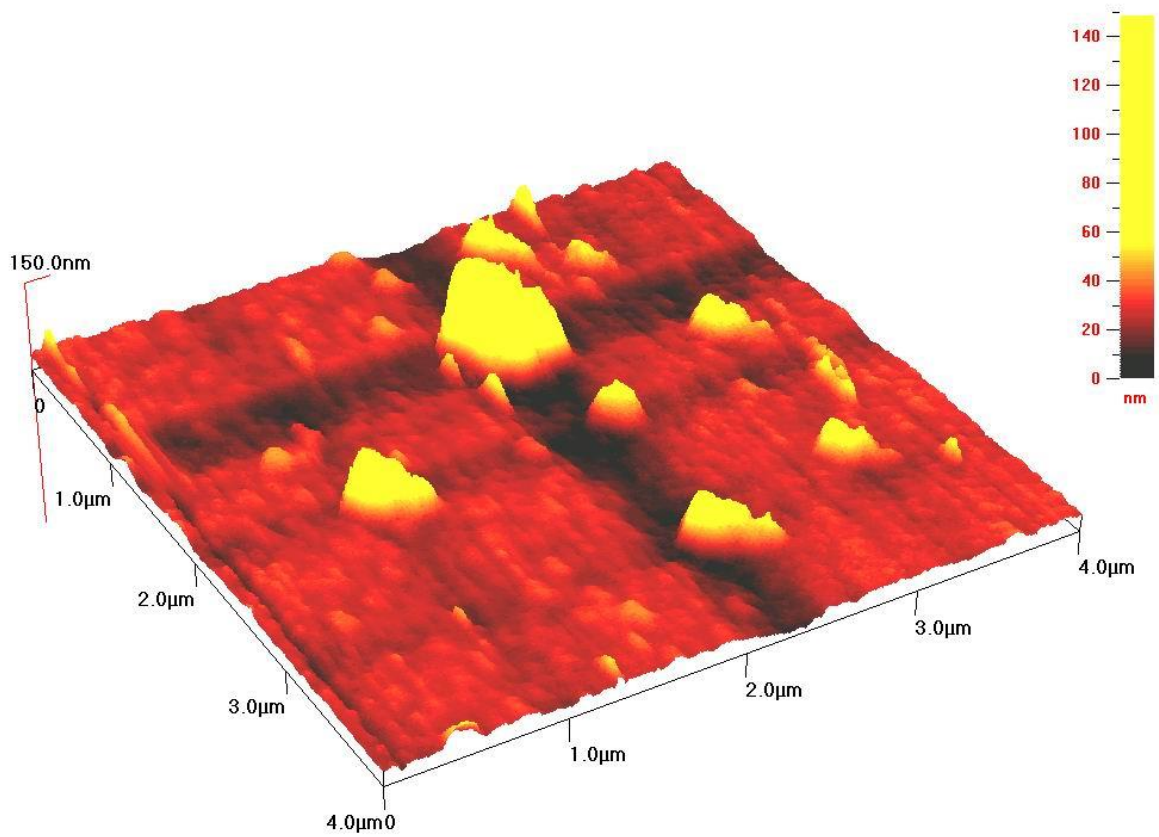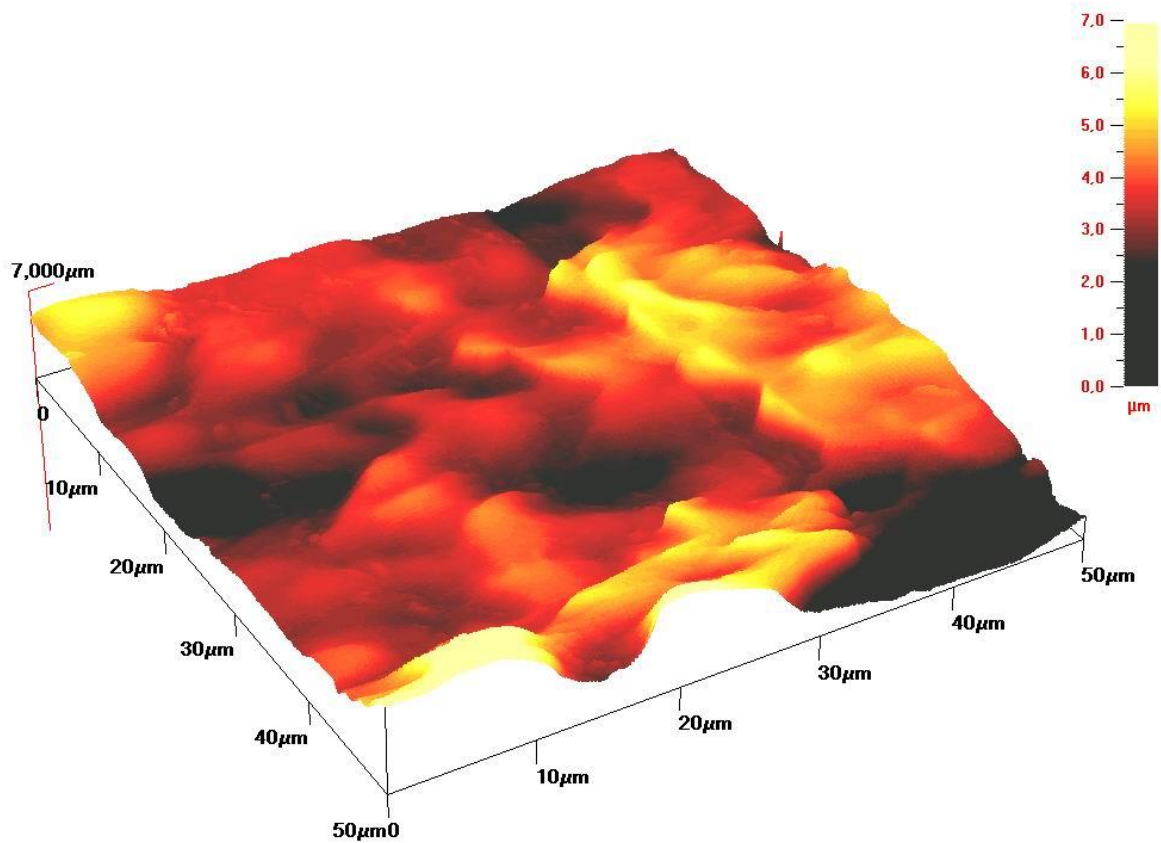
iv) 15 minutes

v) 30 minutes

Figure 3.3 AFM image of nanocomposite: nanocomposite exposed to 172 nm UV-light in 5 mbar NH_3 for i) 0 minutes (untreated), ii) 5 minutes, iii) 10 minutes, iv) 15 minutes and v) 30 minutes. The image shows an area of 4 x 4 µm, while the colour-scale encodes the height information. Due to an image processing artefact, the largest features are accompanied by slightly deeper stripes in horizontal and vertical direction.

3.3.3 Contact Angle Analysis

The UV-treatment of the nanocomposite samples in NH_3 resulted in increased hydrophilicity of the originally amphiphillic surface. Figure 3.4 shows the advancing water contact angle (CA) as function of the irradiation time. It decreased from 87.5 ° on untreated nanocomposite to about 37 ° on UV-treated samples. For longer irradiation times than 5 minutes a saturation effect for the CA was observed.
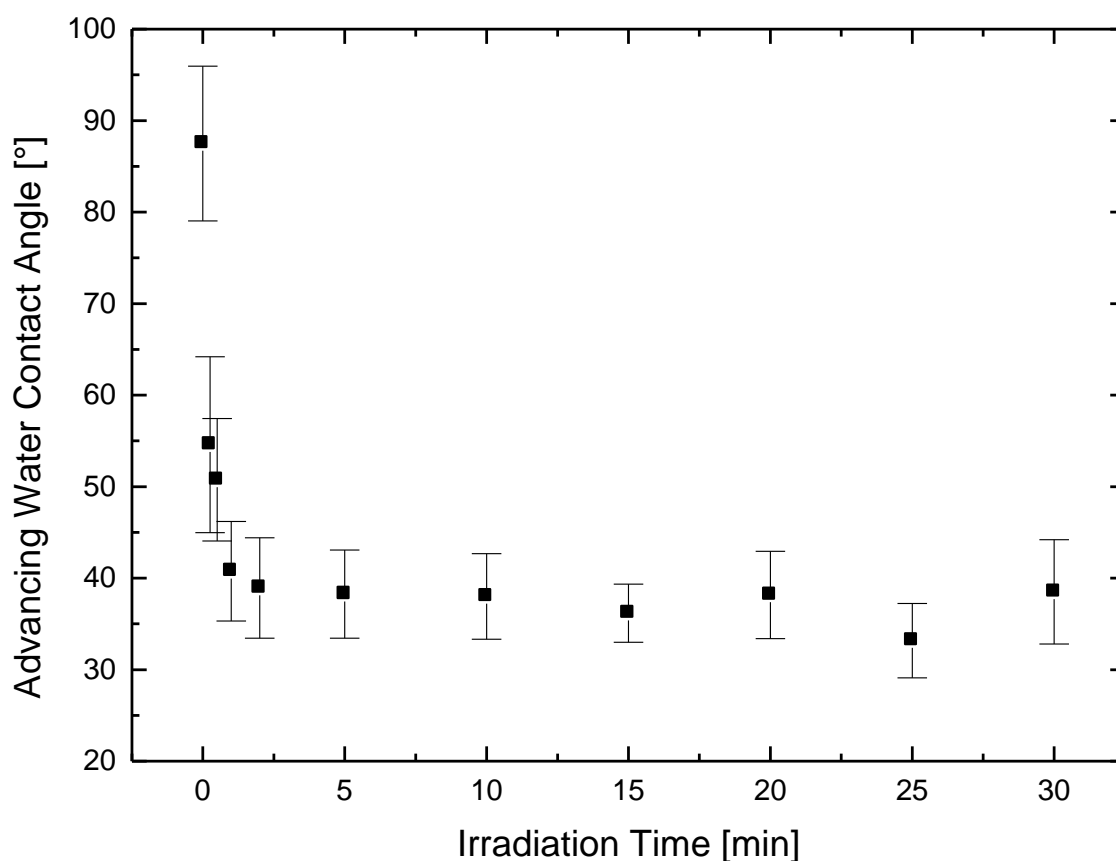
Figure 3.4 CA of UV-irradiated nanocomposite: advancing water contact angle at nanocomposite versus irradiation time (exposure to 172 nm UV-light in 5 mbar NH_3).

3.3.4 X-ray Induced Photo-electron Spectroscopy

Figure 3.5 shows XPS spectra of untreated and irradiated nanocomposite samples which were UV-irradiated for 30 seconds, 5 minutes and 30 minutes in NH_3. For the untreated nanocomposite (Figure 5a) the spectrum consists of peaks which are assigned to oxygen (O), carbon (C) and silicon (Si). No nitrogen (N) peaks could be detected even though the nanocomposite and polyurethane matrix includes N-containing urea and urethane-groups. A possible explanation for that is the short penetration depths of XPS (7 nm) along with surface effects during solidification. In addition traces of chlorine could be detected as in all other spectra in Figure 3.5.

The chlorine content is from the mixture of nano-cages used in the synthesis one of which contains chlorine. The 172 nm UV-irradiation resulted in the introduction of new N- and O-containing groups into the surface. The quantitative evaluations of these spectra are listed in Table 3.1 showing examples for an untreated nanocomposite sample and a nanocomposite sample exposed for 30 minutes to the 172 nm UV-irradiation in 5 mbar NH_3. Detailed spectra of the element peaks (not shown) allow the determination of the chemical bindings of the elements. For the C 1s , O 1s and N 1s electron the intensity of the sub-peaks and their identification are also listed in the Table.

In addition, the sub-peaks and identifications of the Si 2p doublet are listed. For C-groups, the irradiation resulted in the nanocomposite surface showing a strong depletion of C-C bonds (suggesting a reduction of CH_2 groups) and the formation of C=C double bonds and of various C-O and C-N bonds. For Si-groups, higher values of binding were detected in the samples irradiated for 5 and 30 minutes than in the unirradiated sample. This can be interpreted as an oxidation of the Si-atoms in the surface layer. The newly found N-peaks can be assigned to C-bond N-H groups, mainly near C=O groups, or to Si-N bonds. The detailed

analysis in the N-region of the sample of Figure 2.5b revealed a peak, which could be interpreted as N^+ (for example from ammonium groups). The other features of the spectra of the samples irradiated for 30 seconds and 5 minutes are qualitatively similar to those of the spectrum of irradiated for 30 minutes, but less pronounced.
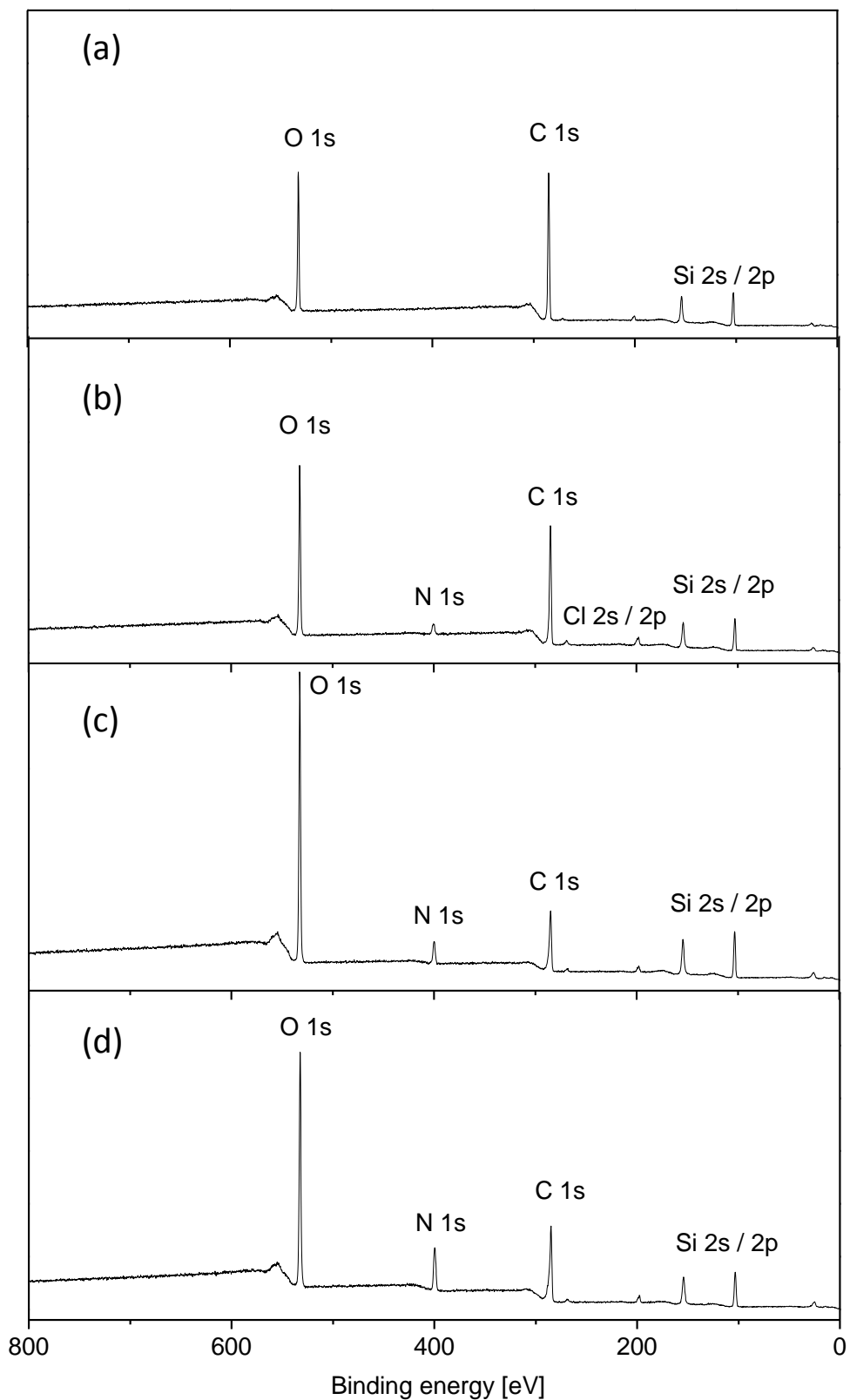
Figure 2.5 XPS spectra of nanocomposite: (a) nanocomposite untreated, (b) nanocomposite exposed to 172 nm UV-light in 5 mbar NH_3 for 30 seconds, (c) nanocomposite exposed for 5 minutes and (d) nanocomposite exposed for 30 minutes.

Sample	Peak	Conc. at %	Subpeak	Pos. eV	Conc. %	Binding
UN	C	61.4	C 1s 1	285.0	94.5	C-C
			C 1s 2	286.5	5.5	C-O
	O	22.9	O 1s 1	530.9	1.7	O-Si
			O 1s 2	532.3	87.2	O-Si,O=
		O 1s 3	533.1	11.1		-O-
	Si	14.9	Si $2p^{3/2}$ 1	102.6	66.7	Si-C
			Si $2p^{1/2}$ 1	103.2	33.3	Si-C
IN	C	38.5	C1s 1	284.6	43.0	C
			C1s 2	285.0	13.4	C-C
			C1s 3	285.7	14.2	C-N, C-
			C1s 4	286.5	15.1	C-O
			C1s 5	287.8	10.0	O-C-O,C=O,N-CO
			C1s 6	288.9	4.2	O=C-O
	O	35.1	O 1s 1	530.9	6.3	O-Si
			O 1s 2	532.4	89.1	O-Si, O=
			O 1s 3	533.8	4.6	-O-
	Si	13.6	Si $2p^{3/2}$ 1	101.9	3.4	Si-C
			Si $2p^{1/2}$ 1	102.6	1.7	Si-C
			Si $2p^{3/2}$ 2	103.1	63.3	Si-O
			Si $2p^{1/2}$ 2	103.8	31.7	Si-O
	N	11.7	N 1s 1	398.6	22.8	Si-N, C-N-
			N 1s 3	399.9	77.2	N-C=O

Table 3.1: Detailed evaluation of XPS spectra. Key: UN; Untreated Nanocomposite, IN; Irradiated Nanocomposite (30 minutes exposure to 172nm UV-light in 5 mbar NH_3)

3.3.5 Attenuated Total Reflection- Fourier Transformed Infra Red Spectroscopy

Figure 3.6 shows the ATR-FTIR spectra of untreated nanocomposite and nanocomposite samples irradiated for 30 seconds, 5 minutes or 30 minutes. In Figure 3.7 the identified peaks are marked by labels indicating the corresponding vibrations. The peaks of the untreated sample could be correlated to vibration modes of the components of the nanocomposite polymer (Figure 2.7a). The peak at 3340 cm^{-1} could be identified as N-H

vibration, probably from the urea and urethane groups in the polymer. The large peak at 2960 cm^{-1} was assigned to C-H vibrations from methylene segments in the polymer chain, the side peak at 2865 cm^{-1} to C-H vibrations from CH$_3$-groups bonded to phenol groups in the carbonate segments. The peak at 1735 cm^{-1} was identified as C=O vibration, probably from carbonate or urethane segments. The small peaks between 1430 and 1625 cm^{-1} were assigned to ring vibrations of phenol groups.

The peak at 1250 cm^{-1} was assigned either to C-C or O-CO-O vibrations in the polymer backbone. The peak at 1085 cm^{-1} could be assigned to Si-O-Si vibrations from the silsequioxane groups. The identification of the peak at 945 cm^{-1} was to some extent ambiguous, but may be the vibration of an Si-O group bond to a phenol ring. Compared to untreated nanocomposite, the main difference in the spectra of the irradiated samples was the appearance of a broad peak between 2630 and 3690 cm^{-1} (Figure 3.7b), which was more pronounced for the samples with longer irradiation times.

This peak can be assigned to a combination of various O-H, N-H and N-H$_2$ vibrations. Besides the peak at 1085 cm^{-1}, an additional peak at 1050 cm^{-1} appeared in the irradiated samples. Both could be associated with Si-O-Si vibrations.
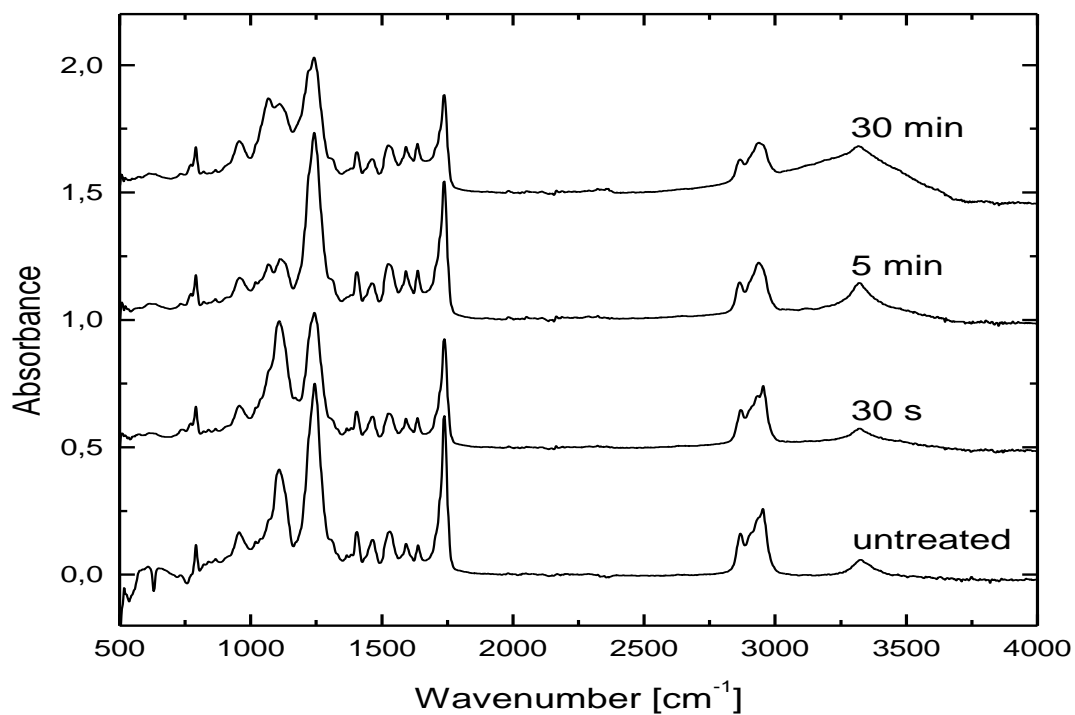
Figure 3.6 ATR-FTIR spectra of nanocomposite: nanocomposite untreated and nanocomposite exposed to 172 nm UV-light in 5 mbar NH_3 for 30 seconds, 5 minutes and 30 minutes, respectively. For sake of clarity, an off-set is added to the spectra of irradiated samples.
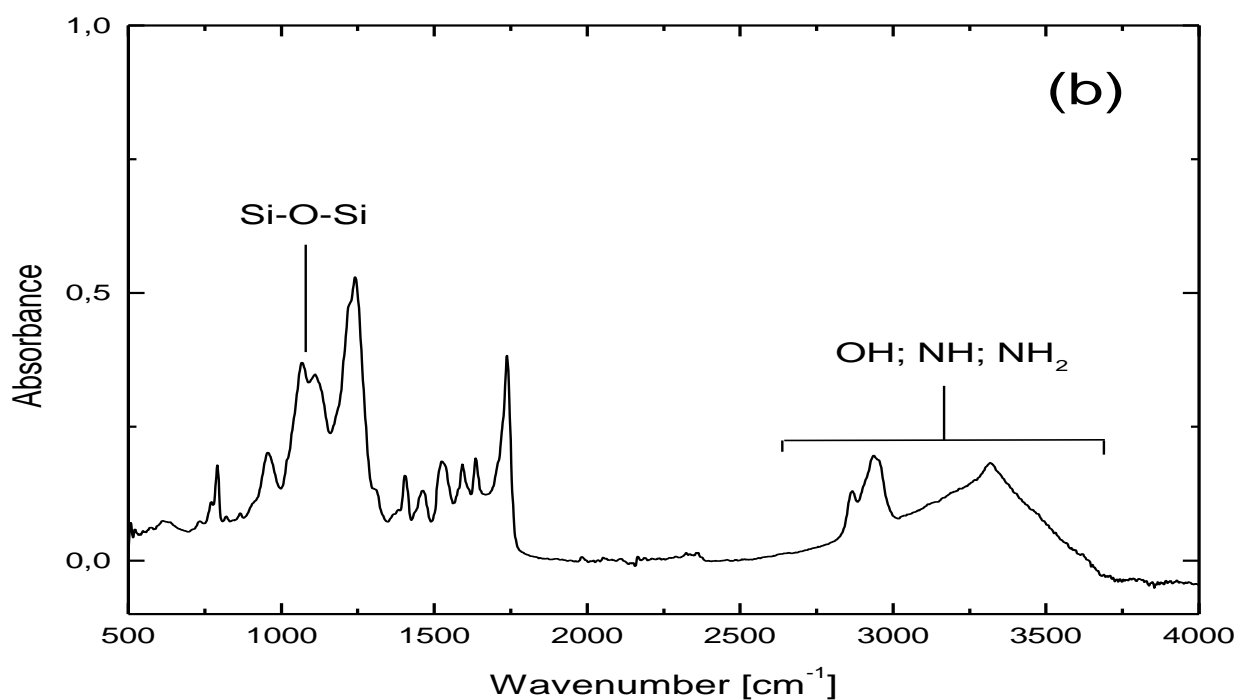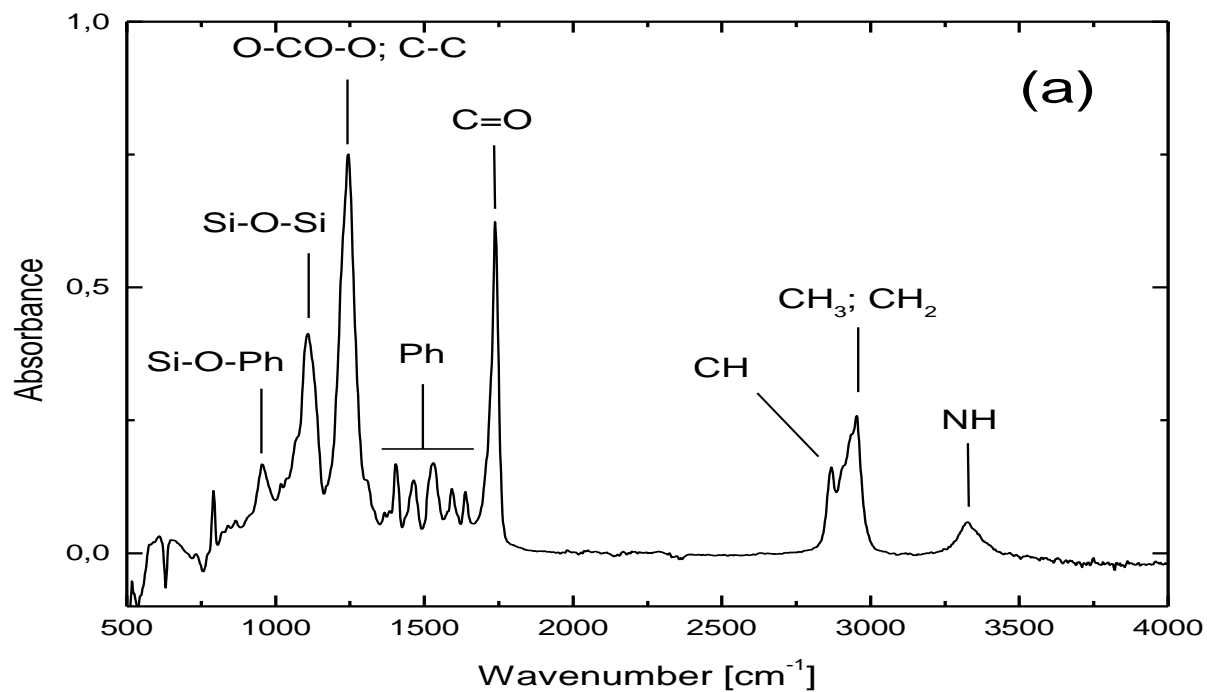
Figure 3.7 Peak assignment in ATR-FTIR spectra: peak assignment in spectrum of (a) untreated nanocomposite and (b) nanocomposite exposed to 172 nm UV-light in 5 mbar NH_3 for 30 minutes. Ph is the abbreviation of phenol-ring.

3.3.6 Determination of optimal seeding density

Figure 3.8a) shows the amount of DNA extracted from adherent cells on unmodified nanocomposite after a two-hour seeding period for four cell concentrations. It can be seen that as the seeding density increases there is a significant ($p<0.001$ vs. Previous column) increase in the amount of DNA (and hence cell numbers).

The percentage of cells seeded after two hours is shown in Figure 3.8b). Approximately 40% to 50% of the total number of cells appear to be attached after two hours.

The relative LDH release following two hours' cell seeding is shown in Figure 3.8c). It can be seen that there was no significant difference in LDH release for any of the treatments over the period examined.

Based on the above results it was determined to use a 1 x 10^5 seeding density and seeding periods of one and two hours to determine if UV modification of the nanocomposite improved initial cell adhesion or growth.
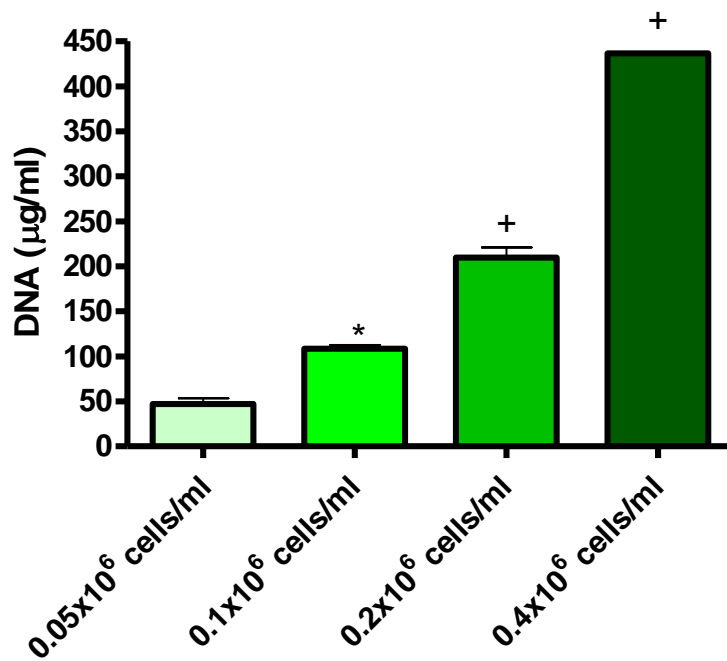
Figure 3.8a Pico green assay for total DNA amount from cells seeded on unmodified nanocomposite graft after two hour seeding with 0.5, 1, 2 and 4 x 10^5 HUVEC/ml (n=4). $^+$ indicates p<0.001 vs. previous column.
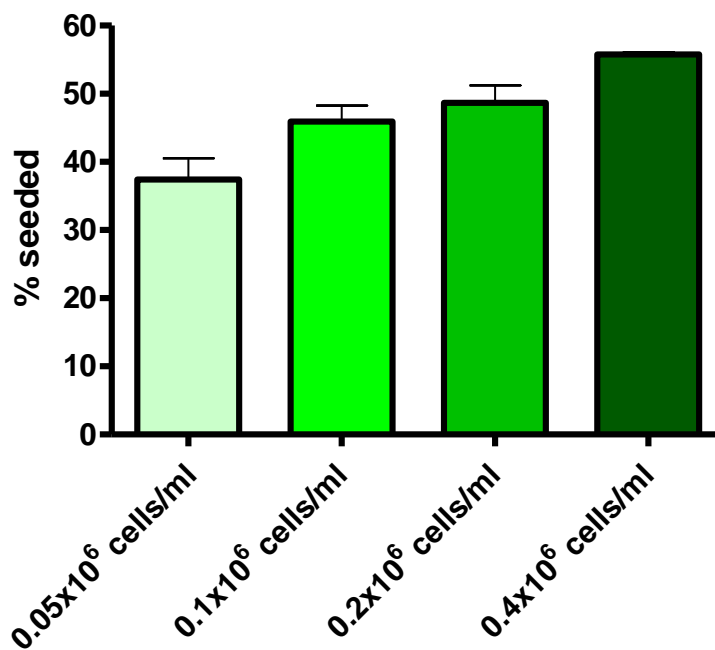
Figure 3.8b Percentage of cells seeded on nanocomposite after two hour seeding with 0.5, 1, 2 and 4 x 10^5 HUVEC/ml (n=4).
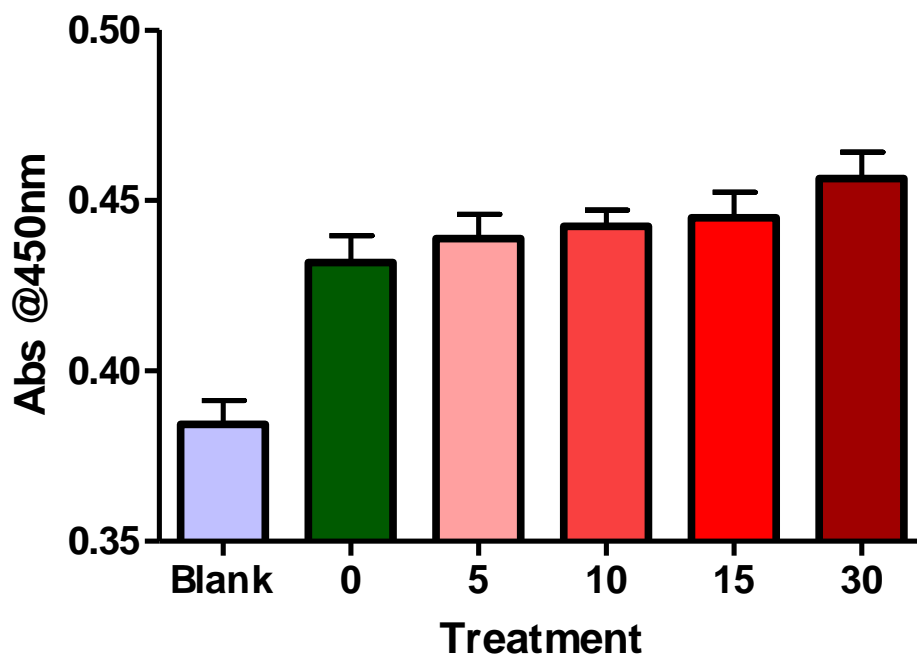
Figure 3.8c LDH activity for unmodified (0), 5, 10, 15 and 30 minutes irradiated at 5mbar NH$_3$ atmosphere modified Prep 11 graft after 2 hours seeding (n=4). Cell seeding density 1 x 10^5 cells/well.

3.3.7 Assessment of cell viability and metabolism on UV modified nanocomposite

The results of the assessment of cell viability and metabolism for the initially seeded cells and after 24, 48 and 72 hours' incubation for each seeding time are shown in figures 3.9a) to d).

It can be seen that there was little difference between any of the groups at the time points investigated for either a one hour or two hour seeding period. The nanocomposite irradiated for 10 minutes appears to be slightly worse at most time points in the two-hour seeding experiment.
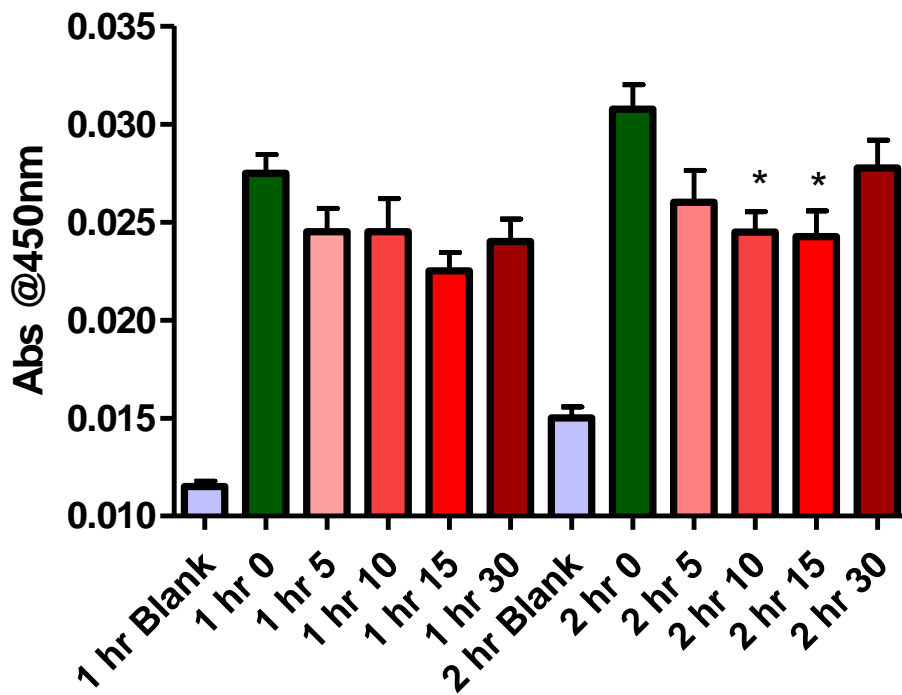
a)
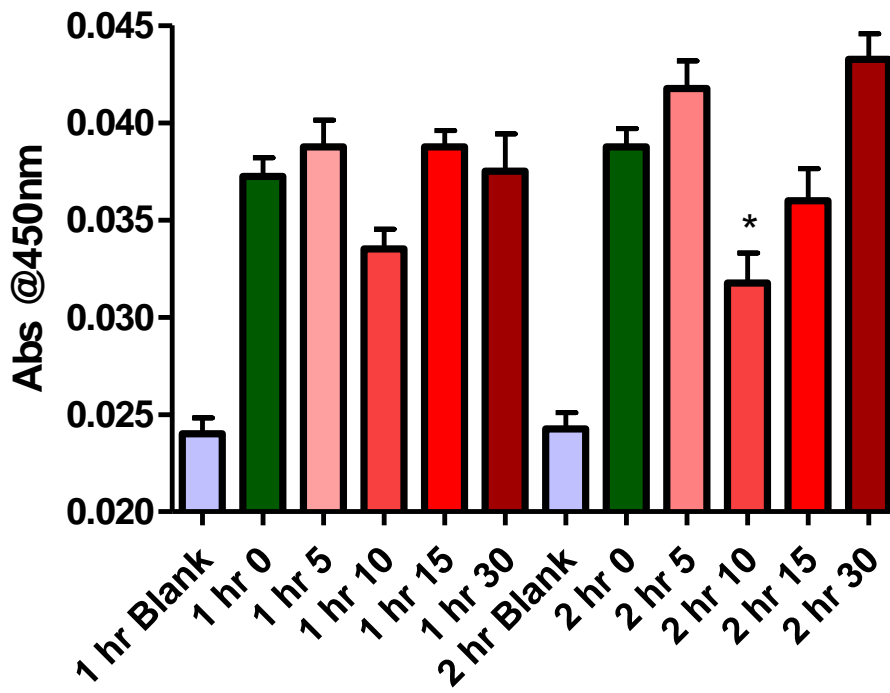
b)
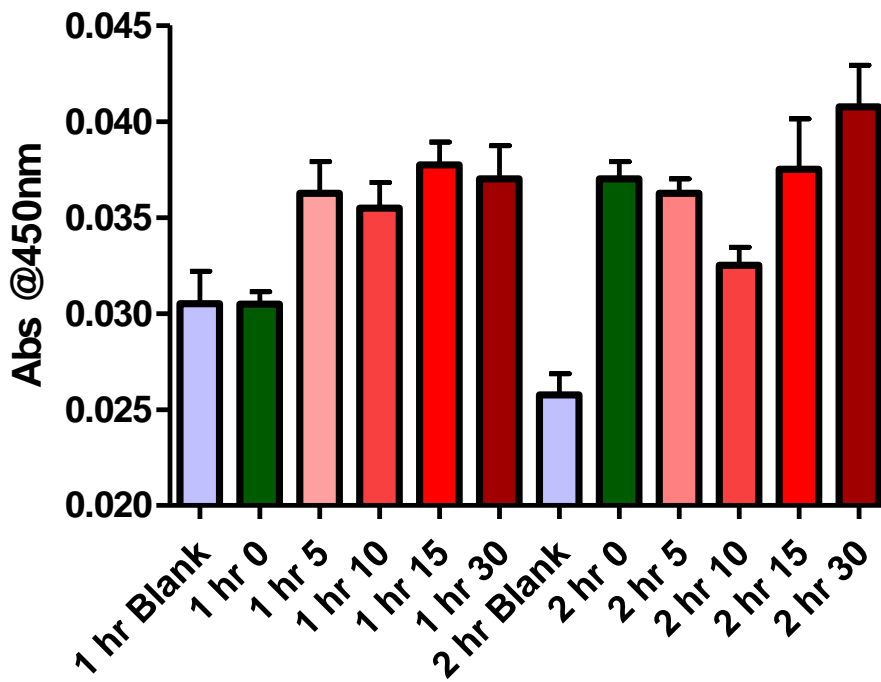
c)
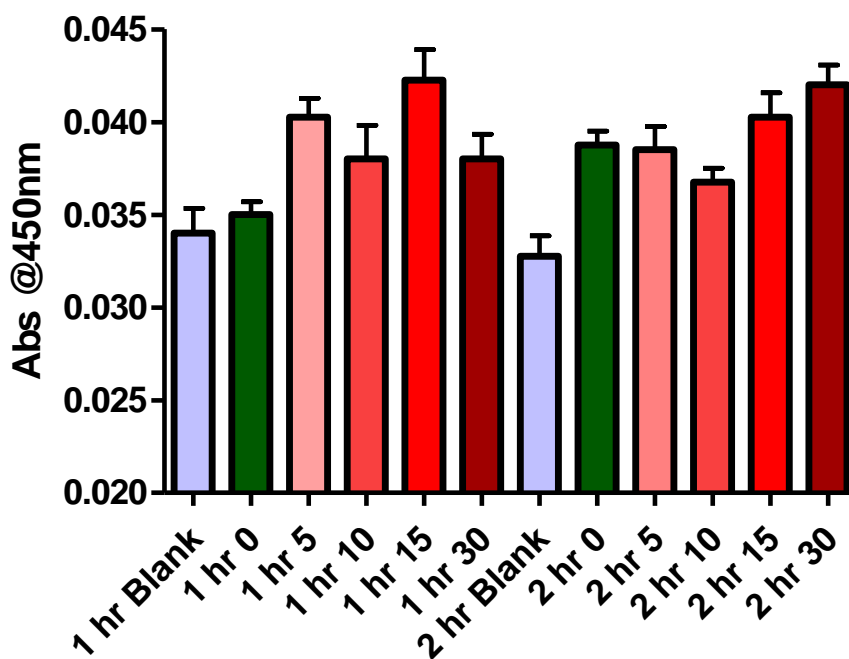
d)

Figure 3.9: AB assay for unmodified (0), 5, 10, 15 and 30 minutes irradiated at 5mbar NH_3 atmosphere modified nanocomposite a) after initial seeding, b) 24 hours; c) 48 hours and d) 72 hours after initial 1 hour and 2 hour seeding (n=4). Cell seeding density 1 x 10^5 cells/well. [*] indicates $p<0.05$ vs. 2 hour unmodified.

3.4 Discussion

The XPS results of the unmodified sample are consistent with the nanocomposite composition except the lack of N explainable by the low penetration depth of the XPS assay method NMR studies (data not shown) and ATR measurements demonstrated that this lack of N is not representative of the bulk material . XPS and ATR-FTIR spectra showed an increasing amount of N for the irradiated nanocomposite samples. Photochemical surface modification of the polymer is responsible for this increase, comparable with the

incorporation of N into the surface of other polymers as described previously (Heitz *et al.*, 2004; Gumpenberger *et al.*, 2003). The new N-containing groups could be NH, NH_2 or NH_3^+. The irradiated nanocomposite samples showed higher O-contents as compared to the untreated nanocomposite. This increase in O could be due to residual O in the irradiation chamber or to oxidation of remaining radicals in the sample surface during exposure to air after the treatment (Heitz *et al.*, 2004). Another source could be O-groups from within the nano-cages themselves.

This is supported by the fact that the Si at the surface arising from the nano-cages is oxidized to a degree as is indicated in the XPS results as well as in the ATR-FTIR. For untreated nanocomposite, one peak at 285 eV is dominant in the detailed XPS spectra in the C-region. This is commonly associated with CH groups. With increasing irradiation time the C peak becomes more complex consisting of several subpeaks. This indicates that carbon is involved in the chemical reactions or that the surface composition changes during modification.

The width of the XPS C-peak is relatively large for the irradiated samples, indicating a broad variation of the chemical surrounding of the C-atoms under consideration. This would be consistent with photoreactions in the nanocomposite chain being induced due to UV-irradiation. The appearance of a broad peak between 2630 and 3690 cm^{-1} the ATR-FTIR clearly shows that there are new N- or O- containing groups incorporated in to the surface which are polar. Therefore, the photochemical surface modification is in accordance with the observed considerable reduction of CA resulting in a change from an amphiphillic surface to a more hydrophilic surface.

No obvious changes to the surface morphology of the nanocomposites were observed by SEM and AFM investigations. However small changes could occur due to irradiation that may influence the interaction of the cells with the surface and structural changes well below 100 nm can be of great significance.

The cell adhesion and proliferation results show clearly that there is little improvement in HUVEC adhesion and proliferation on the photochemically modified nanocomposite surfaces under the circumstances investigated. Interestingly further study using a HUVEC EA.hy926 cell line which was derived from HUVEC (Edgell *et al.*, 1983; Bouis *et al.*, 2001) did demonstrate an improvement in cell adhesion and proliferation for the 5 and 15 minute UV modified surfaces (Olbrich *et al.*, 2007).

It was anticipated that the potential enhancement of the adhesion and proliferation on the photochemically modified regions may be due to the improved hydrophillicity of the modified surface. This is supported by the change of polarity/wettability demonstrated by the CA measurements. The improved wettability facilitates the adsorption of cell adhesion-mediating proteins, present in the serum of the culture media, in an amount, spectrum and conformation favourable for the binding of specific amino acid sequences of these proteins to the integrin receptors of the cells (Arnold *et al.*, 2004). On the modified nanocomposite samples there is a relatively high content of positively chargeable amine groups. These are reported to have a good interaction with the mainly negative charged cell membrane and this could be favourable for cell adhesion. In addition the new chemical groups include functional groups typically found in amino acids suggesting that cell adhesion may be supported by direct cellular interaction with these newly formed chemical groups on the surface.

3.5 Conclusion

A decrease in contact angle from 87.5^O for the untreated nanocomposite to approximately 37° for the UV-treated samples shows a significant increase in hydrophilicity which is supported by the ATR-FTIR and XPS analysis. The difference in outcome for the primary HUVEC cells reported in this chapter which were largely unaffected by the surface modification and the HUVEC cell line used in the follow up study demonstrates the difficulties involved in extrapolating results obtained using cell lines to primary cells. In conclusion, it can be said that the successful modification of the nanocomposite investigated in this study by UV-irradiation in an ammonia atmosphere has been demonstrated by the results obtained and that the technique may have potential for future employment to develop an EC seeded prosthesis.

4

4 Human Peripheral Blood derived Endothelial Cell Seeding of Nanocomposite.

4. 1 Introduction

The use of prosthetic grafts in vascular surgery has increased since the introduction of a fabric arterial graft in mid twentieth century. Although much work has been carried out since then to improve the prosthetic grafts employed in this field, cardiac and peripheral vascular disease remain the major causes of death in the Western world. In UK, it is estimated that one in three deaths could be attributed to diseases of the circulatory system or heart and this is likely to be a continuing problem in the future as the life expectancy of the population increases. In an ideal situation, an autologous vein or artery is the most suitable conduit choice for bypass operations (the internal mammary being employed for coronary bypass and the saphenous for lower limb arterial bypass) and these results in a 5-year patency rate of

around 75%. In around 30% of cases a suitable autologous conduit is not available for lower limb bypass and a similar situation occurs for coronary bypass (Kannan *et al.*, 2005a) leading to a requirement to use an artificial conduit (Rashid *et al.*, 2004).

There are two major types of prosthetic graft in clinical usage currently, based on either expanded polytetrafluoroethylene (ePTFE) or polyethylene terephthalate (Dacron®). Current prosthesis employed have low patency rate due to the low compliance and thrombogenicity of the materials used.

Several approaches have been taken to attempt to improve the patency of prosthetic grafts, including surface modification of existing grafts, endothelial seeding and recently development of tissue engineering bypass graft (Baguneid *et al.*, 2006; Sarkar *et al.*, 2007b; Isenberg *et al.*, 2006) and development of new compliance prosthesis with active biomolecules and endothelialisation (Kidane *et al.*, 2004).

The most interesting material our group has been working on is an novel nanocomposite based on polyhedroligomeric silsesquioxane-poly (carbonate-urea)urethane nanocomposite. The potential advantages of the UCL-Nano™ have been reviewed previously (Kannan *et al.*, 2005a). The nanocomposite has been demonstrated to have similar viscoelastic properties to a native artery and be resistant to degradation (Kannan *et al.*, 2005c). Several previous studies have also indicated that the nanocomposite can sustain HUVEC seeding (Punshon *et al.*, 2005; Vara *et al.*, 2006).

Another aspect which has been investigated to overcome this problem is seeding the artificial material with EC's to improve the blood compatibility of the device. This idea was first reported by Herring *et* al (Herring *et al.*, 1978; Stanley *et al.*, 1985) in 1978 and has

since attracted considerable interest with numerous studies being carried out in this area. Sources of material from which to obtain suitable cells to attempt seeding include the patient's own veins (Herring *et al.*, 1978; Stanley *et al.*, 1985) omentum or subcutaneous fat and peritoneal lavage (Tiwari *et al.*, 2003a) all of which have the disadvantages of being invasive to obtain (requiring an operation) and difficult to extract cells from in adequate numbers. These factors limit their potential in both a research and clinical situation.

In a clinical context two-stage seeding, in which EC are extracted from tissue then cultured for a period of time in the laboratory has been demonstrated to be successful in a number of studies with a significant increase in graft patency. One study by Zilla *et al* and published in 1994 (Zilla *et al.*, 1994) seeded autologous EC from the external jugular vein onto 70 cm long 6 mm internal diameter PTFE grafts coated with fibrin glue in 33 patients with either disabling claudication or critical ischemia. The average culture time required after vein incision was 25 days and growth failure occurred in 27% of the cases. Cases were followed up by angiography, platelet adhesion studies, assessment of the ankle-brachial index and duplex sonography. After 32 months' the patency of the endothelialised grafts was 85% compared to 55% for the unseeded control grafts thus demonstrating an improvement in patency similar to that found when employing autologous grafts. These results were confirmed by further long-term studies by the same group reporting similar results (Deutsch *et al.*, 1999; Meinhart *et al.*, 2001).

Despite this demonstration of the potential of the two-stage seeding technique developed by this group such techniques have not, to date, been taken up in widespread practice. There are several reasons why uptake of this technique has been limited. Firstly, it requires the patient to undergo an extra operation to collect the tissue required to extract EC prior to

culture in the laboratory. This exposes the patients to additional risk in undergoing an extra surgical procedure to obtain tissue and has considerable cost implications over and above those for the cell culture stage where a dedicated facility is required. Secondly the period required to grow up the cells and seed the device is considerable (three to four weeks) and, in a number of cases, the cells fail to multiply sufficiently to seed the graft.

There has been much interest in the potential for using human stem cells to treat a wide variety of medical conditions in the future (Sales *et al.*, 2005). Much of this research is based on using embryonic stem cells, cells obtained from bone marrow or cells obtained from umbilical cord blood. Whilst the potential for such work is great it is associated with grave problems from the ethical viewpoint when working with human tissue in the case of embryonic stem cells, difficulty in obtaining adequate samples for research in the case of bone marrow or clinical practicality in the case of umbilical cord blood.

It has recently been demonstrated however that human peripheral blood contains both circulating EC's and EPC, a type of stem cell with the potential to expand. The first report on the isolation of progenitor cells from peripheral blood was made by Ashara *et al* in 1997 (Asahara *et al.*, 1997) using magnetic beads to separate CD34$^+$ cells. Further studies by groups such as Hill *et al* demonstrated that it was possible to extract progenitor cells without the use of magnetic beads and correlated the numbers in blood with cardiovascular risk factors (Hill *et al.*, 2003). Several other studies have demonstrated the potential of progenitor cells isolated from this source (Shirota *et al.*, 2003; Hur *et al.*, 2004; Ingram *et al.*, 2004).

In view of the above the aim of this chapter was to develop a system with the potential to deliver an EC-seeded bypass graft in a realistic time-frame and in a manner such that general

uptake of the process would be possible. This could be achieved by building on the proven clinical success of two stage seeding whilst attempting to overcome the potential pitfalls of cell source by employing peripheral blood as a source of cells and using nanocomposite as a scaffold for seeding.

4.2 Materials and Methods

4.2.1 Preparation of nanocomposite polymer films

The synthesis of the nanocomposite inorganic urethane is made from 4,4'-methylenebis (phenyl isocyanate) (MDI), poly (hexamethylene carbonate)diol, and silsesquioxane dissolved in tetrahydrofuran here bis [3- (trimethoxysilyl)propyl]amine and chain extended with DMAC.

Glass Petri dishes (40mm diameter) were then coated with 4mls of nanocomposite (15 % in DMAC) and cured overnight at 55ºC. The resulting films were then thoroughly washed with sterile PBS and sterilized by immersion in 70% ethanol followed by air-drying.

4.2.2 Blood Collection

Blood samples were collected following consent from healthy adult human volunteers. 20ml samples were collected by venepuncture in EDTA blood tubes (Sarstedt, U.K.). Following collection samples were mixed and used for cell isolation within one hour of collection.

4.2.3 Cell Isolation

The mononuclear fraction of the blood was then isolated using Lymphoprep (Axis-Shield, U.K.). Briefly 20ml of blood was transferred to a 50 ml centrifuge tube (Falcon, U.K.) and

gently mixed with 20ml Hank's Balanced Salt Solution (HBSS) (Invitrogen, U.K.). 5ml Lymphoprep was then added to each of eight 12ml polystyrene centrifuge tubes (Falcon, U.K.) and 5ml of the blood/HBSS mixture then layered carefully on top. The tubes were then centrifuged at 1500 rpm and 20°C for 25 minutes. The mononuclear fraction was then separated from each and placed equally into two 30 ml universal tubes (Falcon, U.K.). 10ml of HBSS was then added slowly to each tube and the contents mixed. The tubes were then centrifuged at 1500 rpm and 20°C for 15 minutes. The supernatant was then discarded and the cells resuspended in 2 ml HBSS. The volume was then made up to 10ml and the cells centrifuged at 1200 rpm and 20°C for 15 minutes to remove red blood cells. The supernatant was again discarded and the cell pellet resuspended in 10ml HBSS. A final centrifugation step at 1500 rpm and 20°C for 15 minutes was then performed. Finally, the supernatant was again discarded and the cells resuspended in 5ml cell culture medium (CCM): RPMI 1640 supplemented with 20% fetal bovine serum and penicillin/streptomycin (Invitrogen U.K.). The cells were then counted using a haemocytometer.

4.2.4 FACS analysis for CD133$^+$/VEGFR2$^+$ EPC

100μl of initial cell isolation was incubated with a murine IgG, for 15 minutes at 4°C to block non-specific binding/specific binding via FcR, followed by incubation with a novel cocktail of antibodies comprising FITC-conjugated mouse anti-human CD2, CD13 and CD22 (BD Biosciences), PE-conjugated mouse anti-human VEGFR2 (R&D Systems, U.K) and biotin-conjugated mouse anti-human CD133 (Miltenyi Biotec, U.K) monoclonal antibodies for 10 minutes at 4°C, then washed. Following this, streptavidin-PeCy7 (Beckman Coulter, U.K) was added and the samples further incubated for 10 minutes at 4°C. Red cells were lysed and the samples were fixed using the Coulter TQ-prep system (Beckman Coulter, U.K). The samples were resuspended in HBSS and fluorescent particles (Sphero™Accucount

fluorescent particles (ACFP-100-3), 10 μm; Spherotech Inc, U.K) were added to calculate absolute cell numbers. The calculation was performed as follows:

Samples included the count of 10,000 fluorescent particles to give a total of $0.5–1×10^6$ mononuclear events. The samples were analysed immediately on a FACScan using CellQuest 3.1 software (Becton Dickinson, U.K.).

The instrument was standardised daily with Calibration beads (FluoroSpheres 6-Peak; DakoCytomation, U.K) and thoroughly cleaned before data acquisition to exclude any trace amounts of cellular debris or residual cells from a previous tube. The cleaning process comprised of sequential tubes with water, bleach and water again for about 30 minutes.

4.2.5 Cell Culture

Isolated cells were cultured for an initial two days in a 6-well plate (Falcon, U.K) at a seeding density of $9.2x10^6$ cells/well following which the supernatant (containing the non-attached cells) from two wells was transferred to a nanocomposite film coated Petri dish. Cells were then cultured in CCM for a further five days. The supernatant was then removed from the UCL-Nano™ film coated Petri dishes and the remaining adherent cells cultured in CCM with the medium being changed every two to three days for a total of 35 days. Cells were also cultured on 8-well slides (Falcon, U.K.) for characterisation studies. Experiments were repeated between three and five times.

4.2.6 Measurement of Cell Metabolism

Cell metabolism was assessed by Alamar blue^{TM} (AB) (Serotec, U.K.) assay at Day 7, 14, 21, 28 and 35. Medium was removed from the nanocomposite film coated Petri dishes and 4ml 10% AB in CCM added. After a 4-hour incubation, duplicate 100μl samples of AB/CCM

were removed and measured on a Fluroskan Ascent FL (Thermo Labsystems, U.K.) fluorescent plate reader (excitation 530nm, emission at 620nm). Unseeded nanocomposite film coated Petri dishes were used as a control. The AB/CCM mixture was then removed and replaced with fresh CCM.

4.2.7 RNA Isolation and Investigation

RNA was extracted from initial cell isolates, confluent cell cultures on 6-well plates and Day 35 confluent cell cultures seeded on nanocomposite by using an "RNeasy™" kit (Qiagen Ltd, U.K.). The RNA concentration and purity was calculated by measuring the absorbance at 260nm and 280nm using an Eppendorf Biophotometer (Eppendorf^{AG}, Germany). The quality of the RNA was assessed by 2% agarose gel electrophoresis and the mRNA obtained was used for polymerase chain reaction (PCR) for CD14, CD34, CD133, PECAM-1 and vWF. RT-PCR was performed using an One-Step PCR kit (Qiagen Ltd, U.K.). A master mix containing 10 μl 5x Qiagen One-Step RT-PCR buffer, 10 μl 5x Q-Solution, 400 μM from each of the deoxynucleoside triphosphate's, 2 μl Qiagen One-Step RT-PCR enzyme mix and 0.5 μM from each of the primers (Table 4.1) was added. 0.25 μg of template RNA was used for each PCR reaction. RNase free water was added to give a total volume of 50 μl. Cycle conditions were as follows: CD14 30 cycles at 94°C, 57°C and 72°C; CD34 35 cycles at 94°C, 54°C and 72°C; CD133 35 cycles at 94°C, 52°C and 72°C; VEGFR2 35 cycles at 94°C, 59°C and 72°C; vWF 35 cycles at 94°C, 50°C and 72°C; PECAM-1 35 cycles at 94°C, 50°C and 72°C and amplification was carried out using a MasterCycler Gradient PCR machine (Eppendorf^{AG}, Germany). In the case of vWF and PECAM-1 RNA extracted from HUVEC was used as a positive control. PCR products were then analysed by 2% agarose gel electrophoresis and a GeneGenius darkroom with 'GeneSnap' version 6.02. (Syngene, U.K.).

Marker	Sense (5' to 3')	Antisense (5' to 3')
CD14	CCTCCCAAGTTTTAGGACAA	CAGCTGGTGATAAGGGTTAG
CD34	CCTCCCAAGTTTTAGGACAA	CAGCTGGTGATAAGGGTTAG
CD133	CAGTCTGACCAGCGTGAAAA	GGCCATCCAAATCTGTCCTA
VEGFR2	GTGACCACATGGAGTCGTG	CCAGAGATTCCATGCCACTT
CD31	GCTGTTGGTGGAAGGAGT	GAAGTTGGCTGGAGGTGCTC
vWF	TGCTGACACCAGAAAAGTGC	AGTCCCCAATGGACTCACAG

Table 4.1: Primer sequences for CD14, CD34, CD133, VEGFR2, CD31 and vWF gene expression analysis.

4.2.8 Giemsa Staining

CCM was removed from the cell sample to be stained. Cells were then washed thoroughly with 5mls PBS. 500μl ice-cold methanol was then added for 5 minutes to fix the cells. Following fixing the methanol was removed and the cells air-dried. 200μl Giemsa stain (Invitrogen, U.K.) was then added and the cells left to stain for 15 minutes at room temperature. The stain was then removed and the cells destained with PBS as required then examined microscopically. Cells were stained at Day 5, Day 14, Day 21 and Day 35.

4.2.9 Scanning Electron Microscopy

Seeded nanocomposite at Day 35 was examined by SEM to visualise whether cells were still present on the nanocomposite surface.

4.2.10 Immunohistochemistry for CD34, CD133 and vWF

4.2.10.1 Preparation of Cells for Staining

Cell samples were collected from the initial cell isolation and cytospun onto polylysine-coated slides (VWR, U.K.) at 500 rpm for 5 minutes. Confluent cell cultures were grown on 8-well slides. Slides were then fixed in ice-cold methanol (VWR, U.K.) for 10 minutes, air-dried and stored at 4°C until stained.

4.2.10.2 CD34 Staining of Initial Cell Isolations and Confluent Cells

CD34 staining was carried out using an FITC conjugated CD34 antibody (Milteyni, U.K). 10µl CD34-FITC antibody was added to 90µl buffer (Phosphate buffered saline (PBS) containing 0.5 % bovine serum albumin (BSA) and 2 mM EDTA). Diluted antibody was then added gently to the cell sample and incubated at 4°C in the dark for 10 minutes. Excess antibody was then removed by washing with 10 to 20 times volume of buffer following which the cells were covered with a drop of mounting medium (Vector, U.K.) and examined microscopically.

4.2.10.3 CD133 Staining of Initial Cell Isolations and Confluent Cells

CD133 staining was carried out using a biotin conjugated CD133 primary antibody and visualized using an anti-biotin Allophycocyanin (APC) secondary antibody (both Miltenyi, U.K.). Briefly 20µl CD133-biotin antibody was added to 80µl buffer (PBS containing 0.5 % BSA and 2 mM EDTA). Diluted antibody was then added gently to the cell sample and incubated at 4°C in the dark for 10 minutes. Excess antibody was then removed by washing with 10 to 20 times volume of buffer. 10µl Anti-biotin-APC in 100µl buffer was then applied with a further incubation for 10 minutes at 4°C. Excess antibody was then again removed by

washing with 10 to 20 times volume of buffer following which the cells were covered with a drop of mounting medium and examined microscopically.

4.2.10.4 von Willebrand Factor Staining of Initial Cell Isolations and Confluent Cells

Staining for von Willebrand Factor (vWF) was carried out using a mouse monoclonal primary antibody to vWF and visualized using a goat polyclonal to mouse IgG H&L (FITC conjugated) secondary antibody (ABCAM, U.K.). Briefly cells were permeabilized by incubating for 10 minutes in PBS with 0.25% Triton X-100 (Sigma Chemical Company, U.K.). Cells were then washed 3 times with 1ml PBS after which cells were incubated for 30 minutes with 1% BSA PBST (PBS plus 0.2% Tween-20 (Sigma Chemical Company, U.K.) to block unspecific binding. Cells were then incubated in diluted primary antibody (3µl to 100 µl 1% BSA PBST) for 1 hour at room temperature. Cells were then washed 3 times with 1ml PBS after which cells were incubated in diluted secondary antibody (3µl to 100µl 1% BSA PBST) in 1% BSA PBST for 1 hour at room temperature in the dark. Cells were then washed a further three times in PBS, mounted as above and examined microscopically.

4.2.10.5 PECAM-1 (CD31) Staining of Initial Cell Isolations and Confluent Cells

CD31 staining was carried out using an APC conjugated CD31 antibody (Milteyni, U.K.). Briefly 10µl CD31-APC antibody was added to 90µl buffer (PBS containing 0.5 % BSA and 2 mM EDTA). Diluted antibody was then added gently to the cell sample and incubated at 4°C in the dark for 10 minutes. Excess antibody was then removed by washing with 10 to 20 times volume of buffer following which the cells were covered with a drop of mounting medium and examined microscopically.

4.3 Results

4.3.1 Number of Cells Isolated

The total numbers of cells isolated for 22 isolations (11 from the same test subject) from 20mls blood are shown in Figure 4.1. In general, the average number of cells isolated was $37.5x10^6 \pm 2.414$ (SEM) cells/20ml blood (maximum $54x10^6$, minimum $19x10^6$). For the 11 extractions from the same subject the average number of cells isolated was $42.18x10^6 \pm 3.440$ (SEM) cells/20ml blood (maximum $54x10^6$, minimum $21x10^6$ cells/ml). Cells were successfully isolated from all blood samples taken.
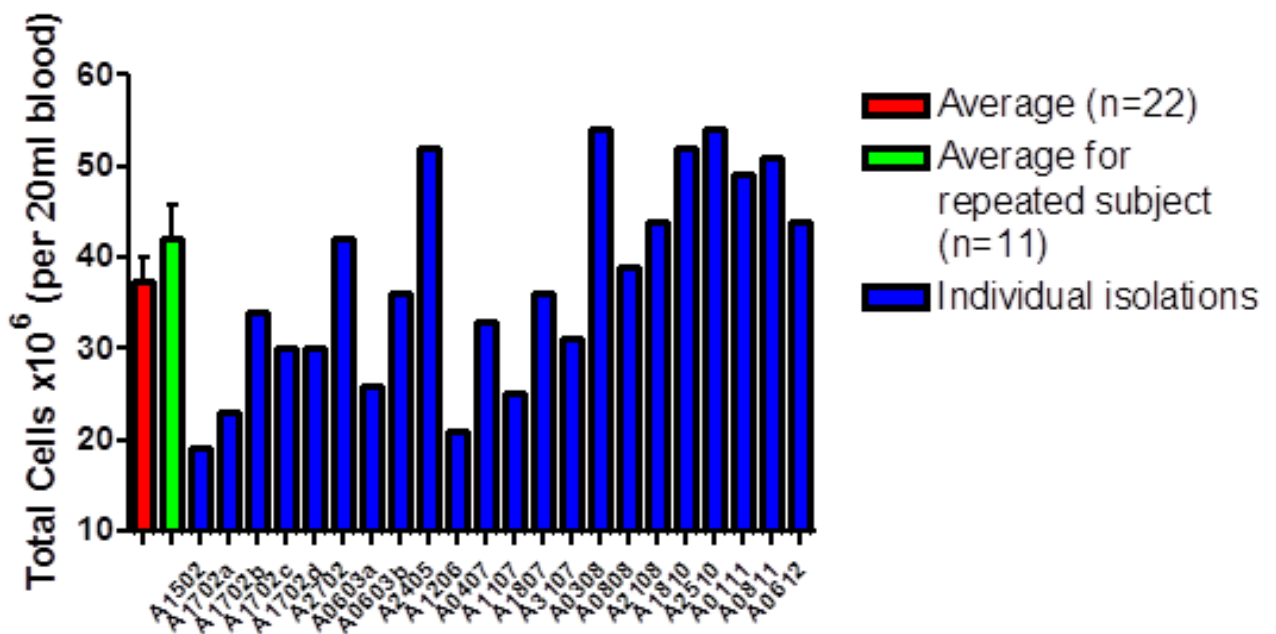
Figure 4.1: Cell isolations by density centrifugation from 20ml human blood. Cells counted by haemocytometer and number adjusted for volume of blood taken. Alphanumeric on the X axis refer to extract codes.

4.3.2 FACS analysis for CD133$^+$/VEGFR2$^+$ EPC

Figure 4.2 shows the number of CD133$^+$ cells per ml of initial cell isolation (all isolations 5ml) as determined by FACS analysis was 131±13.53 cells per ml of cell isolation. For CD133$^+$/VEGFR2$^+$ (EPC) cells 13.65±6.21 were produced per ml of cell isolation.
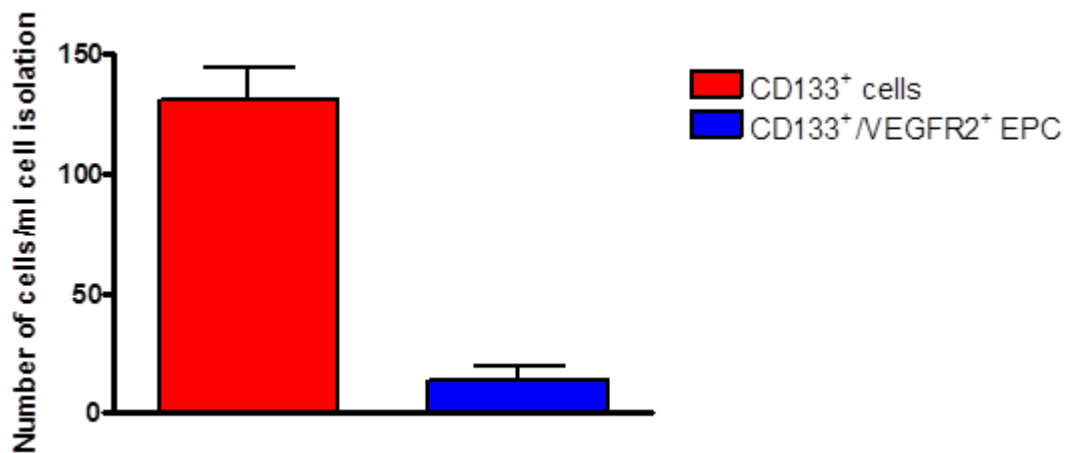
Figure 4.2: FACS analysis of initial cell isolations. Number of CD133+ and CD133+/VEGFR2+ (EPC) cells shown per ml of cell isolation.

4.3.3 Assessment of Cell Metabolism of Cells Seeded on Nanocomposite

Cell metabolism was measured over a 35-day period on seeded nanocomposite films. Cells were present at all time-points measured and there was no significant reduction in cell metabolism over the course of the investigation (Figure 4.3).
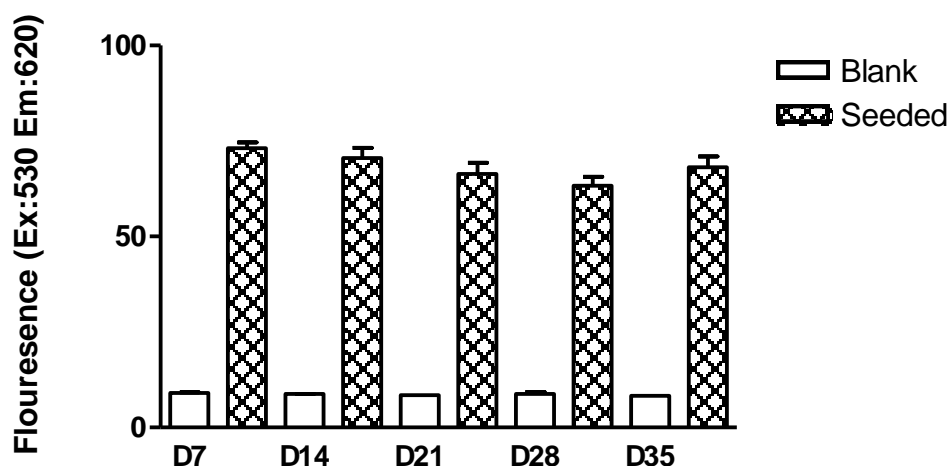
Figure 4.3: Cell metabolism determined by an Alamar blue^{TM} assay up to 35 days (n=5).

4.3.4 RNA Isolation and Investigation of Initial Cell Isolations, Confluent Cells and Day 35 Confluent Cells Seeded on Nanocomposite

Figure 4.4a) demonstrates a 2% agarose gel of three initial cell isolations (A, B and C) examined by RT-PCR for CD14, CD34, CD133 and VEGFR2. All isolations were positive for CD14, CD34, CD133 and VEGFR2. Figure 4.4b) similarly shows a 2% agarose gel of three confluent cell cultures (A, B and C) examined in the same way. CD14, CD34 and VEGFR2 were still detected while CD133 was not found to be present. All negative controls showed no PCR product present. Figure 4.4c) shows a 2% agarose gel of an initial cell isolation (A) and two Day 35 nanocomposite seeded confluent cell samples (B) and (C). The results are similar to those obtained from confluent cells on 6-well plates. Figure 4.4d) shows a 2% agarose gel of two HUVEC cell samples (A and B), two initial cell isolations (C and D) and two Day 35 nanocomposite seeded confluent cell samples (E and F) examined for PECAM-1 and vWF. All the isolations are positive for both genes.
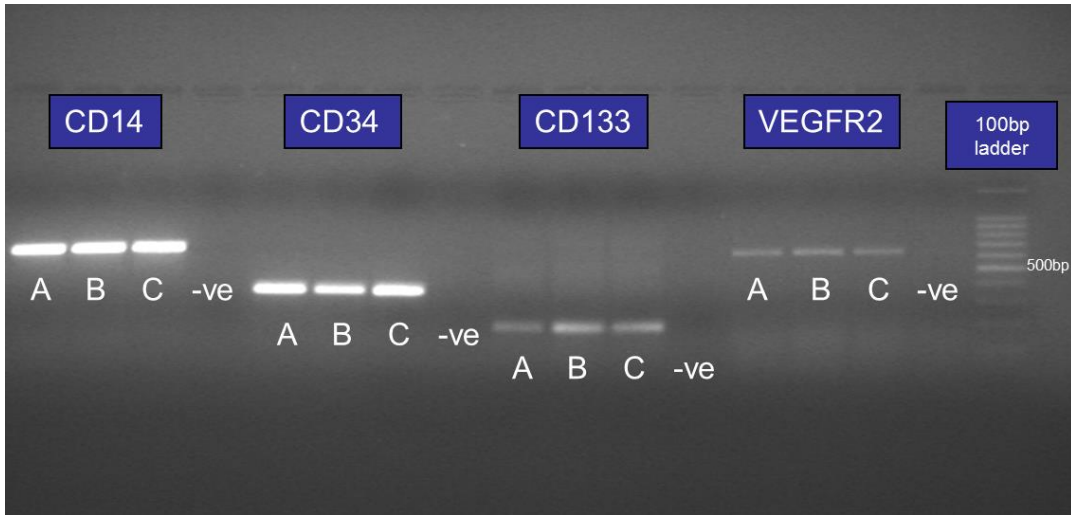
Figure 4.4a) 2% agarose gel of RT-PCR for three initial cell isolations (A, B and C) with CD14, CD34, CD133 and VEGFR2

Figure 4.4b) 2% agarose gel of RT-PCR for three confluent cell isolations A, B and C with CD14, CD34, CD133 and VEGFR2
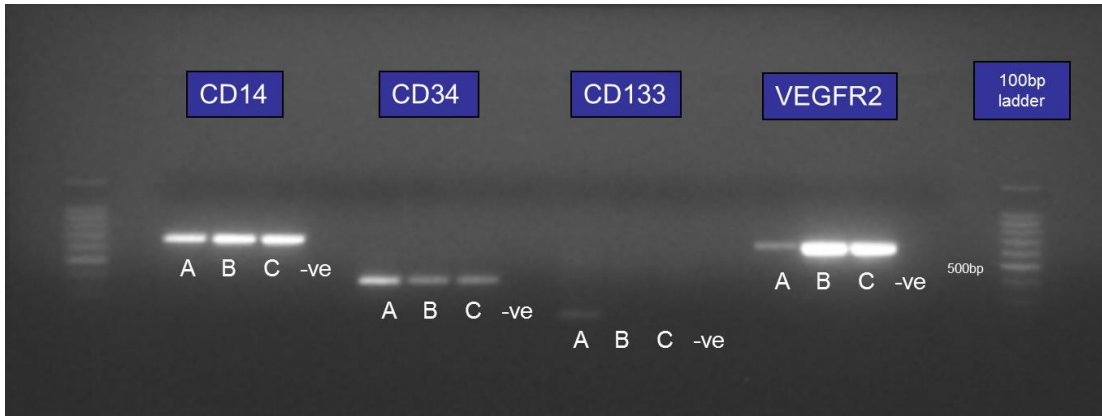
Figure 4.4c) 2% agarose gel of RT-PCR for an initial cell isolation A and two Day 35 nanocomposite confluent seeded samples B and C with CD14, CD34, CD133 and VEGFR2
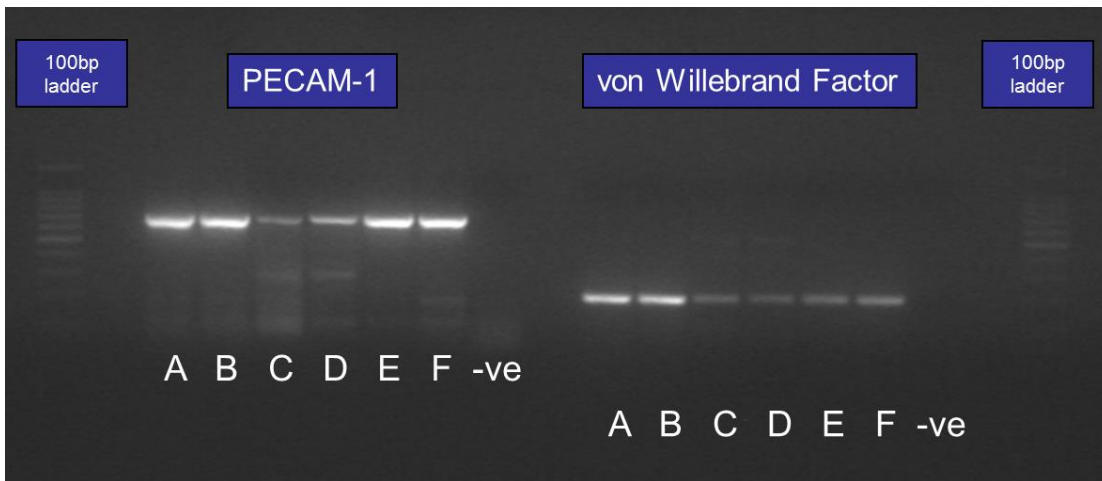
Figure 4.4d) 2% agarose gel of RT-PCR for two HUVEC cell isolations A, B, two initial cell isolations C, D and two Day 35 nanocomposite confluent seeded samples E, F for PECAM-1 and vWF

4.3.5 Giemsa Staining of Cells Seeded on Nanocomposite

Cells seeded on nanocomposite were stained with Giemsa stain at Day's 5, 14, 21 and 35. At Day 5 several Hill Colonies were present. By Day 14 the majority of the nanocomposite is covered by cells with some dense areas of cells where Hill Colonies had developed and this was maintained to Day 35 (Figure 4.5).
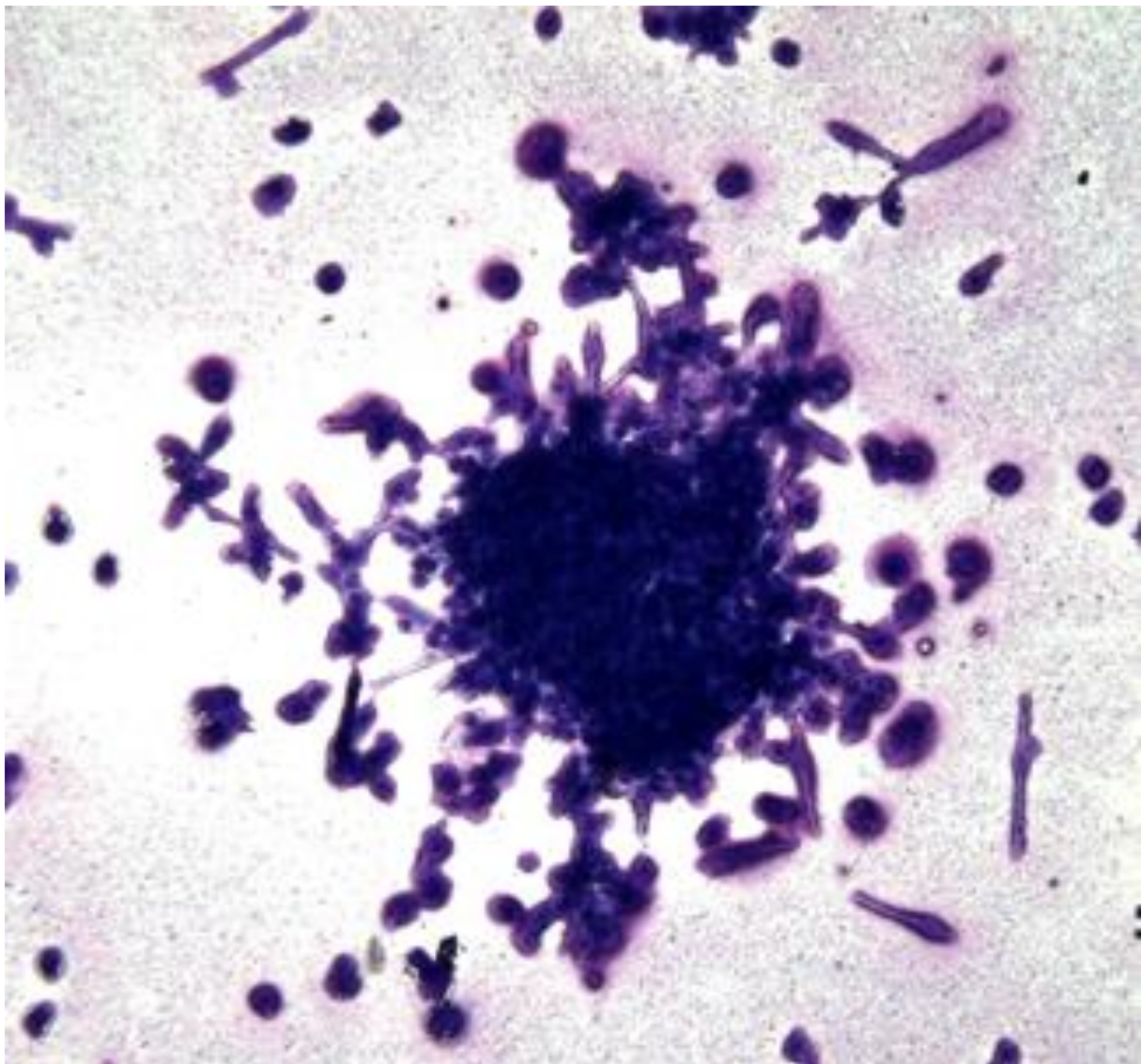
Figure 4.5a): Cells seeded on nanocomposite and stained with Giemsa at Day 5 (x10 magnification)
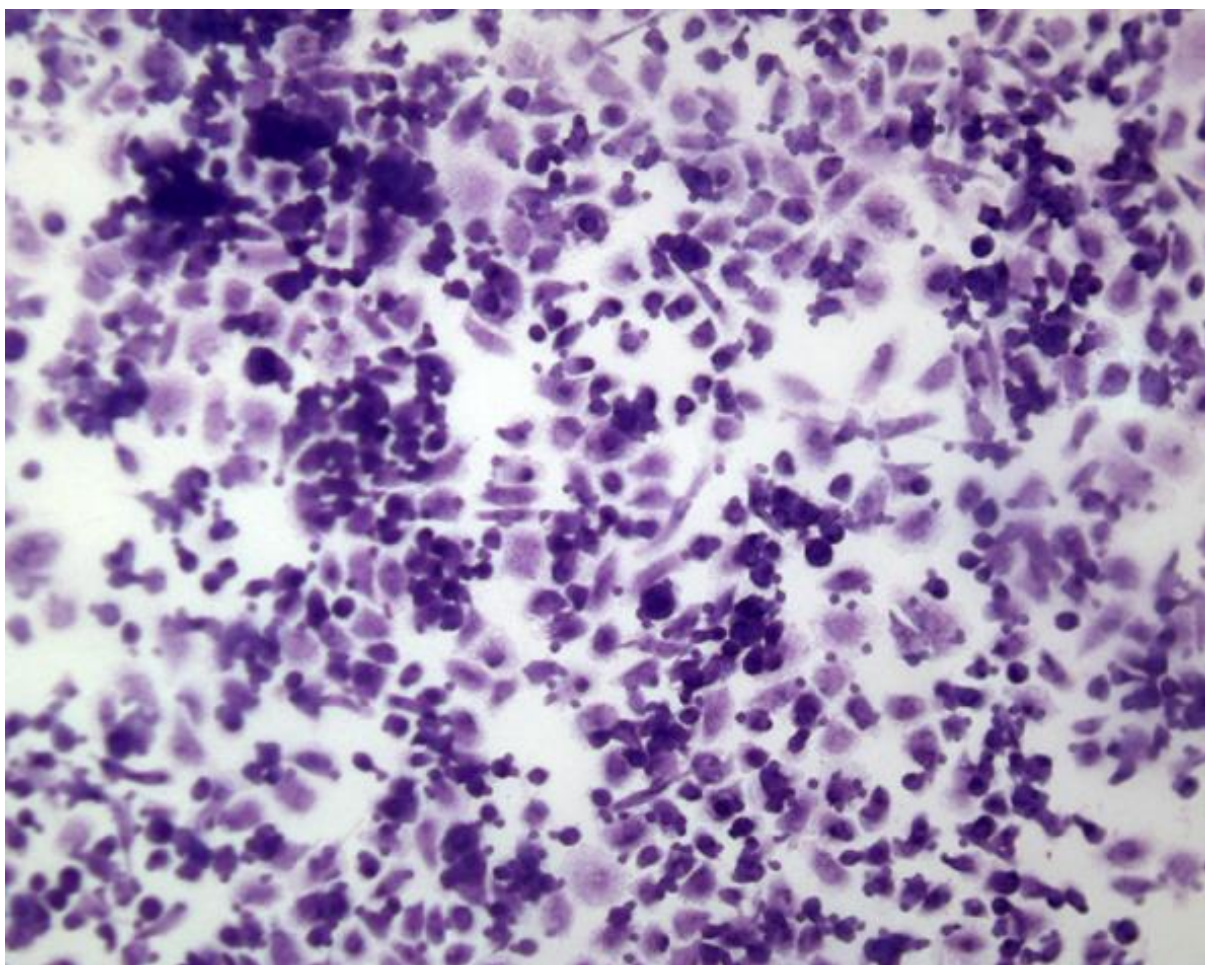
Figure 4.5b): Cells seeded on nanocomposite and stained with Giemsa at Day 14 (x10 magnification)
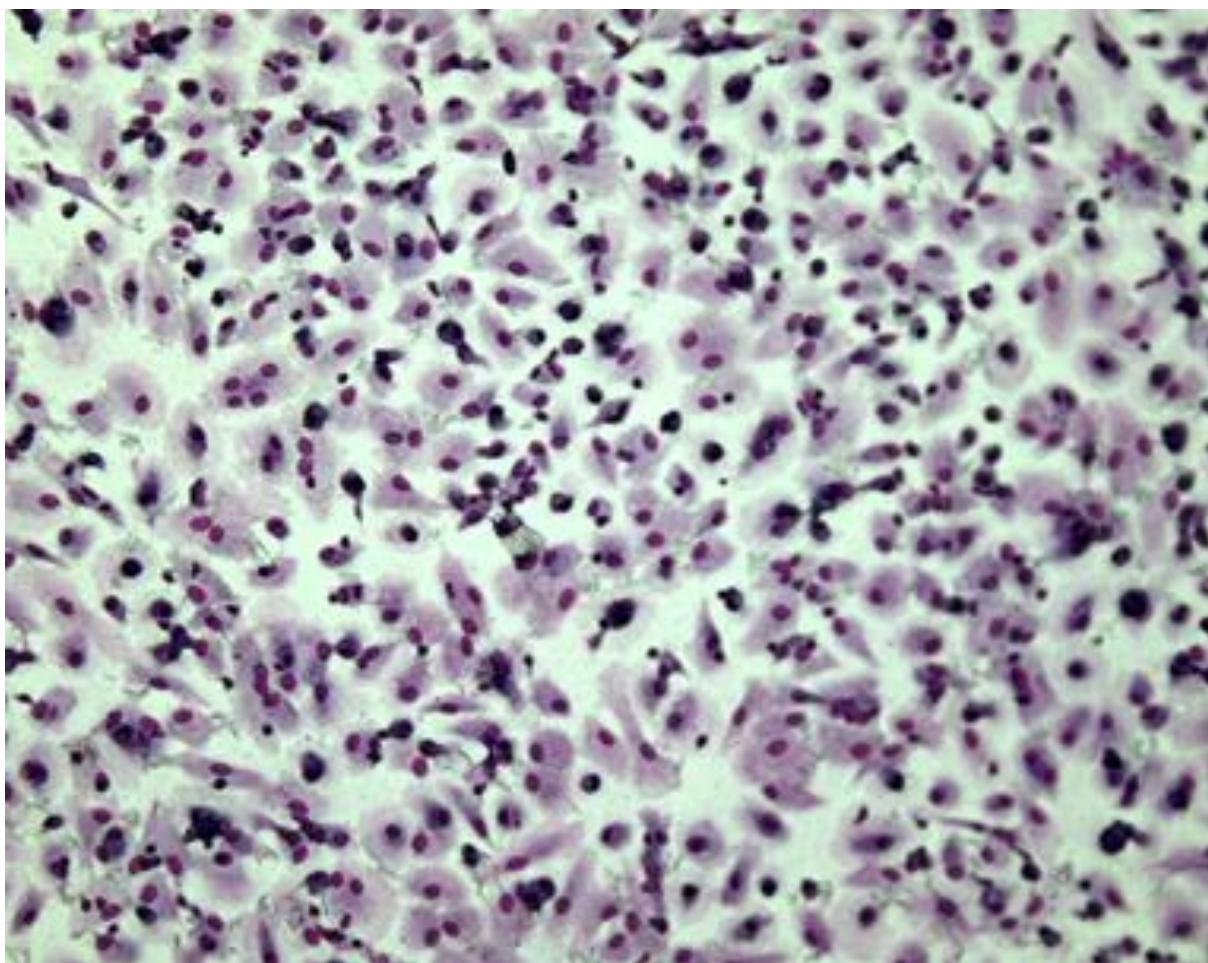
Figure 4.5c): Cells seeded on nanocomposite and stained with Giemsa at Day 21 (x10 magnification)
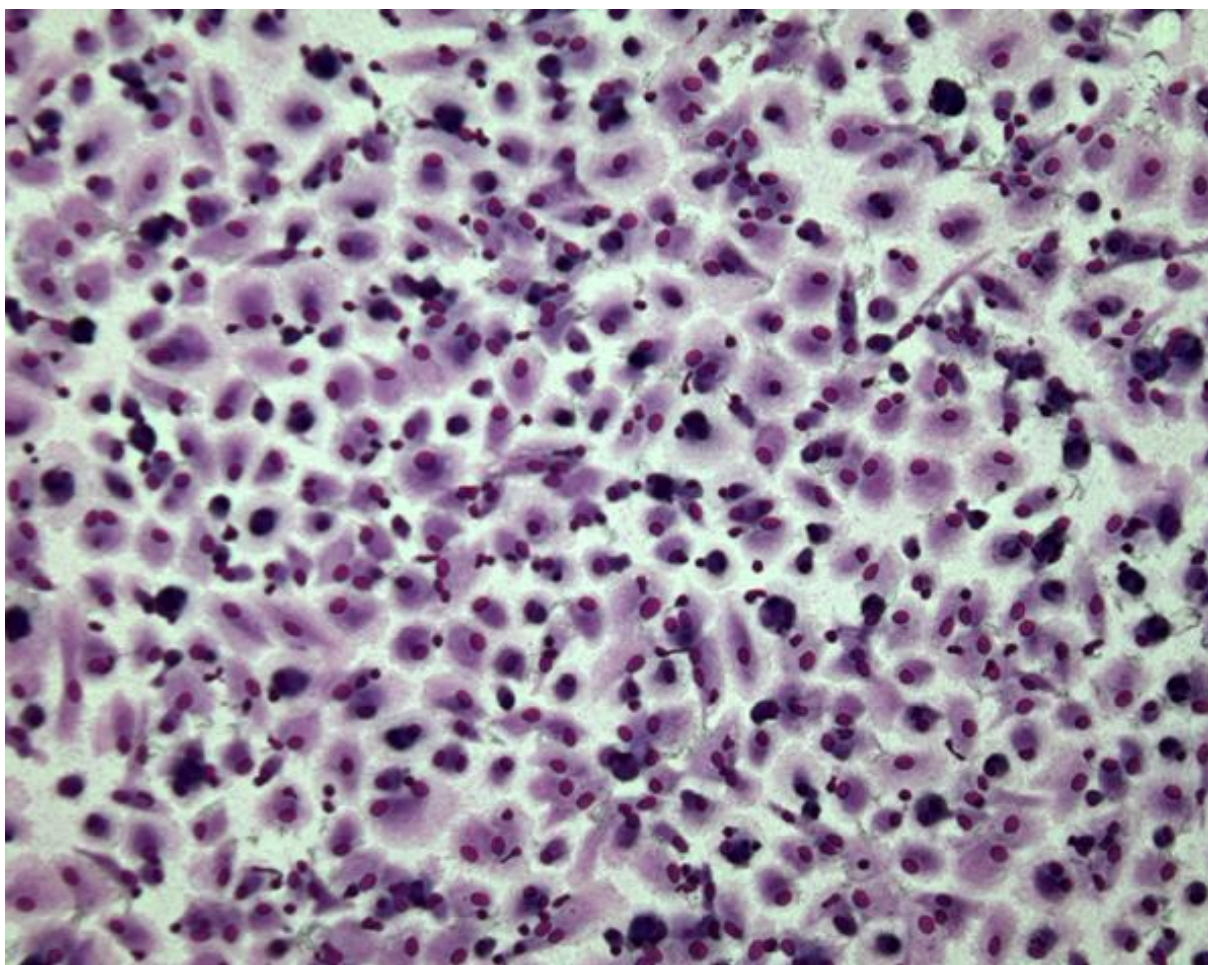
Figure 4.5d): Cells seeded on nanocomposite and stained with Giemsa at Day 35 (x10 magnification).

4.3.6 Scanning Electron Microscopy

Cells were observed in a confluent layer on the nanocomposite (Figure 4.6).
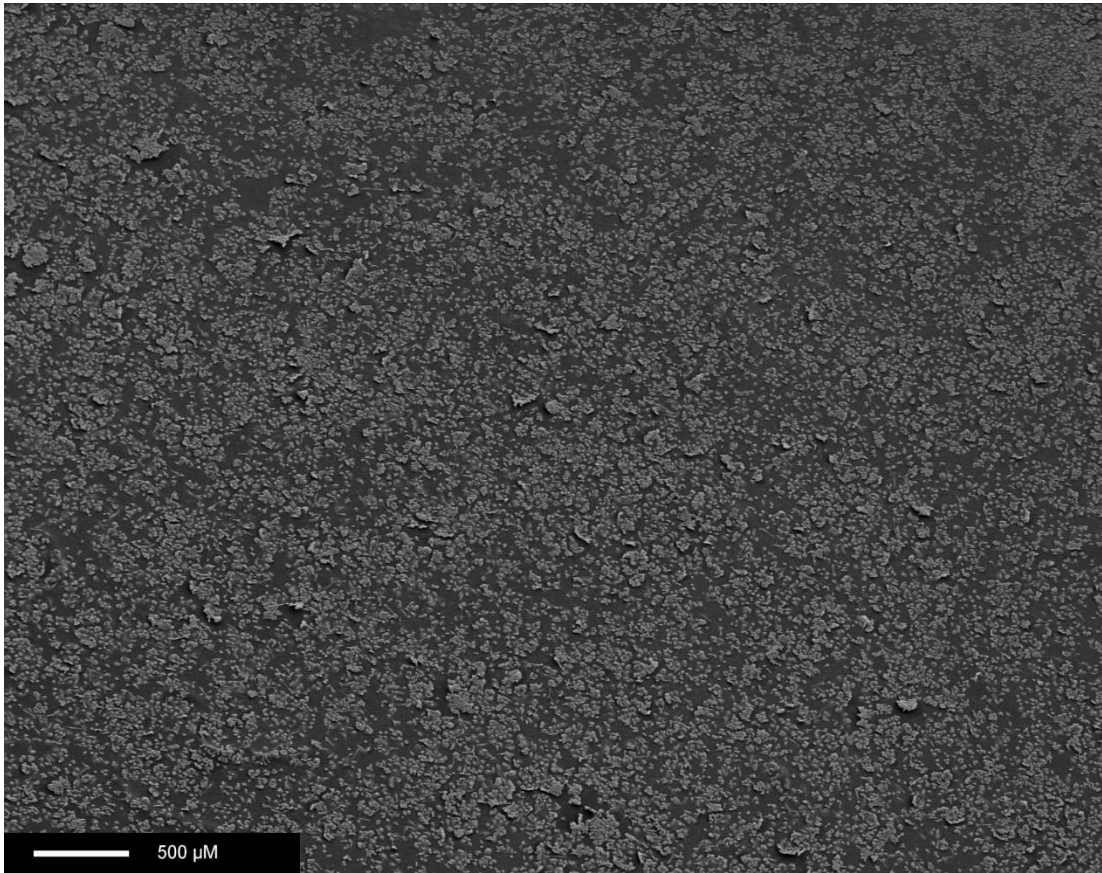
Figure 4.6: Cells were observed in a confluent layer on the nanocomposite at day 35 demonstrated with SEM.

4.3.7 CD34 and CD133 Staining of Initial Cell Isolations, Hill Colonies and Confluent Cells

Figure 4.7 shows staining for CD34 and CD133 on an initial cell isolation sample. All views are of the same cell population. Figure 4.7a) shows a large mixed cell population present with two basic cell types, small round cells and larger round cells. Figure 4.7b) shows cells staining positive for CD34 (FITC (green)). All the larger cells present are stained positive for CD34 whereas only a small proportion of the smaller cells stain CD34^{+ve}. Figure 4.7c) shows cells staining positive for CD133 (Allophycocyanin (red)). All of the larger

CD34^{+ve} cells appear to be CD133^{-ve} whereas again a small proportion of the smaller cells appear to be CD133^{+ve}. Figure 4.7d) shows dual staining for CD34 and CD133. A low proportion of the smaller cells can clearly be seen to be both CD34^{+ve} and CD133^{+ve}.

Figure 4.8 shows three different Hill Colonies i) unstained, ii) stained for CD34 and iii) stained for CD133. All three colonies show clear evidence of CD34^{+ve} and CD133^{+ve} cells.

Figure 4.9 shows staining for CD34 and CD133 on a confluent cell culture sample. All views are of the same cell population. Figure 3.9a) shows a fairly consistent cell population. Figure 4.9b) shows cells staining positive for CD34 (FITC (green)). The majority of cells present are stained positive for CD34. Figure 4.9c) shows cells staining positive for CD133 (Allophycocyanin (red)). Again, the majority of cells express CD133, with a few cells expressing high levels. Figure 4.9d) shows dual staining for CD34 and CD133. The majority of the cells appear to be both CD34^{+ve} and CD133^{+ve} at confluence.
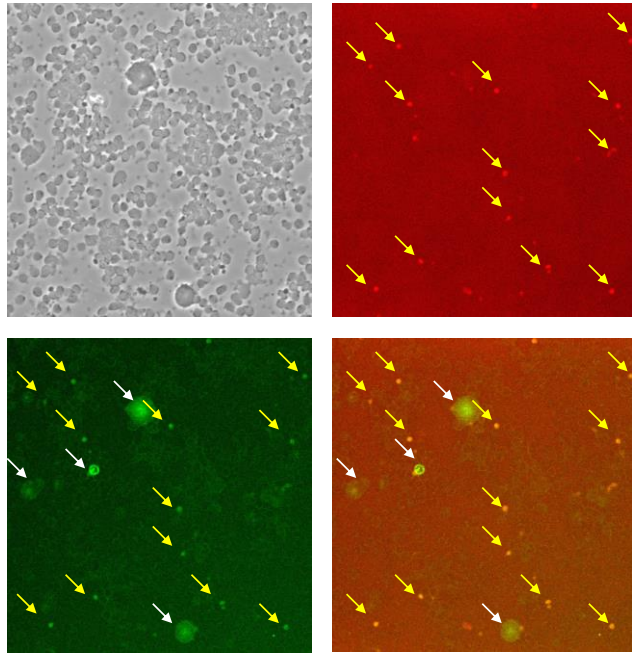
Figure 4.7. Initial cell isolation stained for CD34 and CD133. a) unstained, b) CD34 stained, c) CD133 stained and d) dual stained. All views are of the same cell population (magnification X100).
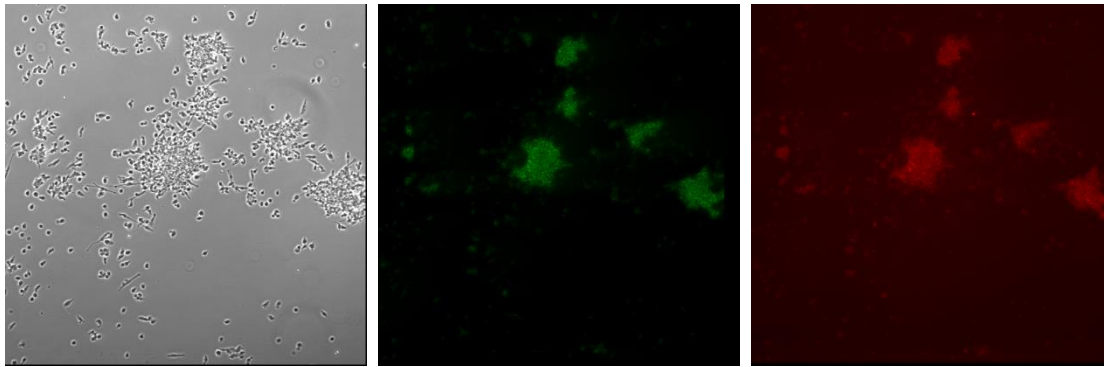
a)
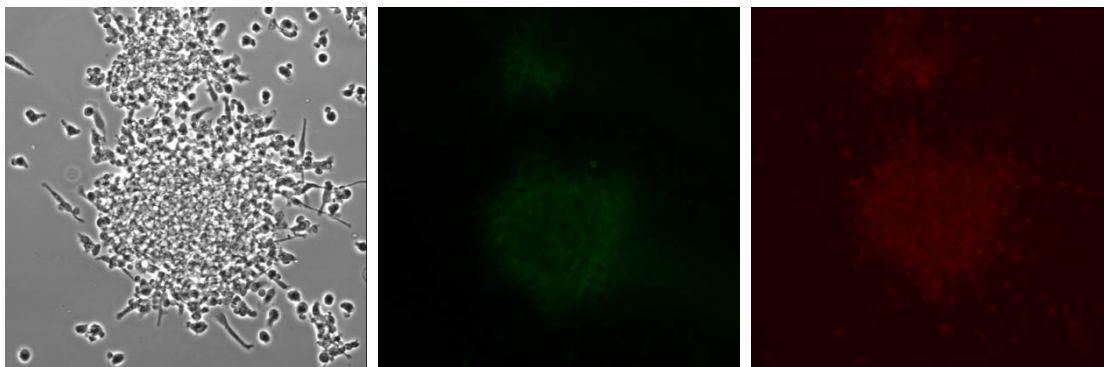
b)
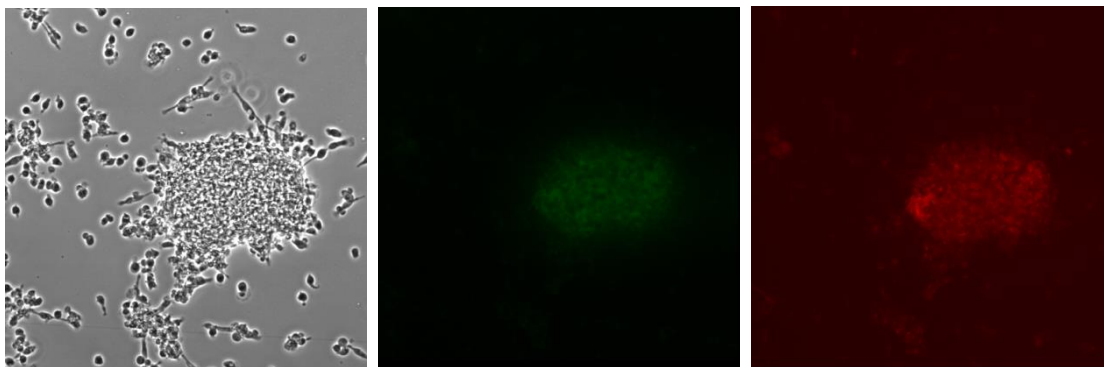
c)

Figure 4.8: Staining of Hill Colonies: three views each stained for i) no fluorescence ii) CD34 (FITC(green)) and iii) CD133 (Allophycocyanin(red)).
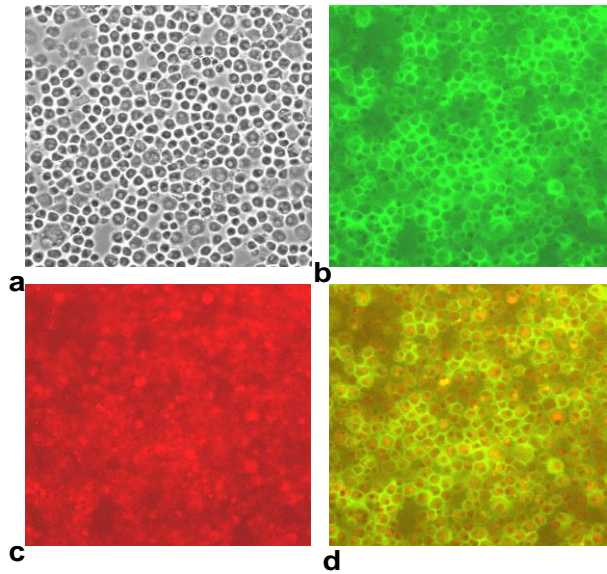
Figure 4.9: Confluent cell culture stained for CD34 and CD133: a) unstained, b) CD34 stained, c) CD133 stained and d) dual stained. All views are of the same cell population (magnification X100).

4.3.8 von Willebrand Factor Staining of Initial Cell Cultures and Confluent Cells

Staining for vWF is demonstrated in Figure 4.10. Figure 4.10a) and c) shows an initial cell isolation stained for vWF with a mixed cell population of small and larger cells. The larger cells are stained strongly positive for vWF. There is also some staining in the smaller cell population in addition. Figure 4.10b) and d) show confluent cell cultures stained for vWF and demonstrates that the majority of the cells are vWF positive.
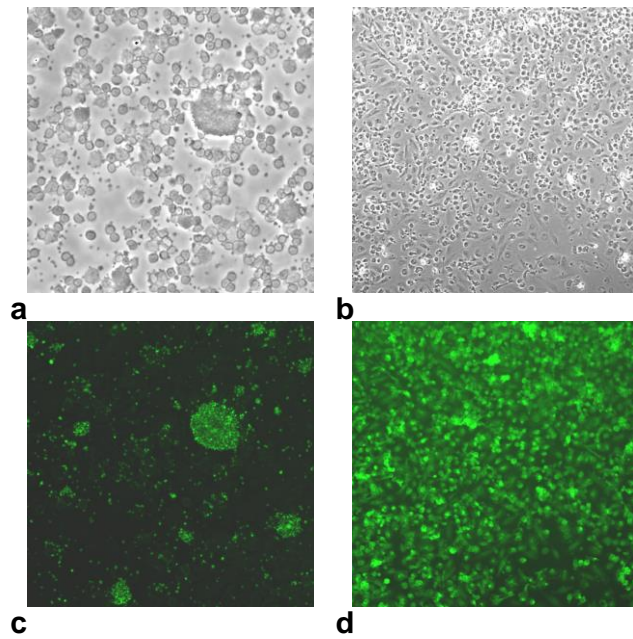
Figure 4.10: Initial cell isolation and confluent cells stained for vWF: a) initial isolation unstained b) confluent cells unstained, c) initial isolation stained for vWF and d) confluent cells stained for vWF (magnification X100).

4.3.9 PECAM-1 (CD31) Staining of Initial Cell Isolations and Confluent Cells

Initial cell isolations stained for CD31 have a small minority of cells stained positive (Figure 4.11a) and c). Confluent cultures demonstrate a low overall level of staining (Figure 4.11b) and d).
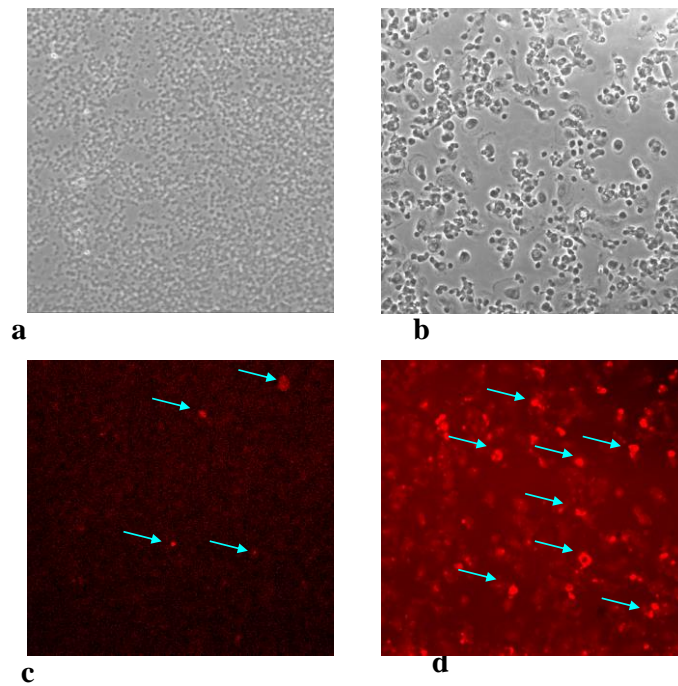
Figure 4.11: Initial cell isolations and confluent cells stained for PECAM-1: a) initial isolation unstained b) confluent cells unstained, c) initial isolation stained for PECAM-1 and d) confluent cells stained for PECAM-1 (magnification X100).

4.4 Discussion

Recent research on adult stems cells has focused upon turning bone marrow cells into a variety of cell types. This is a promising area of study but has many potential pitfalls and the mechanisms involved are complex. More practical at this time from the viewpoint of developing a functional EC-seeded vascular prosthesis may be the use of the EPC first isolated and differentiated into EC by Asahara in 1997 (Asahara *et al.*, 1997). This chapter investigates isolating these cells and their culture on a novel nanocomposite material previously shown to be an excellent candidate for vascular grafts. The results presented in this chapter demonstrate that not only can this material support colonies of EPC but also that they will differentiate into EC then grow to near confluence on the graft and remain viable for a considerable period of time on the nanocomposite surface.

To characterise the initial cell extract a variety of techniques were employed. FACs analysis for $CD133^+/VEGFR2^+$ cells which is the current standard for FACs analysis of EPC {74} demonstrated that EPC were present in the initial cell isolation in numbers similar to those obtained in other studies (George *et al.*, 2006). RNA analysis confirms that in the initial cell extract the monocyte marker CD14 and the EPC/ mature EC marker CD34 are strongly expressed. The stem cell marker CD133 is also expressed to a lesser extent. PECAM-1, VEGFR2 and vWF were also expressed in the initial cell isolations. CD34, CD133, vWF and PECAM-1 were also examined by immunohistochemistry. The initial cell isolation was dual stained for CD34 and CD133 which also indicates the presence of EPC. Initially a mixed population of cells can be seen with some larger cells among a larger number of small cells. When stained for CD34 with the larger cells are clearly positive with a low proportion of the smaller cells also staining positive. When dual stained for CD133 the larger cells which were

positive for CD34 are clearly negative for CD133 (and may thus perhaps be identified as CEC) while the low proportion of the smaller cells which were CD34 positive are also CD133 positive (potentially identified as EPC). When the initial cell extract was stained for vWF again the larger cells are clearly vWF positive (supporting the suggesting that they are CEC) with some fragmentary staining of the smaller cell population. Taken together the above results in this study this suggests that the isolation of EPC from peripheral blood was successfully achieved in line with reports from other groups.

The process for culturing EPC once isolated is currently a matter for debate and experimentation. Many groups use a 'pre-plating' stage after which non-adherent cells are collected and cultured to remove rapidly adhering cells (such as CEC, monocytes and macrophages) which varies from one hour (Asahara *et al.*, 1997; Shirota *et al.*, 2003) to 48 hours (Hill *et al.*, 2003; George *et al.*, 2006). Others omit a 'pre-plating' stage and allow cells to seed for a variety of times ranging from 24 hours (Ingram *et al.*, 2004) to three days (Zhang *et al.*, 2006a) or six days (Hur *et al.*, 2004). In this study a 48-hour pre-plating period was employed. Some samples of the initially adherent cells were continued in culture but failed to prosper (data not shown). Following the pre-plating period cells were left for five days to adhere after which non-adherent cells were disposed of. Again, some samples of the non-adherent cells after five days seeding were continued in culture but did not grow to any extent (data not shown).

All isolations cultured produced viable cell populations and developed a number of colonies with Hill Colony characteristics when seeded on the nanocomposite. Cultures on nanocomposite achieved confluence in 14 days and resulted in cells with a cobblestone appearance by day 21. Cultures were maintained at confluence for a total of 35 days. AB

studies confirmed that metabolically active cells were present over the 35-day period of the study. While the level of cell metabolism does not increase greatly in the initial period this may be due to a combination of monocytes dying off with EPC and CEC proliferating at the same time leading to little net change in the overall level of cell metabolism.

RNA analysis of confluent cells confirms that CD14, CD34 and VEGFR2 expression was maintained though CD133 expression was lost which may be attributed to the conversion of EPC to EC over time. PECAM-1 and vWF expression was also maintained and increased in comparison to that in the initial cell isolations. Immunostaining for CD34 and CD133 again showed that the majority of confluent cells expressed both markers and, in addition, also expressed vWF and PECAM-1. Thus, the conditions employed in this study may be optimal for differentiation (due to the presence of growth factors in the FBS) but not for prolonged division.

The results obtained in this chapter suggest that it is possible to obtain a confluent layer of cells with endothelial-like properties on the nanocomposite after 14 days of culture following extraction from human blood. All the extractions produced viable cells. Previous work has demonstrated that HUVEC attach to the nanocomposite and (particularly with the employment of pre-conditioning) survive on the nanocomposite when exposed to physiological flow (Vara *et al.*, 2006). Thus, the cell extraction method employed compares favourably with the 25 day time-period and failure rates quoted by the clinical studies in two-stage seeding with the added advantage of the ease of blood collection compared to the difficulty of obtaining cells from other sources and the requirement for an additional operation. While it is possible that a mixed population of cells may ensue from the extraction method employed (including monocytes, EPC and CEC) this should not be a major problem

in the application envisaged as the long-term studies carried out in humans suggest that with 9 year patencies EC must be renewing on the graft either by infiltration from the anastomosis or by EPC or CEC attaching from the blood. Thus the initial presence of a seeded layer of cells would seem to be the significant factor in producing a successful graft and improving patency (Asahara *et al.*, 1997; Salven *et al.*, 2003).

4.5 Conclusion

In conclusion, the results presented in this chapter demonstrate that the nanocomposite employed in this study can be successfully seeded with cells derived from human peripheral blood with a confluent layer of cells being observed after 14 days' culture. The cells remained viable and confluent on the nanocomposite for 35 days over the course of the study. These results suggest that this process has potential both for a realistic and achievable two-stage seeding process for vascular bypass grafts or for the potential development of a device with the aim of achieving in-situ seeding once implanted. Further optimisation and development of the technique may result in a clinically successful method for improving the patency of vascular bypass grafts in the future.

5

5 The effect of shear stress on human endothelial cells seeded on cylindrical nanocomposite conduits

5.1. Introduction

Physiological fluid mechanical stimuli are important modulators of vascular cell phenotype and function (Dolan *et al.*, 2011). The major biomechanical forces that have been characterised are a) shear stress, which is the frictional force applied by flowing blood on the inner vessel wall tangential to the vessel wall and b) cyclic stretch (tensile stress), which results from pulsatile pressure (blood pressure) acting perpendicular to the vessel wall (Sarkar *et al.*, 2006). Although the entire vessel wall, including EC's, SMC and the extracellular matrix (ECM) (collagen, elastin, proteoglycans), is subjected to stretch as a consequence of pulsatile pressure, the shear stress is received principally at the EC surface. Experimental studies have been widely carried out where mechanical force-induced changes in cell

function have been measured *in vitro*, using EC cultured mainly on glass or plastic (Boo *et al.*, 2002; Chien, 2008). Shear stress is experimentally generated *in vitro* by flowing fluid across an EC monolayer under controlled kinematic conditions, usually in a laminar flow regime. Flow circuits have been used as an *in vitro* system to investigate the responses of cultured EC to hemodynamic forces at the cellular and molecular level (Illi *et al.*, 2003; Wasserman and Topper, 2004; Chen *et al.*, 2001). EC exposed to shear stress undergo changes in cell shape, alignment and microfilament network remodelling in the direction of flow.

The patency rate of small diameter (<6 mm) cardiovascular grafts has been poor due to the development of anastomotic intimal hyperplasia (IH) and thrombus formation (Kannan *et al.*, 2005a). The formation of an EC layer is a critical factor in the development of a tissue engineered vascular graft (Heyligers *et al.*, 2005) as the endothelium provides a thromboresistant barrier between circulating blood and the surface of the graft. It also controls blood flow and vessel tone (Furchgott *et al.*, 1984; Furchgott and Zawadzki, 1980), platelet activation, adhesion and aggregation (Cucina *et al.*, 2003), leukocyte adhesion (Iiyama *et al.*, 1999) and SMC migration and proliferation (Ward *et al.*, 2001). Currently attempts to seed EC on vascular prosthesis materials are problematic with the major concern being the low number of EC that remain on the graft surface after exposure to *in vivo* shear stress. In an effort to improve cell retention, one approach has been to condition the seeded EC by applying *in vitro* shear stress prior to implantation. Exposure of EC seeded grafts to shear stress has been shown to increase cell retention (Baguneid *et al.*, 2004) and decrease cell loss post implantation (Dardik *et al.*, 1999). There has been considerable interest in studying the effect of applying shear stress to vascular prosthesis seeded with cells and

recently the importance of examining gene expression in this situation has become very apparent.

The development of a polymer containing silsesquioxane in the form of nano-bridges; poly(carbonate-silsesquioxane-bridge-urea)urethane nanocomposite intended for the development of cardiovascular devices (Seifalian *et al.*, 2005) has been reported and patented. This nanocomposite has been characterized and further studies have also demonstrated that it can be successfully seeded with EC and that, once seeded, the EC remain viable for a period of days (Punshon *et al.*, 2005).

EC *in vivo* are highly robust and can resist disruption by haemodynamic shear stress at levels that far exceed physiological conditions. In cell culture, EC rapidly lose many of their differentiated features, and when seeded on vascular graft material they are not sufficiently adherent or differentiated to resist physiologic shear stress. Studies have found that EC exposed to shear stress *in vitro*, applied in a stepwise fashion over days, are induced to become tightly adherent to the substratum and exhibit more differentiated features (Baguneid *et al.*, 2004; Ballermann *et al.*, 1998; Dardik *et al.*, 1999). Therefore, it has long been postulated that the pre-conditioning of EC seeded on vascular grafts with shear stress *in vitro* could be used to improve EC retention and differentiation for subsequent *in vivo* use and avoid or reduce the problems associated with rapid cell loss observed when cells are exposed to physiological shear stress without a prior period of preconditioning.

It has been previously shown that preconditioning prior to exposure to physiological shear stress using a flow circuit developed in-house can significantly enhance EC retention, viability and morphology (Tiwari *et al.*, 2003b). Significantly studies showed the

development of a functional and stable endothelium on the prosthetic vascular graft in response to low shear stress (1-2 dyne/cm^2) (Baguneid *et al.*, 2004; Dardik *et al.*, 1999). One potential mechanism for this observed improvement has been suggested to be regulated by the expression of growth factors and matrix enhancing factors (Passerini *et al.*, 2003). To attempt to elucidate the molecular basis of the behaviour of EC when exposed to shear stress examined the gene expression of EC seeded on a nanocomposite conduit demonstrated that transforming growth factor beta-1 (TGFβ-1), collagenase-1 (COL-1) and platelet endothelial cell adhesion molecule-1 (PECAM-1) gene expression was upregulated after 4 hours of physiological shear stress (Vara *et al.*, 2006).

The aim of this Chapter was to initially examine the application of shear stress for 1 and 4 hours on EC seeded nanocomposite conduits. To provide a comparison to the nanocomposite and validate the methods employed initially identically sized and seeded glass conduits were also examined.

Following this initial investigation, the impact of low flow preconditioning on EC adhesion and retention on cylindrical nanocomposites prior to exposure to physiological flow rates and pressures was examined. Further the effect of a period of recovery under static conditions between the preconditioning episode and the exposure to physiological shear stress is examined and finally potential changes in gene expression which may explain the effects observed monitored.

To examine the effect of preconditioning on cell retention and adherence EC seeded conduits were exposed to a variety of preconditioning regimes with appropriate static and non-preconditioned controls. Conduits were preconditioned by exposure to a low shear stress

of 1-2 dynes/cm^2 for a period of 1 or 4 hours with or without a 24 hour recovery period and then subjected to physiological shear stress of 15 dynes/cm^2 for 4 hours. Cell retention and adherence was then measured using an AB metabolic activity assay and examination by SEM.

5.2. Methods

5.2.1. Preparation of Nanocomposite Polymer Conduits

The inorganic urethane is made from 4,4'-methylenebis(phenyl isocyanate) (MDI), poly(hexamethylene carbonate)diol, and bridged silsesquioxane here bis[3-(trimethoxysilyl)propyl]amine and then chain extended with ethylene diaminell in DMAC.

An automated bio-processor was used to extrude the nanocomposite into conduits with an internal diameter of 5mm and length of 5cm. Conduits were sterilised by autoclaving prior to use.

5.2.2. Glass Conduits

Glass conduits of 5cm length and 5mm internal diameter were manufactured to order (Scientific Laboratory Supplies, Wilford, U.K.). Conduits were sterilised by autoclaving prior to use.

5.2.3. Human Umbilical Vein Cell Culture

HUVEC were isolated from human umbilical cord vein following a previously described method (Jaffe *et al.*, 1973). Cell numbers were amplified by tissue culture in culture medium; prepared as follows: 157 ml M199 medium, 4.5 ml Sodium Bicarbonate (7.5%), 1.5 ml Penicillin/Streptomycin (10,000 U/ml and 10 mg/ml respectively), 40 ml Foetal Bovine Serum and 3.6 ml 200 mM L-Glutamine (Invitrogen Ltd, Paisley, U.K.) at 37° C and 5 %

$CO_2/95 \%O_2$. At confluence cells were removed using 0.25% Trypsin-EDTA (Sigma-Aldrich Company Ltd, Poole, U.K.) and split in a 1:2 ratio. Confluent cultures at passage three were used in all experiments.

5.2.4 Optimisation of Conduit Seeding

HUVEC were cultured to passage three and seeded in five-centimetre length, five-millimetre internal diameter tubular nanocomposite conduits. Following trypsinisation, and resuspension in complete tissue culture medium, a cell count was obtained and diluted in 1ml of complete medium to three cell seeding concentrations; 0.5×10^6 cells, 1×10^6 cells and 2×10^6 cells per conduit. Cells were added as a suspension to each graft segment, the ends of the graft plugged, and the graft segments rotated 90° every 15 minutes for the first two hours to achieve an even covering of HUVEC on each graft. To assess the efficiency of cell adhesion on the nanocomposite, grafts were incubated for four, eight, 12 and 24 hours at 37°C. Unseeded grafts were placed with complete medium and incubated at 37°C. As a comparison and to ensure each technique was carried out accurately the same densities of cells were seeded onto 6-well polystyrene tissue culture plates as above.

5.2.5 Estimation of Cell Damage during Seeding

To assess cell damage over seeding conditions, LDH levels were examined in the media following cell seeding. Fifty microliters cell culture medium from each sample was transferred to a 96-well plate. Fifty microliters substrate mixes (1 vial substrate plus 12 mls assay buffer) was added to each well and the plate covered in foil to prevent light access. Samples were then incubated at room temperature for 30 minutes after which the reaction was stopped by the addition of 50 μl stop solution (1 M acetic acid). Absorbance was then read at 450 nm using a Multiscan MS UV visible spectrophotometer.

5.2.6 Conduit Seeding for Exposure to Physiological Flow

Glass and nanocomposite conduits were seeded with HUVEC at 1×10^6 cells per conduit. Cells were added as a suspension to each conduit, the ends of the conduit plugged, and the conduits rotated 90° every 15 minutes for 2 hours to achieve an even covering of HUVEC on each conduit. Conduits were then left overnight at 37° C and 5 % CO_2/95 %O_2 for efficient cell adhesion and used the next day.

5.2.7 Assessment of Seeding Efficiency and Cell Viability

Viability of seeded cells was assessed using an AB assay (Serotec Ltd., Kidlington, Oxford, U.K.). Following overnight seeding conduits were washed with phosphate buffered saline (PBS) and the washings collected for cell counting to assess seeding efficiency. 1 ml of AB (10%) in complete medium was added to each conduit and incubated for four hours at 37° C and 5 % CO_2/95 %O_2. Duplicate 100 μl samples were removed and the absorbance's read spectroscopically at wavelengths of 570 nm and 630 nm using a Labsystems Multiscan MS UV visible spectrophotometer (Labsystems, Ashford, U.K.). All conduits were washed prior to exposure to flow. Cell viability on nanocomposite conduits was also assessed following exposure to flow.

5.2.8 Design and Validation of a Physiological Pulsatile Flow Circuit

To test the flow shear stress on the EC, a physiological pulsatile flow circuit was used to simulate the cardiovascular system (Figure 5.1).
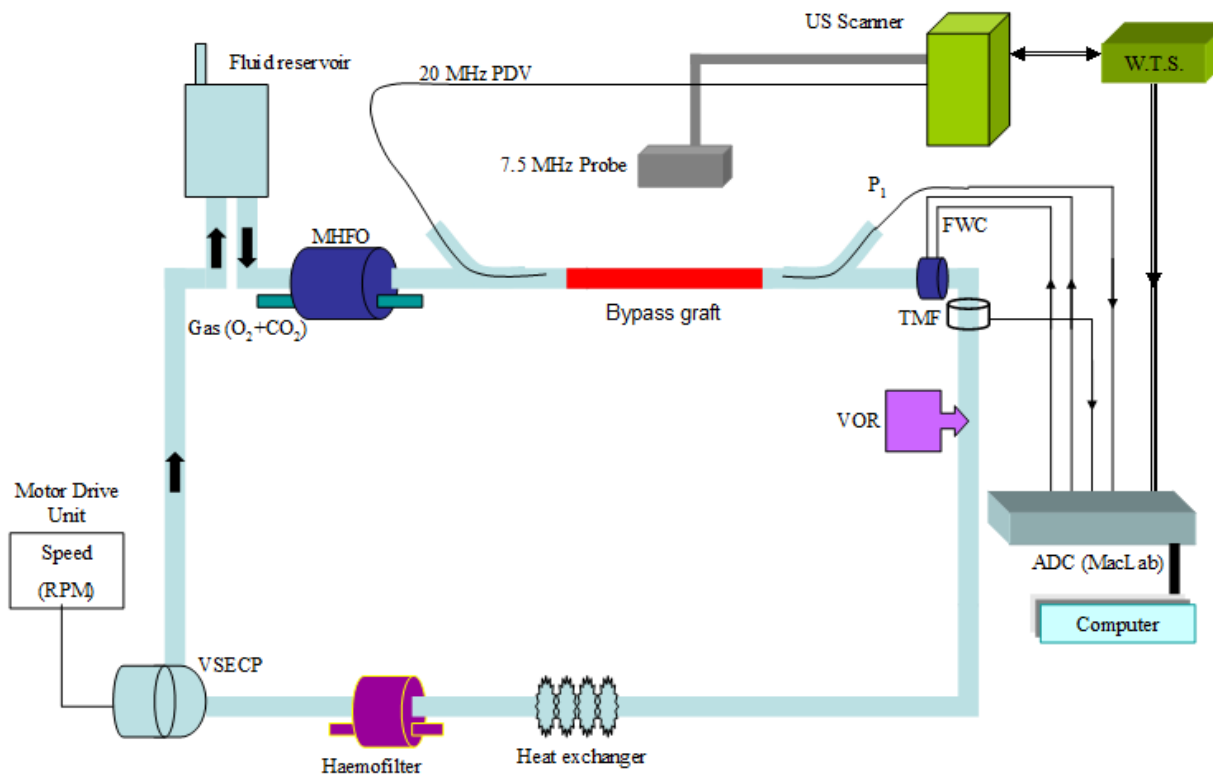
Figure 5.1: The flow circuit comprising a variable-speed electromagnetic centrifugal pump, flexible plastic tubing, fluid reservoir and circulating solution oxygenated through a Maxima hollow fibre oxygenator with 95% air and 5% CO_2. Automatic pH, pO_2 and pCO_2 controller.

A flow waveform conditioner (FWC) sited in series with the circuit is used to generate arterial flow waveforms. This was constructed in-house and consisted of a solenoid connected to an electronic control box from which the frequency and duration of solenoid occlusion could be governed. Instantaneous flow rate is measured using Transonic Medical Flowmeter (TMF) system. Serial intra luminal pressure measurements can be made at discrete sites along the graft using a Millar Mikro-tip catheter transducer introduced via a Y-connection port. Graft radius, flow rate and shear stress are determined using an ultrasound duplex (US) scanner with a wall tracking system (WTS). All outputs are fed into a computer.

The model simulates specifically a given artery such as coronary or lower limb flow waveforms (See caption of Figure 5.1 for further details). The flow circuit was primed with cell culture medium adjusted for viscosity. The whole circuit was kept in a sterilised condition.

Figure 5.2 shows a typical distension and pressure waveform generated from measuring distension and pressure versus time using an ultrasound artery wall tracking system (Wall Track, Pie Medical Systems, Maastricht, Netherlands) and Millar catheter (Millar Instruments, Houston, TX, USA).
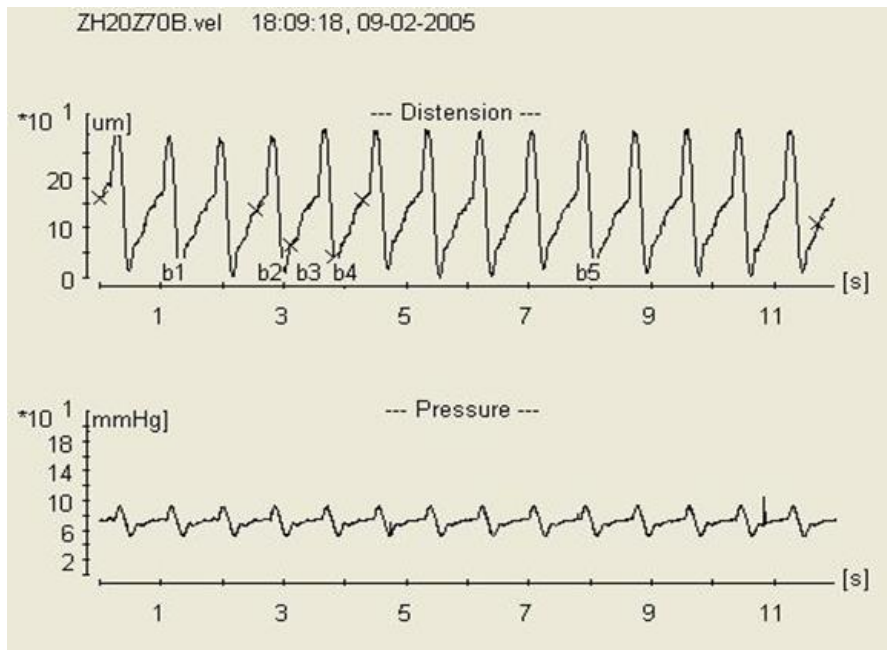
Figure 5.2: Vessel distension detected with ultrasound wall tracking system and pressure with Millar Mikro-tip catheter transducer from circuit in Figure 5.1.

Examples of previously generated plots of the velocity profile inside the artery and shear rate on the wall is shown in Figure 5.3.
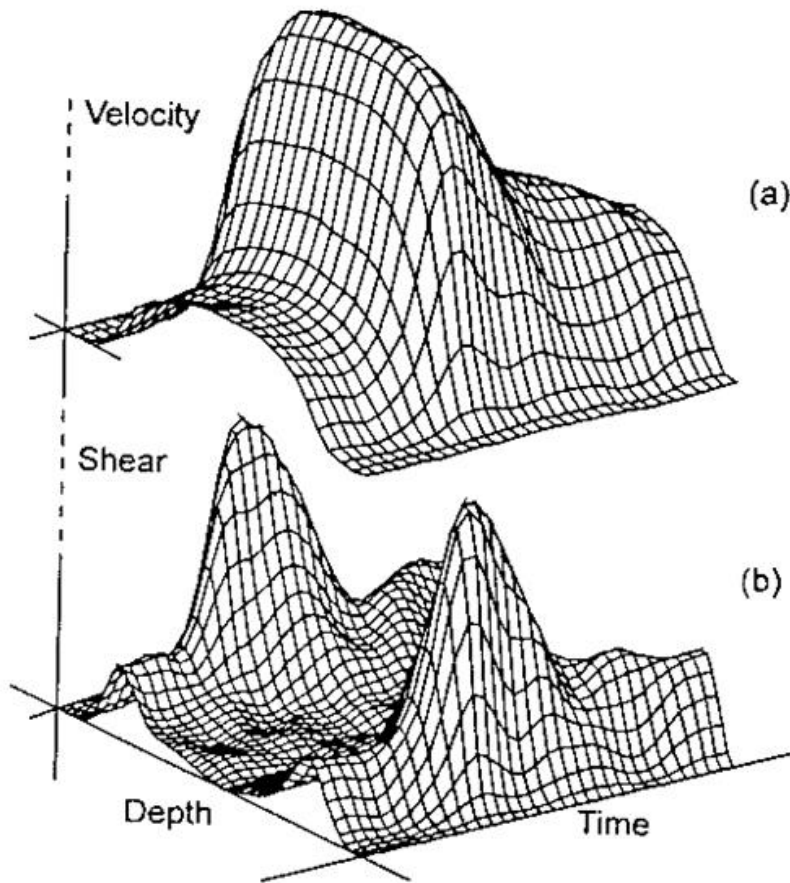
Figure 5.3: A typical time dependent velocity (a) and shear rate distribution (b) acquired by the duplex ultrasound coupled with on-line vessel wall tracking system.

The hemodynamic data including peak and mean shear stresses are computed and recorded in Table 5.1.

Input parameters		Computed parameters	
Frequency of pulsatile cycle	1 Hz	Inlet length (mm)	60
Internal diameter of conduit	5 mm	Peak Reynolds number	512
Temperature	37 ± 1.4	Mean shear stress (dyn/cm^2)	14.0 ± 3.2
Seeded graft length (mm)	50	Systolic shear stress (dyn/cm^2)	30.4 ± 5.8
Seeded density (cells/cm2)	1.2×10^4	Diastolic shear stress (dyn/cm^2)	62.7 ± 9.7
Pressure systolic (mmHg)	120 ± 5	Mean velocity (mm/sec)	436 ± 20
Pressure diastolic (mmHg)	70 ± 6		
pH	7.3 ± 0.1		
pO2 (kPa)	21 ± 2		
pCO2 of solution (kPa)	4.2 ± 0.2		
Viscosity of solution (poise)	0.035 ± 0.2		

Table 5.1: Flow circuit haemodynamic data including peak and mean shear stresses

5.2.9 Application of Shear Stress to EC Seeded Conduits

Seeded conduits were randomly split into two groups, static and flow exposed. Static conduits were placed in fresh medium and incubated at 37°C for either 1 or 4 hrs. Flow exposed conduits were placed in the flow system and a set flow rate of shear stress was applied for either 1 or 4 hrs.

5.2.10.1 Application of Preconditioning Shear Stress on EC Seeded Conduits

The experimental protocol is summarised in Figure 5.4. Seeded conduits were randomly split into two groups (A & B) where preconditioning was tested with or without a static recovery period (see below). Conduits were placed in the flow system and preconditioned at low shear stress rates of 1-2 dynes/cm^2(low flow) and then subjected to pulsatile physiological shear stress of 15 dynes/cm^2 (physiological flow).
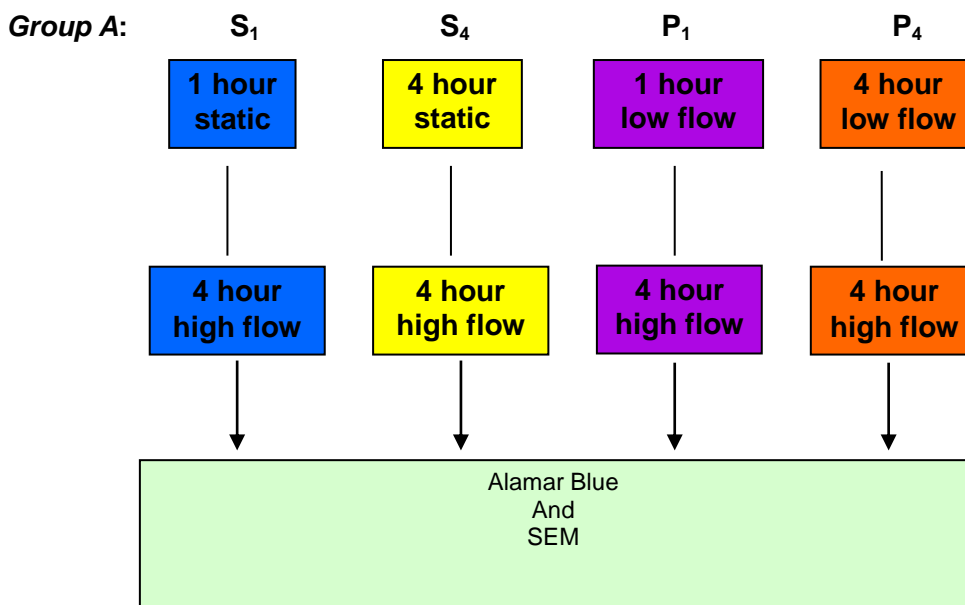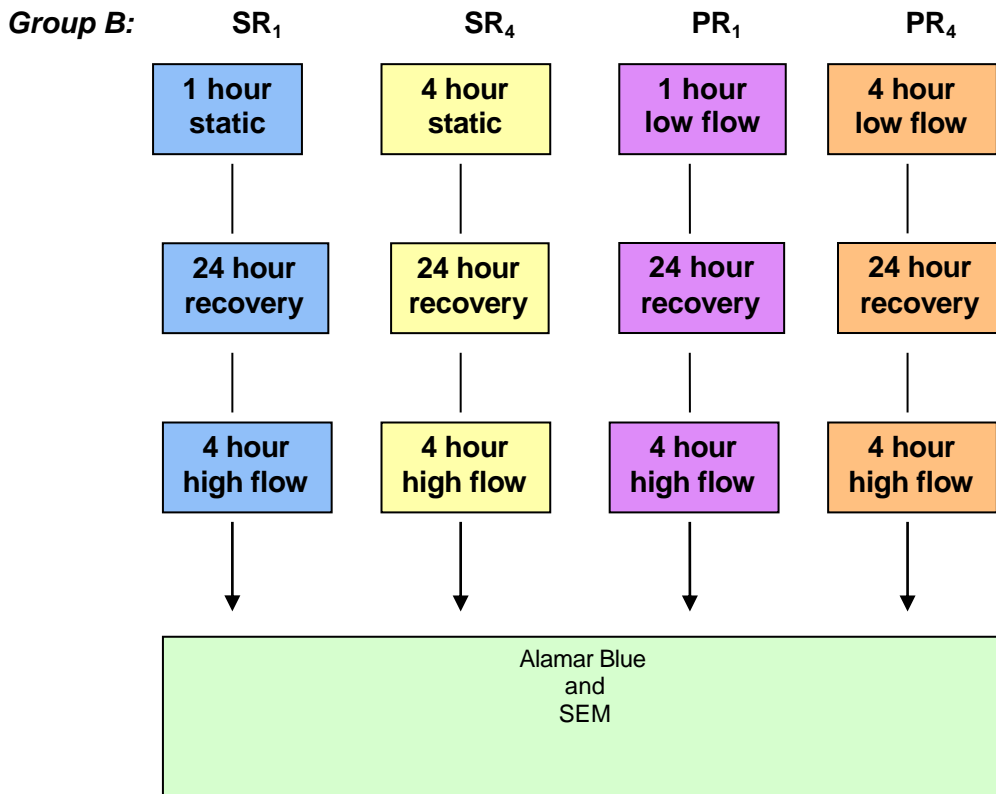
Group A:

S_1	S_4	P_1	P_4
1 hour static	4 hour static	1 hour low flow	4 hour low flow
↓	↓	↓	↓
4 hour high flow	4 hour high flow	4 hour high flow	4 hour high flow

Alamar Blue And SEM

Group B:

| SR₁ | SR₄ | PR₁ | PR₄ |

Figure 5.4: A schematic representation of the experimental procedure illustrating a summary of the treatment carried out to each set of conduits. Group A conduits were exposed to either 1 or 4 hours static (S_1 or S_4) or preconditioning (P_1 or P_4) prior to exposure to 4 hours physiological flow while Group B conduits were exposed to either 1 or 4 hours static (SR_1 or SR_4) or preconditioning (PR_1 or PR_4) followed by a 24 hour static recovery period prior to exposure to 4 hours physiological flow.

5.2.10.2. Preconditioning Shear Stress without a 24-hour recovery period

To test the effect of preconditioning shear stress on EC function without a static recovery period, group A conduits were preconditioned with 1 hour low flow (P_1) or 4 hours of low flow (P_4). Control conduits were also included where conduits were placed with fresh culture medium and incubated under static conditions at 37° C and 5 % CO_2/95 %O_2 for 1 hour (S_1)

or 4 hours (S_4). All conduits were then subsequently exposed to 4 hours of physiological flow.

5.2.10.3 Preconditioning Shear Stress with a 24-hour recovery period

The effect of preconditioning with a 24-hour static recovery period prior to physiological flow was investigated. After 24 hours of seeding, group B conduits were either preconditioned with 1 hour low flow (PR_1) or 4 hours of low flow (PR_4). Control conduits were incubated under static for 1 hour (SR_1) or 4 hours (SR_4). After static or exposure all conduits were then washed with sterile PBS, placed in fresh culture medium and incubated under static conditions for 24 hours. Post recovery period, all conduits were exposed to 4 hours of physiological flow.

5.2.11. RNA Extraction and PCR following Preconditioning Shear Stress

Following exposure to experimental conditions cells were removed from conduits by washing with sterile PBS and then trypsinising using 1ml of trypsin-EDTA (0.25 %) which was added for 5 minutes' incubation at 37oC. RNA was then extracted by using a "Qiagen RNeasy" kit (Qiagen Ltd, Crawley, U.K.).

The RNA concentration and purity was calculated by measuring the absorbance at 260nm and 280nm using an Eppendorf Biophotometer (EppendorfAG, Hamburg, Germany). The quality of the RNA was assessed by 2% agarose gel electrophoresis. The mRNA obtained was used for polymerase chain reaction (PCR) of GAPDH, TGFβ-1, VEGFR-1, PECAM-1 and VEGFR-2 genes (Table 5.2.). RT-PCR was performed using a one-step PCR kit (Qiagen Ltd, Crawley, U.K.). A master mix containing 10 μl 5x Qiagen One-Step RT-PCR buffer, 10 μl 5x Q-Solution, 400 μM from each of the deoxynucleoside triphosphate, 2 μl Qiagen One-

Step RT-PCR enzyme mix and 0.5 μM from each of the primers was added. 0.1 μg of template RNA was used for each gene and RNase free water was added to give a total volume of 50 μl.

Cycle conditions for GAPDH and TGFβ-1 were 40 cycles (94º C, 50º C and 72º C). For PECAM-1 cycle conditions were 35 cycles (94º C, 50º C and 72º C). Finally, for VEGFR-1 and VEGFR-2 cycle conditions were 35 cycles (94º C, 59º C and 72º C). Amplification was carried out using a MasterCycler Gradient PCR machine (EppendorfAG, Hamburg, Germany). PCR products were analysed by 2% agarose gel electrophoresis and semi-quantified using a GeneGenius darkroom with 'GeneSnap' version 6.02. (Syngene, Cambridge, U.K.). The GAPDH band was used as the internal standard to normalise TGFβ-1, VEGFR-1, PECAM-1 and VEGFR-2 signals.

Locus	Sense (5'-'3)	Antisense (5'-'3)
GAPDH	GAAGGTGAAGGTCGGAGT	GAAGATGGTGATGGGATTTC
TGFβ-1	CACCTGCAAGACTATCGACAT	TCGGAGCTCTGATGTGTTGAA
PECAM-1	GCTGTTGGTGGAAGGAGT	GAAGTTGGCTGGAGGTGCTC
VEGFR-1	ATTTGTGATTTTGGCCTTGC	CAGGCTCATGAACTTGAAAGC
VEGFR-2	GTGACCAACATGGAGTCGTG	CCAGAGATTCCATGCCACTT

Table 5.2: GAPDH, TGFβ-1, PECAM-1, VEGFR-1and VEGFR-2 Primer Sequences.

5.2.12 Scanning Electron Microscopy

Seeded nanocomposite conduits were examined by SEM pre- and post-flow to visualise whether cells were present on the grafts surface. SEM images were also taken after trypsinisation of the cells from the conduit in order to determine that complete cell removal was obtained for RNA extraction. Due to the material nature of the glass tubes SEM was not performed for these samples.

5.2.13 Data Analysis and Statistical Methods

The experiments were repeated 4 times. All statistical analysis utilised the Student's t-test comparing flow to static conditions.

5.3. Results

5.3.1 Optimisation of Conduit Seeding Density
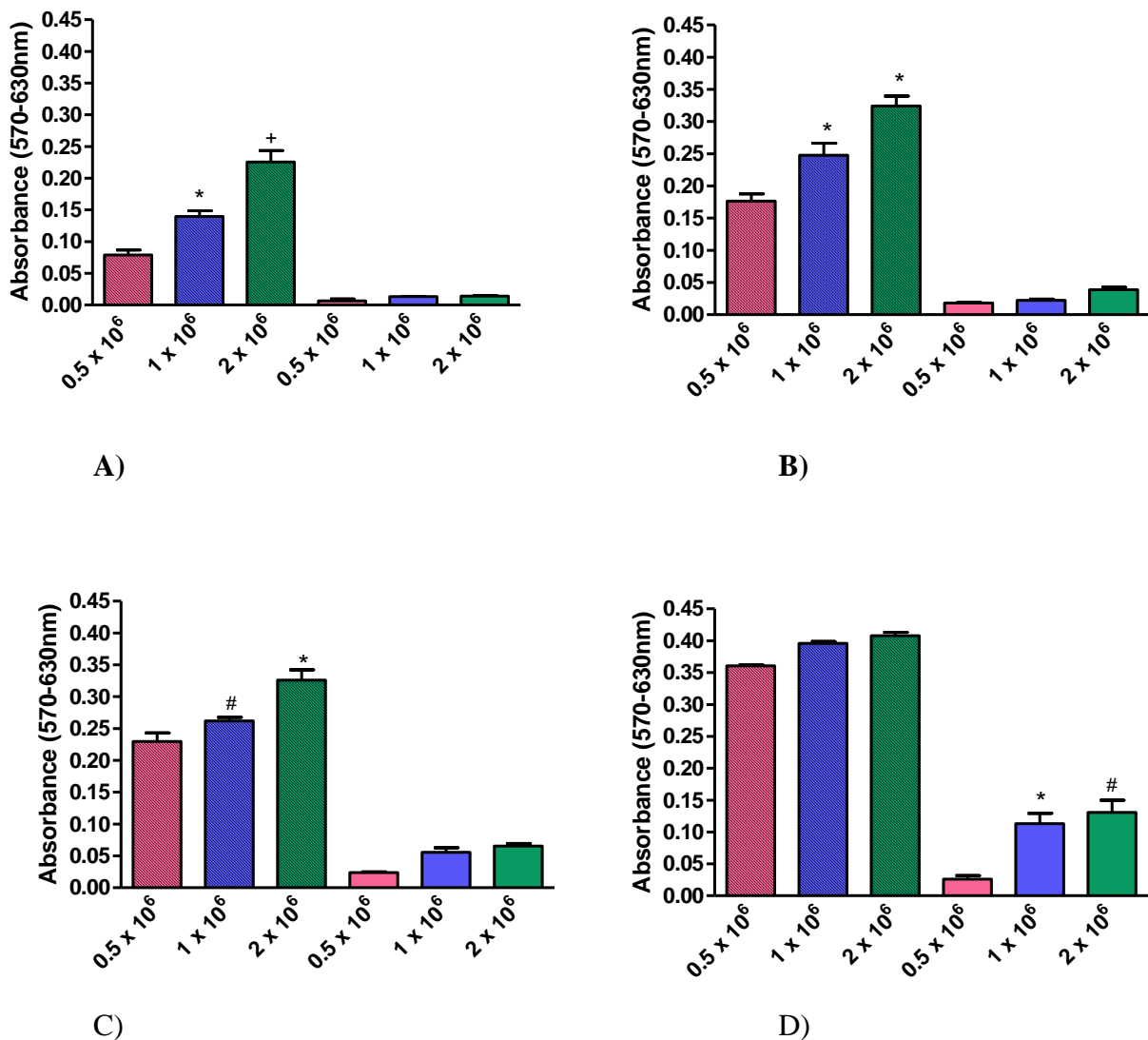
A)

B)

C)

D)

Figure 5.5: Alamar blue[TM] cell viability assay post HUVEC seeded on TCP and nanocomposite conduits at cell seeding densities of 0.5×10^6 cells/cm^2, 1×10^6 cell/cm^2 and 2×10^6 cells/ cm^2 after A) 4 hours, B) 8 hours, C) 12 hours and D) 24 hours of seeding time.

Significant differences ($p< 0.001$) in cell viability were observed between the TCP and nanocomposite groups at all seeding time points. There were no significant differences in cell viability in nanocomposite conduits that were seeded for 4, 8 or 12 hours (Figure 5.4.1 A; B & C respectively) between any of the seeding densities. Significant increases in viability were only seen at 24 hours in nanocomposite conduits seeded with 1×10^6 cells/cm^2($p< 0.01$) and 2×10^6 cells/cm^2($p< 0.001$) compared to 0.5×10^6 cells/cm^2. At 24 hours post seeding, no differences were observed in cell viability in nanocomposite conduits seeded with 1×10^6 cells/cm^2 compared to 2×10^6 cells/cm^2.

Figure 5.5 shows AB cell viability results of nanocomposite conduits seeded at three cell densities of A) 0.5×10^6 cells/cm^2, B) 1×10^6 cells/cm^2 and C) 2×10^6 cells/cm^2 comparing across 4, 8, 12 and 24 hours seeding time. Conduits seeded with 0.5×10^6 cell/cm^2 (Figure 5.5 A) showed significant increases ($p< 0.05$) in cell viability at 12 and 24 hours only compared to 4 hours seeding time. There was no significant difference between any other seeding time points in this seeding density. At 1×10^6 cells/cm^2 (Figure 5.5 B) and 2×10^6 cell/cm^2 (Figure 5.5 C), nanocomposite conduits showed a significant increase in cell viability post 12 ($p< 0.05$) and 24 hours ($p< 0.001$) of seeding compared to 4 hours. Increases were also observed after 24 hours ($p< 0.001$) seeding compared to 8 hours. At this seeding density a significant difference ($p< 0.01$) was seen at 24 hours compared to 12 hours.

A)

B)

C

D)
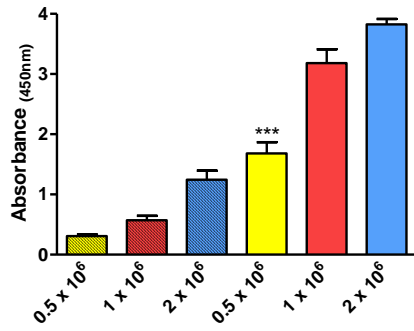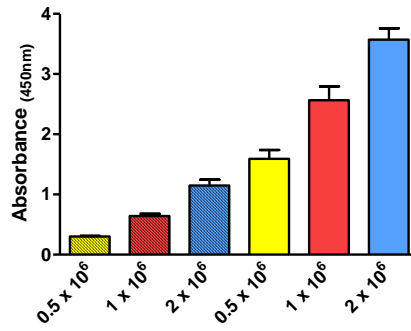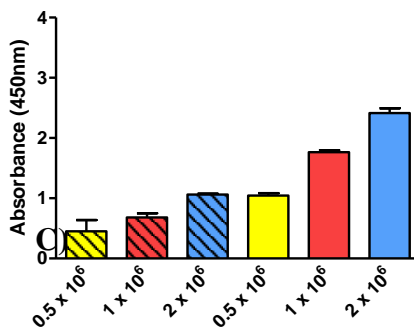
E)
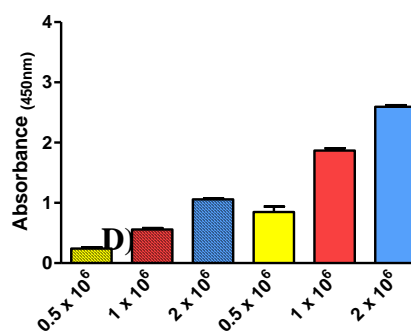
F)

Figure 5.6: LDH assay test measuring cell toxicity on HUVEC seeded on TCP and nanocomposite conduits at 0.5×10^6, 1×10^6 and 2×10^6 for A) 4 hours, B) 8 hours, C) 12 hours and D) 24 hours of seeding time. $*P < 0.05$, $**P < 0.01$ and $***P < 0.001$ using one-way ANOVA with Tukeys

Figure 5.6 shows the LDH assay for cells seeded on nanocomposite conduits and TCP at 0.5 x 10^6, 1x 10^6 and 2 x 10^6 cells/cm²for A) 4 hours; B) 8 hours; C) 16 hours and D) 24 hours of seeding time.

HUVEC seeded on TCP was used as a control. Differences in LDH activity were observed in all cell densities seeded in TCP compared to those seeded in nanocomposite conduits at 4, 8, 12 and 24 hours of seeding.

There was a significant difference between 0.5 x 10^6 and 1 x 10^6 cells/cm² post 4 hours ($p< 0.001$), 8 hours ($p< 0.01$), 12 hours ($p< 0.01$) and 24 hours ($p< 0.001$) seeding time on the nanocomposite conduits. After 4 hours of seeding time there was no significant difference between 1 x 10^6 cells/cm² and 2 x 10^6 cells/cm² seeded on nanocomposite conduits. This was significant post 8, 12 hours ($p< 0.01$) and 24 hours ($p< 0.001$).

Figure 5.6 shows the LDH assay for cells seeded on nanocomposite conduits at A) 0.5 x 10^6 cells/cm²; B) 1 x 10^6 cells/cm² and C) 2 x 10^6 cells/cm² for 4, 8, 12 and 24 hours. Cells seeded on nanocomposite conduits at a density of 0.5 x 10^6 cells/cm² (Figure 5.6 A) showed a significant difference between 4 and 24 hours ($p< 0.01$); 4 and 12 and 8 and 24 hours ($p< 0.05$) of seeding time. There was no significant difference in seeding time between 12 and 24 hours of incubation at this cell density.

Nanocomposite conduits seeded with HUVEC at 1 x 10^6 cells/cm² (Figure 5.6 B) showed a higher level of LDH activity at 4 hours compared to 12 and 24 hours ($p< 0.01$). This was also significant for 8 hours compared to 12 hours ($p< 0.05$) of seeding incubation time on the nanocomposite conduits.

HUVEC seeded nanocomposite conduits at 2 x 10^6 cells/cm^2 (Figure 5.6 C) showed a significant higher ($p< 0.001$) LDH activity at 4 hours compared to 12 and 24 hours of seeding. Significant differences were also observed at 8 hours of seeding compared to 12 ($p< 0.001$) and 24 hours ($p< 0.01$) seeding time on the conduits.

5.3.2 Assessment of Seeding Efficiency and Viability

An Alamar blue^{TM} assay pre flow following overnight seeding showed no significant difference in seeding efficiency (data not shown).

5.3.3 Assessment of Cell viability after exposure to flow

Viable cells were present on both the glass conduit group and the nanocomposite conduit group following exposure to flow or static conditions (Fig. 5.7 A (Glass) & B (nanocomposite)) with no significant difference between groups.
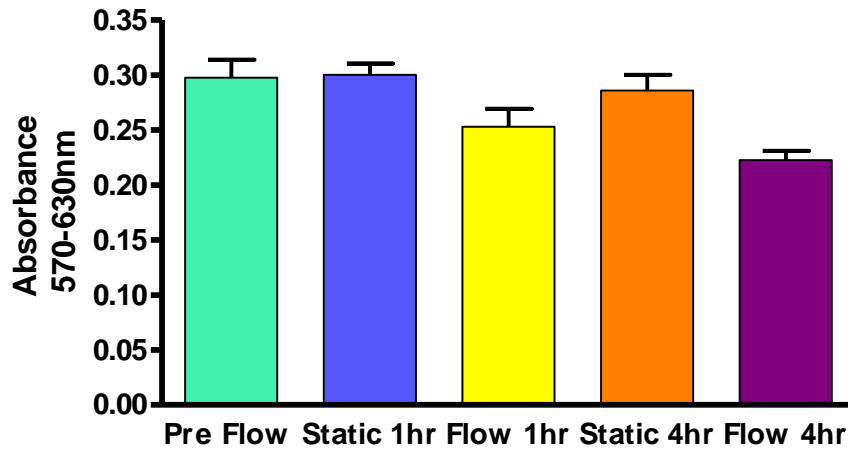
A)
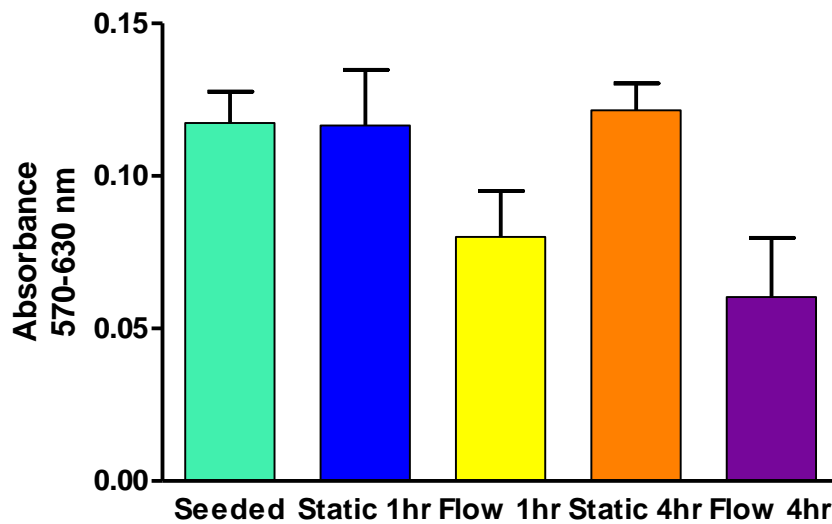
B)

Figure 5.7: Cell seeding efficiency and viability post 1 and 4-hour static and flow exposed on A) glass and B) nanocomposite conduits. No significant differences were seen between the nanocomposite groups (one-way ANOVA).

5.3.4 Scanning Electron Microscopy Analysis of Seeded Conduits

SEM images showed viable cells present on nanocomposite prior to flow (Fig. 5.6, A & B). SEM images also demonstrated cells to be present on nanocomposite post 1 and 4-hour flow (data not shown).
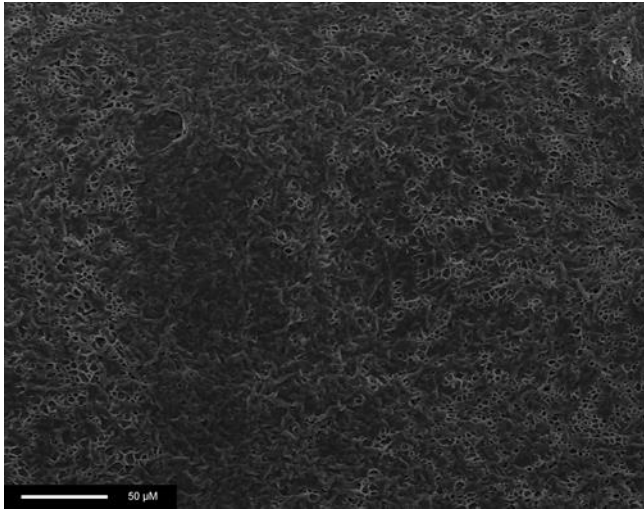
A)
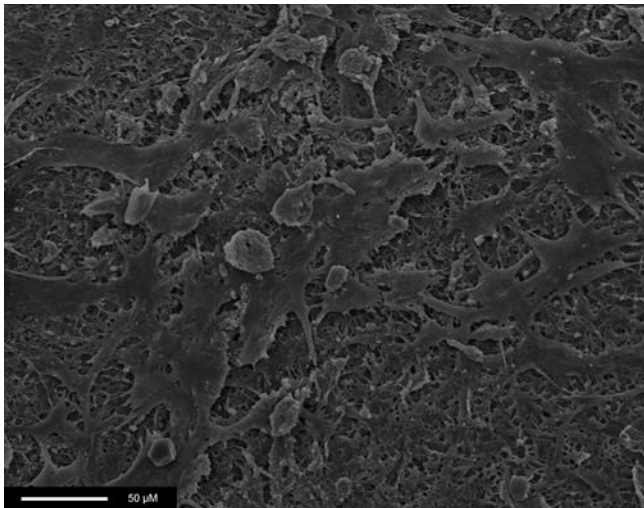
B)

Figure 5.8: Typical SEM of a nanocomposite conduit: A) unseeded, B) seeded with 1 x 10^6 HUVEC overnight

5.3.5 Assessment of Seeding Efficiency and Viability following preconditioning

The AB assays performed pre-flow (following overnight seeding) showed no significant difference in seeding efficiency. Viable cells were present on all seeded nanocomposite conduits.

Figure 5.9 A shows EC viability post 1 and 4 hour static or low flow without a 24 hour recovery period followed by physiological flow. Conduits preconditioned with 1 or 4 hour low flow (P_1 & P_4 respectively) showed no significance difference in cell viability compared to pre-flow. Conduits incubated under static conditions for 4 hours prior to physiological flow (S_4) showed a significant decrease in cell viability ($P < 0.01$) compared to pre-flow, whereas no significant decrease was observed after one hour static incubation (S_1). Despite a noticeable decrease in viability between S_1 and S_4 this was not significant. Comparing P_1 to its static control S_1 also showed no significant difference in cell viability. After four hours of preconditioning P_4, had a significantly higher viability ($P < 0.001$) compared to time matched control S_4.

Pre-conditioning followed by a 24 hour recovery period (Figure 5.9 B) showed significant changes in cell viability in all groups apart from pre-conditioning for one hour (PR_1) to pre-flow. Control conduits not exposed to preconditioning (SR_1 & SR_4) showed significant decreases ($P < 0.01$) in cell viability compared with pre-flow conduits. An increase in cell viability was observed for conduits preconditioned for 1 hour (PR_1) but this was not significant, whereas preconditioning for 4 hours (PR_4) showed a significant increase ($P < 0.01$). Very significant differences ($P < 0.001$) were observed between conduits SR_1 and PR_1 and SR_4 and PR_4.
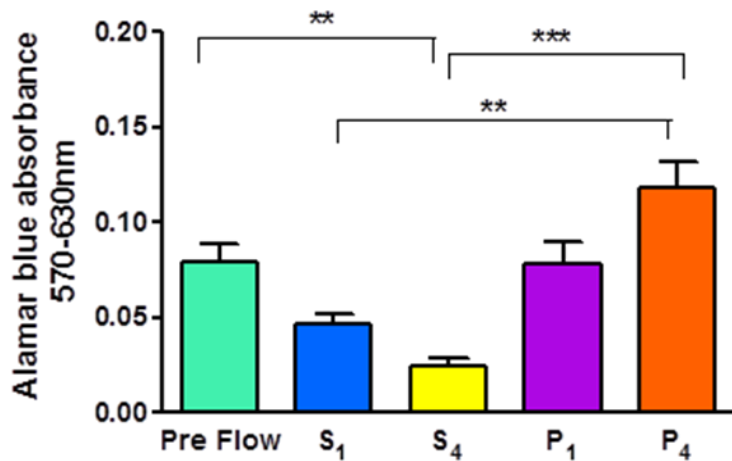
A)
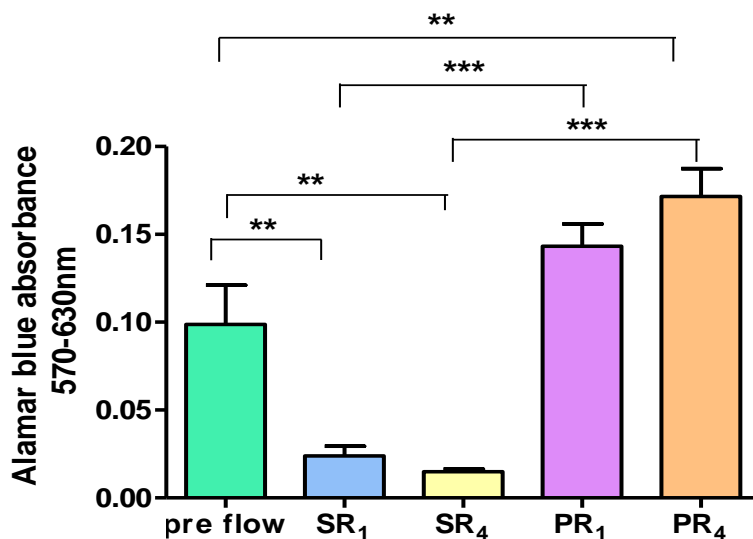
B)

Figure 5.9: Assessment of cell viability by an Alamar blue^{TM} metabolic assay: Figure 4.9 A shows Pre-flow, S_1, S_4, P_1 and P_4 groups. Figure 4.9 B shows Pre-flow, SR_1, SR_4, PR_1 and PR_4 groups. Statistical analysis was carried out by one-way ANOVA (n = 4) with ** $P < 0.01$ and *** $P < 0.001$

5.3.6 Scanning electron microscopy following preconditioning

SEM was employed to further elucidate cell retention following exposure to flow. Figure 5.10 A shows nanocomposite prior to seeding. Figure 5.10 B shows pre-flow seeded

nanocomposite. Figures 5.10 C to F show seeded nanocomposite for treatments S_1, S_4, P_1 and P_4 respectively. Similarly Figures 5.10 G to J show seeded nanocomposite for treatments SR_1, SR_4, PR_1 and PR_4 respectively. All seeded nanocomposites show cells present on the conduit post-treatment in line with the AB results earlier.
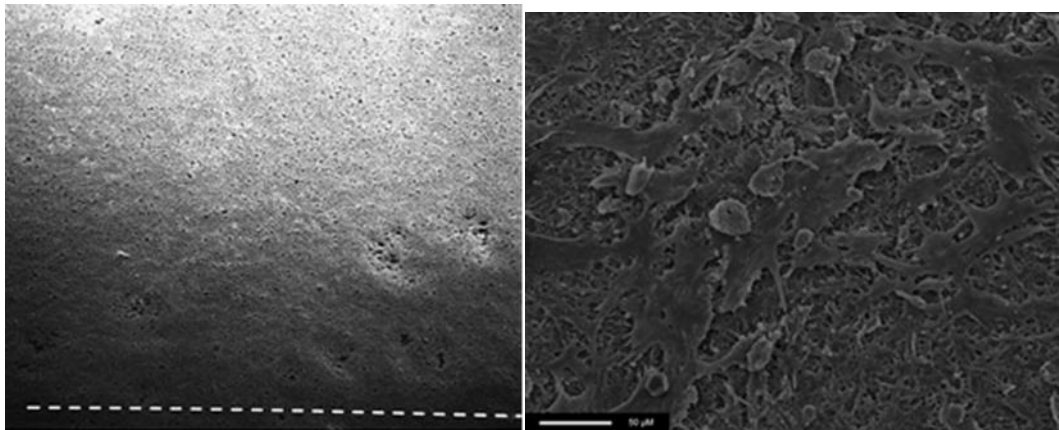
A)   B)
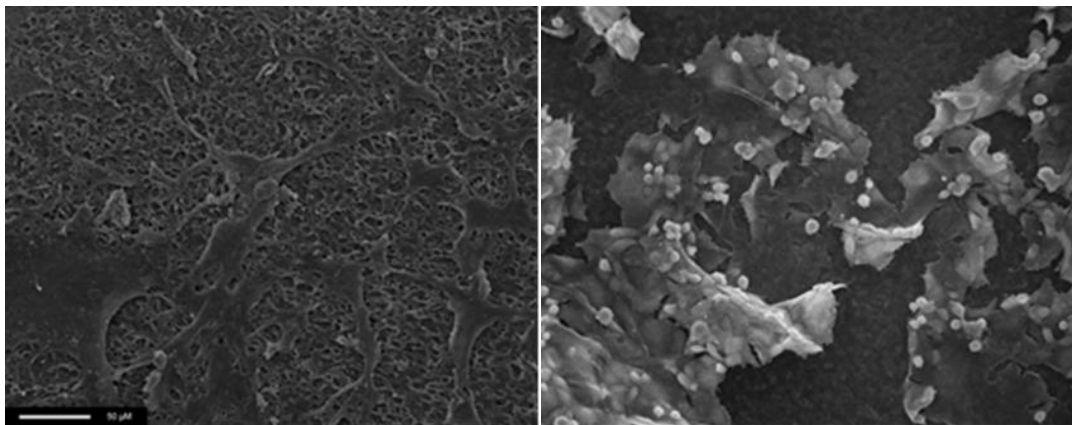
C)   D)
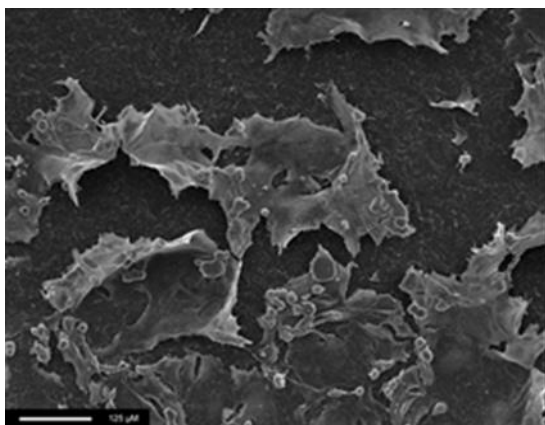
E)
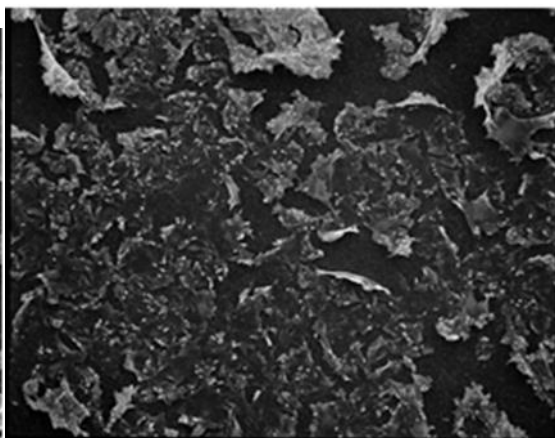
F)
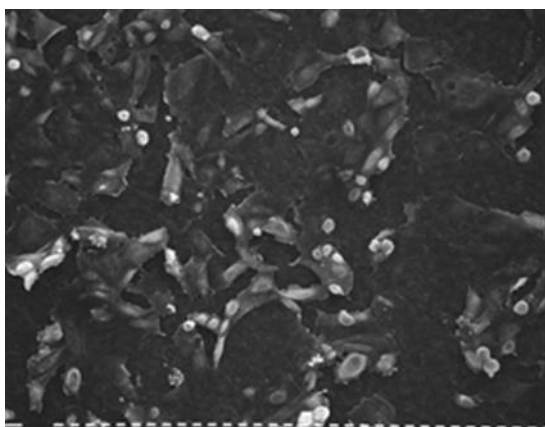
G)
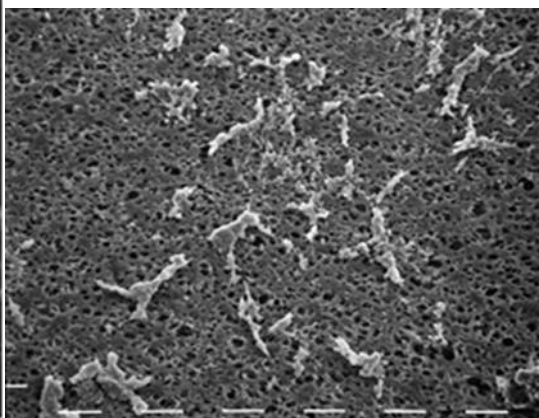
H)
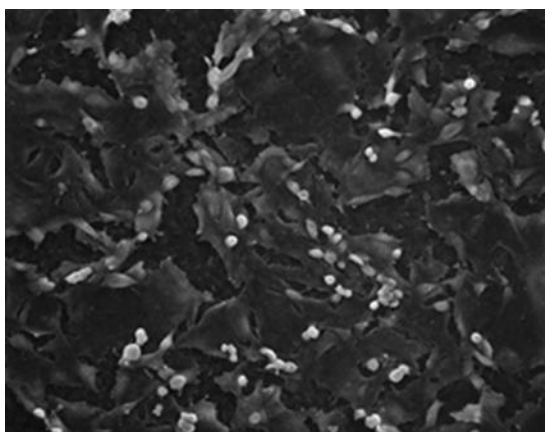
I)
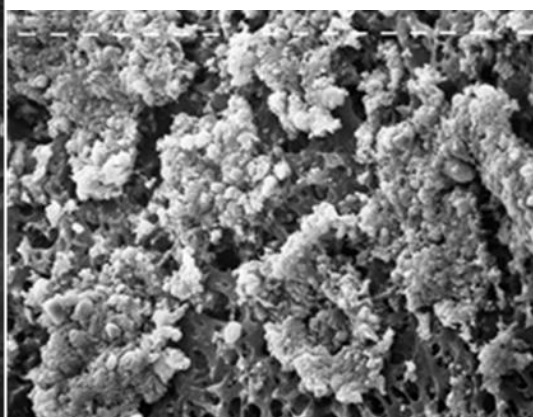
J)

Figure 5.10: Typical SEM of nanocomposite conduits: A (unseeded conduit), B (Pre-flow conduit), C (S_1 conduit), D (S_4 conduit), E (P_1 conduit), F (P_4 conduit), G (SR_1 conduit), 4.8 H (SR_4 conduit), I (PR_1 conduit) and J (PR_4 conduit).

5.3.7 Assessment of Quantity and Quality of RNA Extracted

The amount of RNA extracted from HUVEC is shown in Table 5.3. The purity was high in all samples and in all cases purity was greater than 95%.

Conduit and treatment	RNA Quantity (ng/µl) (mean ± SEM)
Group A	
S_1	4.2 ± 1.2
S_4	2.4 ± 0.7
P_1	12.4 ± 1.3
P_4	18.4 ± 1.5
Group B	
SR_1	2.7 ± 0.6
SR_4	2.0 ± 0.3
PR_1	28.7 ± 3.5
PR_4	36.0 ± 4.9

Table 5.3: RNA yield was measured at absorbance of 260nm and 280nm and quantity determined as ng/µl. Group A shows S_1, S_4, P_1 and P_4 samples. Group B shows SR_1, SR_4, PR_1 and PR_4 samples.

5.3.8 Analysis of GAPDH, TGFβ-1, VEGFR-1, PECAM-1 and VEGFR-2 PCR Products

Figure 5.11 A shows a 2% agarose gel of the PCR products for group A, resulting from 1 and 4-hour exposures respectively to either static conditions (S_1 & S_4) or low flow preconditioning (P_1 & P_4); following four hours of physiological flow on all conduits.

Figure 5.11 B shows a 2 % agarose gel of the PCR products for group B, resulting from 1 and 4-hour exposure respectively to either static conditions (SR_1 & SR_4) or low flow

preconditioning (PR_1 & PR_4); following a 24-hour recovery period on all conduits prior to four hour exposure to high flow for HUVEC seeded on the nanocomposite conduits.

The mRNA levels of GAPDH remained relatively constant in static and preconditioned samples, and changes were observed in the other genes (see below).
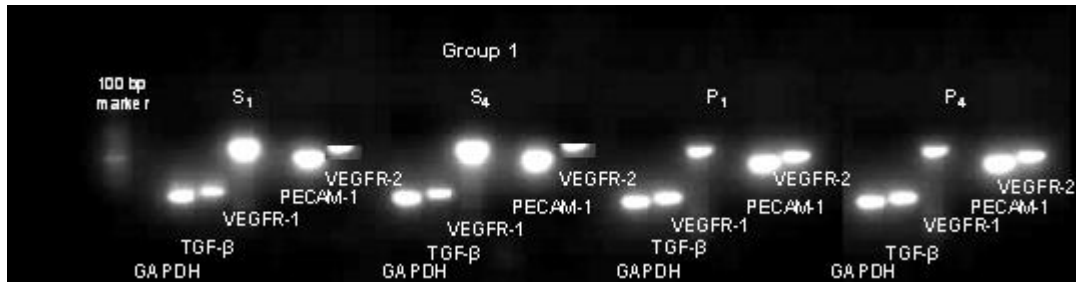
Figure 5.11A
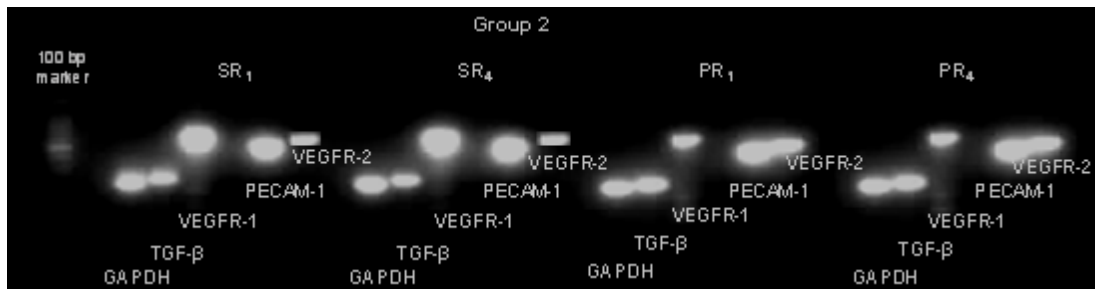
Figure 5.11B

Figure 5.11: Typical 2% agarose gels of PCR products with a 100 bp marker. Each sample was analysed for GAPDH, TGF-β1, VEGFR-1, PECAM-1 and VEGFR-2 expression: Figure 5.11A shows S_1, S_4, P_1 and P_4 samples. Figure 4B shows SR_1, SR_4, PR_1 and PR_4 samples.

5.3.9 Intensity of Gene Expression

Relative levels of GAPDH, TGFβ-1, VEGFR-1, PECAM-1 and VEGFR-2 were determined using Syngene (Syngene, Cambridge, U.K.). After normalisation by the intensity of GAPDH mRNA bands obtained from preconditioning, the levels of gene expression were examined.

Figure 5.12 A shows the intensity of gene expression post 4 hours' physiological flow after either 1 or 4 hours of preconditioning (P_1 & P_4) compared to time matched controls (S_1

& S_4). Differences in gene expression were observed only in the expression of VEGFR-1 and VEGFR-2. Significant decreases (S_1-P_1, $P < 0.01$ & S_4-P_4, $p < 0.001$) in VEGFR-1 and significant increases ($p < 0.001$) in VEGFR-2 were seen after 1 and 4-hour preconditioning compared to time-matched controls. All other genes remained essentially unaltered under these conditions.

Figure 5.12 B shows the intensity of gene expression post 4 hours' physiological flow after either 1 or 4 hours of preconditioning (PR_1 & PR_4) compared to time matched controls (SR_1 & SR_4) with the addition of a 24-hour recovery period after preconditioning. PECAM-1 expression remained relatively unaltered. TGFβ-1 expression was shown to be significantly higher ($P < 0.01$) after 4 hours of preconditioning (PR_4) compared to controls (SR_4). The expression of VEGFR-1 showed a significant decrease after 1 hour only (SR_1-PR_1, $P < 0.05$). Significant increases in VEGFR-2 expression were observed at both time points (SR_1-PR_1, $P < 0.001$ and SR_2-PR_2, $P < 0.001$).
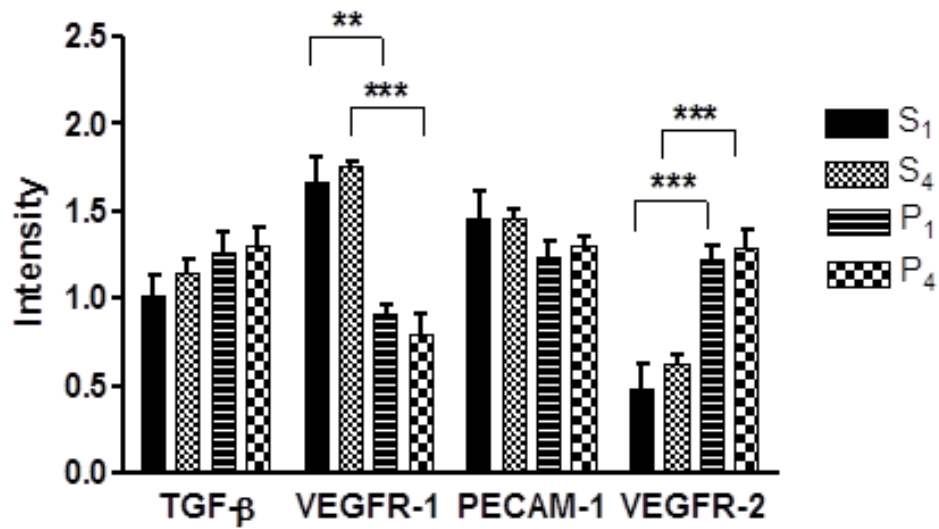
A
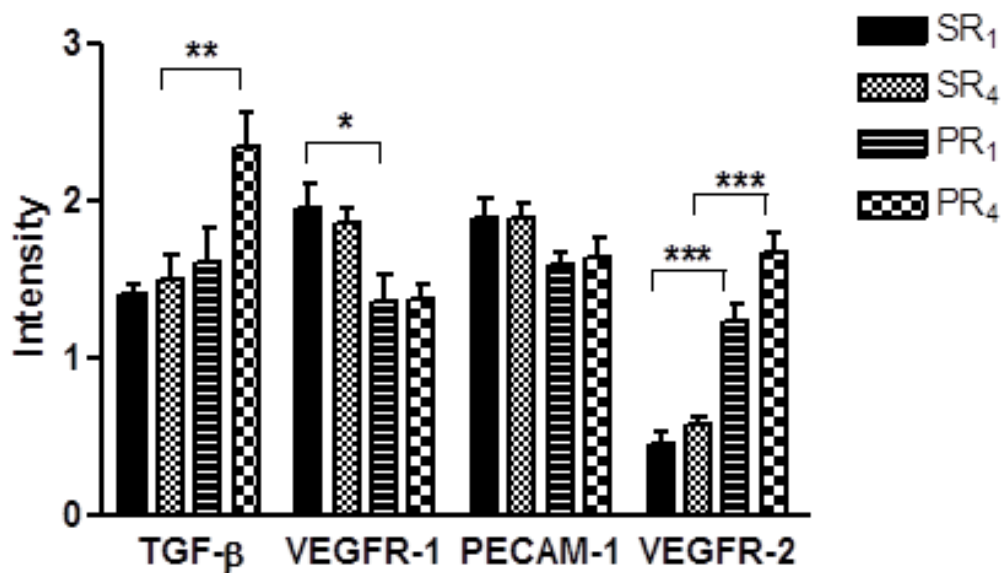
B

Figure 5.12: Intensity analysis of PCR products to determine gene expression levels following normalisation for GAPDH: 4.12A shows S_1, S_4, P_1 and P_4 samples for TGF-β1, VEGFR-1, PECAM-1 and VEGFR-2. 4.12B shows SR_1, SR_4, PR_1 and PR_4 samples for TGF-β1, VEGFR-1, PECAM-1 and VEGFR-2. Statistical analysis was carried out by one-way ANOVA (n = 4) with * $P<0.05$, ** $P < 0.01$ and *** $P < 0.001$

5.4 Discussion

The culture of HUVEC on flat sheets of tissue culture plastic in the absence of flow produces a well-documented change in phenotype; the characteristic cobble stone appearance being one such manifestation. It has long been documented that culture of HUVEC under conditions of shear stress results in a recovery of an *in vivo* phenotype and an alteration of growth pattern with cells becoming aligned to flow in a similar manner to that seen *in vivo* (Zaragoza *et al.*, 2012; Dolan *et al.*, 2011; Malek and Izumo, 1996).

A major problem with EC seeding of vascular prosthesis is that, when exposed to physiological flow, extensive cell loss from the seeded graft surface can occur and that this loss can occur rapidly thus reducing considerably the effectiveness of the cell seeding process (Dardik *et al.*, 1999; Ballermann *et al.*, 1998; Ott and Ballermann, 1995). Various strategies have been employed in an attempt to overcome this problem including modifying the prosthesis surface with moieties such as RGD or fibronectin to improve cell adhesion (Seta *et al.*, 2012; Hoesli *et al.*, 2014) or by the employment of preconditioning to reduce cell loss.

In a previous study by our group, pulsatile physiological shear stress (~14 dynes/cm^2) was shown to result in a significant decrease in cell retention for EC seeded on nanocomposite following exposure to 4 hours of physiological flow (Vara *et al.*, 2011; Tiwari *et al.*, 2003b). This suggested that immediate exposure to physiological levels of shear stress strips EC when seeded on nanocomposite prosthetic materials and is in line with the findings of similar studies by several other groups examining cell retention on a variety of other graft materials (Salehi-Nik *et al.*, 2016; Xiao and Shi, 2004). It has been observed that cell loss under physiological flow conditions can, however, be reduced by exposing the cells to a lower preconditioning flow prior to physiological shear stress and that such prior exposure is

beneficial in promoting cell adherence(Baguneid *et al.*, 2011). Therefore, we tested the hypothesis that exposure of EC seeded on cylindrical nanocomposite conduits to preconditioning shear stress may allow the cells to adapt to the material in an improved manner and enhance cell growth and adhesion. In order to test this hypothesis EC seeded nanocomposite conduits were exposed to a variety of preconditioning shear stress regimes employing either immediate exposure to physiological flow after preconditioning or a recovery period of 24 hours between preconditioning and exposure to physiological flow and compared the results obtained with those for seeded conduits that were exposed to physiological shear stress with no preconditioning. Conduits were preconditioned with a low flow of 1-2 dynes/cm^2 followed by physiological flow.

The AB results prior to flow (pre-flow conduits) demonstrated that the nanocomposite conduits employed in the study were successfully seeded with viable HUVEC in a uniform manner. Pre-flow conduits were taken as a baseline, and the decrease seen after physiological flow was applied without preconditioning suggests that a significant number of cells are lost under these conditions as would be expected and confirming the results of our previous study. The application of preconditioning prior to exposure to physiological flow demonstrated that the seeded nanocomposite retained cells significantly better under this regime and suggests an improvement in cell adherence and an increase in cell numbers or metabolism following preconditioning when compared to the cells not exposed to preconditioning prior to exposure to physiological flow. The changes are more marked after 4 hours compared to 1 hour demonstrating that the effect is time dependent and that a longer period of preconditioning before the application of physiological flow results in greater protection for the cells. There is little difference between the cells exposed to physiological flow immediately post-preconditioning and those given a 24 hour recovery period following preconditioning prior to

exposure suggesting that under the conditions investigated the recovery period results in no further benefit in terms of improved cell retention. However this does demonstrate that even if there is a delay between treatment by preconditioning and implantation of the graft and exposure to physiological flow the potential benefits of preconditioning would not be lost and that the positive effect of preconditioning lasts for at least 24 hours. The SEM studies support these conclusions regarding the relative numbers of cells remaining following exposure to physiological flow.

The investigation of expression levels for a variety of genes was the carried out in an attempt to build upon the information obtained in our previous study to elucidate the potential mechanisms behind the changes observed in cell metabolism and numbers by examining further genes and a wider range of exposure to a variety of flow regimes. In the case of TGFβ1 whilst there was a general increase in expression in the preconditioned groups this increase was only significant in the case of the 4 hour preconditioning followed by a 24 hour recovery period prior to exposure to physiological flow indicating that while TGFβ1 may be involved in the longer term changes observed in this study it's short term effect is limited. PECAM-1 expression remains relatively stable under all treatments suggesting that the remaining HUVEC following exposure to flow retain their EC phenotype regardless of the application of preconditioning. A significant decrease in VEGFR-1 expression was observed in both one and four hour preconditioned cells when followed by immediate exposure to physiological flow and after a 24 hour recovery period. This situation was reversed in the case of VEGF-R2 where a significant increase of gene expression was observed in the preconditioned groups. Both VEGFR-1 and VEGFR-2 are known to bind vascular endothelial growth factor with high affinity and previous studies have shown that VEGFR-2 mediated signalling can result in significant changes in morphology together with alterations in actin

organisation in EC with high expression levels of this receptor (Mustonen and Alitalo, 1995). Significantly other studies have shown that the expression of VEGFR-2 is induced by the application of shear stress associated with a reduction in VEGFR-1 expression in a similar manner to the results obtained in this study (Shay-Salit *et al.*, 2002). This suggests that the reduction in VEGFR-1 and increase in VEGFR-2 expression may be associated with mature EC likely to proliferate in response to shear stress (a situation similar to angiogenesis) and indeed in the case of the PR_4 group a significant increase in cell metabolism or numbers can be seen which may become more apparent if longer term studies were carried out.

In conclusion, the results presented in this chapter confirm that the previous findings regarding the potential benefits of preconditioning can be applied to EC seeded on the nanocomposite employed and demonstrates that preconditioning under the right conditions can result in a significant improvement in EC retention when exposed to physiological flow. This is a major benefit towards achieving a viable seeded conduit for clinical usage. The study also builds upon previous work examining gene expression on cylindrical conduits when exposed to flow by examining VEGFR-1 and VEGFR-2 expression in addition to the previously investigated genes and demonstrates, for the first time, that low flow preconditioning causes alterations in gene expression in this situation. It suggests that such alterations can be determined successfully and that further investigations into other potentially significant genes may well be of benefit in exploring further the potential mechanism by which preconditioning improves cell retention whilst studies into protein expression via techniques such as Western blotting would also be of interest. Such studies would also be valuable in determining the most effective method of preconditioning with regard to the optimal length of time for preconditioning and the potential advantages of a recovery period prior to exposure to physiological flow. Finally, it also demonstrates further

the suitability and potential of the nanocomposite for future use in tissue engineered cardiovascular devices.

6

6 The Extraction of Endothelial Progenitor Cells and Circulating Endothelial Cells from Human Peripheral Blood

6.1 Introduction

One of the most exciting and important areas of medical research in recent years has focused on the potential of employing human stem cells for a wide variety of purposes in both tissue engineering and the treatment of a variety of medical conditions (Sales *et al.*, 2005).

As medical procedures get more complex and the population gets older an ever-larger demand for high quality synthetic prosthesis appears. Regenerative medicine is the best hope for providing high quality hybrid grafts (Baguneid *et al.*, 2011; Motwani *et al.*, 2011). The use of stem cells and adult progenitor cells in regenerative medicine promises access to

sufficient autologous cells for the first time. Previous shortages in, for example, EC's limited the effective production of hybrid grafts (Punshon *et al.*, 2008). The discovery of circulating endothelial progenitors allows regenerative medicine to harness the body's own repair mechanisms in the creation of new medical devices. Regenerative medicine and the use of hybrid technology will result in a more natural 'artificial' implant; thus better mimicking the original and reducing failure rates of such devices.

The majority of this work has focused on cells sourced from embryonic tissue, bone marrow or umbilical cord blood. The future benefits of such work could be considerable but research using such tissue sources faces some practical difficulties. There is considerable debate regarding the ethics of using embryonic tissue as a source of stem cells which has been widely reported. In the case of bone marrow, the availability of samples of bone marrow for research is limited whilst for cells sourced from umbilical cord blood again suitable samples may be limited and the difficulty of donor and recipient compatibility would have to be addressed.

Following the initial report by Ashara *et al* in 1997 on the extraction of CD34$^+$ cells from human peripheral blood (Asahara *et al.*, 1997) there has been some interest in the extraction of endothelial progenitor stem cells (EPSC) from peripheral blood. There are several potential advantages to using peripheral blood as a cell source. Firstly peripheral blood samples are relatively easy to obtain compared to embryonic tissue, bone marrow or cord blood. Secondly the employment of peripheral blood does not encounter the ethical problems associated with embryonic tissue or the compatibility difficulties of using umbilical cord blood.

There are, however, some major problems with peripheral blood as a cell source to be overcome. The major difficulty encountered is that it is possible to extract far fewer cells from peripheral blood compared to embryonic tissue, bone marrow or umbilical cord blood particularly if the blood donor has not been stimulated with granulocyte colony-stimulating factor (GCSF).

This problem is compounded by the lack of a universally accepted method of cell extraction and culture such as exists, for example, in the case of the extraction of HUVEC where the method of Jaffe is generally followed (Jaffe *et al.*, 1973) which has demonstrated its reliability over a number of years.

There is in fact considerable variety in the reported methods employed for the extraction and growth of EPSC from peripheral blood some of which are quite fundamental as a result of which there is currently no generally accepted process for the extraction of these cells. As regards the source of peripheral blood used in studies the majority use 'healthy donors' (Fuchs *et al.*, 2006; Shirota *et al.*, 2003; Zhang *et al.*, 2006a; Ingram *et al.*, 2004) but often the age range is not stated (Fuchs *et al.*, 2006; Salven *et al.*, 2003; Yamamoto *et al.*, 2003) and when it is there is a considerable age range from a mean of 23.05 years (Zhang *et al.*, 2006a) to 56.3 years (Hur *et al.*, 2004). Some methods employ Histopaque for the initial separation (Zhang *et al.*, 2006a; Hur *et al.*, 2004; Ingram *et al.*, 2004; Fuchs *et al.*, 2006; Tepper *et al.*, 2002) while others use Lymphoprep (Punshon *et al.*, 2008). Some studies further employ magnetic beads to purify the initial isolate (Asahara *et al.*, 1997; Salven *et al.*, 2003) while others do not (Hill *et al.*, 2003; Fuchs *et al.*, 2006; Shirota *et al.*, 2003; Tepper *et al.*, 2002). In the majority of studies a two day pre-plating step is employed in which the initial isolate is plated for two days following which the initially adhered cells are disposed of

and the non-adherent cells cultured (Hill *et al.*, 2003; George *et al.*, 2006). Other studies however allow the initial isolation to adhere for two to six days then dispose of the non-adherent cells and culture the initially adherent ones (Zhang *et al.*, 2006a; Hur *et al.*, 2004; Ingram *et al.*, 2004; Rehman *et al.*, 2003).

One isolated there is further variation in the techniques used to culture the isolated cells. Some methods employ coating for the tissue culture surface using materials such as fibronectin (Hill *et al.*, 2003; Fuchs *et al.*, 2006; George *et al.*, 2006), collagen (Howling *et al.*, 2002; Ingram *et al.*, 2004) or gelatin (Hur *et al.*, 2004; Ghanbari *et al.*, 2011). The variety of cell culture medium used also varies with media such as M199 (Wang *et al.*, 2007; George *et al.*, 2006; Hill *et al.*, 2003), EGM-2 (Ingram *et al.*, 2004; Hur *et al.*, 2004; Zhang *et al.*, 2006a) and commercially available specialised media such as the EndoCult Liquid Medium Kit (Stem Cell Technologies, Vancouver BC, Canada) (Yoder *et al.*, 2007) all having been employed in studies. Again a variety of fetal calf serum percentages have been employed, generally ranging from 5% (Tao *et al.*, 2007) to 20% (Wang *et al.*, 2007; Yamamoto *et al.*, 2003; de Mel *et al.*, 2011). The addition of growth factors to the cell culture medium is a further area of complication with some studies using supplements such as human vascular endothelial growth factor, human fibroblast growth factor, insulin-like growth factor-1, human epidermal growth factor, ascorbic acid and hydrocortisone acetate (Zhang *et al.*, 2006b) while others employ supplements such as bovine brain extract (Wang *et al.*, 2007) while some methods report using no supplements other than fetal calf serum (Hill *et al.*, 2003).

The differences in the extraction method and culture process employed in the various studies above make a valid comparison of results obtained from them problematic.

This chapter uses as a base the process for extracting and growing EPSC from peripheral blood in Chapter 4. It then makes a direct comparison of some of the above factors in an attempt to begin to develop a consensus on the method of extraction and culture of EPSC from peripheral blood in the future and facilitate the successful employment of this source of stem cells in clinical practice.

6.2 Materials and Methods

6.2.1 Blood Collection

Blood samples were collected following consent from healthy adult human volunteers. 24ml samples were collected by venepuncture in EDTA blood tubes (Sarstedt, U.K.). Following collection samples were mixed and used for cell isolation within one hour of collection.

6.2.2 Effect of Cell Isolation Techniques

The mononuclear fraction of the blood was then isolated using either Lymphoprep (Axis-Shield, U.K.) or Histopaque 1077 (Sigma-Aldrich, U.K.). Briefly 3ml of either Lymphoprep or Histopaque 1077 was added to each of eight 12ml polystyrene centrifuge tubes (Falcon, U.K.). 3ml of blood was then carefully layered on top. The tubes were then centrifuged at 400 x g for 30 minutes at room temperature. The mononuclear fraction was then separated from each tube and the Lymphoprep and Histopaque 1077 samples pooled separately in 30 ml universal tubes (Falcon, U.K.). 10ml of Hank's Balanced Salt Solution (Invitrogen, U.K.)(HBSS) was then added slowly to each tube and the contents mixed. The tubes were

then centrifuged at 250 x g for 10 minutes at room temperature. The cells were then washed twice by removing the supernatant, re-suspending in 10ml HBSS and centrifuging at 250 x g for 10 minutes at room temperature. Finally the isolated cells were re-suspended in 5ml cell culture medium (CCM): RPMI 1640 supplemented with 20% foetal bovine serum (FBS) and penicillin/streptomycin (both Invitrogen U.K.). Cells were then counted using a haemocytometer and samples of the cell isolates taken for RNA analysis and cell staining. Cells were isolated from four different donors (two male and two female)

6.2.3 Cell Culture

Cells isolated by each method were then cultured for an initial two-day period in a 6-well plate (Falcon, U.K) at a seeding density of 2.5×10^6 cells/well in 5ml CCM (n=5 per individual isolation) following which the supernatant (containing the non-attached cells) was counted using a haemocytometer and transferred to fresh wells (Adherent Group (A)). 5ml CCM was added to the wells containing the initially adherent cells (IA). Cells were then cultured for a further five days. At this stage the medium was removed from the Adherent group wells and transferred to fresh wells (Non adherent group (NA)). Cell metabolism was then assessed in the initially adherent group and the Adherent group using AB (Serotec, U.K.). Two wells from each isolation method were then stained using Giemsa to visualise Hill Colonies. The remaining three wells were the cultured for a further 7 days after which cell metabolism was determined again in all groups and samples taken for RNA analysis.

6.2.4 Effect of Gelatin or Fibronectin Coating

6-well plates were coated overnight with a sterile 1% gelatin solution (Sigma-Aldrich, U.K.) then washed twice with phosphate buffered saline (PBS) (Invitrogen U.K.) prior to use. Human fibronectin coated 6-well plates were obtained from BD Biosciences (BD Biosciences, U.K.). As a control, uncoated 6-well plates were employed. Cells were isolated from human peripheral blood using the Histopaque-1077 method described above. Treated or untreated 6-well plates were then seeded with 2.5×10^6 cells/well in 5ml CCM and cultured as above (n=6 per treatment). Cell metabolism was then measured at day 7 and day 14 and samples taken at day 14 for RNA analysis.

6.2.5 Effect of Foetal Bovine Serum Concentration

Cells were isolated from human peripheral blood as above using the Histopaque-1077 method. Cells were then seeded at 2.5×10^6 cells/well in 5ml cell culture medium supplemented with either 5, 10 or 20% FBS (n=6 per FBS percentage) and cultured as above in the appropriate supplemented media. Cell metabolism was then measured at day 7 and day 14 and samples taken at day 14 for RNA analysis.

6.2.6 Effect of Media Choice

Cells were isolated from human peripheral blood as above using the Histopaque-1077 method. Cells were then seeded at 2.5×10^6 cells/well in 5ml CCM as above but replacing the RPMI 1640 in the CCM with either DMEM, IMDM, M199 (all supplemented with 20% FBS

or EGM-2 (Promocell, U.K.) and cultured (n=5). Cell metabolism was then measured at day 7 and day 14 and samples taken at day 14 for RNA analysis.

6.2.7 Measurement of Cell Metabolism

Cell metabolism was assessed by AB assay at Day 7 and 14. Medium was removed from the wells and 4ml 10% AB in CCM added. After a 4 hour incubation samples of AB/CCM were removed and measured on a Fluroskan Ascent FL (Thermo Labsystems, U.K.) fluorescent plate reader (excitation 530nm, emission at 620nm). Unseeded wells were used as a control.

6.2.8 Giemsa Staining for Hill Colonies

Wells were washed twice with PBS after which 0.5ml ice-cold methanol was added (VWR, U.K.) for 5 minutes to fix the cells. The methanol was then removed and the wells air-dried. 400µl Giemsa stain (Invitrogen U.K.) was then added for 15 minutes after which the wells were destained in distilled water. Colonies were then examined following the criteria of Hill *et al* as described previously(Hill *et al.*, 2003).

6.2.9 RNA Isolation and Investigation

RNA was extracted from initial cell isolates and Day 14 cell samples using an "RNeasy™" kit (Qiagen Ltd, U.K.). The RNA concentration and purity was calculated by measuring the absorbance at 260nm and 280nm using an Eppendorf Biophotometer (Eppendorf[AG], Germany). The quality of the RNA was assessed by 2% agarose gel

electrophoresis and the mRNA obtained was used for polymerase chain reaction (PCR) for CD14, CD34, CD133, Platelet Endothelial Cell Adhesion Molecule-1 (PECAM-1), Vascular Endothelial Growth Factor Receptor-2 (VEGFR2) and von Willebrand Factor (vWF). RT-PCR was performed using an One-Step PCR kit (Qiagen Ltd, U.K.). 0.25 µg of template RNA and 0.5 µM of the appropriate primers (Table 6.1) were used for each PCR reaction. Cycle conditions were as follows: CD14 30 cycles at 94°C, 57°C and 72°C; CD34 35 cycles at 94°C, 54°C and 72°C; CD133 35 cycles at 94°C, 52°C and 72°C; VEGFR2 35 cycles at 94°C, 59°C and 72°C; vWF 35 cycles at 94°C, 50°C and 72°C; PECAM-1 35 cycles at 94°C, 50°C and 72°C and amplification was carried out using a MasterCycler Gradient PCR machine (Eppendorf[AG], Germany). In the case of vWF and PECAM-1 RNA extracted from HUVEC was used as a positive control. PCR products were then analysed by 2% agarose gel electrophoresis and a GeneGenius darkroom with 'GeneSnap' version 6.02. (Syngene, U.K.).

Marker	Sense (5' to 3')	Antisense (5' to 3')
CD14	CCTCCCAAGTTTTAGGACAA	CAGCTGGTGATAAGGGTTAG
CD34	CCTCCCAAGTTTTAGGACAA	CAGCTGGTGATAAGGGTTAG
CD133	CAGTCTGACCAGCGTGAAAA	GGCCATCCAAATCTGTCCTA
VEGFR2	GTGACCACATGGAGTCGTG	CCAGAGATTCCATGCCACTT
PECAM-1	GCTGTTGGTGGAAGGAGT	GAAGTTGGCTGGAGGTGCTC
vWF	TGCTGACACCAGAAAAGTGC	AGTCCCCAATGGACTCACAG

Table 6.1: Primer sequences for CD14, CD34, CD133, VEGFR2, PECAM-1 and vWF gene expression analysis.

6.2.10 Data Analysis and Statistical Methods

Data were presented as mean±SEM. All statistical analysis utilized one way ANOVA with post-hoc Tukey's test.

6.3 Results

6.3.1 Effect of Cell Isolation Techniques

6.3.1.1 Number of Cells Isolated

There was no significant difference between the initial numbers of cells isolated by either method. The initial cell isolation produced $26.01 \times 10^6 \pm 1.54$ cells from the Histopaque 1077 isolations and $26.98 \times 10^6 \pm 5.01$ cells from the Lymphoprep isolations (n=4).

At Day 2 when the non-adherent cells were transferred to fresh wells again there was no significant difference in cells numbers between the two groups: Histopaque 1077 $2.44 \times 10^6 \pm 0.08$ cells compared to Lymphoprep $2.46 \times 10^6 \pm 0.10$ cells (n=20).

6.3.1.2 Assessment of Hill Colonies

All isolations produced Hill Colonies. Figure 6.1 shows typical Hill Colonies from Histopaque 1077 and Lymphoprep isolations.
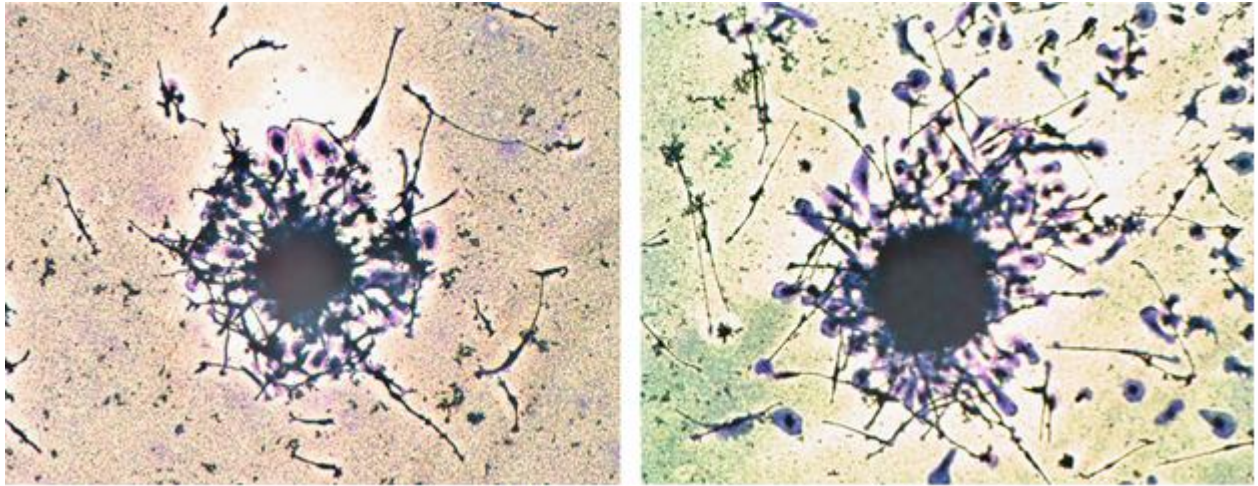
Figure 6.1: Typical Hill Colonies isolated using Histopaque 1077 (left) and Lymphoprep (right).

6.3.1.3 Assessment of Cell Metabolism

Figure 6.2 shows the effect of isolation technique on cell metabolism over a 14 day period. There was a significant increase in cell metabolism between Day 7 and Day 14 in both the Lymphoprep ($p<0.001$) and Histopaque-1077 groups ($p<0.05$) adherent cell group. There was no significant difference between the Lymphoprep and Histopaque-1077 groups at either time point ($p>0.05$). Both the initially adherent cell groups (cells adherent after the first two days) and the cells which had not adhered after 7 days showed minimal metabolic activity at either time point.
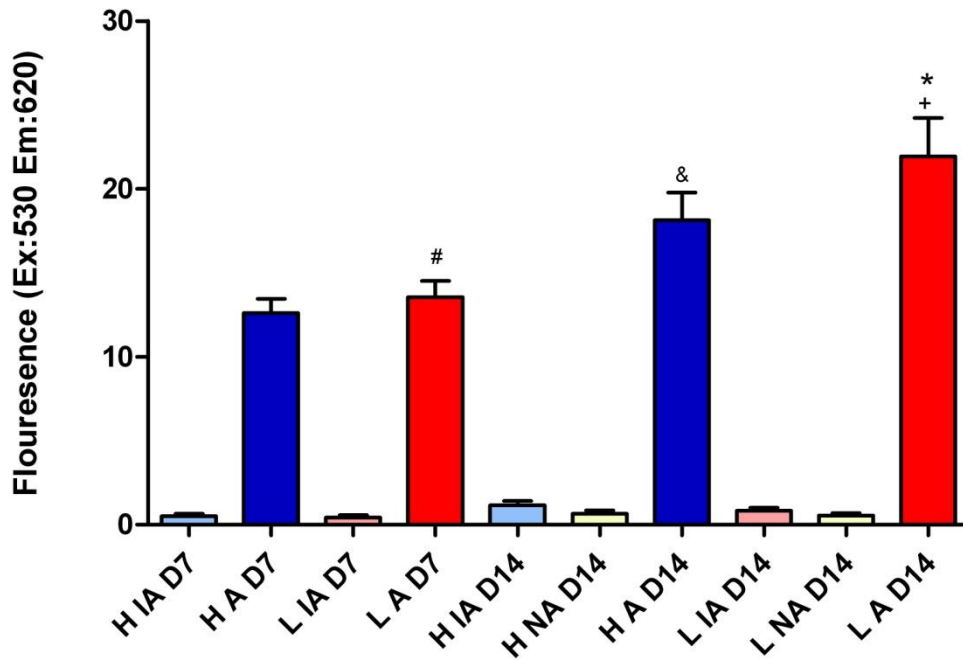
Figure 6.2: Effect of Isolation Technique. Cells isolated by: Histopaque 1077 (H) or Lymphoprep (L). Cell Group: Initially adherent at Day 2 (IA), Adherent at D7 (A) or Non-adherent at D7 (NA). Time point: Day 7 (D7) or Day 14 (D14). [*] $p < 0.001$ L A D14 vs. L A D7; [&] $p < 0.001$ H A D14 vs. L A D7; [#] $p > 0.05$ H A D7 vs. L A D7 and [+] $p > 0.05$ H A D7 vs. H A D14.

6.3.1.4 RNA analysis

RNA analysis for CD14, CD34, CD133, PECAM-1, VEGFR-2 and vWF showed no significant difference between the two groups (Figure 6.3). Figure 6.3a demonstrates a 2% agarose gel of initial cell isolates by either the Histopaque 1077 or Lymphoprep method and Day 14 cultures examined by RT-PCR for CD14, CD34 and CD133. All isolations were positive for CD14 and CD34. The initial isolates were positive for CD133 whereas the Day 14 samples were negative. Figure 6.3b similarly shows a 2% agarose gel of the same samples

examined for vWF, VEGFR-2 and PECAM-1. vWF was positive in both the initial isolations and in the Day 14 samples. VEGFR-2 expression was minimal in the initial isolations and increased in the Day 14 samples. PECAM-1 expression was high in the initial isolates and reduced in the Day 14 isolates.
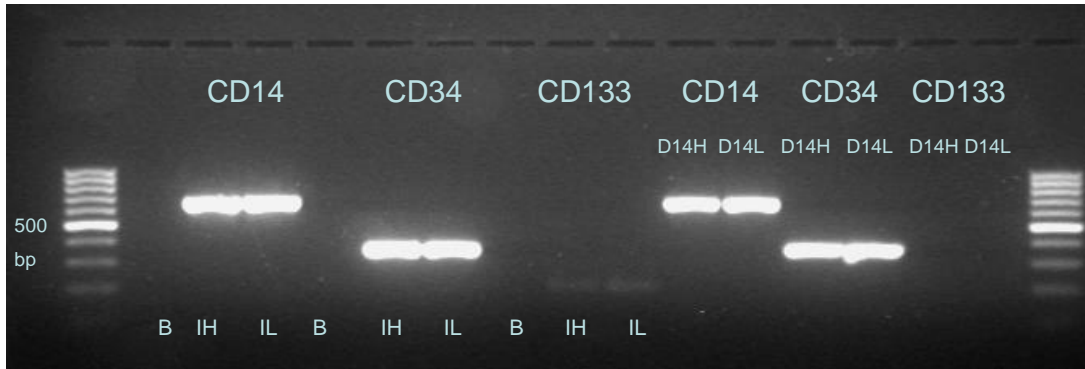
a)

b)

Figure 6.3a): RNA analysis for CD14, CD34 and CD133 on cell extracts isolated by either Histopaque (H) or Lymphoprep (L) techniques from initial (I) or Day 14 (D14) samples. N = Negative Control.

Figure 6.3b): RNA analysis for vWF, VEGFR-2 and PECAM-1 on cell extracts isolated by either Histopaque (H) or Lymphoprep (L) techniques from initial (I) or Day 14 (D14) samples. N = Negative Control.

6.3.2 Effect of Gelatin or Fibronectin Coating

6.3.2.1 Assessment of Cell Metabolism

At Day 7 there was no significant difference in cell metabolism between the uncoated plate group and the fibronectin coated group (p>0.05). Gelatin coating significantly reduced the level of cell metabolism at Day 7 compared to the other two groups (p<0.001). By Day 14 there was a significant increase in cell metabolism for the uncoated plate group compared to Day 7 (p<0.001) whereas the fibronectin coated group failed to show a significant increase in cell metabolism at the same stage (p>0.05). The gelatin coated group showed a significant reduction in cell metabolism at Day 14 compared to Day 7 (p<0.001). Again, in all groups the level of cell metabolism in the initially adherent cells and the cells which failed to adhere in the first 7 days was low (Figure 6.4).
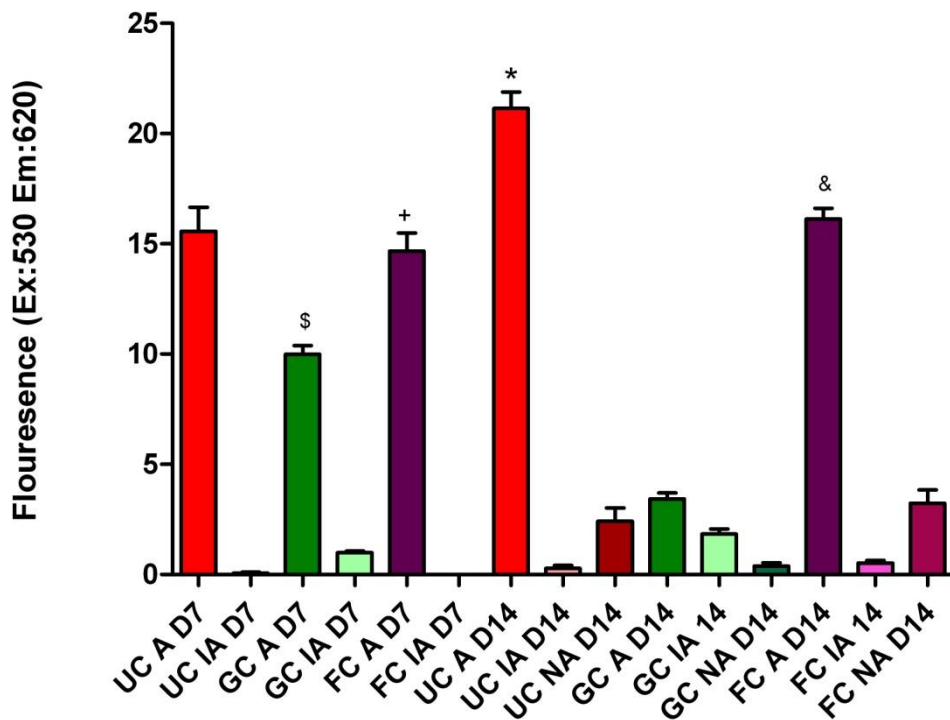
Figure 6.4: Effect of Gelatin or Fibronectin Coating on Cell Metabolism. Coating type: Uncoated (UC); Gelatin Coated (GC) or Fibronectin Coated (FC). Cell Group: Initially adherent at Day 2 (IA), Adherent at D7 (A) or Non-adherent at D7 (NA). Time point: Day 7 (D7) or Day 14 (D14). + p>0.05 FC A D7 vs. UC A D7; $ p<0.001 GC A D7 vs. UC A D7 or FC A D7; * p<0.001 UC A D7 vs. UC A D14 and & p>0.05 FC A D7 vs. FC A D14.

6.3.2.2 RNA analysis

RNA analysis for PECAM-1, VEGFR-2 and vWF showed no significant difference between the three groups (Data not shown).

6.3.3 Effect of Foetal Bovine Serum Concentration

6.3.3.1 Assessment of Cell Metabolism

There is no significant difference between the three FBS concentrations for the adherent cells group at Day 7 ($p>0.05$). At Day 14 only the 20% FBS group shows a significant increase in cell metabolism compared to Day 7 ($p<0.05$). In the case of the 5% FBS group there is a higher cell metabolism in the non-adherent cell group compared to the other two FBS concentrations though this is not statistically significant (Figure 6.5).
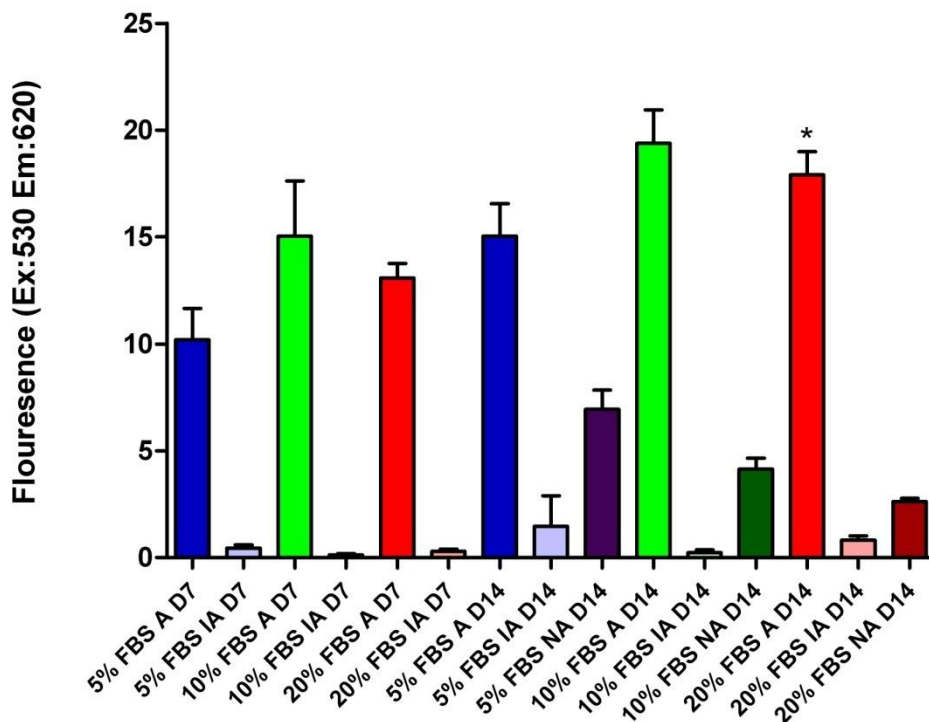
Figure 6.5: The Effect of FBS concentration on cell metabolism. Percentage Fetal Bovine Serum (FBS) 5%, 10% or 20%. Cell Group: Initially adherent at Day 2 (IA), Adherent at D7 (A) or Non-adherent at D7 (NA). Time point: Day 7 (D7) or Day 14 (D14). * p<0.05 20% FBS A D7 vs. 20% FBS A D14.

6.3.3.2 RNA analysis

RNA analysis for PECAM-1, VEGFR-2 and vWF showed no significant difference between the different FBS percentages (data not shown).

6.3.4 Effect of Media Choice

6.3.4.1 Assessment of Cell Metabolism

Figure 6.6 shows the effect of various media on cell metabolism over a 14 day period. All media produced viable cells at Day 7. There was a significant increase in cell metabolism by Day 14 compared to Day 7 in the RPMI 1640, M199, DMEM and IMDM groups ($p<0.001$) and a significant decrease in cell metabolism for the EGM-2 group ($p<0.001$). Comparing the different media between each other at Day 7 the group with the highest cell metabolism, the IMDM group was significantly higher than the M199 group ($p<0.001$) which in turn was significantly higher than the RPMI 1640 group ($p<0.001$) followed by the DMEM group and the EGM-2 group ($p<0.001$). By Day 14 the IMDM and M199 groups showed no significant difference in cell metabolism ($p>0.05$) while both groups were significantly higher than the RPMI 1640, DMEM and EGM-2 groups ($p<0.001$). In the case of the EGM-2 group there was a higher level of cell metabolism in both the initially adherent group of cells at Day 7 and the non-adherent at Day 7 group of cells by Day 14.
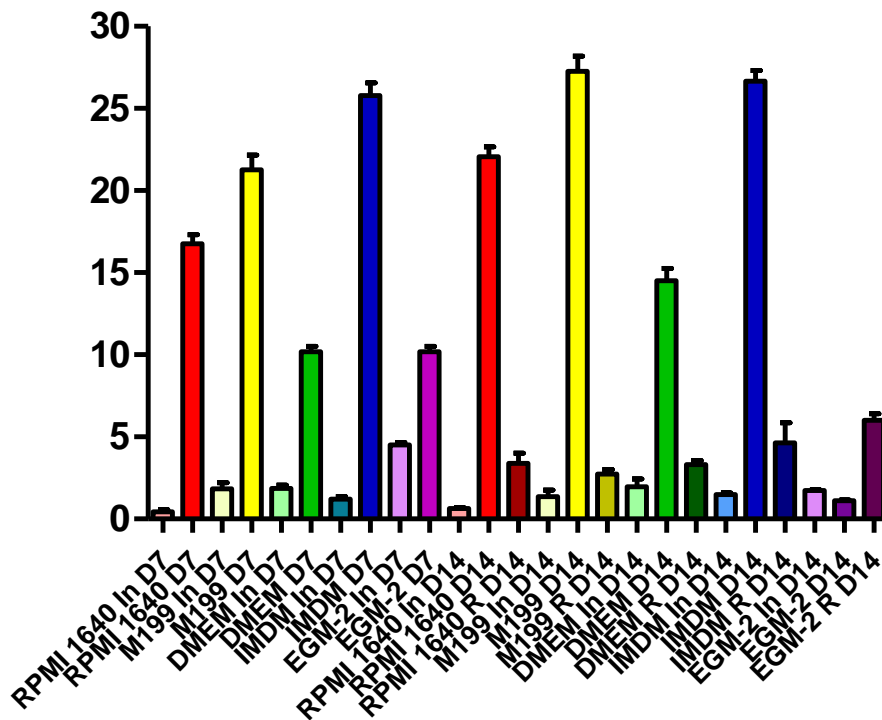
Figure 6.6: The effect of various media on cell metabolism. Media types: RPMI1640; M199; DMEM; IMDM and EGM-2. Cell Group: Initially adherent at Day 2 (IA), Adherent at D7 (A) or Non-adherent at D7 (NA). Time point: Day 7 (D7) or Day 14 (D14). * $p < 0.001$ IMDM A D7 vs. M199 A D7; & $p < 0.001$ M199 A D7 vs. RPMI A D7; + $p < 0.001$ RPMI A D7 vs. DMEM A D7 or EGM-2 A D7; # $p > 0.05$ IMDM A D14 vs. M199 A D14 and $ $p < 0.001$ M199 A D14 or IMDM A D14 vs. RMPI 1640 A D14.

6.3.4.2 RNA analysis

RNA analysis for PECAM-1, VEGFR-2 and vWF showed no significant difference between the various media types (Data not shown).

6.4 Discussion

The use ECs in vascular grafts has for years been sought as an answer to the problems of thrombosis and intimal hypoplasia. Regenerative medicine suffered from the shortage of suitable cells to allow true hybrid grafts to be created in any meaningful clinical scenario. The

discovery, isolation and seeding of grafts with EPSC has allowed the use of regenerative medicine in vascular graft production to move out of a purely experimental field and to become clinically relevant (Sales *et al.*, 2005).

There has been considerable recent interest in the use of progenitor cells extracted from human peripheral blood as a cell source for tissue engineering. Whilst there have been a number of studies published in this field there has been considerable variation in the methods employed to firstly extract the cells from blood and secondly to culture the cells once they have been extracted. Thus the process of isolating and culturing EPSC is still a matter for debate and further investigation to develop a consensus such as that in, for example, the isolation of HUVEC as developed by Jaffe et al (Jaffe *et al.*, 1973).

The initial isolation of the cells has been reported by density centrifugation using either Histopaque-1077 (Yoder *et al.*, 2007; Wang *et al.*, 2007) or Lymphoprep (Punshon *et al.*, 2008). Some groups have then further purified the cell isolate using magnetic beads for CD34 by positive selection (Asahara *et al.*, 1997; Salven *et al.*, 2003; Harraz *et al.*, 2001). Various surfaces to culture the isolated cells on have also been investigated. Examples include human fibronectin coated plates, gelatin coating, collagen coating or uncoated tissue culture plastic.

Once isolated a variety of media compositions have been employed such as EGM-2, M199 or RPMI 1640 supplemented in a variety of ways with some groups using 'simple' media supplemented only with FBS at varying concentrations and penicillin/streptomycin while others employ supplements such as heparin, human VEGF, human Fibroblast Growth Factor, human Epidermal Growth Factor, Insulin-like Growth Factor I and ascorbic acid.

Following isolation many groups use a 'pre-plating' stage after which non-adherent cells are collected and cultured to remove rapidly adhering cells (such as CEC, monocytes and macrophages) which varies from one hour (Asahara *et al.*, 1997; Shirota *et al.*, 2003) to 48 hours (George *et al.*, 2006; Hill *et al.*, 2003). Others omit a 'pre-plating' stage and allow cells to seed for a variety of times ranging from 24 hours (Ingram *et al.*, 2004) to three days (Zhang *et al.*, 2006a) or six days (Hur *et al.*, 2004).

Chapter 4 demonstrated that progenitor cells could be successfully isolated from human peripheral blood using Lymphoprep and differentiated into EC's using a simple culture process on uncoated tissue culture plastic plates employing RPMI supplemented with 20% FBS and penicillin/ streptomycin as a medium (Punshon *et al.*, 2008). Using this study as a base alternate isolation techniques and culture methods were explored and compared.

When comparing extraction using either Lymphoprep or Histopaque-1077 the results obtained in this study suggest that both methods result in similar isolations. There was no significant difference in the number of cells initially isolated by either method or in cell metabolism over the 14 day period studied. RNA analysis demonstrated that in the initial cell extract the monocyte marker CD14 and the EPSC/ mature EC marker CD34 are strongly expressed. The stem cell marker CD133 is also expressed to a lesser extent. PECAM-1 and vWF were also expressed in the initial cell isolations. RNA analysis of the Day 14 cells confirms that CD14 and CD34 expression was maintained though CD133 expression was lost which may be attributed to the conversion of EPSC to EC over time. PECAM-1 and vWF expression was also maintained and VEGFR-2 expression was detected. Thus the RNA analysis confirmed that there was no difference between the cell populations obtained from

either Histopaque 1077 or Lymphoprep isolations with regard to CD14, CD34, CD133, PECAM-1, VEGFR2 or vWF expression.

As Histopaque-1077 was employed by the majority of other studies it was decided to employ this isolation method for the remainder of the study. As regards surface coating of the tissue culture plates uncoated plates were found to be similar to human fibronectin coated plates. Gelatin coating however had a severe detrimental effect by day 14.

Examining the practice of using a 'pre-plating' stage under most conditions this would appear to have little effect as few cells which adhere in the first two days then proliferate further. One observation in initial studies was that this did depend on the vigour with which the cells were washed at day two and that if the cells were gently removed at this stage in some cases the initially adherent cells would proliferate (data not shown) whereas if a vigorous wash was employed the initially adherent cells would not proliferate.

The percentage of FBS in the media had a number of effects on cell culture. Using 20% FBS resulted in most of the proliferating cells adhering between day two and day seven with little metabolic activity being observed in the initially adherent cells or those which failed to attach in the first seven days. Reducing the FBS concentration to 5% lead to changed pattern of cell adherence in which cells appeared to adhere in the initial sample, the day two to seven sample (both of which failed to proliferate in the next seven days) and the day seven to fourteen samples. Employing 10% FBS lead to cells adhering in the initial period, day two to seven, but then failing to proliferate over the next seven days.

Similarly the medium employed had a significant effect on cell culture. M199 produced the highest levels of cell metabolism after 14 days culture with IMDM and to a lesser extent RPMI 1640 producing similar results. Surprisingly in view of its employment in several studies using EGM-2 resulted in a low level of cell metabolism by day 14 despite containing more supplements than the other media examined. It did, however, have only 5% FBS compared to the 20% in all the other media so this could well have had an effect. DMEM also resulted in significantly lower cell metabolism at day 7 and day 14.

Taken together these findings suggest that it difficult to compare studies employing different culture protocols and may explain the wide variety of outcomes reported by other studies into the isolation and culture of progenitor cells from human peripheral blood.

The findings presented in this chapter also demonstrate that while the main isolation methods used to extract progenitor cells from human peripheral blood are comparable varying the culture method can have very significant effects on the final outcome. Based on this study employing fibronectin or gelatin coated culture plates would appear to be unnecessary and the medium of choice should be M199 supplemented with 20% FBS.

In conclusion it can be seen that while this study and previous work can suggest a basis for culture further work to develop an optimised and agreed 'gold standard' culture regime for progenitor cells from human peripheral blood is required in order to maximise the potential of this source of cells for tissue engineering and translate this potential into a valuable and viable process for clinical use in the future.

7

7 The Effect of Varying Sterilization Methods on Nanocomposite

7.1 Introduction

Polyurethanes (PU's) represent a large family of polymers consisting of different organic units linked together by urethane bonds [-NHC(O)O-]. Highly versatile, biocompatible and with excellent mechanical properties PU's are amenable to a number of applications including catheters, biomedical implants and tissue engineering scaffolds (Burke and Hasirci, 2004). However chronic *in vivo* failure, observed upon prolonged implantation, and primarily due to polymer degradation, is a major stumbling block for their continued use (Santerre *et al.*, 2005). The polyester based soft segments of PU's are prone to hydrolysis whereas polyether based PU's are susceptible to oxidative attack.

In order to produce more biostable PU's our group tethered polyhedral oligomeric silsesquioxane (POSS) nanocages to a poly (carbonate-urea) urethane (PCU) backbone. Siloxanes are well known to be biostable and resistant to oxidation and hydrolysis due to the strong intermolecular forces between the constituent molecules and a strong framework with shorter bond lengths. However, siloxanes are mechanically fragile exhibiting particularly poor tear strengths which make siloxane based polymers unsuitable for many applications. By covalently attaching the POSS moiety to the polymer network, our group was able to exploit the beneficial effects of improved biostability afforded by the POSS molecule, without compromising the mechanical integrity of the PU. The polyhedral oligomeric silsesqioxane-poly (carbonate-urea) urethane (POSS-PCU) produced was found to be more resistant to degradation *in vitro* and *in vivo*, possess anti-thrombogenic properties, and sustain cell growth upon its surface; a combination of properties making it suitable for a number of biomedical applications including heart valves, prosthetic grafts, and stents (Kannan *et al.*, 2005b; Kannan *et al.*, 2007; Ahmed *et al.*, 2011). In conjunction with POSS-PCU, a POSS modified biodegradable aliphatic caprolactone polyurethane, poly (caprolactone-urea) urethane (POSS-PCL), was also developed for tissue engineering applications (Gupta *et al.*, 2009).

The risk of infection associated with implantable devices is a significant clinical concern. For example, up to 6% of prosthetic grafts can encounter difficulties with infection resulting in approximately $640m in healthcare costs (Darouiche, 2004). In addition, there are significant associated morbidity and mortality rates with amputation rates approaching 11% and re-infection found in 18% of patients. In 17-40% of patients, graft infection leads to death. Direct implantation of device with microorganisms attached is a common and

avoidable method in which infection can occur necessitating the need for effective sterilisation methods (Nagpal and Sohail, 2011).

Sterilisation can be achieved in a number of ways including steam, gamma irradiation and incubating with ethanol. Whilst numerous investigations have characterised microbial activity following sterilisation, as a marker of efficacy, the impact of sterilisation technique on the material bulk and surface properties is often ignored; whereas it is often the material bulk and surface properties which determine the success of the implant/device. The sterilisation process usually involves physical or chemical treatment which results in the elimination of organic macromolecules and/or microorganisms. Given the nature of their action, the techniques can also react with the biomaterial. Steam sterilisation can lead to hydrolysis, softening and degradation of the polymer due to the high temperature, pressure and humidity (Zhang *et al.*, 1996). Gamma irradiation is known to cause chain scission and cross-linking which can adversely affect material properties (Haugen *et al.*, 2007). Further, both steam and gamma have been known to deform and yellow the polymeric materials. Immersing in ethanol is a milder technique used *in vitro* to disinfect the polymer sample. It is particularly useful for disinfecting biodegradable tissue engineering scaffolds, such as glycolic acid based materials which, by their very nature, tend to be fragile (Shearer *et al.*, 2006).

The purpose of this chapter was to evaluate the impact of the sterilisation technique on the bulk and surface properties of flat sheets and porous membranes of POSS-PCU and POSS-PCL polymers developed in our lab. The treatments include 70% ethanol, steam and gamma irradiation. Changes to the molecular weight, mechanical strength, surface chemistry

and cytotoxicity were evaluated and compared to an unsterilised control. The effectiveness of the sterilisation method was also determined.

7.2 Materials and Methods

7.2.1 Polymer synthesis

7.2.1.1 POSS-PCU nanocomposite

Polycarbonate polyol, 2000 mwt (Bayer Material Science, GmbH) and trans-cyclohexanechlorohydrinisobutyl-polyhedral oligomeric silsesquioxane (Hybrid Plastics Inc) were placed in a 250 mL reaction flask equipped with a stirrer and a nitrogen inlet. The mixture was heated to 135ºC to dissolve the POSS cage into the polyol and then cooled to 70ºC. 4,4'-methylenebis (phenyl isocyanate) (MDI) was added to the polyol blend and reacted at 70 ºC for 90 minutes to form a pre-polymer. DMAC was added slowly to the pre-polymer to form a solution which was cooled to 40^0C. Chain extension of the pre-polymer was carried out by the addition of ethylenediamine and diethylamine in DMAc. 1-butanol in DMAC was added to the mixture to form a POSS-PCU solution.

7.2.1.2 POSS-PCL nanocomposite

Dry polycaprolactone diol (2000mwt) and POSS were placed in a 250ml reaction flask equipped with mechanical stirrer and gas inlet. The mixture was heated to 135°C to dissolve the POSS cage into the polyol and then cooled to 90°C. 4, 4' methylenebis(cyclohexylisocyanate) was added to the polyol blend and then reacted, under nitrogen, at 90°C for 120 minutes with catalyst (Bismuth neodecanoate) to form a pre-polymer. Dry DMAC was added slowly to the pre-polymer to form a solution; the solution was cooled to 40°C. Chain extension of the pre-polymer was carried out by the drop wise addition of a mixture of ethylenediamine and diethylamine in dry DMAC. After completion

of the chain extension, 1-butanol in DMAC was added to the polymer solution forming a POSS-PCL solution.

Unless otherwise stated all chemicals and reagents were supplied by Aldrich Limited, Gillingham, U.K.)

7.2.2 Sample preparation

7.2.2.1 Cast Samples

The 18%(w/w) solutions of polymer in DMAC were cast onto glass petri dishes and left in an oven at 60°C overnight to evaporate the solvent. The resulting solid sheets of polymer were then sterilised accordingly and used for future experiments.

7.2.2.2 Porous Samples

Sodium bicarbonate (NaHCO$_3$, 50%(w/w), 40µm particle size, Bruner Mond, Cheshire, U.K.) was dispersed into an 18% (w/w) solution of the polymers in DMAC containing 2% Tween 80 surfactant. The mixture was mixed and degassed in one process using a Thinky ARE 250 mixer (Intertonics, Oxfordshire, U.K.) resulting in a viscous slurry which was then cast onto a stainless steel sheet and placed in distilled water for 48 hours at room temperature. A sheet of coagulated porous polymer was formed via the immersion precipitation process as a result of solvent exchange with distilled water. The polymer sheets were left immersed in distilled water for a period of 48 hours to ensure complete removal of solvent and NaHCO$_3$. The scaffolds were then removed from the steel support, air dried for a further 48 hrs, and sterilized appropriately for future experiments.

7.2.3 Sterilisation

7.2.3.1 Gamma irradiation

Samples were packed in sterilisation pouches and irradiated with a dose of 28.4 kGy at room temperature, using a 60Co gamma-ray source (Isotron, Berkshire, UK). Samples were exposed to the source on a continuous path for a period of 10 hours.

7.2.3.2 Autoclave

Autoclaving involved exposing the biomaterials to saturated steam at 121°C for a minimum of 15minutes at pressures of 115kPa. The samples were autoclaved and then left overnight for cooling.

7.2.3.3 Ethanol

Polymer discs were incubated with 70% (v/v) ethanol and left in a roller mixer for 10 minutes or 24 hours. Samples were then washed (5×) in distilled water, and stored for future use.

7.2.4 Material characterisation

7.2.4.1 Tensitometry

Samples were cut longitudinally into a dog-bone shaped specimen, 20 × 4mm, using a sharp cutter and mechanical press ensuring a clean cut with no flaws or stress aggregation. However, due to the random nature of pore size and porosity in the coagulated samples, variability is to be expected. The thickness of the samples was determined using an

electronic micrometer. Stress-strain profiles were characterised using a uniaxial load testing machine (Instron 5565, UK) and the Youngs modulus, ultimate tensile strength (UTS) and elongation at break obtained (n=6).

7.2.4.2 Attenuated Total Reflectance –Fourier Transform IinfraRed Spectroscopy

The chemical structure of the PU samples, following exposure to the various methods of sterilisation, was evaluated via attenuated total reflectance Fourier transform infer-red (ATR-FTIR) spectroscopy (JASCO FT/IR 4200). 30 scans were taken for each sample between 600 and 4000 cm^{-1} (n=6).

7.2.4.3 Gel permeation chromatography

Solutions of each sample were prepared by adding 15 mL of Dimethyl formaldehyde (DMF) to 30 mg of sample and left to dissolve on a roller mixer overnight. The samples were analysed using a PL-GPC 50 system (Agilent Technologies) equipped with PLGel column guard and 3 PLGel 5µm mixed bed-C columns (300 x 7.5mm). The measurement was carried out at 50°C in DMF and the eluent was pumped at the constant flow rate of 1.0 mL/min. The system was calibrated by performing Universal Calibration with single PL-polystyrene standard and a set of PL-EasyVial PS-H polystyrene standards of known molecular weights. The detection was done using a PL-BV 400RT viscometer and a PL-RI differential refractometer. The data was been collected and analysed using Varian 'Cirrus Multi detector' software (n=3). Results are presented as percentages of untreated control.

7.2.5 Cytotoxicity

7.2.5.1 Endothelial progenitor cell extraction

Blood samples were collected following consent from healthy adult human volunteers. 24mL samples were collected by venepuncture in EDTA blood tubes (Sarstedt, U.K.). Following collection samples were mixed and used for cell isolation within one hour of collection.

The mononuclear fraction of the blood was then isolated using Histopaque 1077 (Sigma-Aldrich, U.K.). Briefly 3ml of Histopaque 1077 was added to each of eight 12ml polystyrene centrifuge tubes (Falcon, U.K.). 3ml of blood was then carefully layered on top. The tubes were centrifuged at 400 x g for 30 minutes at room temperature. The mononuclear fraction was separated from each tube and the samples pooled in 30 ml universal tubes (Falcon, U.K.). 10ml of Hank's Balanced Salt Solution (Invitrogen, U.K.)(HBSS) was then added slowly to each tube and the contents mixed. The tubes were then centrifuged at 250 x g for 10 minutes at room temperature. The cells were then washed twice by removing the supernatant, resuspending in 10ml HBSS and centrifuging at 250 x g for 10 minutes at room temperature. Finally the isolated cells were resuspended in 5ml cell culture medium (CCM): M199 supplemented with 20% fetal bovine serum (FBS) and penicillin/streptomycin (both Invitrogen U.K.). Cells were then counted using a haemocytometer and seeded onto polymer samples as below.

7.2.5.2 Endothelial progenitor cell culture

Cells were seeded onto polymer discs (n=4) in a 24 well plate (Falcon, U.K.) at a seeding density of 5×10^5 cells/well in 1ml CCM. Cells were then cultured for seven days.

7.2.5.3 Assessment of cell metabolism and viability

Cell metabolism was assessed by AB assay at Day 7. In brief medium was removed from the wells and 1ml 10% AB in CCM added. Following a 4 hour incubation samples of AB/CCM were removed and measured on a Fluroskan Ascent FL (Thermo Labsystems, U.K.) fluorescent plate reader (excitation 530nm, emission at 620nm). Unseeded wells were used as a control.

7.2.6 Efficacy of sterilisation

All samples were tested for the effectiveness of sterilisation. Sterilised samples were immersed in tryptone soya broth (TSB) and fluid thioglycollate medium (THY) for cultivation of microorganisms (Wickham Laboratories, Hampshire) for a period of 14 days at temperatures of 20-25°C for TSB and 30-35°C for THY. Sterile broth was used as a negative control and unsterilized samples as positive controls. The broths were examined macroscopically every 1-3 days with clouding of the broth indicating contamination and inefficient sterilization compared to clear broth which indicates no infection and sterility of the samples (n=3).

7.3.0 Results

7.3.1 Visual inspection

All samples withstood treatment with EtOH well, irrespective of incubation time. Whilst the POSS-PCU samples were unaffected by the autoclaving process, the POSS-PCL samples were destroyed; therefore, it was not possible to examine the autoclaved POSS-PCL samples further. Both the POSS-PCU and POSS-PCL samples held up well against gamma irradiation with slight discolouring/yellowing of the cast sheets of POSS-PCU being observed.

7.3.2 Mechanical test

Figure 7.1 displays the stress-strain curves of the materials following exposure to EtOH, autoclaving and gamma irradiation. The quantitative values are presented in Table 7.1.
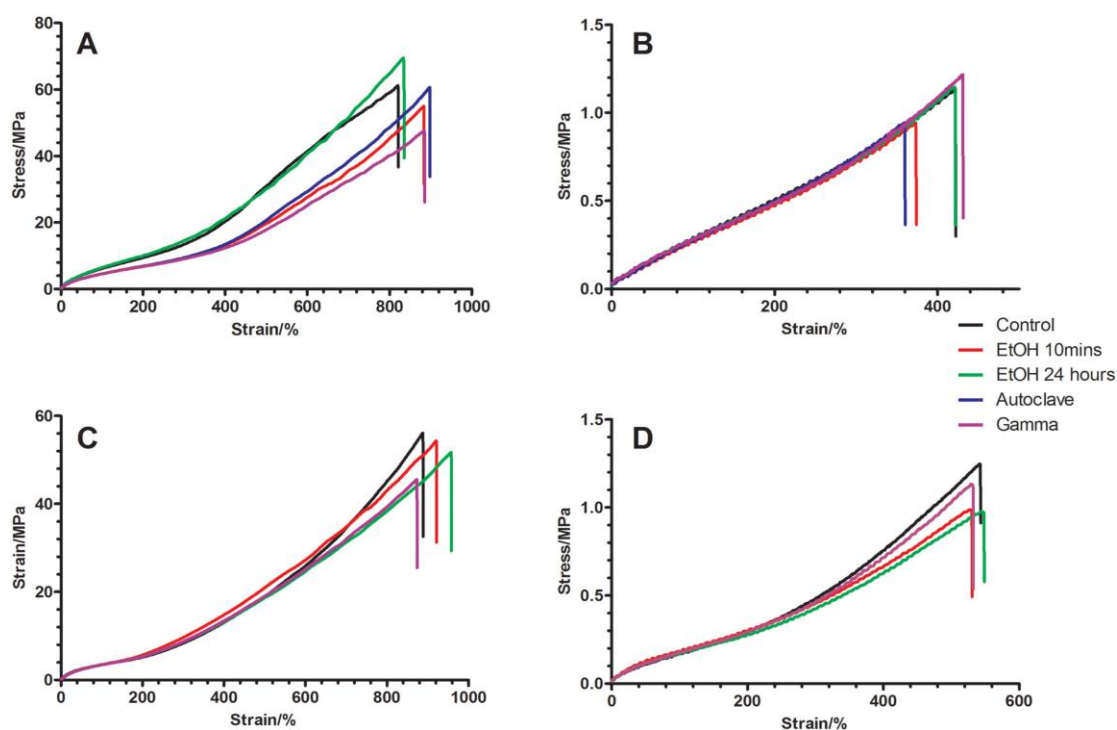
Figure 7.1: ATR-FTIR analysis of (A) cast POSS-PCU, (B) porous POSS-PCU, (C) cast POSS-PCL, and (D) porous POSS-PCL nanocomposites after sterilization with EtOH (10 min and 24 h), autoclave, and gamma irradiation. A summary of the changes in key peak intensities are inset (n ¼ 6, p < 0.05).

Sample		Sterilization Technique	Young's Modulus (MPa)	Tensile Strength (MPa)	Elongation at break (%)
POSS PCU	Cast	Control	8.61±0.81	62.35±6.71	823.96±28.03
		EtOH 10 min	7.75±0.47	56.48±2.98	875.36±47.01
		EtOH 24 hr	7.75±0.64	66.67±3.73	828.59±29.09
		Autoclave	9.16±0.62	62.39±5.72	904.86±37.40[a]
		Gamma	6.49±0.46[a]	48.87±5.04[a]	853.24±51.02[a]
	Porous	Control	0.35±0.02	1.08±0.08	440.76±11.66
		EtOH 10 min	0.32±0.03	0.98±0.06	449.33±25.45
		EtOH 24 hr	0.32±0.04	1.07±0.07	437.51±31.43
		Autoclave	0.33±0.04	0.97±0.05	382.84±35.46[a]
		Gamma	0.35±0.03[a]	1.22±0.05[a]	407.03±9.87[a]
POSS PCL	Cast	Control	6.91±0.93	57.71±2.32	885.73±85.00
		EtOH 10 min	5.61±0.82	55.05±2.42	938.88±54.99
		EtOH 24 hr	5.92±0.60	49.55±4.18	968.32±40.45
		Autoclave	n/a	n/a	n/a
		Gamma	5.03±0.278[a]	42.89±4.82[a]	865.69±114.47[a]
	Porous	Control	0.28±0.04	1.36±0.13	593.76±38.85
		EtOH 10 min	0.22±0.03	1.04±0.11	581.87±29.58
		EtOH 24 hr	0.20±0.01	0.97±0.04	577.52±12.42
		Autoclave	n/a	n/a	n/a
		Gamma	0.23±0.02	1.03±0.07	581.74±31.31

[a]$p < 0.05$

Table 7.1: Mechanical properties (Young's Modulus, ultimate tensile strength and elongation at break) of POSS-PCU and POSS-PCL samples after sterilization by a variety of techniques (n=6)

Both POSS-PCU and POSS-PCL tolerated ethanol treatment well − both for cast and coagulated samples. No significant difference was seen between the Youngs modulus, UTS or elongation at break in any of the samples following incubation with EtOH compared to the untreated control.

Autoclaving the samples of POSS-PCU did not affect the Youngs modulus or UTS. There was a slight significant ($p<0.05$) increase in the elongation at break for the cast sample of POSS-PCU, compared to the control. Autoclaving the porous sample caused a minor decrease in elongation at break.

The porous samples withstood the effects of gamma irradiation well while the cast samples suffered a decrease in their mechanical properties ($p<0.001$). The UTS for POSS-PCU decreased from 62.3 ± 6.7 MPa to 48.9 ± 5.0 MPa whilst POSS-PCL went from 57.7 ± 2.3 MPa to 42.9 ± 4.8 MPa ($p<0.001$). The reduction in UTS translated itself to the Youngs moduli which were both significantly reduced for cast samples of POSS-PCU and POSS-PCL.

7.3.3 ATR-FTIR

Attenuated total reflectance Fourier transform infrared (ATR-FTIR) spectroscopy was used to analyse surface chemical changes upon sterilisation with the results summarised in figure 6.2. The peak assignment was as follows: 1100 cm^{-1} (Si-O-Si), 1240 cm^{-1} (urethane C-O-C), 1400 (C-C aromatic ring), 1540 cm^{-1} (N-H & C=N), 1589 cm^{-1} (C=C aromatic), 1632 cm^{-1} (NH$_2$), 1736 cm^{-1} (C=O).
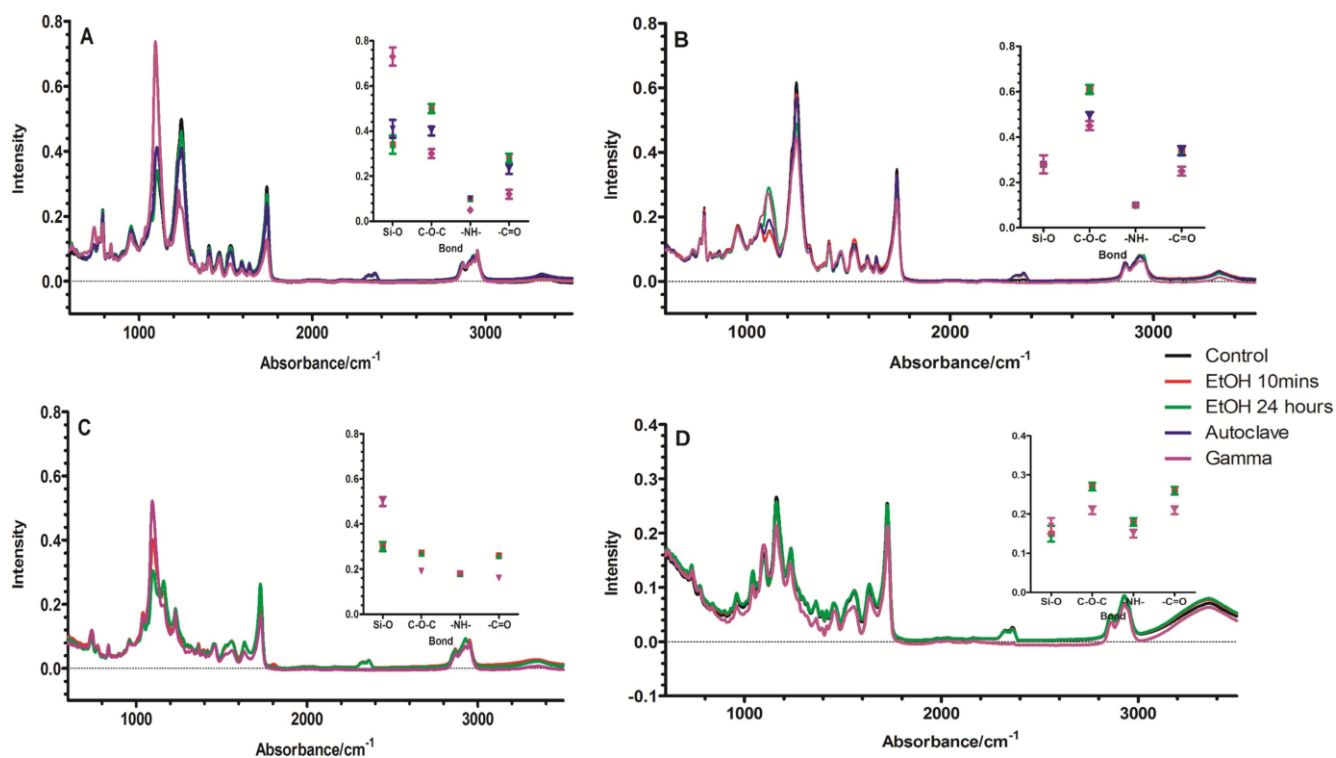
Figure 7.2: ATR-FTIR analysis of POSS-PCU nanocomposites following sterilisation with EtOH (10 mins and 24 hrs), Autoclave and gamma irradiation. With each spectra is a summary of any changes in key peak intensities (n=6, p<0.05).

Ethanol treatment had no significant impact on either of the POSS-PCU or POSS-PCL samples, cast or porous. A slight increase in the peak at 1100 cm^{-1}, attributed to the POSS moiety, was detected for the porous sample incubated in ethanol for 24 hours. Meanwhile autoclaving POSS-PCU caused a slight decrease (p<0.005) in the intensity of the ether peak at 1245 cm^{-1} for both cast and porous samples.

Exposure of POSS-PCU to gamma irradiation led to significant reductions in peak intensity at 1245 cm^{-1}, 1540 cm^{-1} and 1740 cm^{-1} on both cast and coagulated samples. There was, however, an increase in the intensity of the peak at 1095 cm^{-1} for the cast POSS-PCU sample (p<0.001).

Similarly, both POSS-PCL samples demonstrated a reduction in peak intensity, following exposure to gamma irradiation, at 1730 cm^{-1}, 1540 cm^{-1}, 1240 cm^{-1} and 1165 cm^{-1}. However, the cast sample of POSS-PCL also exhibited an increase in peak intensity at 1100 cm^{-1}.

7.3.4 Gel permeation chromatography

GPC results are summarised in figure 7.3.
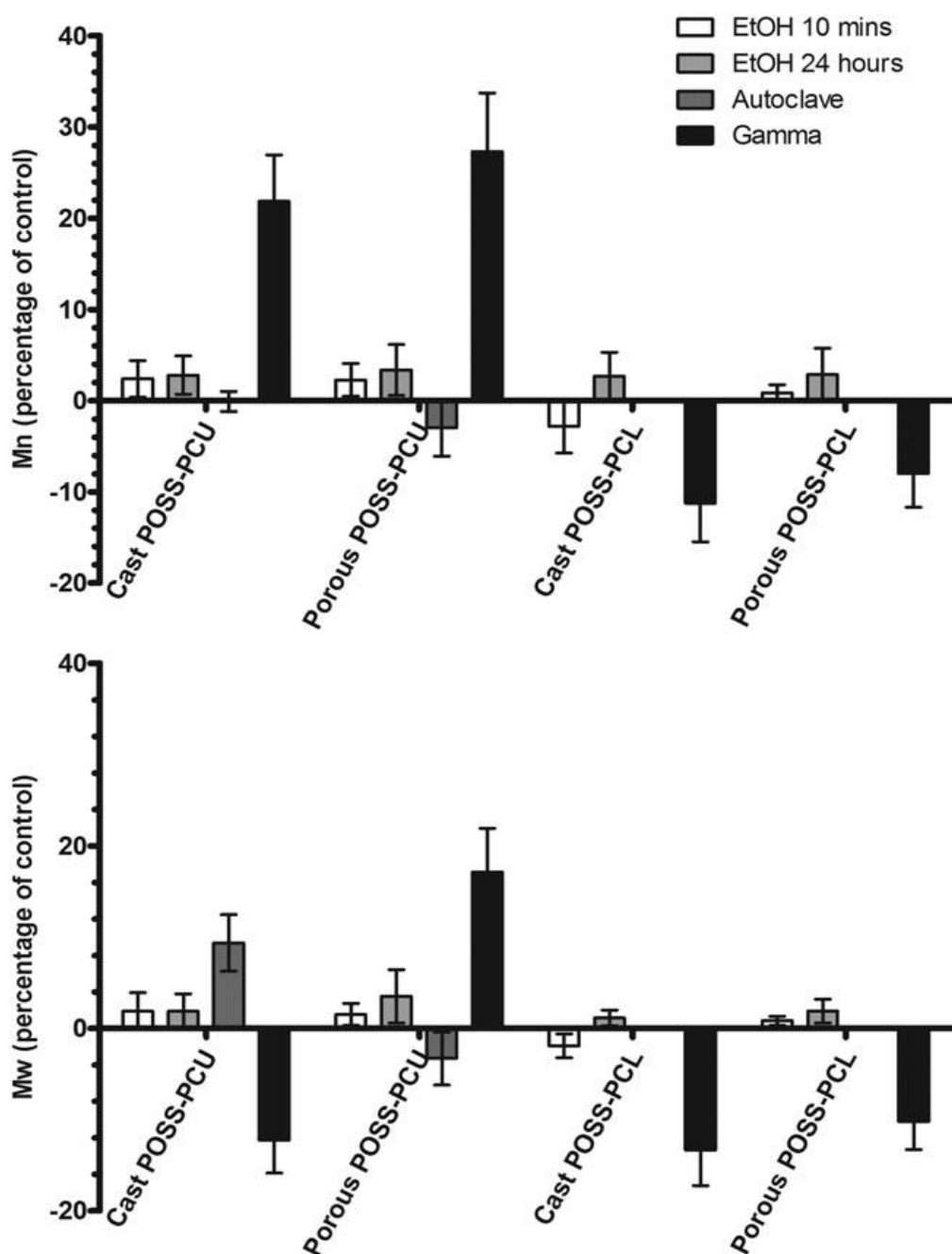
Figure 7.3: The percentage change (compared with unsterilized control) in number average (Mn, top) and weight average (Mw, bottom) molecular weight of POSS-PCU and POSS-PCL, both cast and porous samples after sterilization via a 10-min incubation in EtOH, 24 h incubation in EtOH, autoclaving, and gamma irradiation (mean $\pm$ SD, n=3). The molecular weights of the unsterilized controls were as follows: POSS-PCU ($M_w = 108\,500$, $M_n = 42{,}600$), POSS-PCL ($62\,800$, $M_n = 31{,}200$).

The untreated POSS-PCU was found to have a weight average molecular weight (M_w) of 108,500 and a number average molecular weight (M_n) of 42,600 whereas POSS-PCL had an M_w of 62,800 and an M_n of 31,200. After treatment with ethanol there was a negligible effect on either M_w or M_n regardless of incubation time for any sample. Autoclaving the cast POSS-PCU resulted in a 9.3% increase ($p < 0.005$) in M_w but no change in M_n possibly suggesting a degree of cross linking. No changes in molecular weight distributions were detected in autoclaved porous samples of POSS-PCL. Exposure to gamma irradiation had a significant impact on all of the samples. The M_n of cast POSS-PCU increased significantly by 21.9% whereas the M_w decreased by 12.3% ($p < 0.001$). Meanwhile for porous POSS-PCU both the M_n and M_w increased by 27.3% and 17.1% respectively. Both cast and porous samples of POSS-PCL exhibited a significant ($p < 0.001$) decrease in M_n (11.2% and 7.2%) and M_w (13.4% and 10.4%) respectively after exposure.

7.3.5 Cytotoxicity

The results of the AB assay are presented in figure 6.4 as a ratio of viable cells compared to control cells cultured on the tissue culture plastic, following seven days of incubation. Whilst no significant differences were detected between cell viability on EtOH treated and autoclaved samples, sterilising via gamma irradiation reduced cell viability by approximately 50%, compared to EtOH treated and autoclaved samples, on both cast and porous POSS-PCU samples. Sterilisation technique had no significant impact on cell growth on the cast samples of POSS-PCL samples and no cell growth was observed on the porous POSS-PCL samples.
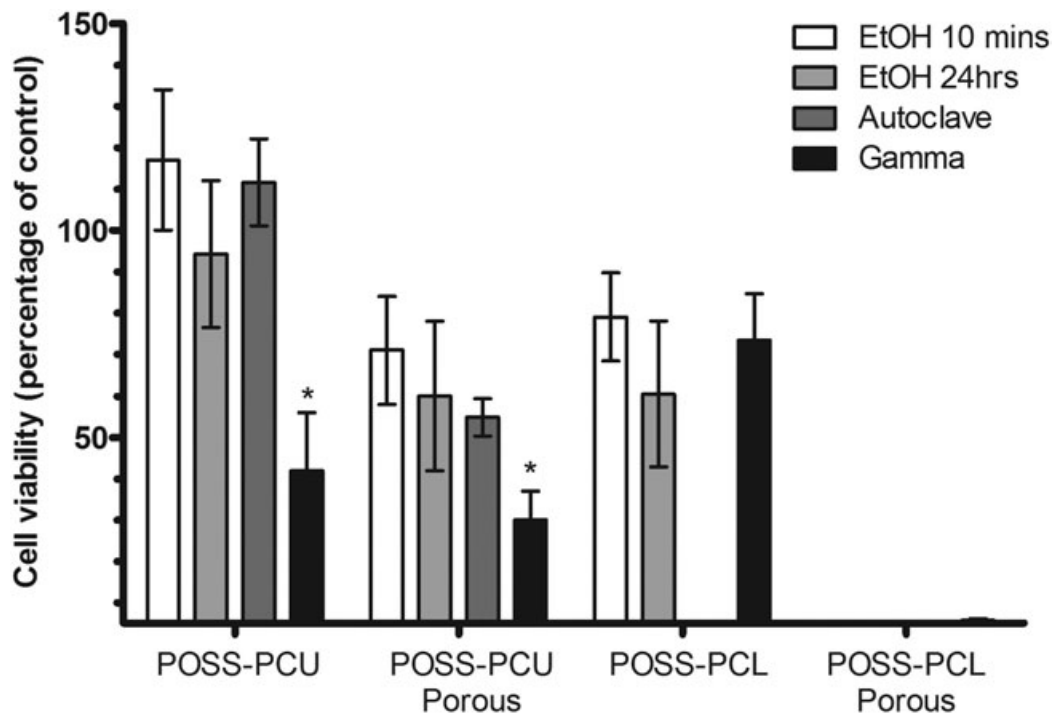
Figure 7.4: Cell viability after 7 day incubation, as determined by Alamar blue assay. Results (mean ± SD) are presented as a percentage of the control cells grown on tissue culture plastic (n=4, * = p<0.001). Gamma irradiation appeared to reduce the number of viable cells by approximately 50% on POSS-PCU whereas no significant differences were observed in cell growth on casted POSS-PCL samples. No cell growth was seen on the coagulated samples of POSS-PCL.

7.3.6 Efficacy of Sterilisation

The polymer materials were incubated in TSB and THY to test the efficiency of sterilization with the resultant level of bacterial growth reported in Table 7.2.

Sample		Sterilization Technique	Growth in Media	
			TSB	THY
POSS-PCU	Cast	EtOH 10 min	3/3	0/3
		EtOH 24 h	2/3	0/3
		Autoclave	0/3	0/3
		Gamma	0/3	0/3
	Porous	EtOH 10 min	2/3	0/3
		EtOH 24 h	3/3	0/3
		Autoclave	0/3	0/3
		Gamma	0/3	0/3
POSS-PCL	Cast	EtOH 10 min	3/3	0/3
		EtOH 24 h	3/3	0/3
		Autoclave	n/a	n/a
		Gamma	0/3	0/3
	Porous	EtOH 10 min	3/3	0/3
		EtOH 24 h	2/3	0/3
		Autoclave	n/a	n/a
		Gamma	0/3	0/3

Table 7.2: Bacterial Growth Observed on Each Sample After Incubation in Tryptone Soya Broth (TSB) and Fluid Thioglycollate Medium (THY) for Cultivation of Microorganisms.

THY is a viscous growth medium with reduced oxygen levels which tests for the growth of anaerobic bacteria and other organisms capable of growing in reduced oxygen tension. No evidence of bacterial growth was observed after incubation of materials in THY. TSB is a general growth media for aerobic microorganisms and is designed for the growth of aerobic bacteria, yeasts and moulds. The materials sterilized by EtOH incubation were not fully sterile and sustained the growth of bacteria for at least 2 out of 3 samples tested of each material. Autoclaving and gamma irradiation appear to be far more effective sterilization techniques based on these results.

7.4.0 Discussion

PU's have found numerous uses as medical devices primarily due to a combination of biocompatibility and suitable mechanical properties. However, degradation through oxidation and hydrolysis, once implanted, has limited their use. Siloxane based polymers, on the other hand, are resistant to oxidation and hydrolysis, and also show good biocompatibility; but they are not mechanically robust enough and are prone to mechanical failure. In a bid to utilise the mechanical integrity of PU'ss and the biostability of siloxanes, our group has tethered a polyhedral siloxane cage to the PU backbone. An *in vitro* examination demonstrated it to be more resistant to hydrolysis and oxidation, results which were later confirmed *in vivo*.

However, the impact of sterilising technique is as yet unknown. Sterilisation can be achieved in a number of ways including steam and gamma irradiation. Depending on the chemical nature of the material and the processing method; sterilisation techniques have been reported to induce changes in material properties. In this study we investigated the effects of sterilisation on two POSS polyurethane nanocomposites: a non-degradable POSS-PCU with

an aromatic hard segment and carbonate based soft segment, and a biodegradable POSS-PCL based on an aliphatic hard segment and caprolactone soft segement. Further, we investigated the effect of sterilisation on phase separated POSS-PCU and POSS-PCL. Phase separation is a popular method to create a porous, 3D environment for tissue engineering applications (Wei and Ma, 2008). The properties of the sterilised samples were compared to untreated controls.

The four samples assessed were incubated with 70% ethanol for a period of 10 minutes and 24 hours. ATR-FTIR analysis indicated that no changes in the surface chemical composition took place. Further, there were no significant variations in molecular weight or mechanical properties suggesting that neither surface nor bulk properties of POSS-PCU or POSS-PCL were affected by ethanol irrespective of incubation time. Whilst ethanol has been shown to be useful in disinfecting lipophilic viruses and gram-positive, gram-negative, and acid-fast bacteria; hydrophilic viruses and bacterial spores are resistant to the microbial effects of ethanol making it unsuitable for sterilising biomedical devices for *in vivo* applications (Holy *et al.*, 2001). However, in this study no signs of bacterial infection or cytotoxicity were observed with cell growth being in excess of control cells cultured on tissue culture plastic following 7 days of culture for the cast sheets and 75%   for coagulated samples.

The process of autoclaving requires samples to be exposed to high pressure saturated steam at temperatures of 121°C or more. The combination of high temperature, humidity and pressure has been shown to be quite detrimental to PU's with decreases in UTS, hydrolysis and oxidation being reported in polyether based PU's (Simmons *et al.*, 2006). The caprolactone based POSS-PCL also could not withstand the effects of autoclaving with extensive deformation of the samples being observed. It is likely that the aliphatic hard

segment of the POSS-PCL decrystallises and loses its structural integrity upon exposure to high temperatures. The result of which was that further examination of the autoclaved POSS-PCL samples was not possible.

The non-degradable POSS-PCU samples were, however, relatively unaffected by exposure to autoclaving with the cast and coagulated samples retaining their shape and structure. GPC analysis suggested there was a minor increase in Mw of the cast sample which may explain the slight increase in elongation at break experienced by the autoclaved POSS-PCU. The small changes in behaviour may be due to a minimal degree of cross linking experienced by the material. The coagulated sample of POSS-PCU exhibited a small decrease in elongation at break alongside a reduction in ATR-FTIR peak intensity at 1245cm^{-1}. These results are consistent with chain scission of the hard segment. The porous, coagulated sample has a significantly increased surface area, compared to the cast sample, offering a possible explanation for the difference in behaviour between the cast and coagulated samples. Chain scission may be induced by the moist environment at the surface of the material as opposed to the high temperatures being experienced by the bulk. No significant changes were recorded in the molecular weight profile of the coagulated POSS-PCU sample further reinforcing the belief that chain scission is a surface effect as opposed to bulk.

Mixed findings have been reported regarding the effects of gamma irradiation on PU's. Whilst some investigators have found no change in material properties following exposure to gamma irradiation, an equally significant number of publications indicate severe degradation of material (Haugen *et al.*, 2007; Simmons *et al.*, 2006; Grad *et al.*, 2003). Gamma irradiation is advantageous in that it is a rapid and highly effective sterilisation

technique. However, in the case of both the POSS samples that were tested it caused severe damage and displayed cytotoxic effects upon the cultured mononuclear cells. Whilst cell growth on the POSS-PCL samples was unaffected by sterilisation technique, gamma irradiation reduced cell viability by more than half on POSS-PCU. Whilst the exact mechanism behind this observation is unclear, there are reports in the literature of PU'ss with MDI based hard segments releasing 4,4'-methylene dianiline as a degradation product (Haugen *et al.*, 2007; Tang *et al.*, 2003). Aromatic amines are known to be highly cytotoxic and gamma irradiation has been shown to release 4,4'-methylene dianiline previously giving rise to cytotoxic side effects (Shintani, 1995; Golli-Bennour *et al.*, 2011).

No changes were observed in the appearance of POSS-PCL samples after exposure to gamma irradiation; however, the POSS-PCU samples had discoloured and became yellow. The difference between the two samples is most likely due to the MDI in the aromatic hard segment of POSS-PCU. Exposure to gamma irradiation may have oxidised the central methylene group of the biphenyl leading to a highly conjugated quinone chromophore (fig 6).

Analysis of the surface functional groups of the cast and coagulated samples of POSS-PCU via ATR-FTIR provided further evidence of material degradation. Reductions in peak intensities at $1245cm^{-1}$, $1540cm^{-1}$ and $1740\ cm^{-1}$ are all consistent with hydrolysis of the hard segment. The significant reductions in Mw for both samples, as well as Mn for the coagulated sample would appear to corroborate those findings. The Mn for casted samples of POSS-PCU increased suggesting that cross linking is taking place. As Mn is a more sensitive parameter to the lower end of the molecular weight distribution, these results would suggest that chain scission is taking place followed by cross linking of the low molecular weight chains of the casted POSS-PCU. An increase in ATR-FTIR peak intensity at $1095\ cm^{-1}$

would reinforce these findings as ~1100cm^{-1} is the region where we would expect to find ether peak as a result of cross linking. However, it is difficult to assign this peak with any certainty as the Si-O-Si of POSS is also expected in this region.

There is no evidence to suggest any cross linking is taking place in the POSS-PCL samples. GPC data showed significant reductions in Mn, Mw and Pd for both the cast and coagulated samples suggesting severe degradation of samples. These findings were reinforced by the ATR-FTIR results which found reductions in peaks at 1730 cm^{-1}, 1540 cm^{-1} 1240 cm^{-1} and 1165 cm^{-1} indicating chain scission in both the hard and soft segments.

The effect of polymer degradation was seen in the mechanical testing of the samples. The UTS and Youngs modulus decreased significantly for the casted samples of both POSS-PCU and POSS-PCL. The coagulated samples did not display any significant changes in their mechanical properties. This is probably due to the highly porous nature of the coagulated samples meaning that the true cross sectional area upon which force was applied was considerably lower than the measured area resulting in lower than expected values. The force range upon which the samples were examined may not be large enough to determine any detrimental effects on the polymer chains.

7.5.0 Conclusion

Sterilising POSS modified polyurethanes via EtOH resulted in no observable damage. Whilst the high temperatures involved in autoclaving, destroyed the biodegradable POSS-PCL samples, the non-degradable POSS-PCU withstood autoclaving well. Gamma irradiation however led to significant degradation in both samples and had a cytotoxic effect upon cell culture. The results indicate that autoclaving is the optimal sterilisation procedure for POSS-PCU; however, more suitable methods to sterilise biodegradable materials is needed. Tissue engineering scaffolds are purposefully designed to degrade over time; however their fragile nature also makes them unsuitable for the standard forms of sterilisation. Therefore, new methods capable of sterilising without affecting them chemically, mechanically or morphologically are needed for *in vivo* use of biodegradable scaffolds.

8

8. Summary

Over the course of this thesis the aim of the project developed and changed as the work progressed. Initially the project was designed to look at the possibility of developing an improved scaffold for use in vascular prosthesis using the novel nanocomposite developed by our group and seeded with human cells derived from a human umbilical cord source.

This series of experiments has demonstrated that it is possible to extract stem cells from human peripheral blood and seed endothelial tissue within a reasonable timeframe. Flow circuit studies demonstrate that cells remain adherent on the graft surface even simulated physiological flow.

It is generally acknowledged that in order for a vascular prosthesis to approach the patency of autologous saphenous vein the development of an endothelium on the prosthesis lumen would be essential.

As the project progressed it became apparent that both the single-stage and two-stage EC seeding processes which had been attempted by a number of groups including my own previously were not, when translated to clinical practice, very successful. This was due to a number of factors including the difficulty of obtaining an adequate number of cells to seed prosthesis and the requirement to undergo two surgeries in order to obtain the initial cell sample. Other challenges could include cost, lack of specialist facilities/staffing, regulatory matters and ethical issues.

As a result, it became necessary to consider if a different approach to the issue of cell sourcing would be more realistic. During the lifetime of this thesis, there was increasing interest in the new field of stem cell technology. While many of the most commonly used sources of stem cells would face the same problems as the cell sources previously investigated for vascular prosthesis seeding (such as lack of availability for cord blood and the difficulty of extraction for bone marrow derived cells) one other cell source, peripheral blood derived endothelial stem cells, appeared to be very promising. Peripheral blood is relatively easily obtained from patients with minimal risk and inconvenience to the patient.

It was therefore postulated that it may be possible to design a practical process to produce an EC seeded vascular prosthesis within a clinically realistic timescale and this became the revised aim of the thesis. Such a process would involve initially extracting a sufficient amount of blood from the patient after which the EPC and circulating EC's would be extracted in the laboratory. The extracted cells would then be either cultured until there were an adequate number of cells to seed the prosthesis or seeded directly onto the prosthesis and

allowed to attach firmly. If necessary, the seeded prosthesis could also be exposed to pre-conditioning prior to implantation. Once successfully seeded the vascular prosthesis could then be implanted into the patient in more routine clinical settings.

Such a process has many theoretical advantages. As the cells used would be derived from each patient individually there should be no issues with immune reactions to foreign cells. Should insufficient cells be extracted or the extracted cells fail to progress then either a second blood sample could be taken or the patient could still have an unseeded prosthesis implanted in urgent cases. In either case the patient would not have been exposed to a preliminary operation with its attendant costs and risks.

The work presented in this thesis demonstrates that the nanocomposite used to manufacture the vascular prosthesis is suitable for cell seeding (Chapters 2 and). Chapters 4 and 6 provided evidence that it is possible to extract sufficient cells from human peripheral blood in a suitable timescale to seed a prosthesis and that the cells so extracted and grown demonstrate EC properties. Chapter 3 examined the possibility of modifying the surface of the nanocomposite to improve cell adhesion and growth and this is an area in which much further work could be carried out. Finally, Chapter 5 investigated the effect of flow on seeded nanocomposite both with and without preconditioning. Chapter 7 examined some potential methods of sterilizing the vascular prosthesis prior to cell seeding.

Given the above it can be concluded that the postulated process for developing a seeded vascular prosthesis which can be implanted into a patient in a realistic timeframe is a potentially viable approach to the problem and provides a solid base for further investigation and progress to clinical usage.

All of the work presented in this thesis has been published in peer-reviewed journals as has much of the work on which it is based. A full list of publications is included in Appendix A.

8.1 Further Work

Vascular disease represents a huge healthcare burden. In the United Kingdom, there were more than 1.6 million episodes related to cardiovascular disease in NHS hospitals, accounting for 10% of all inpatient episodes among men and 6.2% among women. With a mortality rate of 28% and a cost burden to the NHS in England of £6.8 billion in 2012/13 (British Heart Foundation 2014) there is sound clinical and economic reasoning to pursue this area of research.

There are numerous areas in which further work could be carried out and great opportunities for further progress in the field. The area of surface modification of prosthesis is a vast subject with numerous new approaches being investigated constantly. There is still no generally accepted method of extracting EPC from peripheral blood and this area would also be very interesting to investigate further as would the effect of age and other health related factors on extracted cell numbers. There are also still some practical issues to resolve such as problems with using non-human licensed tissue culture media and supplements (such as FBS) to extract and grow the cells as well as making available the facilities to do this.

Finally of course eventually there would be the need to assess the process in a clinical trial with human patients for safety, quality of life, cost effectiveness and other clinical outcomes.

8.2 Conclusion

The work presented in this thesis demonstrates that the development of a two stage seeding process for peripheral vein grafting using autologous peripheral blood is a viable possibility according to these early experiments.

Challenges remain in developing this methodology for clinical use. Given further work, these challenges such as the cost, ethical and practical issues could be overcome to develop a clinical solution to the burden of cardiovascular disease in future.

References

Adamson, A. W. and Gast, A. P. (1997) *Physical chemistry of surfaces.* 6. ed. ed. New York [u.a.]: Wiley.

Ahmed, M., Ghanbari, H., Cousins, B. G., Hamilton, G. and Seifalian, A. M. (2011) Small calibre polyhedral oligomeric silsesquioxane nanocomposite cardiovascular grafts: influence of porosity on the structure, haemocompatibility and mechanical properties, *Acta Biomaterialia,* 7 (11), pp. 3857-3867.

Amaral, M., Lopes, M. A., Santos, J. D. and Silva, R. F. (2002) Wettability and surface charge of Si3N4-bioglass composites in contact with simulated physiological liquids, *Biomaterials,* 23 (20), pp. 4123-4129.

Armitage, D. A., Parker, T. L. and Grant, D. M. (2003) Biocompatibility and hemocompatibility of surface-modified NiTi alloys, *Journal of Biomedical Materials Research,* 66A (1), pp. 129-137.

Arnold, M., Cavalcanti-Adam, E. A., Glass, R., Blummel, J., Eck, W., Kantlehner, M. *et al.* (2004) Activation of integrin function by nanopatterned adhesive interfaces, *Chemphyschem.,* 5 (3), pp. 383-388.

Asahara, T., Murohara, T., Sullivan, A., Silver, M., van der, Z. R., Li, T. *et al.* (1997) Isolation of putative progenitor endothelial cells for angiogenesis, *Science,* 275 (5302), pp. 964-967.

Assmann, A., Delfs, C., Munakata, H., Schiffer, F., Horstkotter, K., Huynh, K. *et al.* (2013) Acceleration of autologous in vivo recellularization of decellularized aortic conduits by fibronectin surface coating, *Biomaterials,* 34 (25), pp. 6015-6026.

Azhim, A., Yamagami, K., Muramatsu, K., Morimoto, Y. and Tanaka, M. (2011) The use of sonication treatment to completely decellularize blood arteries: a pilot study, *Conference Proceedings : ...Annual International Conference of the IEEE Engineering in Medicine and Biology Society.IEEE Engineering in Medicine and Biology Society.Annual Conference,* 2011 , pp. 2468-2471.

Baguneid, M. S., Seifalian, A. M., Salacinski, H. J., Murray, D., Hamilton, G. and Walker, M. G. (2006) Tissue engineering of blood vessels, *The British Journal of Surgery,* 93 (3), pp. 282-290.

Baguneid, M., de Mel, A., Yildirimer, L., Fuller, B. J., Hamilton, G. and Seifalian, A. M. (2011) In vivo study of a model tissue-engineered small-diameter vascular bypass graft, *Biotechnology and Applied Biochemistry,* 58 (1), pp. 14-24.

Baguneid, M., Murray, D., Salacinski, H. J., Fuller, B., Hamilton, G., Walker, M. *et al.* (2004) Shear-stress preconditioning and tissue-engineering-based paradigms for generating arterial substitutes, *Biotechnology and Applied Biochemistry,* 39 , pp. 151-157.

Baiguera, S. and Ribatti, D. (2013) Endothelialization approaches for viable engineered tissues, *Angiogenesis,* 16 (1), pp. 1-14.

Baker, L. D., Johnson, J. M. and Goldfarb, D. (1976) Expanded polytetrafluoroethylene (PTFE) subcutaneous arteriovenous conduit: an improved vascular access for chronic hemodialysis, *Transactions - American Society for Artificial Internal Organs,* 22 , pp. 382-387.

Ballermann, B. J., Dardik, A., Eng, E. and Liu, A. (1998) Shear stress and the endothelium, *Kidney International.Supplement,* 67 , pp. 100.

Banerjee, S., Xu, H., Fuh, E., Nguyen, K. T., Garcia, J. A., Brilakis, E. S. *et al.* (2012) Endothelial progenitor cell response to antiproliferative drug exposure, *Atherosclerosis,* 225 (1), pp. 91-98.

Belanger, M. C., Marois, Y., Roy, R., Mehri, Y., Wagner, E., Zhang, Z. *et al.* (2000) Selection of a polyurethane membrane for the manufacture of ventricles for a totally implantable artificial heart: blood compatibility and biocompatibility studies, *Artificial Organs,* 24 (0160-564; 11), pp. 879-888.

Berger, K., Sauvage, L. R., Rao, A. M. and Wood, S. J. (1972) Healing of arterial prostheses in man: its incompleteness, *Annals of Surgery,* 175 (1), pp. 118-127.

Blakemore, A. H. and Voorhees, A. B. (1954) The use of tubes constructed from vinyon N cloth in bridging arterial defects; experimental and clinical, *Annals of Surgery,* 140 (3), pp. 324-334.

Boo, Y. C., Sorescu, G., Boyd, N., Shiojima, I., Walsh, K., Du, J. *et al.* (2002) Shear stress stimulates phosphorylation of endothelial nitric-oxide synthase at Ser1179 by Akt-independent mechanisms: role of protein kinase A, *The Journal of Biological Chemistry,* 277 (5), pp. 3388-3396.

Bouis, D., Hospers, G. A., Meijer, C., Molema, G. and Mulder, N. H. (2001) Endothelium in vitro: a review of human vascular endothelial cell lines for blood vessel-related research, *Angiogenesis,* 4 (2), pp. 91-102.

British Heart Foundation (2014) Cardiovascular Statistics. British Heart Foundation Centre on Population Approaches for Non‑Communicable Disease Prevention. Nuffield Department of Population Health, University of Oxford

Brothers, T. E., Stanley, J. C., Burkel, W. E. and Graham, L. M. (1990) Small-caliber polyurethane and polytetrafluoroethylene grafts: a comparative study in a canine aortoiliac model, *Journal of Biomedical Materials Research,* 24 (6), pp. 761-771.

Bu, X., Yan, Y., Zhang, Z., Gu, X., Wang, M., Gong, A. *et al.* (2010) Properties of extracellular matrix-like scaffolds for the growth and differentiation of endothelial progenitor cells, *The Journal of Surgical Research,* 164 (1), pp. 50-57.

Buijs, J., Ramstrom, M., Danfelter, M., Larsericsdotter, H., Hakansson, P. and Oscarsson, S. (2003) Localized changes in the structural stability of myoglobin upon adsorption onto silica particles, as studied with hydrogen/deuterium exchange mass spectrometry, *Journal of Colloid and Interface Science,* 263 (2), pp. 441-448.

Burke, A. and Hasirci, N. (2004) Polyurethanes in biomedical applications, *Advances in Experimental Medicine and Biology,* 553 , pp. 83-101.

Carr, H. M., Vohra, R., Sharma, H., Smyth, J. V., Rooney, O. B., Dodd, P. D. *et al.* (1996) Endothelial cell seeding kinetics under chronic flow in prosthetic grafts, *Annals of Vascular Surgery,* 10 (5), pp. 469-475.

Cebotari, S., Lichtenberg, A., Tudorache, I., Hilfiker, A., Mertsching, H., Leyh, R. *et al.* (2006) Clinical application of tissue engineered human heart valves using autologous progenitor cells, *Circulation,* 114 (1 Suppl), pp. 132.

Chamiot-Clerc, P., Copie, X., Renaud, J. F., Safar, M. and Girerd, X. (1998) Comparative reactivity and mechanical properties of human isolated internal mammary and radial arteries, *Cardiovascular Research,* 37 (3), pp. 811-819.

Chen, B. P., Li, Y. S., Zhao, Y., Chen, K. D., Li, S., Lao, J. *et al.* (2001) DNA microarray analysis of gene expression in endothelial cells in response to 24-h shear stress, *Physiological Genomics (Online),* 7 (1), pp. 55-63.

Chen, Z., Ward, R., Tian, Y., Malizia, F., Gracias, D. H., Shen, Y. R. *et al.* (2002) Interaction of fibrinogen with surfaces of end-group-modified polyurethanes: a surface-specific sum-frequency-generation vibrational spectroscopy study, *Journal of Biomedical Materials Research,* 62 (2), pp. 254-264.

Chien, S. (2008) Effects of disturbed flow on endothelial cells, *Annals of Biomedical Engineering,* 36 (4), pp. 554-562.

Chiesa, R., Astore, D., Frigerio, S., Garriboli, L., Piccolo, G., Castellano, R. *et al.* (2002) Vascular prosthetic graft infection: epidemiology, bacteriology, pathogenesis and treatment, *Acta Chirurgica Belgica,* 102 (4), pp. 238-247.

Christenson, E. M., Dadsetan, M. and Hiltner, A. (2005) Biostability and macrophage-mediated foreign body reaction of silicone-modified polyurethanes, *Journal of Biomedical Materials Research.Part A,* 74 (2), pp. 141-155.

Cucina, A., Borrelli, V., Randone, B., Coluccia, P., Sapienza, P. and Cavallaro, A. (2003) Vascular endothelial growth factor increases the migration and proliferation of smooth muscle cells through the mediation of growth factors released by endothelial cells, *The Journal of Surgical Research,* 109 (1), pp. 16-23.

Cunningham, J. J., Nikolovski, J., Linderman, J. J. and Mooney, D. J. (2002) Quantification of fibronectin adsorption to silicone-rubber cell culture substrates, *BioTechniques,* 32 (4), pp. 880 passim.

Dahl, S. L., Koh, J., Prabhakar, V. and Niklason, L. E. (2003) Decellularized native and engineered arterial scaffolds for transplantation, *Cell Transplantation,* 12 (6), pp. 659-666.

Dardik, A., Liu, A. and Ballermann, B. J. (1999) Chronic in vitro shear stress stimulates endothelial cell retention on prosthetic vascular grafts and reduces subsequent in vivo neointimal thickness, *Journal of Vascular Surgery,* 29 (1), pp. 157-167.

Darouiche, R. O. (2004) Treatment of infections associated with surgical implants, *The New England Journal of Medicine,* 350 (14), pp. 1422-1429.

de Mel, A., Murad, F. and Seifalian, A. M. (2011) Nitric oxide: a guardian for vascular grafts? *Chemical Reviews,* 111 (9), pp. 5742-5767.

Debakey, M. E., Crawford, E. S. and Cooley, D. A. (1957) Chronic arterial insufficiency of the lower extremities, *Disease-a-Month : DM,* , pp. 3-45.

Desai, M., Seifalian, A. M. and Hamilton, G. (2011) Role of prosthetic conduits in coronary artery bypass grafting, *European Journal of Cardio-Thoracic Surgery : Official Journal of the European Association for Cardio-Thoracic Surgery,* 40 (2), pp. 394-398.

Deutsch, M., Meinhart, J., Fischlein, T., Preiss, P. and Zilla, P. (1999) Clinical autologous in vitro endothelialization of infrainguinal ePTFE grafts in 100 patients: a 9-year experience, *Surgery,* 126 (5), pp. 847-855.

Dolan, J. M., Meng, H., Singh, S., Paluch, R. and Kolega, J. (2011) High fluid shear stress and spatial shear stress gradients affect endothelial proliferation, survival, and alignment, *Annals of Biomedical Engineering,* 39 (6), pp. 1620-1631.

Duchateau, R., Dijkstra, T. W., van Santen, R. A. and Yap, G. P. (2004) Silsesquioxane models for silica surface silanol sites with adjacent siloxide functionalites and olefin polymerization catalysts thereof, *Chemistry (Weinheim an Der Bergstrasse, Germany),* 10 (16), pp. 3979-3990.

Echave, V., Koornick, A. R., Haimov, M. and Jacobson, J. H. (1979) Intimal hyperplasia as a complication of the use of the polytetrafluoroethylene graft for femoral-popliteal bypass, *Surgery,* 86 (6), pp. 791-798.

Edgell, C. J., McDonald, C. C. and Graham, J. B. (1983) Permanent cell line expressing human factor VIII-related antigen established by hybridization, *Proceedings of the National Academy of Sciences of the United States of America,* 80 (12), pp. 3734-3737.

EDWARDS, W. S. (1959) Progress in synthetic graft development; an improved crimped graft of teflon, *Surgery,* 45 (2), pp. 298-309.

Fasol, R., Zilla, P., Deutsch, M., Grimm, M., Fischlein, T. and Laufer, G. (1989) Human endothelial cell seeding: evaluation of its effectiveness by platelet parameters after one year, *Journal of Vascular Surgery,* 9 (3), pp. 432-436.

Filova, E., Brynda, E., Riedel, T., Chlupac, J., Vandrovcova, M., Svindrych, Z. *et al.* (2014) Improved adhesion and differentiation of endothelial cells on surface-attached fibrin structures containing extracellular matrix proteins, *Journal of Biomedical Materials Research.Part A,* 102 (3), pp. 698-712.

Fiore, A. C., Brown, J. W., Turrentine, M. W., Ruzmetov, M., Huynh, D., Hanley, S. *et al.* (2011) A bovine jugular vein conduit: a ten-year bi-institutional experience, *The Annals of Thoracic Surgery,* 92 (1), pp. 2.

Fuchs, S., Hermanns, M. I. and Kirkpatrick, C. J. (2006) Retention of a differentiated endothelial phenotype by outgrowth endothelial cells isolated from human peripheral blood and expanded in long-term cultures, *Cell and Tissue Research,* 326 (0302-766; 1), pp. 79-92.

Furchgott, R. F., Cherry, P. D., Zawadzki, J. V. and Jothianandan, D. (1984) Endothelial cells as mediators of vasodilation of arteries, *Journal of Cardiovascular Pharmacology,* 6 Suppl 2 , pp. 336.

Furchgott, R. F. and Zawadzki, J. V. (1980) The obligatory role of endothelial cells in the relaxation of arterial smooth muscle by acetylcholine, *Nature,* 288 (5789), pp. 373-376.

Garrido, L., Pfleiderer, B., Papisov, M. and Ackerman, J. L. (1993) In vivo degradation of silicones, *Magnetic Resonance in Medicine,* 29 (6), pp. 839-843.

George, J., Shmilovich, H., Deutsch, V., Miller, H., Keren, G. and Roth, A. (2006) Comparative analysis of methods for assessment of circulating endothelial progenitor cells, *Tissue Engineering,* 12 (2), pp. 331-335.

Ghanbari, H., Cousins, B. G. and Seifalian, A. M. (2011) A nanocage for nanomedicine: polyhedral oligomeric silsesquioxane (POSS), *Macromolecular Rapid Communications,* 32 (14), pp. 1032-1046.

Goh, E. T., Wong, E., Farhatnia, Y., Tan, A. and Seifalian, A. M. (2014) Accelerating in situ endothelialisation of cardiovascular bypass grafts, *International Journal of Molecular Sciences,* 16 (1), pp. 597-627.

Golli-Bennour, E. E., Kouidhi, B., Dey, M., Younes, R., Bouaziz, C., Zaied, C. *et al.* (2011) Cytotoxic effects exerted by polyarylsulfone dialyser membranes depend on different sterilization processes, *International Urology and Nephrology,* 43 (2), pp. 483-490.

Grad, S., Kupcsik, L., Gorna, K., Gogolewski, S. and Alini, M. (2003) The use of biodegradable polyurethane scaffolds for cartilage tissue engineering: potential and limitations, *Biomaterials,* 24 (28), pp. 5163-5171.

Graham, L. M., Burkel, W. E., Ford, J. W., Vinter, D. W., Kahn, R. H. and Stanley, J. C. (1980a) Immediate seeding of enzymatically derived endothelium in Dacron vascular grafts. Early experimental studies with autologous canine cells, *Archives of Surgery (Chicago, Ill.: 1960),* 115 (11), pp. 1289-1294.

Graham, L. M., Vinter, D. W., Ford, J. W., Kahn, R. H., Burkel, W. E. and Stanley, J. C. (1980b) Endothelial cell seeding of prosthetic vascular grafts: early experimental studies with cultured autologous canine endothelium, *Archives of Surgery (Chicago, Ill.: 1960),* 115 (8), pp. 929-933.

Greisler, H. P., Gosselin, C., Ren, D., Kang, S. S. and Kim, D. U. (1996a) Biointeractive polymers and tissue engineered blood vessels, *Biomaterials,* 17 (3), pp. 329-336.

Greisler, H. P., Petsikas, D., Cziperle, D. J., Murchan, P. M., Henderson, S. C. and Lam, T. M. (1996b) Dacron stimulation of macrophage transforming growth factor-beta release, *Cardiovascular Surgery (London, England),* 4 (2), pp. 169-173.

Greisler, H. P., Tattersall, C. W., Henderson, S. C., Cabusao, E. A., Garfield, J. D. and Kim, D. U. (1992) Polypropylene small-diameter vascular grafts, *Journal of Biomedical Materials Research,* 26 (10), pp. 1383-1394.

Gumpenberger, T., Heitz, J., Bauerle, D., Kahr, H., Graz, I., Romanin, C. *et al.* (2003) Adhesion and proliferation of human endothelial cells on photochemically modified polytetrafluoroethylene, *Biomaterials,* 24 (28), pp. 5139-5144.

Gupta, A., Vara, D. S., Punshon, G., Sales, K. M., Winslet, M. C. and Seifalian, A. M. (2009) In vitro small intestinal epithelial cell growth on a nanocomposite polycaprolactone scaffold, *Biotechnology and Applied Biochemistry,* 54 (4), pp. 221-229.

Habal, M. B. (1984) The biologic basis for the clinical application of the silicones. A correlate to their biocompatibility, *Archives of Surgery (Chicago, Ill.: 1960),* 119 (7), pp. 843-848.

Harish, A. and Allon, M. (2011) Arteriovenous graft infection: a comparison of thigh and upper extremity grafts, *Clinical Journal of the American Society of Nephrology : CJASN,* 6 (7), pp. 1739-1743.

Harraz, M., Jiao, C., Hanlon, H. D., Hartley, R. S. and Schatteman, G. C. (2001) CD34^{-} Blood-Derived Human Endothelial Cell Progenitors, *Stem Cells (Dayton, Ohio),* 19 (4), pp. 304-312.

Haugen, H. J., Brunner, M., Pellkofer, F., Aigner, J., Will, J. and Wintermantel, E. (2007) Effect of different gamma-irradiation doses on cytotoxicity and material properties of porous polyether-urethane polymer, *Journal of Biomedical Materials Research.Part B, Applied Biomaterials,* 80 (2), pp. 415-423.

Heitz, J., Gumpenberger, T., Kahr, H. and Romanin, C. (2004) Adhesion and proliferation of human vascular cells on UV-light-modified polymers, *Biotechnology and Applied Biochemistry,* 39 , pp. 59-69.

Heitz, J., Svorcik, V., Bacakova, L., Rockova, K., Ratajova, E., Gumpenberger, T. *et al.* (2003) Cell adhesion on polytetrafluoroethylene modified by UV-irradiation in an ammonia atmosphere, *J. Biomed. Mater. Res. A,* 67 (1), pp. 130-137.

Herring, M., Gardner, A. and Glover, J. (1984) Seeding human arterial prostheses with mechanically derived endothelium. The detrimental effect of smoking, *Journal of Vascular Surgery,* 1 (2), pp. 279-289.

Herring, M., Gardner, A. and Glover, J. (1978) A single-staged technique for seeding vascular grafts with autogenous endothelium, *Surgery,* 84 (4), pp. 498-504.

Hess, F. (1985) History of (micro) vascular surgery and the development of small-caliber blood vessel prostheses (with some notes on patency rates and re-endothelialization), *Microsurgery,* 6 (2), pp. 59-69.

Heyligers, J. M., Arts, C. H., Verhagen, H. J., de Groot, P. G. and Moll, F. L. (2005) Improving small-diameter vascular grafts: from the application of an endothelial cell lining to

the construction of a tissue-engineered blood vessel, *Annals of Vascular Surgery,* 19 (3), pp. 448-456.

Hill, J. M., Zalos, G., Halcox, J. P., Schenke, W. H., Waclawiw, M. A., Quyyumi, A. A. *et al.* (2003) Circulating endothelial progenitor cells, vascular function, and cardiovascular risk, *The New England Journal of Medicine,* 348 (7), pp. 593-600.

Hirsch, A. T., Allison, M. A., Gomes, A. S., Corriere, M. A., Duval, S., Ershow, A. G. *et al.* (2012) A call to action: women and peripheral artery disease: a scientific statement from the American Heart Association, *Circulation,* 125 (11), pp. 1449-1472.

Hoesli, C. A., Garnier, A., Juneau, P. M., Chevallier, P., Duchesne, C. and Laroche, G. (2014) A fluorophore-tagged RGD peptide to control endothelial cell adhesion to micropatterned surfaces, *Biomaterials,* 35 (3), pp. 879-890.

Holy, C. E., Cheng, C., Davies, J. E. and Shoichet, M. S. (2001) Optimizing the sterilization of PLGA scaffolds for use in tissue engineering, *Biomaterials,* 22 (1), pp. 25-31.

Howling, G. I., Dettmar, P. W., Goddard, P. A., Hampson, F. C., Dornish, M. and Wood, E. J. (2002) The effect of chitin and chitosan on fibroblast-populated collagen lattice contraction, *Biotechnology and Applied Biochemistry,* 36 (Pt 3), pp. 247-253.

Hur, J., Yoon, C. H., Kim, H. S., Choi, J. H., Kang, H. J., Hwang, K. K. *et al.* (2004) Characterization of two types of endothelial progenitor cells and their different contributions to neovasculogenesis, *Arteriosclerosis, Thrombosis, and Vascular Biology,* 24 (2), pp. 288-293.

Igreja, C., Courinha, M., Cachaco, A. S., Pereira, T., Cabecadas, J., da Silva, M. G. *et al.* (2007) Characterization and clinical relevance of circulating and biopsy-derived endothelial progenitor cells in lymphoma patients, *Haematologica,* 92 (4), pp. 469-477.

Iiyama, K., Hajra, L., Iiyama, M., Li, H., DiChiara, M., Medoff, B. D. *et al.* (1999) Patterns of vascular cell adhesion molecule-1 and intercellular adhesion molecule-1 expression in rabbit and mouse atherosclerotic lesions and at sites predisposed to lesion formation, *Circulation Research,* 85 (2), pp. 199-207.

Illi, B., Nanni, S., Scopece, A., Farsetti, A., Biglioli, P., Capogrossi, M. C. *et al.* (2003) Shear stress-mediated chromatin remodeling provides molecular basis for flow-dependent regulation of gene expression, *Circulation Research,* 93 (2), pp. 155-161.

Ingram, D. A., Mead, L. E., Tanaka, H., Meade, V., Fenoglio, A., Mortell, K. *et al.* (2004) Identification of a novel hierarchy of endothelial progenitor cells using human peripheral and umbilical cord blood, *Blood,* 104 (9), pp. 2752-2760.

Isenberg, B. C., Williams, C. and Tranquillo, R. T. (2006) Small-diameter artificial arteries engineered in vitro, *Circulation Research,* 98 (1), pp. 25-35.

Ivarsson, M. L., Holmdahl, L., Falk, P., Molne, J. and Risberg, B. (1998) Characterization and fibrinolytic properties of mesothelial cells isolated from peritoneal lavage, *Scandinavian Journal of Clinical and Laboratory Investigation,* 58 (3), pp. 195-203.

Jaffe, E. A., Nachman, R. L., Becker, C. G. and Minick, C. R. (1973) Culture of human endothelial cells derived from umbilical veins. Identification by morphologic and immunologic criteria, *The Journal of Clinical Investigation,* 52 (11), pp. 2745-2756.

Julio, C. A., de-Queiroz, A. A., Higa, O. Z., Marques, E. F. and Maizato, M. J. (1994) Blood compatibility of tubular polymeric materials studied by biological surface interactions, *Brazilian Journal of Medical and Biological Research = Revista Brasileira De Pesquisas Medicas E Biologicas / Sociedade Brasileira De Biofisica ...[Et Al.],* 27 (11), pp. 2565-2568.

Kannan, R. Y., Salacinski, H. J., Butler, P. E., Hamilton, G. and Seifalian, A. M. (2005a) Current status of prosthetic bypass grafts: a review, *J. Biomed. Mater. Res. B Appl. Biomater.,* 74 (1), pp. 570-581.

Kannan, R. Y., Salacinski, H. J., Butler, P. E. and Seifalian, A. M. (2005b) Polyhedral oligomeric silsesquioxane nanocomposites: the next generation material for biomedical applications, *Accounts of Chemical Research,* 38 (11), pp. 879-884.

Kannan, R. Y., Salacinski, H. J., De, G. J., Clatworthy, I., Bozec, L., Horton, M. *et al.* (2006) The antithrombogenic potential of a polyhedral oligomeric silsesquioxane (POSS) nanocomposite, *Biomacromolecules.,* 7 (1), pp. 215-223.

Kannan, R. Y., Salacinski, H. J., Ghanavi, J. E., Narula, A., Odlyha, M., Peirovi, H. *et al.* (2007) Silsesquioxane nanocomposites as tissue implants, *Plastic and Reconstructive Surgery,* 119 (6), pp. 1653-1662.

Kannan, R. Y., Salacinski, H. J., Odlyha, M., Butler, P. E. and Seifalian, A. M. (2005c) The degradative resistance of polyhedral oligomeric silsesquioxane nanocore integrated polyurethanes: An in vitro study, *Biomaterials, .*

Kannan, R. Y., Salacinski, H. J., Sales, K., Butler, P. and Seifalian, A. M. (2005d) The roles of tissue engineering and vascularisation in the development of micro-vascular networks: a review, *Biomaterials,* 26 (14), pp. 1857-1875.

Kerdjoudj, H., Moby, V., Berthelemy, N., Gentils, M., Boura, C., Bordenave, L. *et al.* (2007) The ideal small arterial substitute: Role of cell seeding and tissue engineering, *Clinical Hemorheology and Microcirculation,* 37 (1-2), pp. 89-98.

Kidane, A. G., Salacinski, H. J., Punshon, G., Ramesh, B., Srai, K. S. and Seifalian, A. M. (2003) Synthesis and evaluation of amphiphilic RGD derivatives: uses for solvent casting in polymers and tissue engineering applications, *Medical & Biological Engineering & Computing,* 41 (6), pp. 740-745.

Kidane, A. G., Salacinski, H., Tiwari, A., Bruckdorfer, K. R. and Seifalian, A. M. (2004) Anticoagulant and antiplatelet agents: their clinical and device application(s) together with usages to engineer surfaces, *Biomacromolecules.,* 5 (3), pp. 798-813.

Kidson, I. G. and Abbott, W. M. (1978) Low compliance and arterial graft occlusion, *Circulation,* 58 (3 Pt 2), pp. 1.

Klinkert, P., Post, P. N., Breslau, P. J. and van Bockel, J. H. (2004) Saphenous vein versus PTFE for above-knee femoropopliteal bypass. A review of the literature, *European Journal of Vascular and Endovascular Surgery : The Official Journal of the European Society for Vascular Surgery,* 27 (4), pp. 357-362.

Klinkert, P., van Dijk, P. J. and Breslau, P. J. (2003) Polytetrafluoroethylene femorotibial bypass grafting: 5-year patency and limb salvage, *Annals of Vascular Surgery,* 17 (5), pp. 486-491.

Kottke-Marchant, K., Anderson, J. M., Miller, K. M., Marchant, R. E. and Lazarus, H. (1987) Vascular graft-associated complement activation and leukocyte adhesion in an artificial circulation, *Journal of Biomedical Materials Research,* 21 (3), pp. 379-397.

Lappan, U., Geißler, U. and Lunkwitz, K. (1999) Modification of polytetrafluoroethylene by electron beam irradiation in various atmospheres, *Nuclear Inst. and Methods in Physics Research, B,* 151 (1), pp. 222-226. DOI: 10.1016/S0168-583X(99)00115-9.

Lasseter, T. L., Clare, B. H., Abbott, N. L. and Hamers, R. J. (2004) Covalently modified silicon and diamond surfaces: resistance to nonspecific protein adsorption and optimization for biosensing, *Journal of the American Chemical Society,* 126 (33), pp. 10220-10221.

Lee, S. W., Lee, Y. S., Hong, J. W., Wye, M. Y., Kim, J. H. and Kang, H. J. (2004) Surface modification and adhesion improvement of PTFE film by ion beam irradiation, *Nuclear Inst. and Methods in Physics Research, B,* 219 , pp. 963-967. DOI: 10.1016/j.nimb.2004.01.197.

Leseche, G., Penna, C., Bouttier, S., Joubert, S. and Andreassian, B. (1997) Femorodistal bypass using cryopreserved venous allografts for limb salvage, *Annals of Vascular Surgery,* 11 (3), pp. 230-236.

L'Heureux, N., McAllister, T. N. and de la Fuente, L M (2007) Tissue-engineered blood vessel for adult arterial revascularization, *The New England Journal of Medicine,* 357 (14), pp. 1451-1453.

Liu, T., Liu, S., Zhang, K., Chen, J. and Huang, N. (2014) Endothelialization of implanted cardiovascular biomaterial surfaces: the development from in vitro to in vivo, *Journal of Biomedical Materials Research.Part A,* 102 (10), pp. 3754-3772.

Liu, X., Zhang, Y., Wang, S., Lei, Z., Li, X. and Fan, D. (2016) The use of expanded polytetrafluoroethylene in depressed deformities of the face, *Experimental and Therapeutic Medicine,* 12 (5), pp. 3151-3154.

Magometschnigg, H., Kadletz, M., Vodrazka, M., Dock, W., Grimm, M., Grabenwoger, M. *et al.* (1992) Prospective clinical study with in vitro endothelial cell lining of expanded polytetrafluoroethylene grafts in crural repeat reconstruction, *Journal of Vascular Surgery,* 15 (3), pp. 527-535.

Malek, A. M. and Izumo, S. (1996) Mechanism of endothelial cell shape change and cytoskeletal remodeling in response to fluid shear stress, *Journal of Cell Science,* 109 (Pt 4) (Pt 4), pp. 713-726.

Mangold, S., Schrammel, S., Huber, G., Niemeyer, M., Schmid, C., Stangassinger, M. *et al.* (2015) Evaluation of decellularized human umbilical vein (HUV) for vascular tissue engineering - comparison with endothelium-denuded HUV, *Journal of Tissue Engineering and Regenerative Medicine,* 9 (1), pp. 13-23.

Marchal, J. A., Picon, M., Peran, M., Bueno, C., Jimenez-Navarro, M., Carrillo, E. *et al.* (2012) Purification and long-term expansion of multipotent endothelial-like cells with potential cardiovascular regeneration, *Stem Cells and Development,* 21 (4), pp. 562-574.

Marois, Y., Guidoin, R., Roy, R., Vidovsky, T., Jakubiec, B., Sigot-Luizard, M. F. *et al.* (1996) Selecting valid in vitro biocompatibility tests that predict the in vivo healing response of synthetic vascular prostheses, *Biomaterials,* 17 (19), pp. 1835-1842.

Martin, D. J., Warren, L. A., Gunatillake, P. A., McCarthy, S. J., Meijs, G. F. and Schindhelm, K. (2000) Polydimethylsiloxane/polyether-mixed macrodiol-based polyurethane elastomers: biostability, *Biomaterials,* 21 (10), pp. 1021-1029.

Mary, C., Marois, Y., King, M. W., Laroche, G., Douville, Y., Martin, L. *et al.* (1998) Comparison of the in vivo behavior of polyvinylidene fluoride and polypropylene sutures used in vascular surgery, *ASAIO Journal (American Society for Artificial Internal Organs : 1992),* 44 (3), pp. 199-206.

Mathapati, S., Verma, R. S., Cherian, K. M. and Guhathakurta, S. (2011) Inflammatory responses of tissue-engineered xenografts in a clinical scenario, *Interactive Cardiovascular and Thoracic Surgery,* 12 (3), pp. 360-365.

Matsumoto, H., Hasegawa, T., Fuse, K., Yamamoto, M. and Saigusa, M. (1973) A new vascular prosthesis for a small caliber artery, *Surgery,* 74 (4), pp. 519-523.

Meinhart, J. G., Deutsch, M., Fischlein, T., Howanietz, N., Froschl, A. and Zilla, P. (2001) Clinical autologous in vitro endothelialization of 153 infrainguinal ePTFE grafts, *The Annals of Thoracic Surgery,* 71 (5), pp. S331.

Meinhart, J., Deutsch, M. and Zilla, P. (1997) Eight years of clinical endothelial cell transplantation. Closing the gap between prosthetic grafts and vein grafts, *ASAIO Journal (American Society for Artificial Internal Organs : 1992),* 43 (5), pp. M521.

Mikulikova, R., Moritz, S., Gumpenberger, T., Olbrich, M., Romanin, C., Bacakova, L. *et al.* (2005) Cell microarrays on photochemically modified polytetrafluoroethylene, *Biomaterials,* 26 (27), pp. 5572-5580.

Moroni, F. and Mirabella, T. (2014) Decellularized matrices for cardiovascular tissue engineering, *American Journal of Stem Cells,* 3 (1), pp. 1-20.

Moss, A. H., Vasilakis, C., Holley, J. L., Foulks, C. J., Pillai, K. and McDowell, D. E. (1990) Use of a silicone dual-lumen catheter with a Dacron cuff as a long-term vascular access for hemodialysis patients, *American Journal of Kidney Diseases : The Official Journal of the National Kidney Foundation,* 16 (3), pp. 211-215.

Motwani, M. S., Rafiei, Y., Tzifa, A. and Seifalian, A. M. (2011) In situ endothelialization of intravascular stents from progenitor stem cells coated with nanocomposite and functionalized biomolecules, *Biotechnology and Applied Biochemistry,* 58 (1), pp. 2-13.

Mozaffarian, D., Benjamin, E. J., Go, A. S., Arnett, D. K., Blaha, M. J., Cushman, M. *et al.* (2016) Executive Summary: Heart Disease and Stroke Statistics--2016 Update: A Report From the American Heart Association, *Circulation,* 133 (4), pp. 447-454.

Murphy, J. G., Schwartz, R. S., Edwards, W. D., Camrud, A. R., Vlietstra, R. E. and Holmes, D. R.,Jr. (1992) Percutaneous polymeric stents in porcine coronary arteries. Initial experience with polyethylene terephthalate stents, *Circulation,* 86 (5), pp. 1596-1604.

Mustonen, T. and Alitalo, K. (1995) Endothelial receptor tyrosine kinases involved in angiogenesis, *The Journal of Cell Biology,* 129 (4), pp. 895-898.

Nagpal, A. and Sohail, M. R. (2011) Prosthetic vascular graft infections: a contemporary approach to diagnosis and management, *Current Infectious Disease Reports,* 13 (4), pp. 317-323.

Nemeno-Guanzon, J. G., Lee, S., Berg, J. R., Jo, Y. H., Yeo, J. E., Nam, B. M. *et al.* (2012) Trends in tissue engineering for blood vessels, *Journal of Biomedicine & Biotechnology,* 2012 , pp. 956345.

Nylander, T., Tiberg, F., Su, T. J., Lu, J. R. and Thomas, R. K. (2001) Beta-casein adsorption at the hydrophobized silicon oxide-aqueous solution interface and the effect of added electrolyte, *Biomacromolecules,* 2 (1), pp. 278-287.

Olbrich, M., Punshon, G., Frischauf, I., Salacinski, H. J., Rebollar, E., Romanin, C. *et al.* (2007) UV surface modification of a new nanocomposite polymer to improve cytocompatibility, *Journal of Biomaterials Science.Polymer Edition,* 18 (4), pp. 453-468.

Ott, M. J. and Ballermann, B. J. (1995) Shear stress-conditioned, endothelial cell-seeded vascular grafts: improved cell adherence in response to in vitro shear stress, *Surgery,* 117 (3), pp. 334-339.

Park, J. H., Park, K. D. and Bae, Y. H. (1999) PDMS-based polyurethanes with MPEG grafts: synthesis, characterization and platelet adhesion study, *Biomaterials,* 20 (10), pp. 943-953.

Passerini, A. G., Milsted, A. and Rittgers, S. E. (2003) Shear stress magnitude and directionality modulate growth factor gene expression in preconditioned vascular endothelial cells, *Journal of Vascular Surgery,* 37 (1), pp. 182-190.

Pellegata, A. F., Asnaghi, M. A., Zonta, S., Zerbini, G. and Mantero, S. (2012) A novel device for the automatic decellularization of biological tissues, *The International Journal of Artificial Organs,* 35 (3), pp. 191-198.

Peng, T., Gibula, P., Yao, K. D. and Goosen, M. F. (1996) Role of polymers in improving the results of stenting in coronary arteries, *Biomaterials,* 17 (7), pp. 685-694.

Pennel, T., Zilla, P. and Bezuidenhout, D. (2013) Differentiating transmural from transanastomotic prosthetic graft endothelialization through an isolation loop-graft model, *Journal of Vascular Surgery,* 58 (4), pp. 1053-1061.

Peters, K., Unger, R. E., Kirkpatrick, C. J., Gatti, A. M. and Monari, E. (2004) Effects of nano-scaled particles on endothelial cell function in vitro: studies on viability, proliferation and inflammation, *Journal of Materials Science: Materials in Medicine,* 15 (4), pp. 321-325.

Prokopowicz, M., Banecki, B., Lukasiak, J. and Przyjazny, A. (2003) The measurement of conformational stability of proteins adsorbed on siloxanes, *Journal of Biomaterials Science.Polymer Edition,* 14 (2), pp. 103-118.

Puckett, M. A., DeFriend, D., Williams, M. P. and Roobottom, C. A. (2004) A leaking breast prosthesis presenting as an abdominal mass, *The British Journal of Radiology,* 77 (921), pp. 790-791.

Punshon, G., Sales, K. M., Vara, D. S., Hamilton, G. and Seifalian, A. M. (2008) Assessment of the potential of progenitor stem cells extracted from human peripheral blood for seeding a novel vascular graft material, *Cell Proliferation,* 41 (2), pp. 321-335.

Punshon, G., Vara, D. S., Sales, K. M., Kidane, A. G., Salacinski, H. J. and Seifalian, A. M. (2005) Interactions between endothelial cells and a poly(carbonate-silsesquioxane-bridge-urea)urethane, *Biomaterials,* 26 (32), pp. 6271-6279.

Punshon, G., Vara, D. S., Sales, K. M. and Seifalian, A. M. (2011) A novel method for the extraction and culture of progenitor stem cells from human peripheral blood for use in regenerative medicine, *Biotechnology and Applied Biochemistry,* 58 (5), pp. 328-334.

Raithel, D. and Groitl, H. (1980) Small artery reconstruction with a new vascular prosthesis, *World Journal of Surgery,* 4 (2), pp. 223-230.

Ramires, P. A., Mirenghi, L., Romano, A. R., Palumbo, F. and Nicolardi, G. (2000) Plasma-treated PET surfaces improve the biocompatibility of human endothelial cells, *Journal of Biomedical Materials Research,* 51 (3), pp. 535-539.

Rashid, S. T., Salacinski, H. J., Fuller, B. J., Hamilton, G. and Seifalian, A. M. (2004) Engineering of bypass conduits to improve patency, *Cell Proliferation,* 37 (5), pp. 351-366.

Rehman, J., Li, J., Orschell, C. M. and March, K. L. (2003) Peripheral blood "endothelial progenitor cells" are derived from monocyte/macrophages and secrete angiogenic growth factors, *Circulation,* 107 (8), pp. 1164-1169.

Rosenman, J. E., Kempczinski, R. F., Pearce, W. H. and Silberstein, E. B. (1985) Kinetics of endothelial cell seeding, *Journal of Vascular Surgery,* 2 (6), pp. 778-784.

Salacinski, H. J., Goldner, S., Giudiceandrea, A., Hamilton, G., Seifalian, A. M., Edwards, A. *et al.* (2001) The mechanical behavior of vascular grafts: a review, *Journal of Biomaterials Applications,* 15 (3), pp. 241-278.

Salacinski, H. J., Odlyha, M., Hamilton, G. and Seifalian, A. M. (2002a) Thermo-mechanical analysis of a compliant poly(carbonate-urea)urethane after exposure to hydrolytic, oxidative, peroxidative and biological solutions, *Biomaterials,* 23 (10), pp. 2231-2240.

Salacinski, H. J., Tai, N. R., Carson, R. J., Edwards, A., Hamilton, G. and Seifalian, A. M. (2002b) In vitro stability of a novel compliant poly(carbonate-urea)urethane to oxidative and hydrolytic stress, *Journal of Biomedical Materials Research,* 59 (2), pp. 207-218.

Salacinski, H. J., Tai, N. R., Punshon, G., Giudiceandrea, A., Hamilton, G. and Seifalian, A. M. (2000) Optimal endothelialisation of a new compliant poly(carbonate-urea)urethane vascular graft with effect of physiological shear stress, *European Journal of Vascular and Endovascular Surgery : The Official Journal of the European Society for Vascular Surgery,* 20 (4), pp. 342-352.

Salehi-Nik, N., Banikarimi, S. P., Amoabediny, G., Pouran, B., Shokrgozar, M. A., Zandieh-Doulabi, B. *et al.* (2016) Flow Preconditioning of Endothelial Cells on Collagen-Immobilized Silicone Fibers Enhances Cell Retention and Antithrombotic Function, *Artificial Organs, .*

Sales, K. M., Salacinski, H. J., Alobaid, N., Mikhail, M., Balakrishnan, V. and Seifalian, A. M. (2005) Advancing vascular tissue engineering: the role of stem cell technology, *Trends in Biotechnology,* 23 (9), pp. 461-467.

Salven, P., Mustjoki, S., Alitalo, R., Alitalo, K. and Rafii, S. (2003) VEGFR-3 and CD133 identify a population of CD34+ lymphatic/vascular endothelial precursor cells, *Blood,* 101 (1), pp. 168-172.

Santerre, J. P., Woodhouse, K., Laroche, G. and Labow, R. S. (2005) Understanding the biodegradation of polyurethanes: from classical implants to tissue engineering materials, *Biomaterials,* 26 (35), pp. 7457-7470.

Sarkar, S., Salacinski, H. J., Hamilton, G. and Seifalian, A. M. (2006) The mechanical properties of infrainguinal vascular bypass grafts: their role in influencing patency, *European Journal of Vascular and Endovascular Surgery : The Official Journal of the European Society for Vascular Surgery,* 31 (6), pp. 627-636.

Sarkar, S., Sales, K. M., Hamilton, G. and Seifalian, A. M. (2007a) Addressing thrombogenicity in vascular graft construction, *J. Biomed. Mater. Res. B Appl. Biomater.,* 82 (1), pp. 100-108.

Sarkar, S., Schmitz-Rixen, T., Hamilton, G. and Seifalian, A. M. (2007b) Achieving the ideal properties for vascular bypass grafts using a tissue engineered approach: a review, *Medical & Biological Engineering & Computing,* 45 (4), pp. 327-336.

Sato, Y., Yamaguchi, D., Katoh, T., Ikeda, S., Aoki, Y., Oshima, A. *et al.* (2003) Surface modification of polytetrafluoroethylene by synchrotron radiation, *Nuclear Inst. and Methods in Physics Research, B,* 208 , pp. 231-235. DOI: 10.1016/S0168-583X(03)01108-X.

Schuurman, H. J., Cheng, J. and Lam, T. (2003) Pathology of xenograft rejection: a commentary, *Xenotransplantation,* 10 (4), pp. 293-299.

Seetharam, A., Tiriveedhi, V. and Mohanakumar, T. (2010) Alloimmunity and autoimmunity in chronic rejection, *Current Opinion in Organ Transplantation,* 15 (4), pp. 531-536.

Seifalian, A. M., Handcock, S. and Salacinski, H. J. (2005) Polymer for use in conduits and medical devices, *Patent Number: WO2005070998:,* http://v3.espacenet.com/textdoc?DB=EPODOC&IDX=WO2005070998&F=0] .

Seifalian, A. M., Salacinski, H. J., Punshon, G., Krijgsman, B. and Hamilton, G. (2001) A new technique for measuring the cell growth and metabolism of endothelial cells seeded on vascular prostheses, *Journal of Biomedical Materials Research,* 55 (4), pp. 637-644.

Seifalian, A. M., Salacinski, H. J., Tiwari, A., Edwards, A., Bowald, S. and Hamilton, G. (2003) In vivo biostability of a poly(carbonate-urea)urethane graft, *Biomaterials,* 24 (14), pp. 2549-2557.

Seifalian, A. M., Tiwari, A., Hamilton, G. and Salacinski, H. J. (2002) Improving the clinical patency of prosthetic vascular and coronary bypass grafts: the role of seeding and tissue engineering, *Artificial Organs,* 26 (0160-564; 4), pp. 307-320.

Seta, N., Okazaki, Y., Izumi, K., Miyazaki, H., Kato, T. and Kuwana, M. (2012) Fibronectin binding is required for acquisition of mesenchymal/endothelial differentiation potential in human circulating monocytes, *Clinical & Developmental Immunology,* 2012 , pp. 820827.

Sgarioto, M., Vigneron, P., Patterson, J., Malherbe, F., Nagel, M. D. and Egles, C. (2012) Collagen type I together with fibronectin provide a better support for endothelialization, *Comptes Rendus Biologies,* 335 (8), pp. 520-528.

Shay-Salit, A., Shushy, M., Wolfovitz, E., Yahav, H., Breviario, F., Dejana, E. *et al.* (2002) VEGF receptor 2 and the adherens junction as a mechanical transducer in vascular endothelial cells, *Proceedings of the National Academy of Sciences of the United States of America,* 99 (14), pp. 9462-9467.

Shearer, H., Ellis, M. J., Perera, S. P. and Chaudhuri, J. B. (2006) Effects of common sterilization methods on the structure and properties of poly(D,L lactic-co-glycolic acid) scaffolds, *Tissue Engineering,* 12 (10), pp. 2717-2727.

Shintani, H. (1995) Formation and elution of toxic compounds from sterilized medical products: methylenedianiline formation in polyurethane, *Journal of Biomaterials Applications,* 10 (1), pp. 23-58.

Shirota, T., He, H., Yasui, H. and Matsuda, T. (2003) Human endothelial progenitor cell-seeded hybrid graft: proliferative and antithrombogenic potentials in vitro and fabrication processing, *Tissue Engineering,* 9 (1), pp. 127-136.

Simmons, A., Hyvarinen, J. and Poole-Warren, L. (2006) The effect of sterilisation on a poly(dimethylsiloxane)/poly(hexamethylene oxide) mixed macrodiol-based polyurethane elastomer, *Biomaterials,* 27 (25), pp. 4484-4497.

Simoons, M. L. and Windecker, S. (2010) Controversies in cardiovascular medicine: Chronic stable coronary artery disease: drugs vs. revascularization, *European Heart Journal,* 31 (5), pp. 530-541.

Singh, N., Van Craeyveld, E., Tjwa, M., Ciarka, A., Emmerechts, J., Droogne, W. *et al.* (2012) Circulating apoptotic endothelial cells and apoptotic endothelial microparticles independently predict the presence of cardiac allograft vasculopathy, *Journal of the American College of Cardiology,* 60 (4), pp. 324-331.

Sottiurai, V. S. (1999) Distal Anastomotic Intimal Hyperplasia: Histocytomorphology, Pathophysiology, Etiology, and Prevention, *The International Journal of Angiology : Official Publication of the International College of Angiology, Inc,* 8 (1), pp. 1-10.

Sottiurai, V. S., Kollros, P., Glagov, S., Zarins, C. K. and Mathews, M. B. (1983) Morphologic alteration of cultured arterial smooth muscle cells by cyclic stretching, *The Journal of Surgical Research,* 35 (6), pp. 490-497.

Stanley, J. C., Burkel, W. E., Graham, L. M. and Lindblad, B. (1985) Endothelial cell seeding of synthetic vascular prostheses, *Acta Chirurgica Scandinavica. Supplementum,* 529 , pp. 17-27.

Stauffer, B. L., Maceneaney, O. J., Kushner, E. J., Cech, J. N., Greiner, J. J., Westby, C. M. *et al.* (2008) Gender and Endothelial Progenitor Cell Number in Middle-Aged Adults, *Artery Research,* 2 (4), pp. 156-160.

Tang, Y. W., Labow, R. S. and Santerre, J. P. (2003) Isolation of methylene dianiline and aqueous-soluble biodegradation products from polycarbonate-polyurethanes, *Biomaterials,* 24 (17), pp. 2805-2819.

Tao, J., Yang, Z., Wang, J. M., Wang, L. C., Luo, C. F., Tang, A. L. *et al.* (2007) Shear stress increases Cu/Zn SOD activity and mRNA expression in human endothelial progenitor cells, *Journal of Human Hypertension,* 21 (5), pp. 353-358.

Tepper, O. M., Galiano, R. D., Capla, J. M., Kalka, C., Gagne, P. J., Jacobowitz, G. R. *et al.* (2002) Human endothelial progenitor cells from type II diabetics exhibit impaired proliferation, adhesion, and incorporation into vascular structures, *Circulation,* 106 (22), pp. 2781-2786.

Tiwari, A., Kidane, A., Punshon, G., Hamilton, G. and Seifalian, A. M. (2003a) Extraction of cells for single-stage seeding of vascular-bypass grafts, *Biotechnology and Applied Biochemistry,* 38 (Pt 1), pp. 35-41.

Tiwari, A., Kidane, A., Salacinski, H., Punshon, G., Hamilton, G. and Seifalian, A. M. (2003b) Improving endothelial cell retention for single stage seeding of prosthetic grafts: use of polymer sequences of arginine-glycine-aspartate, *European Journal of Vascular and Endovascular Surgery : The Official Journal of the European Society for Vascular Surgery,* 25 (4), pp. 325-329.

Tiwari, A., Salacinski, H. J., Punshon, G., Hamilton, G. and Seifalian, A. M. (2002) Development of a hybrid cardiovascular graft using a tissue engineering approach, *FASEB*

Journal : Official Publication of the Federation of American Societies for Experimental Biology, 16 (8), pp. 791-796.

Tseng, D. Y. and Edelman, E. R. (1998) Effects of amide and amine plasma-treated ePTFE vascular grafts on endothelial cell lining in an artificial circulatory system, *Journal of Biomedical Materials Research,* 42 (2), pp. 188-198.

Twine, C. P. and McLain, A. D. (2010) Graft type for femoro-popliteal bypass surgery, *The Cochrane Database of Systematic Reviews,* (5):CD001487. doi (5), pp. CD001487.

Vara, D. S., Punshon, G., Sales, K. M., Hamilton, G. and Seifalian, A. M. (2006) The effect of shear stress on human endothelial cells seeded on cylindrical viscoelastic conduits: an investigation of gene expression, *Biotechnology and Applied Biochemistry,* 45 (Pt 3), pp. 119-130.

Vara, D. S., Punshon, G., Sales, K. M., Hamilton, G. and Seifalian, A. M. (2011) Haemodynamic regulation of gene expression in vascular tissue engineering, *Current Vascular Pharmacology,* 9 (2), pp. 167-187.

Vara, D. S., Punshon, G., Sales, K. M., Sarkar, S., Hamilton, G. and Seifalian, A. M. (2008) Endothelial cell retention on a viscoelastic nanocomposite vascular conduit is improved by exposure to shear stress preconditioning prior to physiological flow, *Artificial Organs,* 32 (12), pp. 977-981.

Veith, F. J., Moss, C. M., Sprayregen, S. and Montefusco, C. (1979) Preoperative saphenous venography in arterial reconstructive surgery of the lower extremity, *Surgery,* 85 (3), pp. 253-256.

Wang, X. B., Huang, J., Zou, J. G., Su, E. B., Shan, Q. J., Yang, Z. J. *et al.* (2007) Effects of resveratrol on number and activity of endothelial progenitor cells from human peripheral blood, *Clinical and Experimental Pharmacology & Physiology,* 34 (11), pp. 1109-1115.

Ward, M. R., Tsao, P. S., Agrotis, A., Dilley, R. J., Jennings, G. L. and Bobik, A. (2001) Low blood flow after angioplasty augments mechanisms of restenosis: inward vessel remodeling, cell migration, and activity of genes regulating migration, *Arteriosclerosis, Thrombosis, and Vascular Biology,* 21 (2), pp. 208-213.

Wasserman, S. M. and Topper, J. N. (2004) Adaptation of the endothelium to fluid flow: in vitro analyses of gene expression and in vivo implications, *Vascular Medicine (London, England),* 9 (1358-863; 1), pp. 35-45.

Weber, B., Emmert, M. Y., Schoenauer, R., Brokopp, C., Baumgartner, L. and Hoerstrup, S. P. (2011) Tissue engineering on matrix: future of autologous tissue replacement, *Seminars in Immunopathology,* 33 (3), pp. 307-315.

Wei, G. and Ma, P. X. (2008) Nanostructured Biomaterials for Regeneration, *Advanced Functional Materials,* 18 (22), pp. 3566-3582.

Weinberg, C. B. and Bell, E. (1986) A blood vessel model constructed from collagen and cultured vascular cells, *Science (New York, N.Y.),* 231 (4736), pp. 397-400.

Whalen, R. L., Cardona, R. R. and Kantrowitz, A. (1992) A new, all silicone rubber small vessel prosthesis, *ASAIO Journal (American Society for Artificial Internal Organs : 1992),* 38 (3), pp. 207.

White, R. A., Klein, S. R. and Shors, E. C. (1987) Preservation of compliance in a small diameter microporous, silicone rubber vascular prosthesis, *The Journal of Cardiovascular Surgery,* 28 (5), pp. 485-490.

Wilshaw, S. P., Rooney, P., Berry, H., Kearney, J. N., Homer-Vanniasinkam, S., Fisher, J. *et al.* (2012) Development and characterization of acellular allogeneic arterial matrices, *Tissue Engineering.Part A,* 18 (5-6), pp. 471-483.

World Health Organisation (2016) *Cardiovascular Disease (CVD) Factsheet.* Available from: http://www.who.int/mediacentre/factsheets/fs317/en/ [Accessed 18th September 2016].

Xiao, L. and Shi, D. (2004) Role of precoating in artificial vessel endothelialization, *Chinese Journal of Traumatology = Zhonghua Chuang Shang Za Zhi,* 7 (5), pp. 312-316.

Xu, H., Yan, F., Monson, E. E. and Kopelman, R. (2003) Room-temperature preparation and characterization of poly (ethylene glycol)-coated silica nanoparticles for biomedical applications, *Journal of Biomedical Materials Research.Part A,* 66 (4), pp. 870-879.

Xue, L. and Greisler, H. P. (2003) Biomaterials in the development and future of vascular grafts, *Journal of Vascular Surgery : Official Publication, the Society for Vascular Surgery [and] International Society for Cardiovascular Surgery, North American Chapter,* 37 (2), pp. 472-480.

Yamamoto, K., Takahashi, T., Asahara, T., Ohura, N., Sokabe, T., Kamiya, A. *et al.* (2003) Proliferation, differentiation, and tube formation by endothelial progenitor cells in response to shear stress, *Journal of Applied Physiology: Respiratory, Environmental and Exercise Physiology,* 95 (5), pp. 2081-2088.

Yoder, M. C., Mead, L. E., Prater, D., Krier, T. R., Mroueh, K. N., Li, F. *et al.* (2007) Redefining endothelial progenitor cells via clonal analysis and hematopoietic stem/progenitor cell principals, *Blood,* 109 (5), pp. 1801-1809.

Zaragoza, C., Marquez, S. and Saura, M. (2012) Endothelial mechanosensors of shear stress as regulators of atherogenesis, *Current Opinion in Lipidology,* 23 (5), pp. 446-452.

Zenni, G. C., Ellinger, J., Lam, T. M. and Greisler, H. P. (1994) Biomaterial-induced macrophage activation and monokine release, *Journal of Investigative Surgery : The Official Journal of the Academy of Surgical Research,* 7 (2), pp. 135-141.

Zhang, F., Kang, E. T., Neoh, K. G., Wang, P. and Tan, K. L. (2001) Modification of Si(100) surface by the grafting of poly(ethylene glycol) for reduction in protein adsorption and platelet adhesion, *Journal of Biomedical Materials Research,* 56 (3), pp. 324-332.

Zhang, S. J., Zhang, H., Wei, Y. J., Su, W. J., Liao, Z. K., Hou, M. *et al.* (2006a) Adult endothelial progenitor cells from human peripheral blood maintain monocyte/macrophage function throughout in vitro culture, *Cell Research,* 16 (6), pp. 577-584.

Zhang, S. J., Zhang, H., Wei, Y. J., Su, W. J., Liao, Z. K., Hou, M. *et al.* (2006b) Adult endothelial progenitor cells from human peripheral blood maintain monocyte/macrophage function throughout in vitro culture, *Cell Research,* 16 (6), pp. 577-584.

Zhang, Y. Z., Bjursten, L. M., Freij-Larsson, C., Kober, M. and Wesslen, B. (1996) Tissue response to commercial silicone and polyurethane elastomers after different sterilization procedures, *Biomaterials,* 17 (23), pp. 2265-2272.

Zilla, P., Bezuidenhout, D. and Human, P. (2007) Prosthetic vascular grafts: wrong models, wrong questions and no healing, *Biomaterials,* 28 (34), pp. 5009-5027.

Zilla, P., Deutsch, M., Meinhart, J., Puschmann, R., Eberl, T., Minar, E. *et al.* (1994) Clinical in vitro endothelialization of femoropopliteal bypass grafts: an actuarial follow-up over three years, *Journal of Vascular Surgery : Official Publication, the Society for Vascular Surgery [and] International Society for Cardiovascular Surgery, North American Chapter,* 19 (3), pp. 540-548.

Appendix 1 List of Publications

*Ahmed, M., **Punshon, G**., Darbyshire, A. and Seifalian, A. M. (2013) Effects of sterilizatio n treatments on bulk and surface properties of nanocomposite biomaterials, *Journal of Biome dical Materials Research.Part B, Applied Biomaterials,* 101 (7), pp. 1182-1190.

Conn, G., Kidane, A. G., **Punshon, G**., Kannan, R. Y., Hamilton, G. and Seifalian, A. M. (20 06) Is there an alternative to systemic anticoagulation, as related to interventional biomedical devices? *Expert Review of Medical Devices,* 3 (2), pp. 245-261.

de Mel, A., **Punshon, G**., Ramesh, B., Sarkar, S., Darbyshire, A., Hamilton, G. *et al.* (2009) I n situ endothelialization potential of a biofunctionalised nanocomposite biomaterial-based sm all diameter bypass graft, *Bio-Medical Materials and Engineering,* 19 (4-5), pp. 317-331.

Gupta, A., Vara, D. S., **Punshon, G**., Sales, K. M., Winslet, M. C. and Seifalian, A. M. (2009) In vitro small intestinal epithelial cell growth on a nanocomposite polycaprolactone scaffold , *Biotechnology and Applied Biochemistry,* 54 (4), pp. 221-229.

Kidane, A. G., **Punshon, G**., Salacinski, H. J., Ramesh, B., Dooley, A., Olbrich, M. *et al.* (20 06) Incorporation of a lauric acid-conjugated GRGDS peptide directly into the matrix of a pol y(carbonate-urea)urethane polymer for use in cardiovascular bypass graft applications, *Journ al of Biomedical Materials Research.Part A,* 79 (3), pp. 606-617.

Kidane, A. G., Salacinski, H. J., **Punshon, G**., Ramesh, B., Srai, K. S. and Seifalian, A. M. (2 003) Synthesis and evaluation of amphiphilic RGD derivatives: uses for solvent casting in pol ymers and tissue engineering applications, *Medical & Biological Engineering & Computing,* 41 (6), pp. 740-745.

Krijgsman, B., Seifalian, A. M., Salacinski, H. J., Tai, N. R., **Punshon, G**., Fuller, B. J. *et al.* (2002) An assessment of covalent grafting of RGD peptides to the surface of a compliant poly(carbonate-urea)urethane vascular conduit versus conventional biological coatings: its role in enhancing cellular retention, *Tissue Engineering,* 8 (4), pp. 673-680.

Leary, A., Cook, R., Jones, S., Smith, J., Gough, M., Maxwell, E. *et al.* (2016) Mining routinely collected acute data to reveal non-linear relationships between nurse staffing levels and outcomes, *BMJ Open,* 6 (12), pp. 011177.

Leary, A., Greenwood, P., Hedley, B., Agnew, J., Thompson, D. and **Punshon, G**. (2008) An analysis of use of crowd medical services at an English football league club, *International Emergency Nursing,* 16 (3), pp. 193-199.

*Olbrich, M., **Punshon, G**., Frischauf, I., Salacinski, H. J., Rebollar, E., Romanin, C. *et al.* (2007) UV surface modification of a new nanocomposite polymer to improve cytocompatibility, *Journal of Biomaterials Science.Polymer Edition,* 18 (4), pp. 453-468.

Punshon, G. and Fuller, B. (1998) Changes in ferrozine detectable iron in liver cells during hypoxia and hypothermia, *Biochemical Society Transactions,* 26 (2), pp. S102.

***Punshon, G**., Sales, K. M., Vara, D. S., Hamilton, G. and Seifalian, A. M. (2008) Assessment of the potential of progenitor stem cells extracted from human peripheral blood for seeding a novel vascular graft material, *Cell Proliferation,* 41 (2), pp. 321-335.

***Punshon, G**., Vara, D. S., Sales, K. M., Kidane, A. G., Salacinski, H. J. and Seifalian, A. M. (2005) Interactions between endothelial cells and a poly(carbonate-silsesquioxane-bridge-urea)urethane, *Biomaterials,* 26 (32), pp. 6271-6279.

Punshon, G., Vara, D. S., Sales, K. M. and Seifalian, A. M. (2011a) The long-term stability in gene expression of human endothelial cells permits the production of large numbers of cells suitable for use in regenerative medicine, *Biotechnology and Applied Biochemistry,* 58 (5), pp. 371-375.

*Punshon, G., Vara, D. S., Sales, K. M. and Seifalian, A. M. (2011b) A novel method for the extraction and culture of progenitor stem cells from human peripheral blood for use in regenerative medicine, *Biotechnology and Applied Biochemistry,* 58 (5), pp. 328-334.

Salacinski, H. J., **Punshon, G**., Krijgsman, B., Hamilton, G. and Seifalian, A. M. (2001) A hybrid compliant vascular graft seeded with microvascular endothelial cells extracted from human omentum, *Artificial Organs,* 25 (12), pp. 974-982.

Salacinski, H. J., Tai, N. R., **Punshon, G**., Giudiceandrea, A., Hamilton, G. and Seifalian, A. M. (2000) Optimal endothelialisation of a new compliant poly(carbonate-urea)urethane vascular graft with effect of physiological shear stress, *European Journal of Vascular and Endovascular Surgery : The Official Journal of the European Society for Vascular Surgery,* 20 (4), pp. 342-352.

Seifalian, A. M., Salacinski, H. J., **Punshon, G**., Krijgsman, B. and Hamilton, G. (2001) A new technique for measuring the cell growth and metabolism of endothelial cells seeded on vascular prostheses, *Journal of Biomedical Materials Research,* 55 (4), pp. 637-644.

Tiwari, A., Kidane, A., **Punshon, G**., Hamilton, G. and Seifalian, A. M. (2003a) Extraction of cells for single-stage seeding of vascular-bypass grafts, *Biotechnology and Applied Biochemistry,* 38 (Pt 1), pp. 35-41.

Tiwari, A., Kidane, A., Salacinski, H., **Punshon, G**., Hamilton, G. and Seifalian, A. M. (2003 b) Improving endothelial cell retention for single stage seeding of prosthetic grafts: use of pol ymer sequences of arginine-glycine-aspartate, *European Journal of Vascular and Endovascul ar Surgery: The Official Journal of the European Society for Vascular Surgery,* 25 (4), pp. 32 5-329.

Tiwari, A., **Punshon, G**., Kidane, A., Hamilton, G. and Seifalian, A. M. (2003c) Magnetic be ads (Dynabead) toxicity to endothelial cells at high bead concentration: implication for tissue engineering of vascular prosthesis, *Cell Biology and Toxicology,* 19 (5), pp. 265-272.

Tiwari, A., Salacinski, H. J., **Punshon, G**., Hamilton, G. and Seifalian, A. M. (2002) Develop ment of a hybrid cardiovascular graft using a tissue engineering approach, *FASEB Journal : Official Publication of the Federation of American Societies for Experimental Biology,* 16 (8) , pp. 791-796.

*Vara, D. S., **Punshon, G**., Sales, K. M., Hamilton, G. and Seifalian, A. M. (2006) The effect of shear stress on human endothelial cells seeded on cylindrical viscoelastic conduits: an inve stigation of gene expression, *Biotechnology and Applied Biochemistry,* 45 (Pt 3), pp. 119-130

*Vara, D. S., **Punshon, G**., Sales, K. M., Hamilton, G. and Seifalian, A. M. (2011) Haemody namic regulation of gene expression in vascular tissue engineering, *Current Vascular Pharma cology,* 9 (2), pp. 167-187.

Vara, D. S., **Punshon, G**., Sales, K. M., Salacinski, H. J., Dijk, S., Brown, R. A. *et al.* (2005) Development of an RNA isolation procedure for the characterisation of human endothelial cel l interactions with polyurethane cardiovascular bypass grafts, *Biomaterials,* 26 (18), pp. 3987 -3993.

*Vara, D. S., **Punshon, G**., Sales, K. M., Sarkar, S., Hamilton, G. and Seifalian, A. M. (2008) Endothelial cell retention on a viscoelastic nanocomposite vascular conduit is improved by exposure to shear stress preconditioning prior to physiological flow, *Artificial Organs,* 32 (12), pp. 977-981.

*** publications arising in whole or part from the work presented in this thesis**.